Brain on a chip : to reconstruct multi-nodal neuronal networks in vitro for neurodegenerative disease modelling

Teng Pan

SORBONNE UNIVERSITÉ

École Doctorale Cerveau Cognition Comportement (Paris, n°158)

Laboratoire Neuroscience Paris Seine, Équipe Régénération et Croissance de l'axone
Laboratoire Physico-Chimie Curie, Équipé Macromolécules et Microsystèmes en Biologie et en Médecine

Spécialité : Neurosciences et Micro-ingénierie

Brain on a chip to reconstruct multi-nodal neuronal networks *in vitro* for neurodegenerative disease modelling

Présentée par

Teng PAN

Pour obtenir le grade de

DOCTEUR DE SORBONNE UNIVERSITÉ

Dirigée par

Jean-Michel PEYRIN et Catherine VILLARD

Présentée et soutenue publiquement le 24/05/2022,
devant un jury composé de:

Dr Jean-Michel PEYRIN	Directeur de recherche, Paris	Directeur de thèse
Dr Catherine VILLARD	Directeur de recherche, Paris	Co-directrice de thèse
Dr Benoît CHARLOT	Directeur de recherche, Montpellier	Rapporteur
Dr Devrim KILINC	Chargé de recherche - Habilitation à diriger des recherche (CR-HDR), Lille	Rapporteur
Dr Ayako YAMADA	Chargé de recherche, Paris	Examinatrice
Dr Rachel SHERRARD	Professeure des universités, Paris	Président de jury

PhD Thesis

Brain on a chip to reconstruct multi-nodal neuronal networks *in vitro* for neurodegenerative disease modelling

PAN Teng

Sorbonne University - PhD Thesis

Title : Brain on a chip to reconstruct multi-nodal neuronal networks in vitro for neurodegenerative disease modelling

Author : PAN Teng

Address : 7 Quai Saint-Bernard, IBPS, Sorbonne University, A301,75005, Paris.

Acknowledgement

Paris is a beautiful, romantic and tolerant city. I was very fortunate to spend forty-two months of my PhD research at Sorbonne University, which is located adjacent to the Seine River. I still remember my first encounter with Sorbonne University, it was called Université Pierre-et-Marie-Curie. When I was a child, Marie Curie used to be a role model of female scientists in my mind， and I wanted to be a scientist like her. With this longing and my efforts, I was eventually granted the opportunity to study in Paris.

In this blossoming season, I am coming to the end of my doctoral career, a process that has been full of ups and downs, setbacks and misfortunes, but more than that, growth, acquisition and strength, all of which are my precious memories. Looking back over the past thirty years, I think it is my perseverance and effort that has taken me so far. The weighty thesis is not only the accumulation of my PhD, but also the most important creation in my life. And it will also inspire me towards the future.

First of all, I would like to thank my mother who made it possible for me to do my PhD in France. She is a great mother. Her strength, concentration and passion for her career and continuous pursuit of knowledge have been a great inspiration for me. Moreover, she gave me a new life again when I was at the lowest point of my life. It was also her decision that led me to come to France. Of course, I can't ignore the fact that I seem to have inherited some design talent from her as well. Likewise, I am grateful to my father, who, like all Chinese fathers, is a quietly giving and committed man. The support from my family is the prerequisite that enabled me to make this choice.

Secondly, I would like to thank my supervisors, Jean-Michel PEYRIN and Catherine VILLARD. They have transferred me enormous knowledge on Neurobiology and Microfluidics, guided and helped me to solve problems in my research. I feel very fortunate to be their Ph.D. student. Therefore, in my acknowledgements, I would like to express my gratitude and admiration for them all. Dr. PEYRIN is a very kind,

responsible and patient supervisor. He is very brilliant and knowledgeable. He always responsive to all my questions and regularly shares the latest research to me. In addition, he is very good at discovering my talents and always guides me in the right way. From him, I learned the attitude and methodology of doing research. Dr. VILLARD is a very nice, enthusiastic and meticulous supervisor. She is very intellectual and experienced in the field of microfluidics. She always encouraged me and gave me a lot of advice on my research. In my mind, she is a very charming academic and I would love to be like her.

Thirdly, I would like to thank my colleagues in our laboratories for their help in my research and my life. They are Audric, Chaimae, Cholé, Charles, Corentin, Josquin, Kadia, Kevin, NA, Simon, Sylvia, Théo, Uz, Xavier, Ya and also our director Fatiha Nothias.

Then, I also would like to thank my friends who have accompanied me at each stage of my life. They are Linde, Fei LIAO, Yonglan, Ning ZHANG, Xiaoming YAN, Xiaoxiao, Cheng YAN, Rongrong, Peng CHEN, Haitao, Huijie, Jianghao, Xuanmeng, Yanan, Qianqian. I would also like to thank the teachers who have influenced my life, Xufu MA, Jianjiang LI, Dahai TANG, Wangxi FAN, Hongxia MA el al.

Finally, and most importantly, I would like to thank the Chinese Scholarship Council for funding my doctoral studies.

Paris，2022.

Remerciements

Paris est une ville magnifique, romantique et tolérante. J'ai eu la chance de passer quarante-deux mois de ma recherche doctorale à l'Université de la Sorbonne, qui est située à côté de la Seine. Je me souviens encore de ma première rencontre avec l'Université de la Sorbonne, qui s'appelait alors Université Pierre-et-Marie-Curie. Quand j'étais enfant, Marie Curie était un modèle de femme scientifique dans mon esprit， et je voulais être une scientifique comme elle. Grâce à ce désir et à mes efforts, j'ai finalement eu l'opportunité d'étudier à Paris.

En cette période de floraison, j'arrive à la fin de ma carrière de doctorante, un processus qui a connu des hauts et des bas, des revers et des malheurs, mais surtout une croissance, une acquisition et une force, qui sont autant de souvenirs précieux pour moi. En regardant ces trente dernières années, je pense que c'est ma persévérance et mes efforts qui m'ont menée si loin. La lourde thèse n'est pas seulement l'accumulation de mon doctorat, mais aussi la création la plus importante de ma vie. Et elle m'inspirera également pour l'avenir.

Tout d'abord, je tiens à remercier ma mère qui m'a permis de faire mon doctorat en France. C'est une mère formidable. Sa force, sa concentration et sa passion pour sa carrière et sa quête permanente de connaissances ont été une grande source d'inspiration pour moi. De plus, elle m'a redonné vie lorsque j'étais au plus bas de ma vie. C'est aussi sa décision qui m'a poussé à venir en France. Bien sûr, je ne peux pas ignorer le fait que je semble avoir hérité d'elle un certain talent pour le design. De même, je suis reconnaissante à mon père qui, comme tous les pères chinois, est un homme discret, généreux et engagé. Le soutien de ma famille est la condition préalable qui m'a permis de faire ce choix.

Ensuite, je tiens à remercier mes superviseurs, Jean-Michel PEYRIN et Catherine VILLARD. Ils m'ont transmis d'énormes connaissances sur la neurobiologie et la microfluidique, m'ont guidé et aidé à résoudre les problèmes de mes recherches. Je me

sens très chanceux d'être leur doctorant. C'est pourquoi, dans mes remerciements, je voudrais exprimer ma gratitude et mon admiration pour eux tous. Le Dr PEYRIN est un superviseur très gentil, responsable et patient. Il est très brillant et bien informé. Il répond toujours à toutes mes questions et me fait régulièrement part des dernières recherches. En outre, il est très doué pour découvrir mes talents et me guide toujours dans la bonne direction. De lui, j'ai appris l'attitude et la méthodologie de la recherche. Le Dr VILLARD est un superviseur très gentil, enthousiaste et méticuleux. Elle est très intellectuelle et expérimentée dans le domaine de la microfluidique. Elle m'a toujours encouragé et m'a donné beaucoup de conseils sur mes recherches. Dans mon esprit, elle est une universitaire très charmante et j'aimerais être comme elle.

Troisièmement, je voudrais remercier mes collègues dans nos laboratoires pour leur aide dans mes recherches et dans ma vie. Ce sont Audric, Chaimae, Cholé, Charles, Corentin, Josquin, Kadia, Kevin, NA, Simon, Sylvia, Théo, Uz, Xavier, Ya et aussi notre directrice Fatiha Nothias.

Ensuite, je tiens également à remercier mes amis qui m'ont accompagné à chaque étape de ma vie. Il s'agit de Linde, Fei LIAO, Yonglan, Ning ZHANG, Xiaoming YAN, Xiaoxiao, Cheng YAN, Rongrong, Peng CHEN, Haitao, Huijie, Jianghao, Xuanmeng, Yanan, Qianqian. Je tiens également à remercier les professeurs qui ont influencé ma vie, Xufu MA, Jianjiang LI, Dahai TANG, Wangxi FAN, Hongxia MA el al.

Enfin, et surtout, je tiens à remercier le Conseil chinois des bourses d'études pour avoir financé mes études doctorales.

Paris，2022.

Abstract

Neurodegenerative diseases are a group of diseases in which neurons undergo degenerative lesions and loss of structural function. Examples of diseases include Parkinson's syndrome and Alzheimer's disease, which lead to poor quality of life for patients in their later years. The occurrence of these diseases is booming in the context of an extremely rapid increase in the global ageing population. Currently, animal models and in vitro cell cultures are commonly used to study the biological mechanisms of these diseases. They involve the spatial spread of neuronal degeneration in the brain's anatomical structures. However, the advantage of in vitro preparations in terms of control and accessibility is balanced by a loss of the original anatomical structure. Moreover, the actual construction of functional neural networks in vitro faces many difficulties.

First, neurons are branched and polarized cells, usually exhibiting one axon and a dendritic tree. To create artificially designed neuron architectures in vitro, we need to locate a given neuronal population's cellular bodies (soma) and guide their axon toward another group of neurons. Then, exploring the propagation of neuronal degeneration of these networks requires manipulating and following independently different neuronal populations.

The emerging microfluidic chip technology has opened up new possibilities for fulfilling these goals. Microfluidics is a technique for handling or manipulating fluids at the micron scale. The field of culturing microtissues and organs in a chip has evolved into a new name, organ-on-a-chip. It is a class of biochips that simplify the structure of real organs to realize the function of the mini-organ. In the field of neuroscience, microfluidics has been used to compartmentalize cells using culture chambers connected by micron-size microchannels guiding axon growth, opening up the possibility of building artificial networks. By converting from 3D to 2D or even 2.5D,

it can solve the situation of neurons in ordinary culture dishes with a crisscrossing of neurites. In addition, microfluidic devices with micron-scale channels and microliter and nanoliter volumes of cell culture medium are capable of both maintaining a stable microenvironment for brain cells and neuronal circuits and changing this environment very rapidly by a fluidic control. Using the response of neuronal cells to chemical or physical stimuli, the change of local molecular concentration can be monitored by precisely controlled sensors which interface with microfluidic chips and some fluorescence indicators. The morphological changes of neurites, soma and nuclei, and cytosolic signals also can be observed. This allows not only to study real-time responses triggered by changes in the microenvironment but also to study the molecular mechanisms of neurodegenerative diseases.

The seminal work of Taylor et al. described the use of microfluidics to build a bi-nodal network. But how to construct multi-nodal networks is still a challenge in this field. Brain connectomics has recently revealed the relationship between topological structure and function of the brain. It inspired our team to combine the compartmentalized microfluidic techniques - which can control axon's directional growth - with the topological principles of brain connectomics to design neural networks. This topology-based design of neural networks more closely resembles the connections between neurons in the real brain and can be used to study how, for example, α-synuclein and b-amyloid aggregates, which are associated with Parkinson's and Alzheimer's diseases, respectively, propagate in neural networks.

In general, the emerging brain-on-a-chip is a promising new class of technology among the current models of multiple neurological diseases.

In the first chapter, this thesis presents the basic knowledge and recent advances in this area. The second section deals with some basic neurobiological knowledge and basic concepts of brain connectomics, the theoretical basis for in vitro construction of neural networks. It introduces the biological features of neurodegenerative diseases and

some mainstream views on their pathogenesis, followed by an overview of some models for studying neurological disorders. In the third section of this chapter, the brain chip section first focuses on the fabrication process of microfluidic chips and related materials and the basis of cell survival in the chip. It reviews and discusses models constructed in recent years using microfluidic chips to study neurological diseases.

In Chapter 2, a platform for the in vitro reconstruction of two-nodes directional neural networks with controlled synaptic connectivity is introduced. The fabrication process involves "in-mold patterning" technique. That allows to enforce both chemical and mechanical constraints on growing neurons. This platform enables micro-positioning groups of neurons inside microfluidic chips and directional axonal guidance to achieve tuneable functional connectivity.

In chapter 3, using the same microfabrication process, I explored the feasibility of reconstructing complex multi-nodal networks in a compartmentalized microfluidic platform. To reach that goal, I studied various parameters to optimize the survival of complex networks in vitro.

In chapter 4, using the two platforms I developed, I study the trans neuronal propagation of alpha-Synuclein aggregates that are proposed to stem for the initiation of neurodegenerative processes such as Parkinson's Disease.

In Chapter 5, based on some final technological experiments, I present few technological perspectives to further optimize the reconstruction of complex networks in vitro.

In Chapter 6, I discuss various aspects underlying the micro-fabrication of platforms to handle neurons and propose some perspectives for the future of brain-on-a-chip approaches.

In summary, the brain-on-a-chip enables in vitro construction as a model for studying diseases. By Constructing a brain on a chip for neurological diseases, this chip

will bring new opportunities for the discovery of new drug targets and the screening of drugs in the nervous system. In the future, high-throughput drug screening on a chip will significantly reduce the time for testing the activity of drug molecules, thus shortening the cycle time for new drug development and replacing animal experiments for drug activity testing more efficiently.

Résumé

Les maladies neurodégénératives sont un groupe de maladies dans lesquelles les neurones subissent des lésions dégénératives et une perte de fonction structurelle. Parmi ces maladies, on peut citer le syndrome de Parkinson et la maladie d'Alzheimer, qui entraînent une mauvaise qualité de vie des patients à un âge avancé. L'apparition de ces maladies est en plein essor dans le contexte d'une augmentation extrêmement rapide de la population mondiale vieillissante. Actuellement, les modèles animaux et les cultures cellulaires in vitro sont couramment utilisés pour étudier les mécanismes biologiques de ces maladies. Elles mettent en jeu la propagation spatiale de la dégénérescence neuronale dans les structures anatomiques du cerveau. Cependant, l'avantage des préparations in vitro en termes de contrôle et d'accessibilité est contrebalancé par une perte de la structure anatomique originale. En outre, la construction effective de réseaux neuronaux fonctionnels in vitro se heurte à de nombreuses difficultés.

Premièrement, les neurones sont des cellules ramifiées et polarisées, présentant généralement un axone et un arbre dendritique. Pour créer des architectures neuronales artificielles in vitro, nous devons localiser les corps cellulaires (soma) d'une population neuronale donnée et guider leur axone vers un autre groupe de neurones. Ensuite, l'exploration de la propagation de la dégénérescence neuronale de ces réseaux nécessite de manipuler et de suivre indépendamment différentes populations neuronales.

La technologie émergente des puces microfluidiques a ouvert de nouvelles possibilités pour atteindre ces objectifs. La microfluidique est une technique permettant de manipuler des fluides à l'échelle du micron. Le domaine de la culture de microtissus et d'organes dans une puce a évolué vers un nouveau nom, celui d'organe sur puce. Il s'agit d'une catégorie de biopuces qui simplifient la structure des organes réels pour réaliser la fonction du mini-organe. Dans le domaine des neurosciences, la microfluidique a été utilisée pour compartimenter les cellules à l'aide de chambres de culture reliées par des microcanaux de l'ordre du micron guidant la croissance des

axones, ouvrant ainsi la possibilité de construire des réseaux artificiels. En passant de la 3D à la 2D ou même à la 2,5D, elle peut résoudre la situation des neurones dans des boîtes de culture ordinaires avec un entrecroisement de neurites. En outre, les dispositifs microfluidiques dotés de canaux à l'échelle du micron et de volumes de microlitres et de nanolitres de milieu de culture cellulaire sont capables à la fois de maintenir un microenvironnement stable pour les cellules du cerveau et les circuits neuronaux et de modifier cet environnement très rapidement par un contrôle fluidique. En utilisant la réponse des cellules neuronales à des stimuli chimiques ou physiques, le changement de la concentration moléculaire locale peut être surveillé par des capteurs contrôlés avec précision qui s'interfacent avec des puces microfluidiques et certains indicateurs de fluorescence. Les changements morphologiques des neurites, du soma et des noyaux, ainsi que les signaux cytosoliques peuvent également être observés. Cela permet non seulement d'étudier en temps réel les réponses déclenchées par les changements du microenvironnement, mais aussi d'étudier les mécanismes moléculaires des maladies neurodégénératives.

Les travaux précurseurs de Taylor et al. ont décrit l'utilisation de la microfluidique pour construire un réseau bionodal. Mais la construction de réseaux multi-nodaux reste un défi dans ce domaine. La connectomique cérébrale a récemment révélé la relation entre la structure topologique et la fonction du cerveau. Cela a inspiré notre équipe à combiner les techniques microfluidiques compartimentées - qui peuvent contrôler la croissance directionnelle des axones - avec les principes topologiques de la connectomique cérébrale pour concevoir des réseaux neuronaux. Cette conception des réseaux neuronaux basée sur la topologie ressemble davantage aux connexions entre les neurones dans le cerveau réel et peut être utilisée pour étudier comment, par exemple, les agrégats d'α-synucléine et de b-amyloïde, qui sont associés respectivement aux maladies de Parkinson et d'Alzheimer, se propagent dans les réseaux neuronaux.

En général, le cerveau sur puce émergent est une nouvelle classe technologique prometteuse parmi les modèles actuels de multiples maladies neurologiques.

Dans le premier chapitre, cette thèse présente les connaissances de base et les avancées récentes dans ce domaine. Le deuxième chapitre traite de certaines connaissances neurobiologiques de base et des concepts fondamentaux de la connectomique cérébrale, la base théorique de la construction in vitro de réseaux neuronaux. Elle présente les caractéristiques biologiques des maladies neurodégénératives et certains points de vue dominants sur leur pathogenèse, puis donne un aperçu de certains modèles d'étude des troubles neurologiques. Dans la troisième section de ce chapitre, la partie consacrée aux puces cérébrales se concentre d'abord sur le processus de fabrication des puces microfluidiques et des matériaux connexes, ainsi que sur les bases de la survie des cellules dans la puce. Elle examine et discute les modèles construits ces dernières années à l'aide de puces microfluidiques pour étudier les maladies neurologiques.

Le chapitre 2 présente une plate-forme pour la reconstruction in vitro de réseaux neuronaux directionnels à deux nœuds avec une connectivité synaptique contrôlée. Le processus de fabrication fait appel à la technique du "patterning in-mold". Cela permet d'appliquer des contraintes chimiques et mécaniques aux neurones en croissance. Cette plateforme permet de micropositionner des groupes de neurones dans des puces microfluidiques et de guider les axones de manière directionnelle pour obtenir une connectivité fonctionnelle réglable.

Dans le chapitre 3, en utilisant le même procédé de microfabrication, j'ai exploré la faisabilité de reconstruire des réseaux multi-nodaux complexes dans une plateforme microfluidique compartimentée. Pour atteindre ce but, j'ai étudié différents paramètres pour optimiser la survie des réseaux complexes in vitro.

Dans le chapitre 4, en utilisant les deux plateformes que j'ai développées, j'étudie la propagation trans neuronale des agrégats d'alpha-Synucléine que l'on propose d'être à l'origine de l'initiation de processus neurodégénératifs tels que la maladie de Parkinson.

Dans le chapitre 5, sur la base de quelques expériences technologiques finales, je présente quelques perspectives technologiques pour optimiser davantage la reconstruction de réseaux complexes in vitro.

Dans le chapitre 6, je discute des divers aspects qui sous-tendent la microfabrication de plates-formes pour manipuler les neurones et je propose quelques perspectives pour l'avenir des approches de type "cerveau sur puce".

En résumé, le cerveau sur puce permet de construire in vitro un modèle pour l'étude des maladies. En construisant un cerveau sur une puce pour les maladies neurologiques, cette puce apportera de nouvelles opportunités pour la découverte de nouvelles cibles médicamenteuses et le criblage de médicaments dans le système nerveux. À l'avenir, le criblage de médicaments à haut débit sur une puce réduira considérablement le temps nécessaire pour tester l'activité des molécules médicamenteuses, ce qui raccourcira la durée du cycle de développement de nouveaux médicaments et remplacera plus efficacement les expériences sur les animaux pour tester l'activité des médicaments.

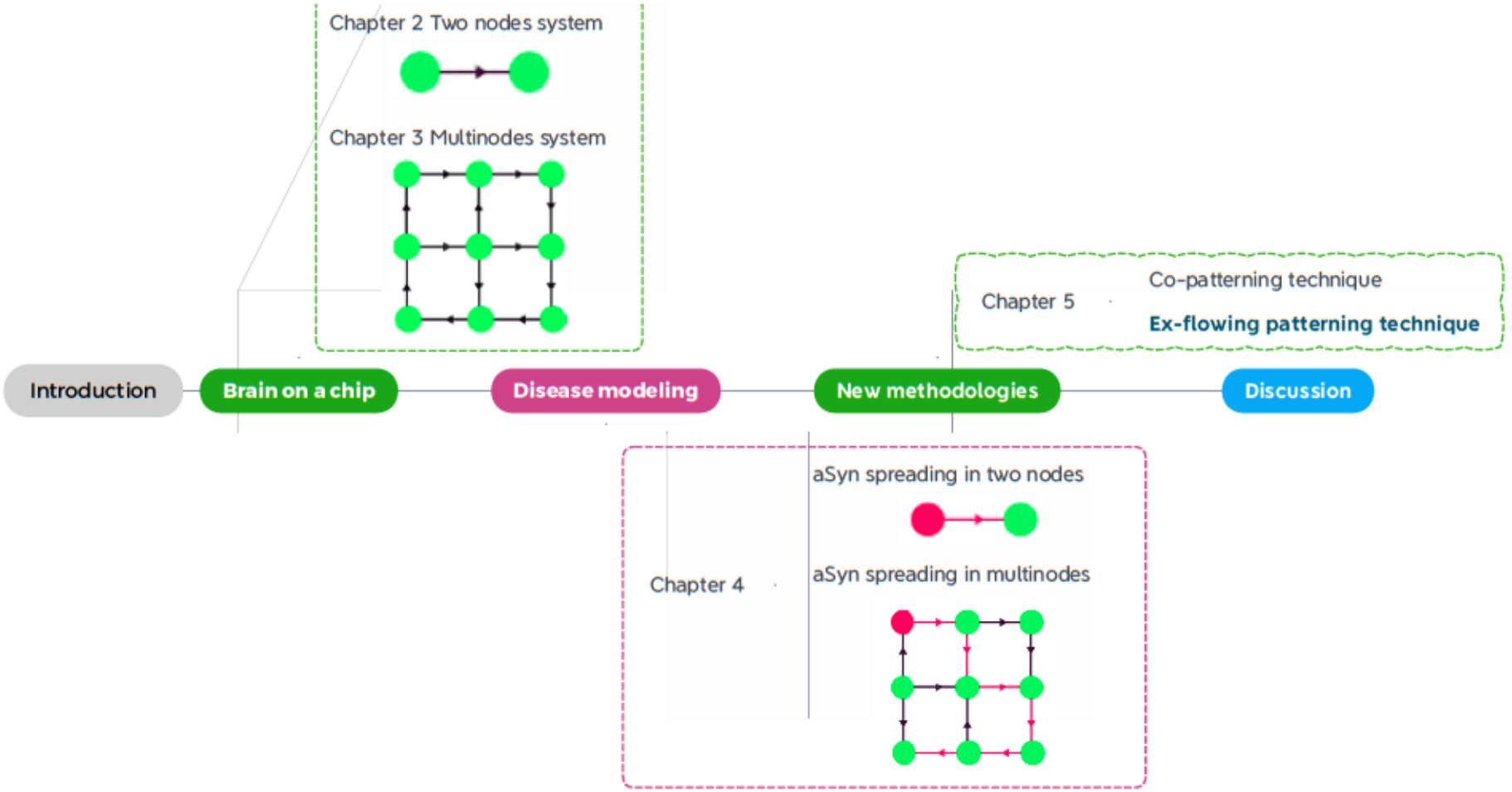
Chapter 2 Two nodes system
Chapter 3 Multinodes system
Chapter 5
Co-patterning technique
Ex-flowing patterning technique
Introduction
Brain on a chip
Disease modeling
New methodologies
Discussion
aSyn spreading in two nodes
Chapter 4
aSyn spreading in multinodes

Table of contents

Abbreviation

AD	Alzheimer's disease
ALS	amyotrophic lateral sclerosis
APP	amyloid precursor protein
Aβ	amyloid beta
BAD	bcl-2-associated death promoter
BiC	bicuculline
BSA	bovine serum albumin
cAMP	cyclic adenosine mono-phosphate
CaN	calcineurin
CNS	central nervous system
CREB	cAMP response element binding protein
DMEM	Dulbecco's modified eagle medium
ECM	extracellular matrix
ERK	extracellular signal-regulated kinase
ESCs	embryonic stem cells
FDA	fluorescein diacetate
FITC	fluorescein isothiocyanate
GAPDH	glyceraldehyde-3-phosphate dehydrogenase
GBSS	Gey's balanced salt solution
HD	Huntington's disease
hiPSCs	human-induced pluripotent stem cells
IA	itaconic acid
JNK	c-Jun N-terminal kinase
MAP2	anti-microtubule associated protein
MAPK	mitogen-activated protein kinase
MRI	magnetic resonance imaging
NDDs:	neurodegenerative diseases
NFT	neurofibrillary tangle
NSCs	neural stem cells
OoC	Organ-on-Chip
OS	oxidative stress
PAAM	polyacrylamide
PC	polycarbonate
PD	Parkinson's disease
PDMS	polydimethylsiloxane

PEG	poly(ethylene) glycol
PET	positron emission tomography
PFA	paraformaldehyde
PFFs	pre-formed α-synuclein fibrils
PHEMA	polyhydroxy ethyl methacrylate
PMMA	polymethylmethacrylate
PVA	polyvinyl alcohol
QA	quinolinic acid
Re	Reynolds number
SCA	spinocerebellar ataxia
SMAC	second mitochondrial activator of caspases
SOD	superoxide dismutase.
TTX	Tetrodotoxin
μCP	microcontact printing

1 Introduction

1.1 Overview

Human beings have always struggled with various diseases, among which diseases related to the nervous system. Specifically neurodegenerative diseases such as Alzheimer, Parkinson or Huntington Diseases targets specific brain areas and promotes chronic and progressive degeneration leading to impaired quality of life and reduced longevity. However, until now, despites several decades of active research, no effective method allows to prevent or cure these degenerative syndromes.

From a historical and cultural perspective, human ingenuity has promoted western medicine based on anatomy, and oriental medicine based on meridian doctrine. Nowadays, human beings mainly rely on surgery, various drugs and adjunctive therapy or interventional medical devices as the main way to fight against diseases. In the near future, there is a good possibility that advanced technologies based on genetic engineering, artificial organs, etc. will enter the clinic as new therapeutic tools. From an historical point of view, human therapeutic yet mostly rely on small organic compound therapeutics the drug development field which accounts for vast majority of available operational therapies. In the process of drug development, the discovery and synthesis of a new drug molecule is the first step, followed by rigorous drug activity screening and pharmaceutical formulation. Normally, after the biologically active molecules (lead compounds or hit) are tested in animals, about 90% of the drugs fails in clinical trials, while more than half of the remaining 10% of the drugs still fail in phase III clinical trials. While this evidence a gap between theoretical concepts underlying target selection / drug development and therapeutical efficacy, this also question the relevance of both cell culture and animal models used in the preclinical studies. Using of animal models, which permitted tremendous advances in both basic and applied biology, is now questioned both at the ethical and operational level. Therefore, alternative technologies that could replace or reduce animal experiments, would allow shortening of screening time, improving efficiency thanks to human stem

cell processes allowing to create human based models, the time and money cost for new drug development, while it can reduce to sacrifice the animals which are living for drug activity screening.

In parallel to human stem cell research field, microfluidics has developed rapidly in the biology and chemistry field. Microfluidic is rapidly pervading analytical chemistry and biological testing fields, as a fast, miniaturized easy to handle way to use conventional laboratory techniques in small portable "lab on chip" devices. It is a technology that is based on the manipulation of fluids in the micron-scale space. Similarly, 20 years of research have now proved that conventional cell culture dishes can be advantageously replaced by miniaturized cell culture devices that allow controlling cell microenvironment at an unprecedented level. Thanks to their inherent properties, these technologies allow controlled reconstruction of co-cultures an approach that paves the way for the rational design of minimalistic "organ-on-a-chip". Microfluidic devices for cell culture contains micron scaled cell culture chambers that allows controlled and continuous perfusion of liquids to renew media, build shaped fluidic gradients, model pulsed flow chambers. Another aspect stems in the possibility to connect in both 2D and 3D manners several chambers to control cell/cell interactions and implement micro technological cues inside the cell culture chambers such as rational mechanical constrains, biochemical or electronic stimulating and sensing devices. It is therefore a cell culture microengineering technology with a high potential for mimicking and reconstructing the physiological functions of human organs. Theoretically, organ-on-a-chip-based model have many advantages compared with the traditional animal models. First of all, the tissue units constructed by can be constructed out of human-derived stem cells. The organ-on-a-chip can achieve a precise control in scale, which can enable studying the quantitative pharmacology, measuring pharmacokinetic parameters such as drug absorption, distribution, metabolism and elimination, and has an irreplaceable advantage in toxicity estimation.

My PhD thesis is rooted in the challenge of developing relevant brain on chip

platform. Due to intrinsic brain complexity with neuronal networks exhibiting ordered topologies that ranges from the cm scale (axons) to nanometric ones (synapses) building brain on chips platforms is a long term run that requires validation of "modules" that permit to capture specific properties of brain networks. In the following chapter, I will therefore introduce some basic knowledge of the nervous system and will intersperse it with the current hypothesis about the mechanisms of neurodegenerative diseases to finally present an overview of current technologies used for brain on chip platforms reconstructions.

1.2 Nervous system

The organism is composed of different organs and systems, each of which having its specific functions. These functional activities are not isolated but interact and coordinate with each other. When the body is in the process of responding to the continuous changes in the external environment, the internal environment is also constantly changing. It is through its regulatory system that the body responds to external environmental changes to restore the stability of the internal environment of the body to survive. The nervous system is an important body system to achieve this regulatory function. When the nervous system degenerates and develops pathologic lesions, it will cause impairment in the body's response to the external environment.

The nervous system is a large and complex system composed of numerous nerve cells that liaise and regulate the function of the body's systems and organs in response to changes in the internal and external environment. Its function is mainly to transmit information from afferent fibers to the brain and spinal cord, the nerve centers. After complex processing in the brain and spinal cord, the information is transformed into efferent signals, which are transmitted via efferent fibers to all systems and organs of the body to regulate their functional activities. The brain, as an important organ for information processing, also possesses advanced functions of memory and learning, and therefore its study implies many fields outside neurobiology such as cognitive

neuroscience. However, in this thesis, I will focus only on the basic biological issues related to neurodegenerative diseases are. This subsection introduces only some basic neurobiological knowledge at the cellular and molecular level, which will help interdisciplinary readers to understand this field, the readers who already have the basic knowledge can directly jump to next section.

1.2.1 The neurons and glial cells in the nervous system

The nervous system is mainly composed of neurons and glial cells. In the late 19th century, the German scientist Franz Nissl used what is nowadays called the Nissl staining to distinguish between neurons and glial cells. Subsequently, the Italian scientist Camillo Golgi used silver-stained brain sections to demonstrate the special structure of neurons. Neurons, like other cells, are composed of a nucleus, cytoplasm and cell membrane. The nucleus is a nearly spheric organelle wrapped by a nuclear membrane, located within the cell body, and contains the chromosomes that hold genetic information. The cytoplasm around the nucleus contains the intracellular fluid rich in potassium ions, the fibrous cytoskeleton and various organelles. The cell membrane consists of a 5 nm thick lipid bilayer, inlaid with membrane proteins. The cell membrane envelops the entire neuron, separating it from the outside world. The structure of neurons is divided into the cell body, dendrites and axons.) The cell body is the main center of neuronal metabolism and is responsible for protein synthesis and energy metabolism to maintain cell survival; the dendrites are the main site where neurons receive external signals; and the axon is responsible for nerve signal transmission. In addition, distant sites of axons with mitochondria, and Golgi also can synthetize proteins.

1.2.1.1 The membranes of Neuron

The cell membrane of nerve cells, like other cells, serves as a barrier between the cell and the environment, allowing the cell to exist relatively independently of the environment. Through the cell membrane, nerve cells can obtain nutrients and excrete

metabolites; they can receive stimuli from environmental changes, generate responses, and transmit information. The molecular structure of nerve cell membranes is composed of lipids, proteins and sugars, as in most other cells. The composition of nerve cell membranes also determines their functions, including the ionic exchanges that trigger depolarization and repolarization of the cell as well as their response to various external substances.

1.2.1.2 Dendrites and axons

The dendrites are one category of outward projections and extensions of the neuronal cell body, which vary in size and shape depending on the neuronal species. The boundary between dendrites and the cell body is sometimes difficult to define. Organelles such as the rough endoplasmic reticulum, free ribosomes and Golgi complex are visible at the proximal end of the dendrites, and most organelles can enter the dendrites from the cell body. A neuron can have multiple dendrites, and the dendrites can regenerate new branches as they extend outward. The morphology of dendrites is maintained by adhesion molecules on the dendritic surface and the cytoskeleton inside the cell. Dendrites can form synapses with the axon terminals of other neurons to receive signal afferents, and are the main site where neurons receive signal transducers. The dendritic spine, which has a variety of receptors and ion channels, is an important site for dendritic synapse formation.

Each neuron has long, thin, uniformly thick and thin axons with few branches and smooth surfaces. The length of axons varies among different classes of neurons, with some axons reaching up to 1 m and others less than 1 mm. Some axons branch during extension and these branches are called axon collaterals. The axon collateral is often perpendicularly emanating from the axon at a distance from the cell body and is essentially the same thickness as the main stem. However, axons contain a large amount of cytoskeleton elements such as microtubules and neurofilaments arranged in parallel, and these filaments play an important role in the formation and maintenance of axons

as well as in the transport of axonal material.

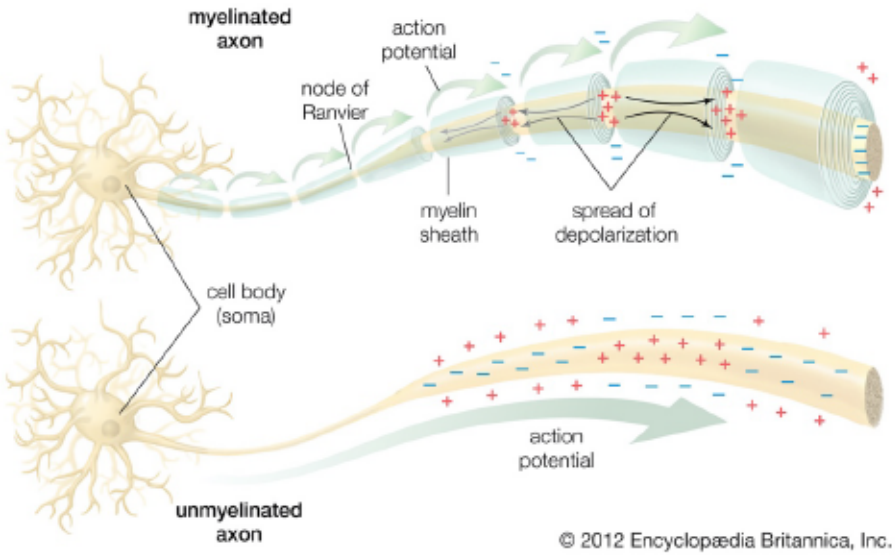

Figure 1. The conduction of the action potential in myelinated axon and unmyelinated axon (copyright: Encyclopædia Britannica, Inc.)

The impulses generated by neurons are called action potentials, which propagate along the axons. Axons can be wrapped into a myelin sheath. Myelinated axons from the central nervous system are surrounded by myelin sheaths formed by the cell membranes of oligodendrocyte or oligodendroglia cells, while the axons from the peripheral nervous system are surrounded by myelin sheaths formed by the cell membranes of Schwann cells. The myelin is not completely wrapped around the axon, but rather in segments. The area between the myelin sheaths where the axon is exposed is called the node of Ranvier, and the cell membrane of the node is rich in voltage-gated sodium channels and rich in intra-membranous particles. The junction is easily activated and action potentials are regenerated here. Action potentials with nerve signals are transmitted jumpily in the myelinated fibers, so that they are transmitted faster in the myelinated fibers than in the unmyelinated fibers. In general, local neurons with shorter axons, such as inhibitory interneurons, have axons that are not myelinated, whereas neurons connecting different regions of the nervous system have longer axons that are myelinated. The end of the axon is enlarged and is called the axon terminal. The axon terminal often gives off many tiny branches that are not covered by myelin,

called the terminal arbor. These axon terminals form synaptic connections with receiving neurons or effector cells (e.g., muscle cells and glandular cells) for intercellular communication.

1.2.1.3 The structure of chemical synapse

The site of information exchange between axon terminals and other neurons or effector cells is called the synapse. The synapse consists of the presynaptic element, which is the axon terminal of the presynaptic neuron, the synaptic cleft between neurons, and the postsynaptic element of the postsynaptic neuron. Depending on the structural and electrophysiological properties of synapses, there are two main types: chemical synapse and electrical synapse.

Chemical synapses consist of a specialized thickened area in the cell membrane of the corresponding part of the two neurons involved in synapse formation and the gap between them. When information is transmitted from one neuron to another, the presynaptic component releases neurotransmitters, which act on neurotransmitter receptors in the postsynaptic component to transmit the signal to the postsynaptic neuron.

Synapses are structures that are specialized for neuronal cell membranes. Each synapse consists of a presynaptic and a postsynaptic structure, which can originate from the same neuron, and form an autapse. Or from different neurons, which form synaptic connections between neurons and thus transmit information. A typical synapse has a synaptic vesicle containing a neurotransmitter at the presynaptic terminal, and the vesicle is in close contact with the presynaptic membrane. Immediately adjacent to the presynaptic membrane is the postsynaptic membrane, which appears as a thickened electron-dense band under electron microscopy, and a special structured postsynaptic dense band formed by a dense arrangement of neurotransmitter receptors and backbone proteins. Synaptic substance transport plays an important role in the development and maturation of synapses. For example, presynaptic structures such as synaptic vesicles,

active zone precursor, mitochondria, and other proteins related to synaptic vesicle fusion and regulation are transported along the microtubule track system by motor proteins such as kinesin. After synthesis in the cytosol, presynaptic membrane proteins are assembled into material transport vesicles. These vesicle structures, which vary in size and shape, are transported along the microtubules to synaptic sites. After reaching the synaptic terminal, these transport vesicles fuse with the presynaptic membrane and release the transport material to build an active zone or reorganize synaptic vesicles. It is only the mature presynaptic endings that are able to complete the process of preparing synaptic vesicles and fusing them with calcium ions (Ca^{2+}) and releasing neurotransmitters. At the same time, this continuous transport process is an important basis for synaptic structural diversity (heterogeneity) and synaptic functional plasticity.

1.2.1.4 The cytoskeleton

The translocation and localization of almost all organelles and biomolecules within neuronal cells are regulated by the cytoskeleton system, including microtubules, microfilaments, and neurofilaments. The cytoskeleton is a complex system of fibrous network structures within cells and is an important organizer of cell structure and function. In neurons, cytoskeletal fibers and their associated proteins form the cytoskeletal system, which accounts for 25% of all neuronal proteins. The cytoskeletal system is the major determinant of cell morphology and the distribution of organelles in the cytoplasm. Neurons are a highly differentiated class of cells with diverse morphologies of cell bodies, dendrites and axons. The cytoskeleton plays a very important role in the formation and maintenance of neuronal morphology. Neurons contain three different cytoskeletal systems: microtubule, actin and neurofilament, which are assembled by different protein subunits. These three cytoskeletal proteins are under dynamic changes and are involved in the maintenance and alteration of neuronal morphology, the alteration of cell membrane shape and secretory activities, and the translocation and regionalization of organelles and proteins, and have important roles in the maintenance of neuronal structure and function. Microtubules are polar hollow

tubular fibers with a diameter of about 24 nm. Microtubules tend to be long fiber-like in the cell and run throughout the interior of the neuron, serving not only for mechanical support but also for transport, localization and organization. Currently, two types of microtubule-related molecular motors have been identified: kinesin, which moves from the negative pole of microtubules to the positive pole, and dynein, which moves from the positive pole of microtubules to the negative pole. Microtubules play an important role in the formation and maintenance of neuronal morphology, the formation and extension of neural protrusions, and axoplasmic transport. Actin maintains and change the shape of the cell membrane, participate in the formation and maintenance of specialized structures of the presynaptic and postsynaptic membranes, mediate the formation and extension of neural protrusions, and participate in important physiological processes such as vesicle secretion. The neurofilament is the intermediate filament in neurons, with a diameter of about 10 nm. In axons, the neurofilaments and microtubules are the most abundant component of the cytoskeleton in axons, which plays an important role in maintaining the morphology of axons.

1.2.1.5 The classification of neurons

Neuronal cells are diverse in shape and function. According to their location, there are two major categories: central neurons and peripheral neurons. The central neurons can be classified into for instance cortical neurons, hippocampal neurons, and cerebellar neurons according to the brain region in which they are located. There are different classifications by neuronal morphology. Neurons can be categorized into unipolar neuron, bipolar neuron, pseudo-unipolar neuron, and multipolar neuron according to their morphology. The unipolar neuron is the simplest neuron because it only extends from the cell body with a single protrusion. This protrusion can give rise to different branches, some of which act as axons and some of which function as dendrites. In the non-vertebrate nervous system, unipolar neurons predominate, whereas in vertebrates, unipolar neurons are found only in the autonomic nervous system. Bipolar neurons contain two protrusions, a dendrite, which serves as a signal-receiving site, and an axon,

which serves as a signal-sending site. The retinal neurons are typical bipolar neurons. The multipolar neuron is the most dominant neuron type in the mammalian nervous system. It has one axon and multiple dendrites. Such as motor neurons in the spinal cord, pyramidal cells in the hippocampus, and Purkinje cells in the cerebellum all are typical multipolar neurons.

1.2.1.6 Glial cells

There is another type of cells in the brain, glial cells, they are involved in the formation of the blood-brain barrier and myelin structures, and have a role in nutrition, support and protection of neurons. It is involved in mediating the growth of synapses and their excitability, and has an important influence on the development of the nervous system. And it mediates the neuroimmune response, participates in pain response, promotes the recycling of neurotransmitters, maintains the dynamic balance of ions, and participates in higher functions of the brain such as cognition and memory. It can be said that with the deepening of neurobiological research, not only the glial cells are found to have multiple functions, but also different types of glial cells are found to have their own unique functions.

Glial cells can be classified into two types: macroglia and microglia. Macroglia are found in both the central and peripheral nervous systems, with astrocytes and oligodendrocytes in the central nervous system and Schwann and satellite cells in the peripheral nervous system. The most numerous of these are astrocytes, which are named for their irregular star-shaped. The number of astrocytes accounts for about half of all neuroglia, and is the most numerous, widely distributed, and voluminous type of neuroglia. Astrocytes can be differentiated from cells in the ventricular zone (VZ) of the neuroepithelium during embryonic development, or from immature cells in the subventricular zone (SVZ) that migrate to the gray or white matter during the perinatal stage. During the developmental stage of the CNS, some glial cells can differentiate into neurons [1]. At the end of neuronal migration, some undifferentiated glial cells

can be transformed into astrocytes. The cytoplasm of astrocytes contains organelles such as rough endoplasmic reticulum, free ribosomes, mitochondria and Golgi complexes, but fewer than neurons, so they cannot be stained with Nissl stain. Astrocytes can express a variety of cell membrane proteins, including ion channel proteins, receptor proteins and transporter proteins. These membrane proteins are closely related to the function of astrocytes. There are abundant gap junctions between astrocytes that allow the passage of inorganic ions and some organic molecules of small relative molecular mass. It is the connexin proteins that are involved in the formation of astrocyte gap junctions. Gap junctions have a role in determining cell phenotype and limiting cell proliferation, thus affecting neural development. There is a two-way information exchange (cross-talk) between neurons and astrocytes, resulting in the concept of "tripartite synapse". The tripartite synapse consists of a presynaptic component, a postsynaptic component, and the protrusions of parasynaptic astrocytes, which reach out to and wrap around the synapse between neurons so that neurons can activate astrocytes by releasing neurotransmitters. The astrocytes can also release gliotransmitters, which provide feedback to neurons.

In the central nervous system, there is an important physiological barrier between the extracellular fluid of the brain and the blood circulation system - the blood brain barrier (BBB). The function of the blood brain barrier is to ensure the stability of the internal environment of the brain tissue from foreign substances (microorganisms, toxins, etc.) from the blood and from hormonal influences from other parts of the body, in order to facilitate the activities of the central nervous system. Among other things, astrocytes are also involved in constituting the blood-brain barrier.

Microglia are a relatively small type of glial cell in the CNS. The number of microglia is small, accounting for 5%-20% of all glial cells. Microglia are distributed in all parts of the brain and are five times more numerous in the gray matter than in the white matter. There are more microglia in the hippocampus, olfactory lobes and basal ganglia than in the thalamus and hypothalamus, and the least in the brainstem and

cerebellum. Microglia are phagocytes present in the brain, belonging to the mononuclear phagocyte family, and are widely considered to be the main immune effector cells within the CNS. In the presence of inflammatory stimuli, their antigenicity is enhanced, their morphology is stretched, and they are functionally active. Microglia are the main source of cytokines within the nervous system as well as the main target cells for their action and play an important role in the neuroimmune and inflammatory response. Microglia are involved in the development of neurological diseases such as Alzheimer's disease, Parkinson's disease, human immunodeficiency virus (HIV) encephalopathy, and multiple sclerosis [2, 3]. Microglia are also one of the major components of amyloid plaques, a characteristic feature of Alzheimer's disease, and together with astrocytes they participate in the neuroinflammatory pathology of Alzheimer's disease. Microglia have a dual role in Alzheimer's disease, both in triggering neuroinflammatory responses and in phagocytic ally removing damaged neurons and abnormal metabolites [4, 5]. In Parkinson's disease, microglia are not simply "reactive proliferators", but are also involved in the development and progression of Parkinson's disease [6-8]. Therefore, the function and role of glial cells cannot be ignored.

1.2.2 The transportation of physiological materials/signals in the nervous system

1.2.2.1 The transportation inside neurons - Axoplasmic transport

Among many neurons with long axons, the axon accounts for most of the total cell volume. Although most of protein synthesis is performed in the cell body, local synthesis exists in axon terminals. In addition, organelles such as mitochondria, have to be transported from the cell body to the axon terminal. This is known as anterograde axonal transport. Therefore, neurons must transport proteins which are synthesized in the cell body to the axon. Also, some organelles that are needed for axon terminals, such as mitochondria, have to be transported from the cell body to the axon terminal

and this is known as anterograde axonal transport. The opposite is retrograde axonal transport, for example, the transport of some endosomes from the axon terminal to the cell body (Figure 2) [9]. The transport of these substances in the axon is collectively referred to as axonal transport or axoplasmic transport. The speed of axoplasmic transport can be very variable, as when transporting some organelles, molecular motor kinesins can bind to secretory vesicles, synaptic vesicle precursors, mitochondria, and large dense-core vesicles which contain neurotransmitters, thus enabling a rapid anterograde axonal transport along microtubules. While transporting endosomes and vesicles from the axon terminal to soma, the cytoplasmic dynein will act as a transport carrier, which can undergo a rapid retrograde transport. Others, such as cytoplasmic proteins that are not assembled into vesicles, will be transported more slowly. If the axoplasmic transport is interrupted, it can lead the axonal disfunction.

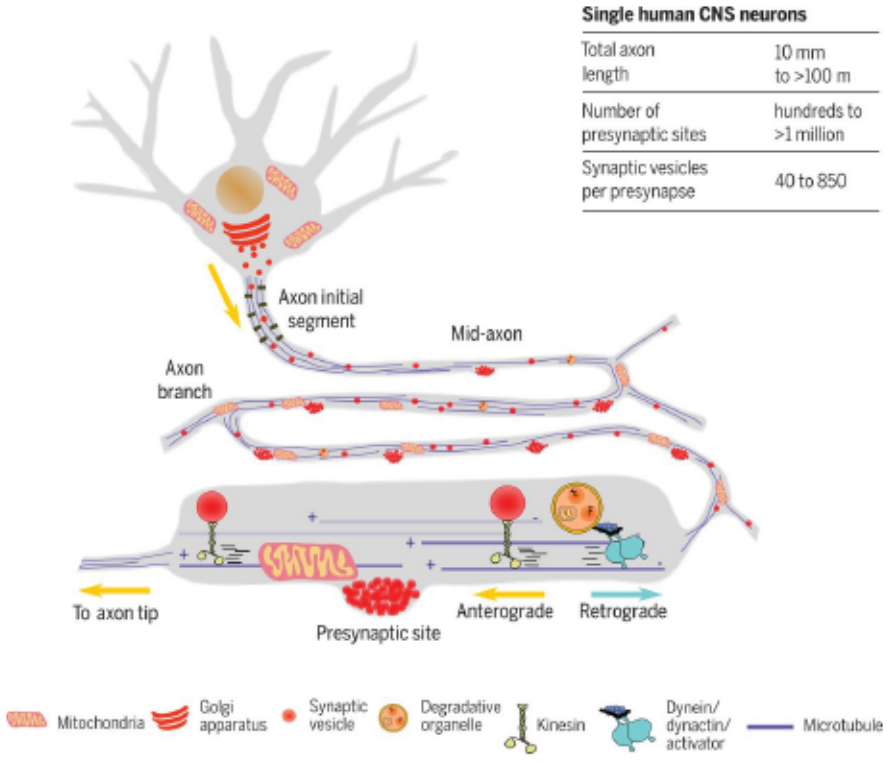

Figure 2. Axoplasmic transport. (Guedes-Dias, 2019)

1.2.2.2 Axonal Transport and Neurodegenerative Diseases

The proper functioning of axonal transport is the basis for enabling neurons to work properly. However, it is clearly observed in some diseases [10-12] that axonal

transport is damaged and the mechanisms inferred from the literature [13, 14] are: motor molecular damaged, microtubule disruption, mitochondrial damage, transported material destruction, etc. Microtubules act as rails in axonal transport, while kinesins are like carrier bins on the rails, mitochondria are the source of energy, and the transported materials are the cargos, any damage to one of these conditions will lead to defects of axonal transport. As mentioned above, kinesins are mainly transported in anterograde on the microtubules， towards the plus ends of the microtubules, while the dynein is opposite. The structures of the two motor proteins are shown in the figure (Figure 3a). Mutant presenilin-induced phosphorylation of kinesin light chain by GSK3β disrupts the binding of kinesin to vesicles and can inhibit transport of vesicles to axon terminals[15, 16]. And the kinesin heavy chain can also be phosphorylated and thus block the binding of motor proteins to microtubules (Figure 3). Besides, regulation and disruption of motor-cargo interaction may disrupt axonal transport in a number of neurodegenerative diseases [9, 17].

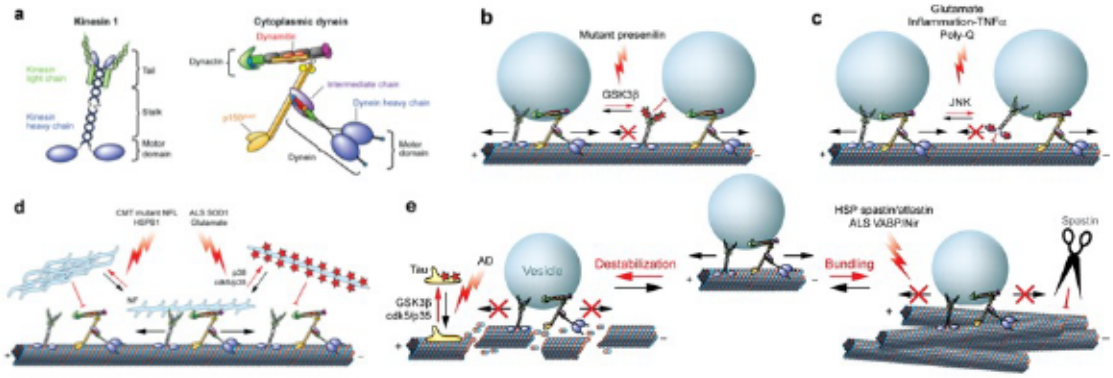

Figure 3. Mechanisms of axonal transport defects: molecular motors, cargoes and microtubules damaged. (Modified based on Kurt J. De Vos, 2008)

Mitochondria use oxidative phosphorylation to produce ATP, but as a byproduct it can produce toxic reactive oxygen species (ROS) [18]. These ROS damage many cellular components, but also damage mitochondria and their DNA. Mitochondria accumulate mutations/damage during their lifetime, which can lead to a decrease in function with aging. Mitochondrial dysfunction may affect axonal transport in at least two ways (Figure 4). First, the anterograde transport of mitochondria and vesicles in

axons is inhibited. Second, the resulting decrease in mitochondria in the axon may reduce the supply of ATP to the molecular motor, resulting in reduced anterograde and retrograde movement of other axoplasmic cargoes. This mitochondrial dysfunction may be part of a vicious cycle mechanism that ultimately leads to axonal death [9, 17]. Mitochondrial damage can be seen in many neurodegenerative diseases. For examples, in Alzheimer's disease, mitochondria are the target of Aβ damage in Alzheimer's disease, and Aβ itself can disrupt the transport of multiple cargoes, as well as mitochondria. [19, 20] The disruption of APP anterograde transport can increase Aβ generation [21], and a variety of Alzheimer's disease-related lesions are now known to impair axonal transport. These damage include changed phosphorylation of KLC2 via mutant presenilin to release cargoes which is motor damaged, and the mutant tau can block the kinesin binding to microtubules, and toxic Aβ can damage mitochondria [22, 23].

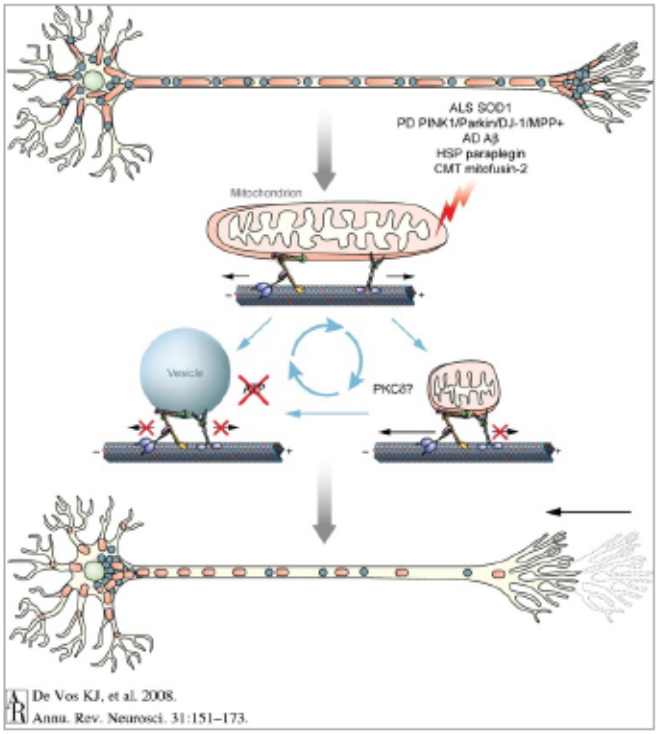

Figure 4. Alteration of Mitochondrial transport are linked to mitochondrial damage (Copyright: Kurt J. De Vos, 2008)

1.2.2.3 The exchange of materials between cells and the environment

The transport of substances inside neurons is mainly by axoplasmic transport, while the exchange of substances such as various soluble nutrients and metabolites

between neurons and the extracellular matrix is dependent on the passive transport, active transport, and vesicular transport which consists of endocytosis and pinocytosis.

Passive transport is the process that allows the molecules on both sides of the cell membrane to cross the membrane via an electrochemical gradient. The small lipid-soluble substances pass directly through the cell membrane following its concentration difference or potential difference. For some non-lipid-soluble or very small lipid-soluble small molecules such as Na^+, K^+, Ca^{2+}, etc., requiring some special proteins on the membrane, which are carriers and ion channels. These proteins are also called Na^+ channels, K^+ channels, Ca^{2+} channels, and they can assist the ions moving from the high concentration to low concentration side. The selectivity of channel proteins for ions is mainly determined by the size of the aqueous pore and the charge of the pore wall when the channel (gate) opens (activation) and closes (inactivation).

Active transport is the process by which nerve cells transport non-lipid-soluble substances across membranes against an electrochemical gradient through an energy-consuming process with the assistance of some functionally specialized protein in the cell membrane, like the sodium-potassium pump, calcium pumps and hydrogen pumps.

Vesicular transport is the main way in which some large molecules enter and exit the cell. The process of exocytosis is the transport of large molecules or clumps of substances from the soma to the extracellular matrix. When some specific chemical signal or the potential changed, it can cause the Ca^{2+} channels opening, then generate Ca^{2+} influx. The Ca^{2+} influx can trigger a series of sequential reactions such as translocation, targeting, membrane melting and breaking of vesicles, resulting in the release of all vesicle components into the extracellular matrix. Furthermore, the inward flow of Ca^{2+} in some cells can also trigger the release of Ca^{2+} from intracellular Ca^{2+} reservoirs. The vesicle contents complete the exocytosis process with a quantum release, that is a single exocytosis can release all the substance of that vesicle. Endocytosis is the opposite of exocytosis. Some substance in the extracellular matrix contacts with the

cell membrane, causing an invagination of the cell membrane there and wrapping the substance, which then splits with the plasma membrane structure and enters the cell plasma together. In addition, there is a receptor in the cell membrane that mediates the process of endocytosis. This process is based on the fact that the substance is first recognized by a specific receptor on the surface of the cell membrane and binds specifically to it. The combined complexes accumulate in the coated vesicle on the cell membrane through lateral movement on the membrane surface, which leads to the depression and disconnection of the cell membrane, where the complexes wrapped in the coated vesicle form a phagocytic vesicle and enter the cytoplasm. Then the receptor is separated from the transporter. The separated receptors are finally transported to the corresponding organelles. The receptors that remain in the intracellular body are then reassociated with some of the membranous structures to form smaller recycling vesicles, which then move back to the cell membrane and fuse with them, allowing the receptors and membrane structures to be reused, a process called membrane recycling. This recycling maintains the total area of the cell membrane relatively constant and allows the corresponding receptors to be reused.

1.2.2.4 The signals/information/substances transfer from neuron to neuron

The information in our brain travels along neurons through action potentials. Action potentials travel down a single neuron cell as an electrochemical cascade, and end at the axon terminal which has vesicles filled with neurotransmitters ready to be released (Figure 5). The neurons communicate from one cell to the other through neurotransmitters. If the neurotransmitter is excitatory, the influx of positive ions will depolarize the cell body. If the neurotransmitter is inhibitory, it will hyperpolarize the cell body. The main excitatory neurotransmitter is glutamate which can trigger more action potentials, and the major inhibitory neurotransmitter is gamma-aminobutyric acid (GABA). When the neuron triggered an action potential, it will release the neurotransmitters. Most neurons tend to have only one type of neurotransmitter – either excitatory or inhibitory. They released by nearly all the inhibitory or excitatory neurons

of the brain. Other well-known neurotransmitters include dopamine, serotonin, adrenaline, and histamine are found at precise points of the brain to help aid in learning, memory, motor function, and other neurologic functions. However, a single vesicle of neurotransmitter isn't enough to depolarize the cell body. Most of the time, the post synapse needs enough vesicles to trigger an action potential.

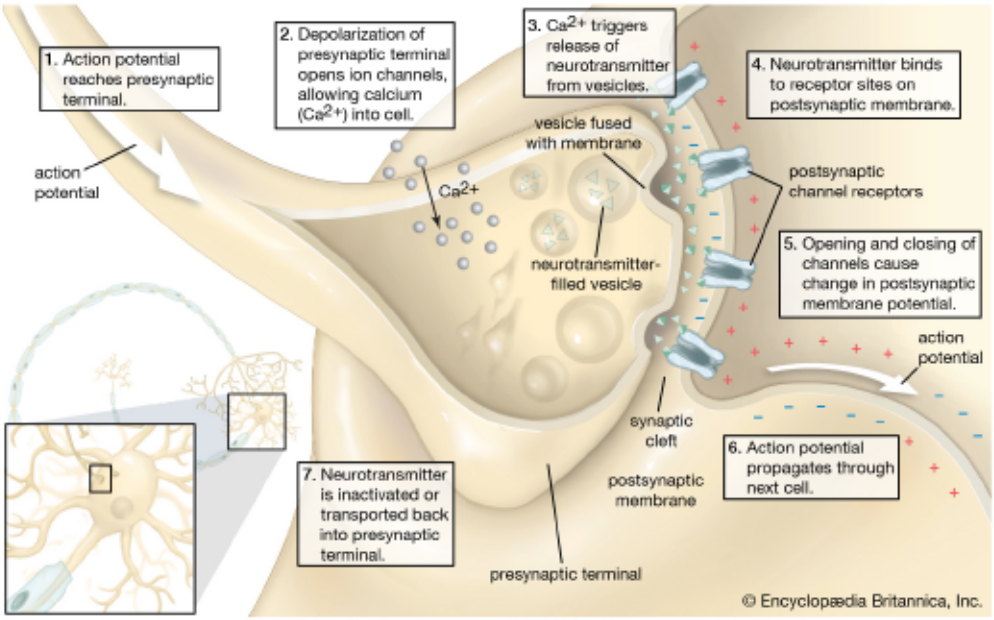

Figure 5. Action potential propagation along axons leads to local synaptic release of neurotransmitter permitting feedforward information flow in neuronal networks. (copyright: Encyclopædia Britannica, Inc.)

More recently, active and regulated modes of intercellular transfer have been described. These encompass releasing of small vesicles (EV's) such as exosomes that mostly derives from intracytoplasmic Multi vesicular Bodies, or structures such as Tunnelling nanotubes [24-27]. Although their relevance in inter - neuronal transfer is debated, EV's have been proposed to permit material (proteins, protein aggregates, RNA) exchange between axons and neighboring glial cells.

1.2.2.5 Ca^{2+} signals in the nervous system

Calcium signaling is being studied in many cells and model organisms to understand the mechanisms of many physiological processes and the pathogenesis of many diseases[28]. Ca^{2+} plays an important role in neurons, and mediates many

important physiological processes, especially in control of synaptic plasticity[29]. Ca^{2+} signaling machinery in nervous system is complex and includes various of calcium-dependent proteins as downstream targets including kinases, phosphatases, transcription factors, enzymes and proteins that induce synaptic vesicle fusion. Also have voltage-gated Ca^{2+} channels (VGCC), N-methyl-D-aspartate receptors (NMDAR), and calcium release-activated channels (CRAC) [30].

Multiple data shown that Ca^{2+} dysregulation plays an important role in neurodegeneration [31, 32]. In Alzheimer, some studies indicate that Aβ may directly bind to and modulate activity of NMDA receptors[33, 34]. The Reduction of NMDAR activity in AD may also be induced by an oxidative stress, most likely due to oxidation of extracellular NMDAR cysteine and intracellular targets such as calmodulin. The disruption of NMDAR signaling further leads to impaired synaptic plasticity, reduced LTP, enhanced LTD and synaptic loss [35, 36]. Also, Ca^{2+} dysregulation happened in PD pathology[37, 38].

There have many ways to image the calcium[39].The discovery of the method for measuring concentration of calcium ions by fluorescent Ca^{2+} indicators[40, 41]. These indicators were the result of the hybridization of highly calcium-selective chelators like EGTA or BAPTA with a fluorescent chromophore. Then after revolution, like fluo-4 [42] dye families are widely used in neuroscience duo to provide large signal-to-noise ratios. The development of the fluorescent indicators was paralleled by the new imaging instrumentation, then generate a lot of new technique and application[43, 44].

1.2.3 The structure and function of the brain

The central nervous system consists of the spinal cord in the vertebral canal and the brain in the cranial cavity. The spinal cord is located within the vertebral canal and is connected to the medulla oblongata at its upper end at the occipital bone. The interior of the spinal cord is composed of the central canal, gray matter and white matter. The gray matter is mainly composed of neuronal cell bodies, short dendrites, and glial cells.

The white matter is composed mainly of crisscrossed myelinated nerve fibers. There are 31 pairs of nerves in the spine that connect the trunk, limbs, and some internal organs and manage their activities through reflexes.

The brain is located in the cranial cavity, and the average adult brain weighs 1400 g. It has 12 pairs of cerebral nerves that connect the facial organs and some internal organs. The spinal nerves of the spinal cord and the cerebral nerves transmit information received from the outside to the brain, where it is integrated to form feelings, emotions, and feelings. The information sent from the brain to the spinal cord and cerebral nerves is mediated by the central system to accomplish movement, instinctive behavior, learning, memory creation, etc. The brain is mainly composed of the brainstem, diencephalon, cerebellum and telencephalon (Figure 6).

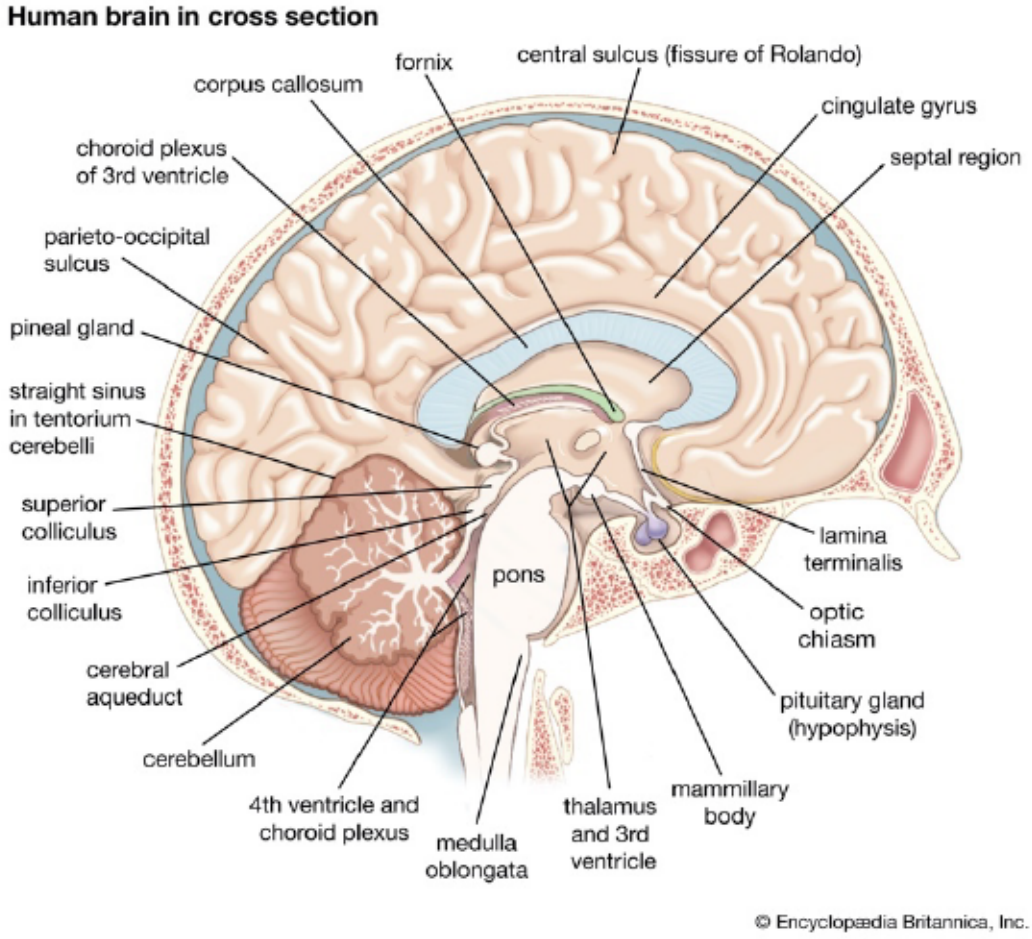

Figure 6. Medial view of the left hemisphere of the human brain. (Copyright: Encyclopædia Britannica, Inc.)

1.2.3.1 Brainstem

The brainstem consists of the medulla oblongata, pons and midbrain, which is a structure between the spinal cord and the diencephalon and is located in the anterior part of the posterior cranial fossa. The internal structure of the brainstem is more complex compared to that of the spinal cord. It can be divided into four main parts, which are gray matter, white matter, mixed gray and white matter areas and central canalicular structures. The function of the brainstem is similar to that of the spinal cord in that it has conduction and reflex functions. The conduction function of the brainstem is to conduct information from the brain, cerebellum and mesencephalon to the spinal cord with the help of its white matter, and to conduct information from the spinal cord and brainstem to the mesencephalon. Different parts of the brainstem control different reflex activities. For example, the midbrain is mainly associated with the reflex activity of the eyes. The medulla oblongata is related to the reflexes of the throat and other internal organs. The pons is associated with the facial reflexes of the head. The brainstem intervenes in reflex arcs such as pupil-to-light reflex, corneal reflex, sneezing reflex, vomiting reflex, cough reflex, etc.

1.2.3.2 Diencephalon

The diencephalon is the region of the embryonic vertebrate neural tube, it including the thalamus, hypothalamus, posterior portion of the pituitary gland, and the pineal gland. The thalamus serves as a relay center for sensory and motor impulses between the spinal cord and medulla oblongata, and the cerebrum. It recognizes sensory impulses of heat, cold, pain, pressure etc. And the hypothalamus has control centers for control of eye movement and hearing responses.

1.2.3.3 Cerebellum

The cerebellum is located in the back of the medulla oblongata and the pons. It is composed mainly of gray matter and white matter. Most of the gray matter is concentrated on the surface forming the cerebellar cortex. The white matter is located

in the deeper cortical layers. The cerebellar cortex is highly laminated and mainly composed of astrocytes, basket cells, etc. Purkinje cells, Golgi II, and granule cells. It is involved in the functions of maintenance of balance and posture, coordination of voluntary movements, motor learning and Cognition.

1.2.3.4 Telencephalon (cerebrum)

The cerebrum, located in the upper part of the mesencephalon and cerebellum, is the highest-level part of the brain and the part that accounts for the largest proportion of the brain. It is mainly composed of gray matter, white matter and the lateral ventricles within it. Most of the gray matter of the telencephalon is concentrated on the surface to form the cerebral cortex; a small portion of the matter is gathered in the deeper medulla, which forms the basal ganglia of the brain. The white matter is located deep in the cortex and is called the medulla. The telencephalon consists of two hemispheres, the left and right. The cavity inside the left and right hemispheres is the lateral ventricle. There is a deep fissure between the left and right hemispheres of the brain called the cerebral longitudinal fissure, which divides the brain into two hemispheres, the bottom of the interhemispheric fissure is a broad fiber plate connecting the two hemispheres, called the corpus callosum. Below the hemispheres and between the cerebellum and the cerebellum there is the cerebral transverse fissure.

The surface area of the human cerebral cortex is about 2200 cm^2, while the volume of the cranial cavity is limited. In order to accommodate the cortex, the cerebral cortex is concave and convex, so the surface of the cerebral hemisphere shows many sulci of different depths, and the elevation before the sulci is the cerebral gyri. In the early embryonic stage, the surface of the cerebral hemisphere is smooth, and later, due to the unbalanced development of the various areas of the cortex, the slow-developing areas are sunken in the depths, and the fast-developing areas are exposed on the surface, forming the sulcus and gyrus. The creation of the sulcus and gyrus are enlarging the surface area of the cerebral hemisphere.

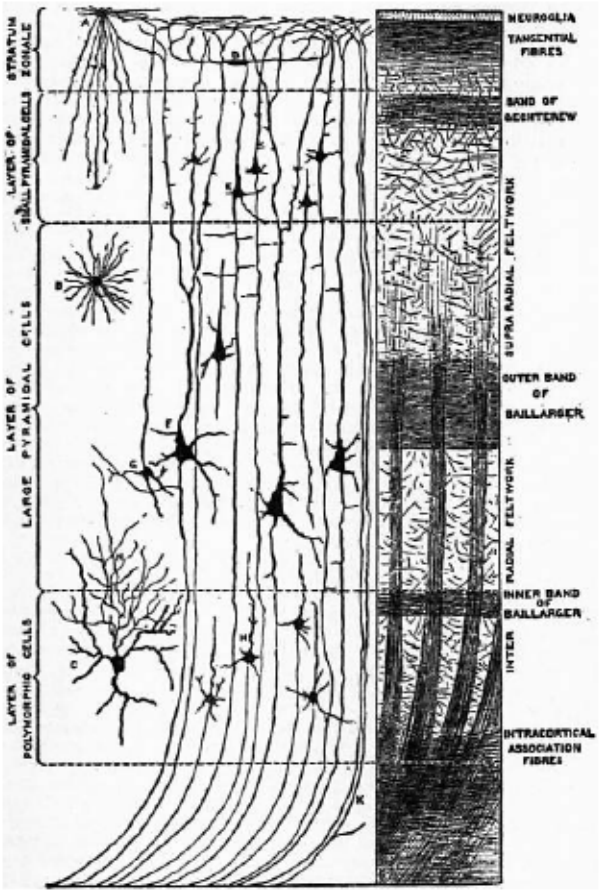

Figure 7. The neuronal layers in the Cortex
(https://fr.wikipedia.org/wiki/Fichier:EB1911_Brain_Fig._15-Cerebral_Cortex.jpg)

One third of the cerebral cortex is exposed on the surface and two thirds on the bottom and wall of the sulcus, with a thickness between 1.5 and 4.5 mm, averaging about 5 mm. The cerebral cortex is composed of a variety of neurons and glial cells, and the number of neurons is extremely large, estimated to be about 100 billion, accounting for 70% of the total number of neurons. The neurons that make up the cerebral cortex are all multipolar neurons, mainly pyramidal cells, granule cells, basket cells and spindle cells. Pyramidal cells are named after their cone-shaped cell bodies. The top of the cone faces the surface and has dendrites at the tip, while the bottom of the vesicle has long axons that reach deep into the white matter, which are projection neurons. The granule cells have polygonal or triangular shaped cell body, and the cell body is small, numerous and granular. They are a class of local neurons that participate in the formation of intracortical microcircuits. Basket cells are inhibitory GABAergic interneurons of the brain, found throughout different regions of the cortex and

cerebellum. Basket cells are multipolar GABAergic interneurons that function to make inhibitory synapses and control the overall potentials of target cells. The fusiform cell is a type of projection neuron with a small number of fusiform cells, mainly located in the deep cortical layer. The axons of these cells can arise from the trunk of the dendrites and enter the medulla, forming projection and association fibers. The nerve cells in the cerebral cortex are arranged in a hierarchical fashion. Morphologically essentially similar nerve cells aggregate into certain layers. Depending on the location, the thickness of each layer, the distribution of various cellular components and other characteristics, the cerebral cortex can be divided into many areas, for example, the frontal lobe is mainly related to random movements and higher mental activities, including somatomotor functions, intelligence and emotional and other activities. The temporal lobe has auditory, perceptual, memory and motor functions. Parietal cortex: The parietal lobe is mainly associated with general somatosensory sensations. In addition to the horizontal stratification, neurons have a very longitudinal columnar structure. Each cortical column is not preceded by distinct glial cells or fiber separations, so it is not considered a structure-based functional unit.

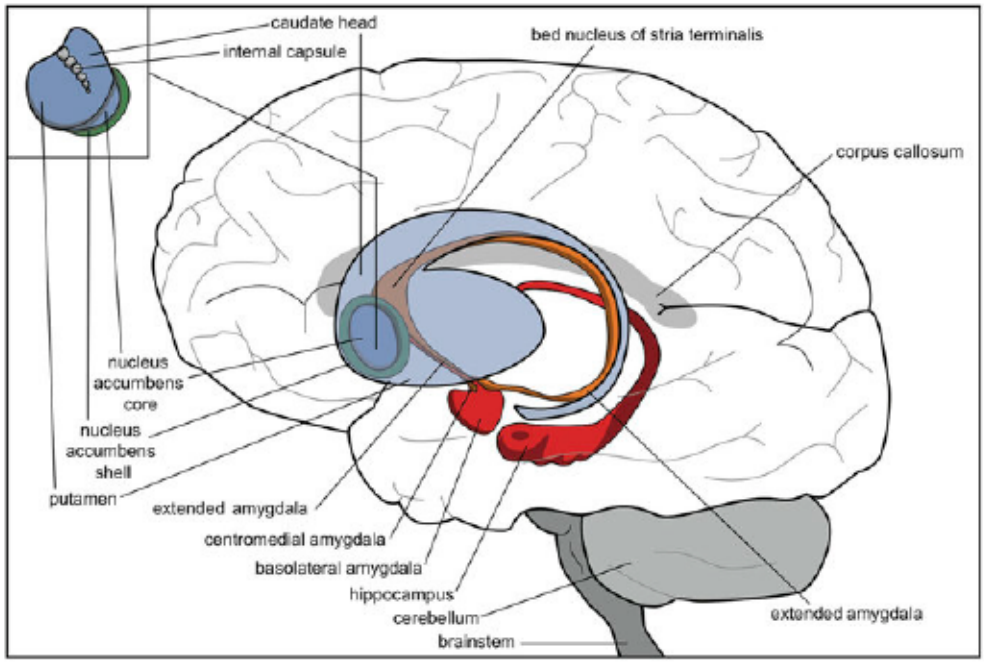

Figure 8. Human brain with striatum (blue), nuclear amygdala (orange), cortical amygdala (red), and hippocampus (red). (copyright : A. J. M. Loonen.)

The basal nucleus is the gray matter nucleus near the base of the medulla of the cerebral hemispheres and includes the amygdaloid body, caudate nucleus, and lentiform nucleus, the latter two collectively known as the corpus striatum. Although the striatum has been subordinated to the control of somatic movements in mammals due to the highly developed cerebral cortex, it still has an important role in motor regulation. In addition to motor regulation, the basal ganglia play an important role in learning, cognition, emotion and many other areas. As one of the subcortical regulators of the motor system, the basal ganglia do not directly initiate or perform movement, but rather play an integrative, optimal, and precise regulatory role, working with the cerebellum to perform motor functions in conjunction with the cortex by regulating muscle tone, modulating joint movements, and maintaining posture. They receive a large number of projections from the cortex, process the information and return it to the cortex via the thalamus. Dysfunction of the basal ganglia will produce a series of neurological disorders accompanied by motor disorders. When the striatum is damaged it leads to slowed casual movements, postural abnormalities and involuntary movements, as in Huntington's disease.

The motor function of the basal ganglia is indirectly realized through the motor-related areas of the cerebral cortex. This connection between basal ganglia circuits and the cerebral cortex can be summarized in three circuits that together form the basic structure of the basal ganglia. In the basal ganglia circuit, the striatum is the gateway to information input and the thalamus is the gateway to information output, projecting integrated nerve impulses to the cerebral motor cortex.

The three circuits are: 1) Cortical-neoportal-pallidum (internal)-thalamus a cortical circuit. 2) Cortical-neoportal-pallidum (external)-basal thalamic nucleus. 3) Cortico-neostriatal-neoplasmic-neoplasmic-thalamic-cortical circuit.

The basal ganglia circuit mediates somatic movements by participating in the planning and initiation of movements, mastery of new movements, sequencing of

movements, and motor responses to new stimulus signals. Therefore, dysfunction of the basal ganglia circuit has the potential to produce severe motor behavior deficits. Currently, there are two main clinical categories of movement disorders due to disorders of the basal ganglia circuitry. The first group is the syndrome with hypermobility and hypotonia, which can be seen in chorea, tardive dyskinesia, and lateral throwing disorder, with lesions mainly located in the striatum. The pathological damage of the disease is mainly in the basal ganglia and cerebral cortex, with the most obvious lesions in the caudate nucleus and the nucleus accumbens. The parenchymal structure of the caudate nucleus head is reduced to a thin band 2-3 mm thick, resulting in a protrusion of the lateral wall of the frontal horn of the lateral ventricle. Deformation and death of striatal neurons as well as a significant decrease in the content of the neurotransmitter GABA and its synthetase, glutamate decarboxylase, in the basal ganglia are accompanied by a decrease in choline acetylase activity and a decrease in acetylcholine. Hyperactivity results from a decrease in the inhibitory amino acids GABA and acetylcholine and a relative increase in the excitatory amino acid dopamine. Another type of syndrome with hypermobility and hypertonia is caused by nigrostriatal and pallidum lesions and is commonly seen in Parkinson's disease. Parkinson's disease is caused by degeneration of dopaminergic neurons in the nigrostriatal dense zone, which weakens their excitatory effect on striatal GABA/SP/DYNergic neurons, resulting in a relative inhibition of the direct circuit, while at the same time GABA/ENKergic neurons lose their inhibitory effect of dopamine, while the thalamus is inhibited and cortical motor area activity is reduced, resulting in reduced and rigid movements, and difficulty in maintaining the movements performed, while This causes changes such as bradykinesia. In addition, Parkinson's disease is also associated with hyperactivity of acetylcholine transmitters.

The limbic system is mainly related to visceral activity, emotions, learning, and memory. One of these structures, the hippocampus, is located at the base of the lateral ventricular horn. The hippocampus and its adjacent structures may be involved in

various learning and memory functions, such as working memory, spatial memory, and associative memory. If this area is disrupted or damaged, it can cause loss of recent memory. The neural structures associated with this function are called hippocampal circuits. In hippocampal structures, long-range synaptic transmission can be induced by monosynaptic activation. This is known as long-term potentiation (LTP). All excitatory transmission pathways in the hippocampus can induce LTP.

1.2.4 The development of nervous system

The early development of the nervous system includes the establishment of the primitive nervous system during the embryonic period, the generation and differentiation of neural precursor cells, the migration of neurons, the growth of axons and the developmental process of a large number of synapses. Each of these events involves a variety of signal-to-signal interactions, signal-receptor interactions and transcriptional regulation of genes. When the growing axons finally reach the target area, the correct connections begin to form and the basic neural circuitry is initially formed. Following birth of embryo, neuronal growth and gene expression change accordingly in response to a variety of experience- and activity-dependent molecular mechanisms, leading to a continuous modification and remodeling of the neural circuits, and the associated behavioral traits are thus shaped and stereotyped. After the individual matures, synaptic connections continue to be modified and renewed, and this structural reconstruction is necessary for the learning and memory of new skills. In addition, new neurons are generated throughout life in certain specific brain regions in adult animals, demonstrating the strong plasticity and repair functions of the central nervous system.

1.2.4.1 The development of brain

In the fourth week of human embryonic development, the anterior part of the neural tube undergoes dramatic changes, and its cephalic end expands to form three primary brain vesicles, which are the prosencephalon, mesencephalon, and rhombencephalon and constitute the basis of the brain. As the dorsal wall of the neural

tube develops faster than the ventral wall, its cephalic end curves ventrally and the first curve, the cephalic flexure, appears. The part of the brain before the cephalic flexure, the forebrain vesicle, continues to expand and becomes the basis of the forebrain; while the midbrain vesicle in the cephalic flexure part develops into the midbrain; and the rhombencephalon vesicle after the cephalic flexure develops into the rhombencephalon. Subsequently, a second bend toward the ventral side, called the cervical flexure, appears at the junction of the rhombencephalon and the spinal cord. At this point, the neural tube of the early embryo has evolved into the prototype of the central nervous system. Once brain regions are established in this manner, the embryo begins further rounds of segmentation to produce new brain regions (Figure 9). The cephalic end of the forebrain vesicle develops into two symmetrical telencephalons, which eventually develop into two hemispheres on either side of the brain. The terminal part of the anterior vesicle develops into the diencephalon, which includes the thalamus, hypothalamus, and a pair of optic cups located laterally, which will develop into retinal neural tissue. The dorsal part of the midbrain vesicles forms the four bulges of the superior and inferior thalamus, while the ventral part forms the nuclei concentrated in the midbrain periaqueductal region. The rhombencephalon evolves into a metencephalon at the cephalic end and a myelencephalon at the caudal. The hindbrain eventually forms the cerebellum and the pons, and the endbrain develops into the medulla oblongata. The lumen of the neural tube in the vesicular area evolves into ventricles at all levels. The anterior vesicular lumen forms the lateral ventricles in the right and left cerebral hemispheres and the third ventricle of the mesencephalon; the midbrain vesicular lumen forms the narrow midbrain aqueduct; and the rhombic vesicular lumen forms the fourth ventricle located dorsal to the pons and medulla oblongata, which continues with the central canal of the spinal cord.

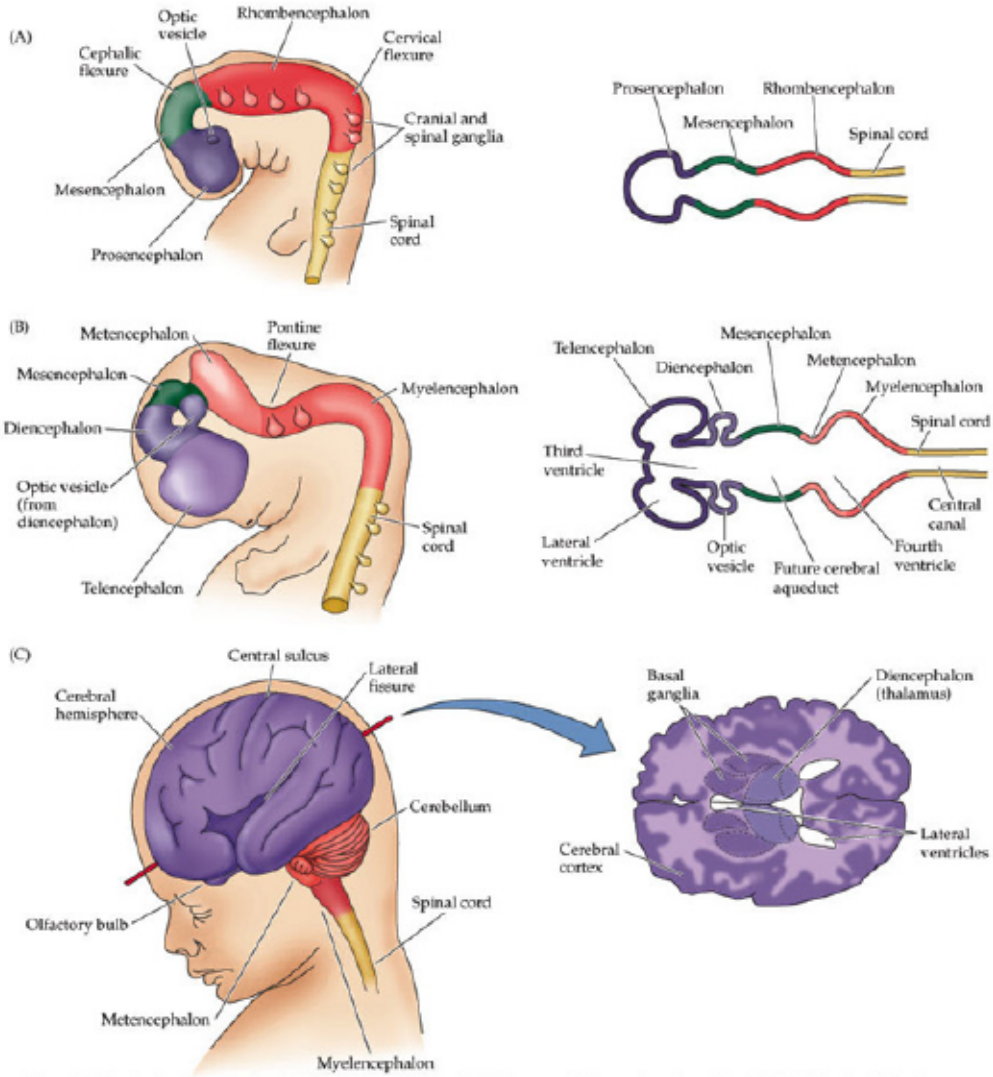

Figure 1.1. The developing human brain. Left, drawings (not to scale) of the neural tube as viewed from the side. Right, top two illustrations drawn as though the tube were stretched out to make it straight and the top were cut off; view is from the top. The bottom right illustration (C) shows the appearance of a section through the forebrain at the level indicating to the left (Figure 22.3 from Neuroscience, 5th Ed.).

Figure 9. The development of human brain. (Copyright: Purves, et al 2011)

1.2.4.2 The development of cells in nervous system

During early embryonic development, after the initial formation of the brain and spinal cord, the persistent cellular components of the central nervous system - neurons and glial cells - begin to arise and differentiate. Almost all of the 100 billion neurons and many more glial cells contained in the adult brain arise within just a few months from a small group of precursor cells. These neural precursor cells (NPCs), or neural stem cells, are located in the ventricular zone (VZ), the innermost layer of the neural tube wall. The mitotic activity in this zone is exceptionally active. During the peak of cell proliferation in the human embryonic period, it is estimated that 250,000 new

neurons can be generated every minute. After birth, most of the cells in this zone disappear, leaving only a very small fraction that continues to produce new neurons.

Early neurogenesis undergoes three temporal phases [45]. The first phase is the expansion of NPCs through multiple rounds of symmetric divisions, called the expansion phase; then the neurogenesis phase, in which most NPCs divide asymmetrically to produce neurons; and the last phase is the gliogenesis, in which NPCs undergo asymmetric divisions to produce mainly astrocytes and oligodendrocytes (Figure 10).

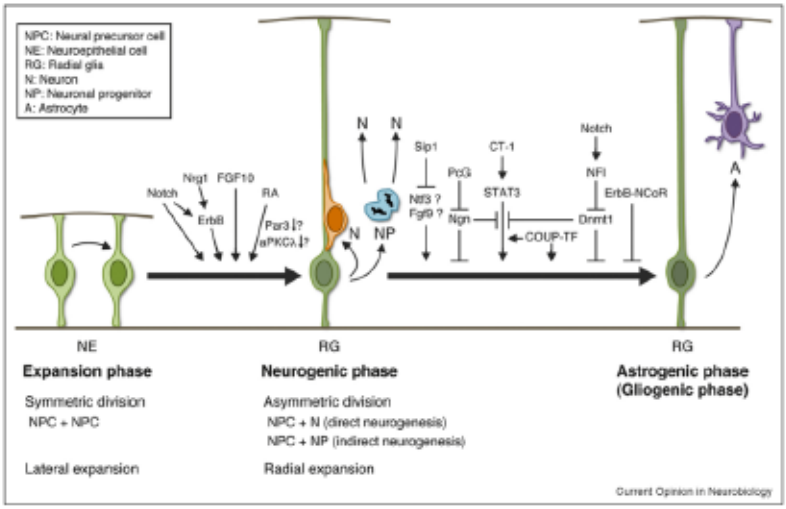

Figure 10. Temporal NPC specification in the neocortical development. (Copyright: Miyata, 2010)

NPCs in the expansion phase usually refer to neuroepithelial cells (NEs). NEs divide symmetrically and expand laterally, which can cause the neocortex to expand laterally and increase the surface area. When neurons undergo phase initiation, NPCs refer to radial glia (RG). RGs generate more differentiated cells through asymmetric division while achieving self-renewal, which can cause radial expansion and thickening of the neocortex. RGs have a typical bipolar morphology with protrusions that run through the wall of the neural tube, extend a long distance from the VZ to reach the soft membrane on the outer surface, and lengthen with the thickening of the neural tube wall, serving as a scaffold for immature neuronal migration. In the late stages of neurogenesis, NPCs give rise mainly to astrocytes and oligodendrocytes, and no longer to neurons. The termination of neurogenesis is synergistically regulated by exogenous factors and

endogenous programs.

1.2.4.3 Neuron migration and axon guidance in the developing nervous system

Neuronal migration and axon guidance During the development of the nervous system, immature neurons arise in the ventricular zone and undergo outward migration, most needing to migrate considerable distances before finally reaching their destination. In the central nervous system, migration, although confined to the neural tube, still involves traversing significant distances, especially in large animals such as primates. As in the formation of the cerebral cortex, neurons need to migrate a few millimeters, through which different types of neurons can come together to form proper spatial connections.

Neurons in different regions of the nervous system adopt different migration strategies. Similar molecular mechanisms may also be used to guide axonal growth at different stages of development. In contrast, neurons in laminarly organized brain regions, including the cerebral cortex, cerebellum and hippocampus, reach their destination along the protrusions of radial glial cells, that is, they migrate in a cell-guided manner. This process is mediated by extracellular matrix adhesion molecules and associated signal transduction molecules. Many of these molecules are also essential for subsequent steps in neural development, such as axon growth and orientation. However, the migration of neurons in many other regions of the brain, particularly those evolving into nucleolus structures, does not depend on the guidance of radial glial cells.

For example (Figure 11), striatal neurons located in the striosome were generated during early neurogenesis, while neurons of the matrix compartment were generated during late neurogenesis. Late-born (matrix) striatal neurons receive cortical input independent and different from the cortical input that early-born (striosomal) striatal neurons receive. Thus, birth-dating results in a different cortical innervation pattern and subsequently, in a different functionality of striatal neurons [46].

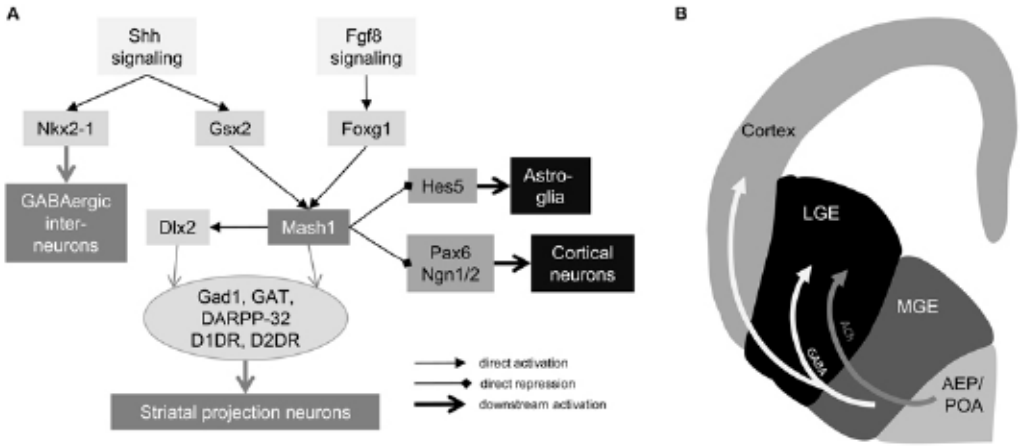

Figure 11. An example of migration with Cortico Striatal.(Marie-Christin Pauly1,2012).

Neurons arise, migrate and, upon reaching their destination, begin to establish neural loops. Firstly, neurons from different brain regions must be connected together by axons and secondly, ordered synaptic connections must be formed between the appropriate pre- and postsynaptic neurons. Thus, the cytological mechanisms of axonal growth and synapse formation are the main determinants in establishing the neural loops that will ultimately control behavior. The directional growth of axons and the identification of synaptic targets are mediated by a special structure at the tip of each growing axon, namely the axonal growth cone. The growth cone constantly detects external signals and responds to them by identifying the correct elongation pathway, inhibiting incorrect growth direction and ultimately promoting the formation of functional synaptic partners. These signals include cell surface adhesion molecules as well as diffusible signaling molecules that can attract or repel growth cones. In addition, secreted growth factors also influence axon growth, synapse formation and regulate the number of axon/target connections. Similar to other intercellular communications, these signals, which are transduced by various receptors and second messenger molecules, initiate intracellular events that lead to the directed growth of axons, the specialization of growth cones to presynaptic components, and the formation of specific postsynaptic sites.

1.2.4.4 The formation of synapses

As axons grow to the correct target, they must make a further choice between a large number of potential local synaptic partners, and select a cell that is specifically innervated by them. The axon terminals that reach the target area begin to form multiple fine terminals and initiate the next process of development, that is, the formation of synapses. Synapse formation involves at least three main stages: (i) The localization of cell-acting factors or adhesion molecules between the presynaptic axon and the postsynaptic cytosol or dendrite, (ii) Presynaptic differentiation, which establishes the transmission structure of the synapse. (iii) Postsynaptic specific differentiation, which allows for the reception of signals from neurotransmitters. There are an extremely large number of synapses in the central and peripheral nervous system, each varying in almost all aspects of morphology, function, location and mode of connection, so that the formation of synaptic specificity may require the induction and integration of multiple signals.

1.2.4.5 Neurogenesis in adults

The classical theory believed that neurogenesis was no longer present in the brains of adult higher vertebrates. Indeed, in a seminal study, using environmental radioactivity as a tracer. Spading KL[47] showed that Cortical neurons in adults are as aged as the individual. These results, substantiated by others, suggest that in most of the brain areas post-mitotic neurons are not renewed during whole life. However, the discovery by Nocdohm and Goldman in 1983 shown that a large number of new neurons were found in the brain of adult canaries in specific brain areas, which attracted a great deal of attention in the scientific field. Following studies have also shown that neurogenesis is present in the adult bird, rodent, primate and even human brain primarily in 2 structures: the olfactory bulb and the hippocampus.

Evidence of localized neurogenesis illustrates that the adult brain has strong plasticity. The plastic changes can occur not only at the molecular or synaptic level, but

also at the more macroscopic cellular, network and systemic levels. It is conceivable that the creation of new neurons and their addition to existing neural circuits, which require new connections to other neurons, will inevitably result in large changes to the existing neural network or system. At the cellular level, newly generated neurons may differ from older neurons, at least for a short period of time, showing some difference in synaptic plasticity. It is possible that at the level of local neural networks, newly generated neurons may be associated with the active properties of some cell populations. Each neural network has the ability to encode information and store operational procedures over a wide range of areas, and the pattern of neurogenesis may be critical to the implementation of these functions. Neural replacement and recovery are an important direction in addressing many neurodegenerative diseases. Much of the loss of many of the underlying cells occurs prior to the discovery of disease symptoms and, to date, no neuroprotective therapeutic technique has been able to prevent the loss of neural cells. The application of neural precursor cells may provide new ideas for the treatment of neurodegenerative diseases due to the ability of various stem cells to generate new neuronal cells and oligodendrocytes.

1.3 Neural connectivity

1.3.1 The neural circuits

1.3.1.1 The projection between cortex and striatum

Neurons in the cortex are connected to multiple structures in the brain by projections. The six layers of the cortex can be divided anatomically into multiple neurons. For example, Intratelencephalic (IT) neurons in the cortex are located mainly in layers 2 to 6 of the cortex, where ITs located in layers 2 to 3 mainly build cortical-cortical connections and ITs located in layers 5 to 6 mainly build cortical-striatal connections, where the cortex mostly communicates with the striatum in a monosynaptic manner. Pyramidal tract (PT) neurons are located in layer 5B of the cortex and receive projections from the IT in layers 2-3, and also project to the striatum,

Thalamus, subthalamic nucleus (STN), and Brainstem. Corticothalamic neurons are located in layer 6 of the cortex, and project to the thalamus and reticular nucleus, and do not make connections to the striatum[48].

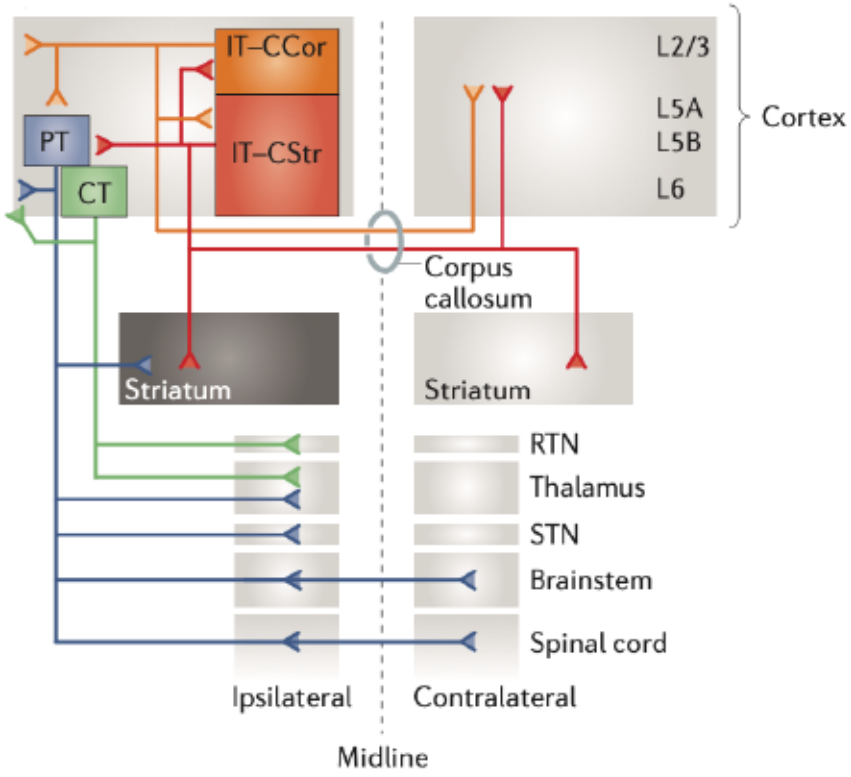

Figure 12. The axonal projection of CStr neurons.

1.3.1.2 The glutamatergic projection in neural circuits

Glutamate is the main excitatory neurotransmitter in the nervous system and belongs to the class of amino acids. There are many glutamatergic pathways in the central nervous system, and five main pathways that project from the cortex. They are cortico-brainstem pathway (ventral tegmental area and dorsal raphe nucleus), cortico-striatal pathway, cortico-hippocampus pathway, cortico-nucleus accumbens pathway, cortico-thalamic pathway (Figure 13, green arrow). And also, cortex have cortico-cortical projection [49, 50]. In addition, the hippocampus and amygdala also have glutamatergic projection to medial prefrontal cortex. These projections support the exhibition of whole brain. Glutamate and glutamate receptors are also involved in the mechanisms of synaptic plasticity (LTP and long-term inhibition, LTD), which is

thought to underlie learning and memory. The lesion of glutamatergic pathways can damage learning and memory off. In Alzheimer's disease (AD) there is loss of pyramidal neurons and their synapses and glutamatergic decrement. The mechanism of glutamatergic (and cholinergic) cell death may be a combination of necrosis and apoptosis caused by multiple factors, and all of these changes are strongly associated with cognitive decline in AD[51, 52].

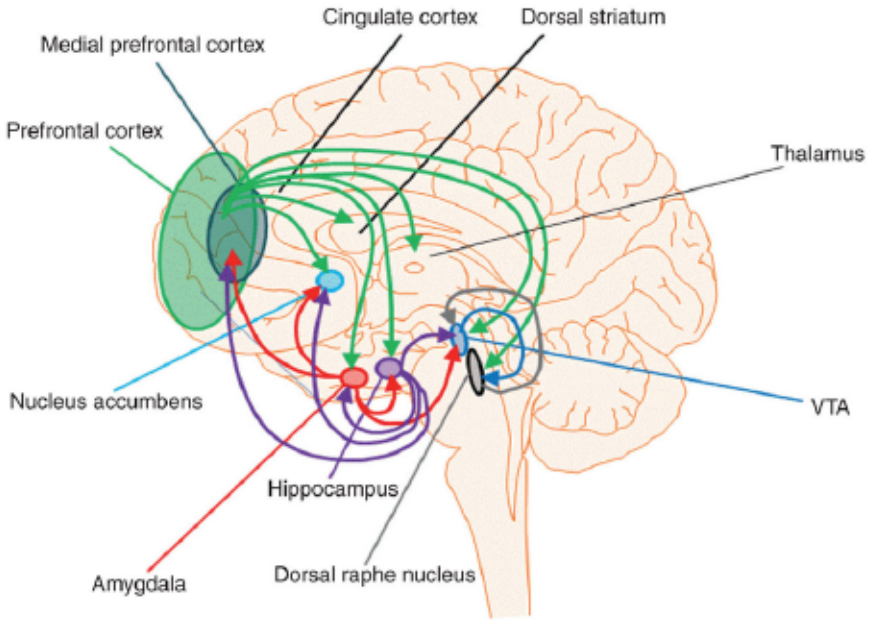

Figure 13. The glutamatergic projection of human brain (Richard L.Bell, 2016).

1.3.1.3 The GABAergic inhibition in neural circuits

The balance between excitatory and inhibitory neurotransmitter systems maintains the normal functioning of the central nervous system (CNS). Excitability is regulated by glutamate, whereas inhibition is regulated by GABA via interneurons. GABA is the major inhibitory neurotransmitter in the CNS and exerts its inhibitory function through ionotropic $GABA_A$ and metabotropic $GABA_B$ receptors [53]. $GABA_A$ receptors can also can be selectively blocked by Bicuculline [54]. When GABA is released into the synaptic gap, it will be reuptaken by GAT-1 and GAT-3 transporter proteins [55]. GABAergic neurons have been found to be present in the amygdala, hippocampus, hypothalamus, prefrontal cortex, olfactory bulb, retina and spinal cord [55].

GABAergic projections are widely distributed throughout the brain and have been found to be mainly from the striatum to the substantia nigra and brainstem, then from the substantia nigra to the thalamus, as well as from the hypothalamus to the occipital and parietal cortices, from the hippocampus to the thalamus and striatum, and from the nucleus accumbens to the thalamus, where GABA projections are also highly innervated by the cerebellum[56] (Figure 14).

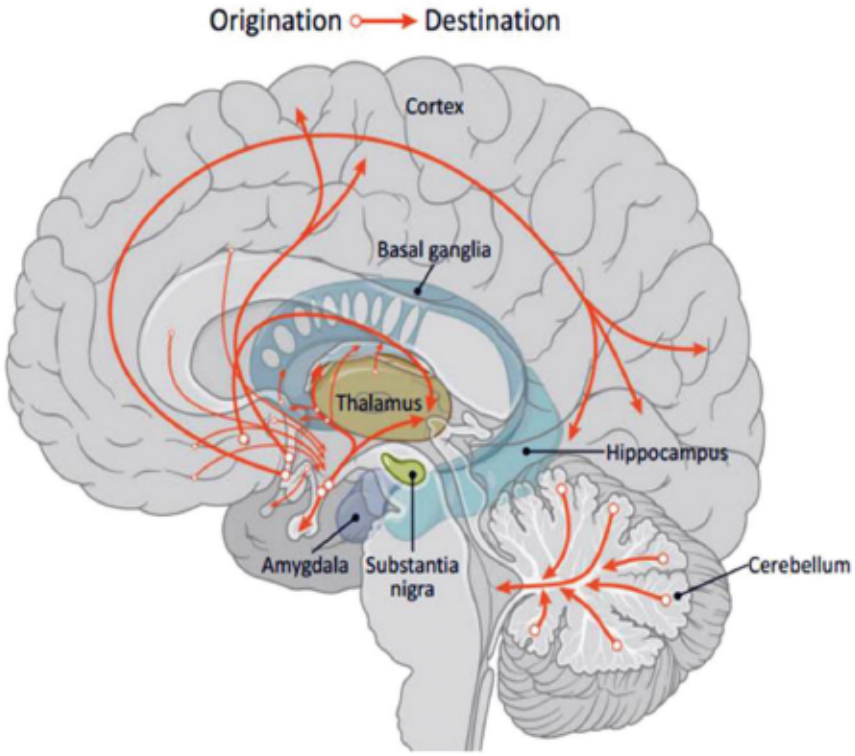

Figure 14. The GABA pathway in human brain (Richard L.Bell, 2016).

From the previously mentioned glutamatergic pathway, it can be found that the partial overlap of these two pathways can form a dynamic inhibitory-excitatory loop. The highly dynamic GABAergic system has a key role in regulating the activity and plasticity of neural networks during development and adulthood [57]. It has also been suggested that dysregulation of GABA action in brain circuits is central to the pathogenesis of NDD [58]. GABAergic pathways are extensively and intricately involved in determining the onset and end of critical periods of development, as well as learning and memory.

1.3.1.4 *The DAergic projection and it's dysfunction in Parkinson's disease*

The striatum is the main input structure to the basal ganglia, receiving the major excitatory input from cortical glutamatergic pyramidal neurons and the densest DAergic innervation of the SNc[59]. GABAergic spiny projection neurons (SPN) are the major neurons in the striatum, accounting for 90% of all striatal cells. The hypokinetic symptoms of PD are due to the selective loss of DAergic neurons in the substantia nigra densa (SNc), which innervates the basal ganglia[60]. In the healthy brain, excitability from the cerebral cortex is transmitted to the striatum and STN, and then to the basal ganglia. Specifically, excitation through the cortex is directly input to the substantial nigra pars reticulata (SNr) or internal segments of the globus pallidus (GPi) via the GABAergic pathway, and indirectly input to external segments of the globus pallidus (GPe), and glutamatergic pathway to STN. SNc regulate cellular activity with dopaminergic projections via D1 or D2 receptors in the basal ganglia (Figure 15). But in Parkinson disease, with the DA neurons degeneration, the DAergic projection lost, the balance was broken. The consequent results are SNr/GPi and STN are hyperactivity, and that inhibit the activity of PPN, thalamus, then reduce the movement.

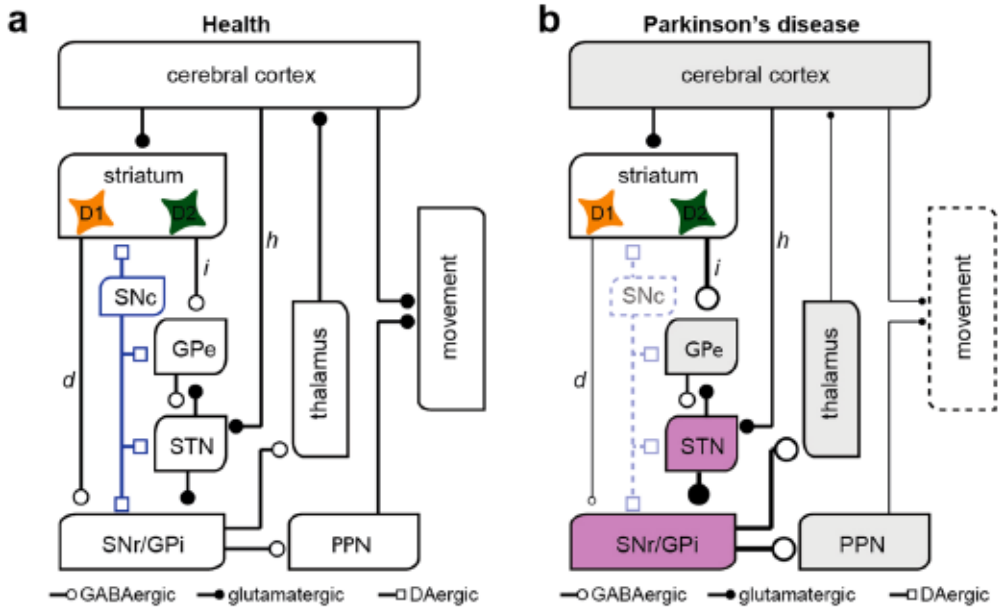

Figure 15. Dysfunction in Cortico-striatal circuits in Parkinson's disease (Hong-Yuan Chu, 2020).

1.3.2 Neural connectomics

We are in an information age with a complex network structure, just like the cells in our brain. In sociology, there are highly structured patterns of connectivity from individual and group human lives, interpersonal interactions to economic behavior, and even disease transmission epidemics and material transport. In biology, the self-organized response of groups in response to external challenges, from single cells to tissues and entire ecosystems, is a reflection of the structure and function of complex systems. The human brain is also composed of small communities of structural modules and networks in which neurons and networks of brain regions are structurally interconnected to form the central nervous system. Studying the role of connectivity in brain function can provide a basis for unravelling brain signaling, behaviors, degenerative pathologies, etc. Connectomics is a way to achieve this, by mapping its elements and connections to create network architectures, and then by quantitative models to determine the relationship between structure and function [61-63].

1.3.2.1 Graph theory and Neural connectomics

Many studies have begun to describe the nervous system mathematically, as a graph or network containing nodes (neurons and/or brain regions) and edges (synaptic connections, inter-regional pathways) [64](Figure 16). Brain networks are constructed from measures of structural or functional relationships between pairs of neurons or brain regions. These paired relationships are summarized in the form of a connectivity matrix that describes the relationships between nodes and edges, i.e., the topology of the network [65]. The main goal of connectome research is to unravel the architecture of brain networks and to explain how the topology of structural networks shapes and regulates brain function. Network science or "graph theory" can be used to elucidate key organizational features of the brain's connectome architecture and to predict the role of network elements and network properties in brain function[61, 62, 66].

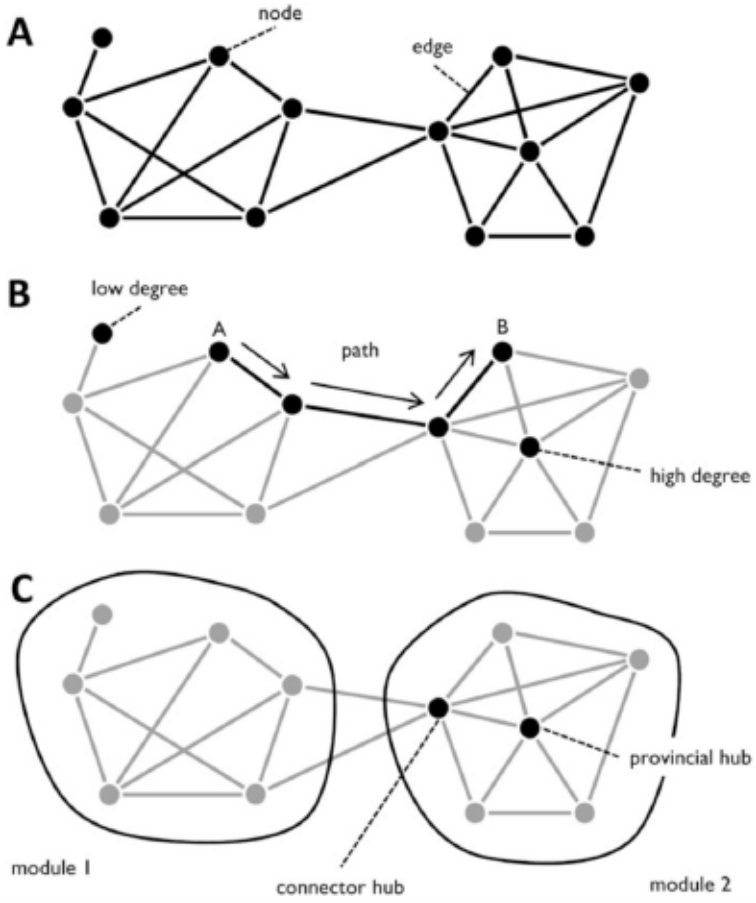

Figure 16. At the macro-connectome level brain can be envisioned as modules of specific topologies made of nodes (neuronal elements) and edges (their interconnections).

Once brain network data are presented in matrix form, they can be used from network science [67]. Hubs in graph theory, for example, represent nodes of particular interest in many network studies because their central embedding in the network topology makes them attractive candidates for information integration and also makes them vulnerable to attack[68]. Hubs can be found to be highly interconnected, similar to the close relationship between modularity and network communities[69]. Hubs that primarily connect nodes within a community are also referred to as "provincial hubs", while hubs that connect multiple communities are referred to as "connector hubs". Increasingly, the cross-cutting features of brain network organization, which simulate capturing isolation, integration, and influence, rely on the decomposition of networks into modules or communities connected by bridge connections and hub nodes[66, 70]. Such modular descriptions of brain networks are particularly attractive because they

can be applied to both structural and functional networks, and the resulting modules have been shown to be relevant to behavior and cognition[71, 72].

1.3.2.2 The relationship between structure and functions in neural network

When exploring the connectivity of the brain, in vitro neural networks formed based on anatomical structures can be considered as structural neural networks, while those based on physiological roles can be counted as functional neural networks. These two domains of brain networks are different in the constructional approach and also have neurobiological differences. An important distinction is between structural and functional brain networks. Structural networks are derived from anatomical data sets and represent physical synaptic connections between neural elements, whereas functional networks are derived from neural recordings and represent their statistical relationships [63, 64].

The relationship between structure and function has also been studied at different scales. A number of studies across micro-, meso-, and macro-scales have shown that patterns of structural connectivity do help shape the dynamics of neural activity. From the micro scale, such as in terms of circuit topology, large-scale recording methods applied to organisms such as zebrafish larvae can produce highly resolved whole-brain recordings of neural population activity [73]. This dynamic circuit activity can be analyzed using time-series methods, and there is evidence that functionally coherent circuits form clusters or modules [74]. Mesoscale data were mainly collected using MRI [75, 76], for example Wang et al. [77] studied the relationship between structural and functional connections within monkey somatosensory cortex at high spatial resolution.

The connections between highly connected nodes and hubs are affected and the default mode network is specially changed. Specific to actual cases of neurodegenerative diseases, some advances in brain imaging suggest that ND triggers deep alterations in brain connectomics. Neuropathological analysis has shown that various pathological signs of ND such as stroke and traumatic brain injury appear to

follow neuroanatomical pathways in the brain. The analysis of brain topology suggests that brain network topology is associated with higher robustness under stress and that ND alters this robustness in space and time [78-80]. From the molecular water, it was shown that the spread of aggregated α-syn, Tau, etc., in the brains of affected patients would be closely related to the functional aspects of the neural network in some way. These results suggest that network topology is involved in the propagation among dementia such as Alzheimer's disease and Lewy body [81]. Studying the relationship between such spatial changes and alterations in physiological function is a key point in understanding the processes of disease and abnormalities occurring in the nervous system.

1.3.3 What we are inspired about reconstructing neural network?

Culturing neurons in vitro is not a difficult task, but the specificity of neuronal morphology predicts that, when building neural networks, it is necessary to mimic the projections of different regions in the human brain, such as the connections between the cortex and the striatum. The signaling of neurons controls the processing and feedback of all information in the brain. This means that the construction of in vitro neural networks must be physiologically active and able to mimic the real functional ones in certain regions of the brain, especially the signaling between neurons. Neural connectomics coupled with graph theory, meanwhile, simplifies the brain into a number of different small information centers. Rather than relying on the cascading of individual neurons, information transfer relies on an orderly integrating of information, followed by the next round of information distribution and transmission from the hub. It is easy to see that a network structure consisting of individual neurons in composition is difficult to achieve both aspects at the same time. But when neurons have their own community or group and then connected to another group, structural projective connectivity and functional information transfer can be achieved at the same time. In addition to this, the overall survivability increases. Therefore, when we design and build the chip, we first aim to capture a certain number of neurons in nodes of our design,

then allow making connection opportunities between these nodes. Hence, the idea of an ordered array of different small communities of neuron populations can be achieved.

1.4 Neurodegenerative disorder

1.4.1 Alzheimer's disease and other dementia disease

Dementia is an acquired, generalized, persistent syndrome of intellectual loss resulting from brain function and mental impairment common in older people. The most common forms of dementia are Alzheimer's disease (AD) and vascular dementia (VD), as well as frontotemporal dementia (including Pick's disease), Lewy body dementia, traumatic brain injury, Parkinson's disease, Huntington's disease, etc. The incidence of Alzheimer's disease is increasing every year as the elderly population grows older.

1.4.1.1 Pathological features of Alzheimer's disease

The typical neuropathological features of AD are senile patches (SP or amyloid plaques) and neurofibrillary tangles (NFT) formed by intracellular over-phosphorylation of tau proteins, which are also the basis for the histopathological diagnosis. The β-amyloid protein (Aβ) is the main component of senile plaques, and the accumulation of extracellular fibrotic β-amyloid protein culminates in the formation of senile plaques.

In AD patients, there is widespread brain atrophy in the temporal, parietal and frontal lobes, mostly symmetrical. The cerebral sulcus becomes shallow, the gyrus becomes narrower, the lateral ventricles become enlarged, the ventricular horn becomes blunt, the gap between the hippocampus and the temporal horn becomes wider, and significant atrophy of the internal olfactory area occurs early. In AD patients, brain tissue destruction spreads from the memory area to the emotional and sensory control areas, with a loss of 5.3% per year in the grey matter of the brain and up to 10% per year in the memory area, compared to 0.9% in normal controls, and the edges of the brain tissue destruction area continue to push outwards, resulting in more brain tissue

damage.

1.4.1.2 Clinical manifestations of Alzheimer's disease

AD mainly occurs in the pre-geriatric and old age. The disease starts insidiously and symptoms usually become apparent after 2-3 years of onset, with a duration of 5-10 years. The main clinical manifestations are dementia syndromes, such as memory loss, cognitive and language dysfunction, etc. Memory impairment is the earliest manifestation of AD, accompanied by emotional and personality changes.

There are various scales to detect dementia [82-85], including the mini-mental state examination (MMSE), the Mattis Dementia Rating Scale (DRS), the Alzheimer's disease assessment scale (ADAS), the Hasegawa Dementia Scale (HDS), the Alzheimer's Disease Assessment Scale (ADAS), the Blessed dementia scale (BDS), Wechsler adult intelligence scale (WAIS) and Wechsler memory scale (WMS). The MMSE is the best-known scale for detecting dementia, designed by Folstein et al [86]. It is easy to use, requiring the patient to draw a clock within a circle, a test that patients with dementia often fail to complete correctly. The clock test has a sensitivity and specificity of 90% for patients with dementia.

The biochemical tests include tau protein levels in the cerebrospinal fluid (SF) and amyloid derivatives in the cerebrospinal fluid. The electrophysiological tests include electroencephalography and evoked brain potentials. The neuroimaging tests include computerized tomographic scanning (CT), magnetic resonance imaging (MRI), single photon emission computed tomography (SPECT), positron emission computed tomography (PET), and proton magnetic resonance spectroscopy (H-MRS), etc [87, 88].

1.4.1.3 The treatments of Alzheimer's disease

According to information released by the World Health Organization, AD is the fifth most common disease-causing death in humans, and to date there is no curative treatment. The aim of treatment is to slow the progression of the disease, maintain

residual brain function and reduce complications [89, 90]. NMDA receptor antagonists [91], for example, reduce the neurotoxic effects of glutamate. Cholinergic agonists such as milameline and xanomeline have shown significant improvements in cognitive function and motor behaviour. Cholinesterase inhibitors [92] such as donepezil, galanthamine and rivastigmine significantly inhibit the activity of acetylcholinesterase in brain tissue and enhance cholinergic synaptic transmission, thus improving the symptoms of AD patients in terms of cognition and memory. Calcium antagonists such as nimodipine, flunarizine and guilizine have different degrees of improvement on certain symptoms of Alzheimer's disease such as memory loss and reduced ability to adapt to the environment [93]. Anti-Aβ drugs [94] such as Alzhemed (tramiprosate) bind solid β-amyloid peptides and inhibit their aggregation. Aβ antibodies bind to the Aβ region of the APP protein on the surface of the cell membrane, accelerating APP endocytosis, and the presence of antibodies in endosomal vesicles enhances the degradation of APP cleavage products, thereby reducing the intracellular Aβ content and achieving a reduction in the Aβ protein content. In addition, there are antioxidant drugs and some hormone replacement therapies [95].

In summary, the course of AD is progressive and non-reversible, the pathogenesis is complex and there are no specific drugs to target.

1.4.2 Parkinson's disease

1.4.2.1 Pathological features of Parkinson's disease

The hallmark histopathology of PD is the loss of dopaminergic neurons in the substantia nigra, accompanied by neuronal inclusions known as Lewy bodies. The cell loss in the substantia nigra occurs in a specific way. There is also significant neuronal loss in the ventricles, dorsal motor nucleus of the vagus, nucleus accumbens, and basal nucleus. And the Lewy bodies may be found in all these sites as well as in many other subcortical structures. The caudate, putamen, globus pallidus, thalamus, and other brainstem structures appear normal [96, 97].

1.4.2.2 Clinical manifestations of Parkinson's disease

The main clinical features of Parkinson's disease include resting tremor, myotonia, bradykinesia and abnormal postural gait movements. The non-motor symptoms include cognitive impairment, neuropsychiatric symptoms, autonomic dysfunction, sleep disturbance and sensory disturbance [98, 99].

1.4.2.3 The treatments of Parkinson's disease

The goal of treatment for Parkinson's disease is mainly to delay the progression of the disease, control the symptoms of the disease and improve the quality of life of patients [100]. It is generally considered that the goal of treatment for young, early-stage patients is to maintain or restore the ability to work. For intermediate and late-stage patients is to have the ability to take care of themselves. For advanced patients is to reduce pain and prolong life.

Patients with Parkinson's disease have a severe deficiency of levodopa in the brain, and the provision of exogenous levodopa can increase the level of dopamine in the brain[101]. Levodopa is a dopamine precursor that is decarboxylated to dopamine by L-amino acid decarboxylase. Dopamine itself cannot cross the blood-brain barrier, but levodopa can cross the blood-brain barrier and become dopamine in the brain tissue by decarboxylase action. Levodopa is currently the most effective drug for Parkinson's disease treatment. Levodopa ethyl ester (LDEE) is a pre-drug of levodopa [102], and levodopa ethyl can be rapidly hydrolyzed into levodopa in the duodenum after taking, and is rapidly absorbed in the form of levodopa, which avoids the disadvantage of unstable absorption of levodopa in Parkinson's disease patients. In addition, dopamine agonists can act directly on striatal dopamine receptors, and their efficacy is not easily affected by the loss of nigrostriatal neurons and can reduce the adverse effects of levodopa [103].

In addition, neural stem cell therapy for PD may be more promising, but it has not been applied to the clinic yet due to the problems of survival and preservation of

transplanted cells and long-term postoperative immune response [104]. Neural stem cells have the ability to differentiate into neurons and glial cells, are capable of self-renewal, and have the potential to provide a large number of brain tissue cells. Therefore, neural stem cell transplantation therapy can repair the damage of striatal dopaminergic pathway caused by nigrostriatal neuronal degeneration, thus achieving the purpose of treating PD[105].

1.4.3 The different hypotheses for mechanisms of neurodegenerative diseases

1.4.3.1 Protein aggregation

One of the most important hypotheses in neurodegenerative diseases is that it is due to abnormal interactions of certain proteins in the brain, which can alter the conformation between normal soluble brain proteins leading to the formation of aggregated insoluble fibers, which are divided into ordered and disordered forms [106]. Normally, proteins are in a dynamic balance between various conformations in synthesis and degradation [107]. While folding is the normal procedure for converting newly synthesized proteins into physiologically functional molecules, abnormal misfolding can lead to changes in protein structure and induce the formation of various supramolecular aggregates (Figure 17). These mistakes can originate from production errors, genetic or acquired amino acid substitutions or damage [108]. These abnormalities can induce a vicious cycle, leading to neuronal and glial cell dysfunction and death [109, 110].

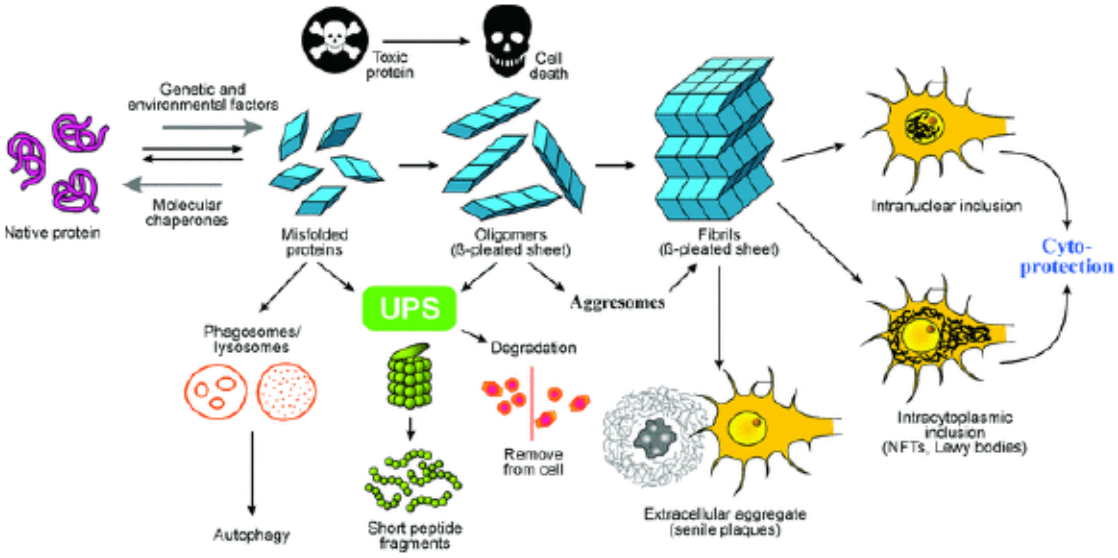

Figure 17. Model of protein misfolding and fibrillation leading to deposition of aggregated proteins in cells and extracellular spaces via actions of the UPS, phagosomes and aggresomes, either causing cell death or cytoprotection. (Kurt, 2010)

This mechanism shares a similar protein aggregation pathway with the cell-cell propagation of prion disease like the Creutzfeldt-Jakob disease, hence that protein aggregation hypotheses of neural degeneration is also called prion-like disease. In prion disease, it is the cellular prion protein (PrP^{C}) converging into PrP^{Sc} which are the abnormal β-sheet-rich form of PrP^{C} [111]. In Prion spreading scenario, PrPSc aggregates are amplified through a seeding/nucleation process that leads to the self-perpetuation of specific supra molecular assembles that behaves like infectious agents in the brain. Similarly, it is now postulated that proteins such as involved in neurodegenerative syndromes β-amyloid (Aβ), Tau, α-synuclein (αSyn) aggregates, and TDP-43 involved in respectively Alzheimer Diseases, Parkinson Disease and Amyotrophic Lateral Sclerosis may acts as "Prion-Like" elements that progressively invades specific brain areas in affected patients. The figure below summarized these prion-like mechanisms involved in the transmission of misfolded proteins which were detected in mammals (Figure 18).

Disease	Normally folded protein "Precursor"	Abnormally folded protein "Prion form"	Protein aggregates detected	Seeding inoculum	Prion-like propagation in mammals
CJD/scrapie	PrP^{C}	PrP^{Sc}	PrP^{Sc} deposits plaques	Various mammalian prions and recPrP fibrils	WT and Tg mice Non-human primates
Alzheimer (AD)	Amyloid precursor protein (APP)	Amyloid beta peptides Aβ	Aβ plaques	Human AD and Tg mice brain extracts blood	Marmosets TgAPP2576 TgAPP23, TgAPP/PS1
Tauopathies	Tau	Tau aggregates	Neurofibrillary tangles (NFTs)	Tg(HuTauP301S) brain extracts	Tg(wt Tau)
Parkinson (PD)	α-Synuclein	α-Synuclein aggregates	Lewy bodies	Human preformed α-Syn fibrils	(i) Fetal tissue grafts in human PD patients (ii) Tg (α-SynA53T) and WT mice

Figure 18. The prion-like mechanism of several misfolded protein transmission in different NDD (Acquatella-Tran, 2013).

Alpha-synuclein (α-Syn) is a 140 amino acid long protein encoded by the SNCA gene that is highly expressed in neuronal tissue. α-Syn is normally involved in vesicular transport by interacting with the SNARE complex protein at the presynaptic terminal [112]. Overexpression of this protein disrupts the homeostasis of the terminal vesicle cycle, thereby inhibiting neurotransmitter release. This protein is naturally unfolded, it is amphipathic and forms an α-helical structure at the N-terminal end when bound to the lipid membrane [113]. When it is cleaved and phosphorylated by proteases, it increases its propensity to aggregate, leading to the formation of β-sheet format. The aggregation process can be divided into primary and secondary nucleation stages. In the primary stage, misfolded monomers form oligomers, which in turn form prefibrillar nuclei, which in turn form larger fibrils. In the second stage, cellulose can create new fibrils by fragmentation and catalyze the formation of new oligomers on the hydrophobic surface of the nucleus [114]. α-Syn aggregation plays a key role in its toxicity.

Tau belongs to a family of microtubule-associated proteins [115] that are involved in regulating microtubule stability mainly in axons. Tau has been shown to have at least 45 possible phosphorylation sites, which are susceptible to phosphorylation and a variety of kinases have the ability to phosphorylate them [116]. In hyperphosphorylation pathologies caused by an imbalance between kinase and phosphatase, it becomes unstable when bound to microtubules as well as the kinesin is

affected, eventually causing impairment of axonal transport [20]. Meanwhile, hyperphosphorylation of tau increases its tendency to self-assemble into larger aggregates, resulting in the accumulation of tau assemblies and the formation of paired helical filaments (PHFs) [117]. Amrit also reviewed the some evidence of tau pathology spreads through prion- like propagation, but it is still not clear that how the prion-like propagation arising from differential spatio-temporal vulnerability of connected neuronal populations[118].

APP (Amyloid precursor protein) is a transmembrane glycoprotein [119]. It is a cell surface receptor that interacts with extracellular matrix proteins [120]. And it is essential for motor neuron development and neuronal migration [121]. Amyloid-β peptide (Aβ) is an approximately 4 kDa fragment derived from the larger amyloid precursor protein (APP) by the concerted action of β- and ɣ-secretases[122]. The Aβ peptides polymerize into insoluble ~10 nm filaments which are the main component of extracellular amyloid plaques. The deposition of amyloid plaques and neurofibrillary tangles (NFT) in the brain is the character of Alzheimer's disease[123]. Tau proteins are mainly distributed in neuronal axons, and in normal brain tissue tau proteins promote tubulin polymerization to form microtubules, reduce dissociation of micro tubulin molecules, and stabilize microtubule structure. Neuronal fiber tangles are one of the main pathological features of AD, which are composed of double-stranded helical filaments, while the main component of PHF in the brain of AD patients is abnormally phosphorylated tau protein. tau protein can also undergo abnormal modifications, such as excessive glycosylation and ubiquitination. The hyperphosphorylated tau protein is partly soluble and partly insoluble deposited in the PHF [124], resulting in neuronal degeneration in the brain. Under pathological conditions, imbalance of kinase and phosphatase activities can lead to hyperphosphorylation of tau protein, thus detaching tau protein from microtubules, causing disintegration of the microtubule system, affecting axonal transport and eventually leading to neuronal degeneration. APP is widely present in the cell membranes of many tissues throughout the body. Aβ is a

normal product of cellular APP, and all cells of the nervous system express Aβ and APP.

1.4.3.2 Genetic factors

Besides "epigenetic" abnormal protein aggregation genetic factors are also involved in initiating and or interfering with the outcome of neurodegenerative syndromes. For example, in Alzheimer Disease, several genes have been linked to susceptibility factor to AD, some of which are directly involved in triggering the formation of aggregates, some being secondarily linked to the duration of the disease. the main genes associated with AD patients are, Tau, amyloid precursor protein (APP), presenilin, and apolipoprotein E (ApoE) [125, 126].

It is not the scope of that PhD to provide an in-depth review of the genetic mechanisms involves in the aetiology and development of AD related process. For in-depth review see these papers [127-130].

Under normal conditions, the production and degradation of Aβ maintain a dynamic balance. APP gene abnormalities in any of the various aspects of transcription, translation, expression of APP molecules, and formation of APP precursor protein and its hydrolysis product Aβ may lead to the formation and deposition of Aβ protein[131, 132]. PS genes have PS-1 and PS-2 type. Defective PS1 gene can reduce the formation of Aβ by inhibiting the occurrence of cleavage by secretase[133]. PS2 can inhibit T cell receptor and Fas-mediated apoptosis of neuronal cells, thus suppressing the occurrence of AD. Mutations in PS2 gene can lead to increased production of Aβ[134].The main role of ApoE is to transport cholesterol in the blood. ApoE is present in both NFT and senile plaques in the brain of AD patients, and the main component of NFT is PHF, while the main component of PHF is abnormally phosphorylated tau protein. It was found that ApoE is associated with abnormal phosphorylation of tau, and the formation of PHF may result from the inability of ApoE to effectively maintain the stability of tau protein-microtubule protein junctions and/or the failure to inhibit the self-aggregation of tau protein[135]. In addition, ApoE can be involved in regulating Aβ production and

can affect the clearance and formation of Aβ by astrocytes and neurons. ApoE can bind to Aβ and accelerate the precipitation of Aβ by prompting the latter to form monofilament fibers [136].

There are five genes clearly associated with Parkinson's disease, namely the alpha-synuclein (α-syn) gene, LRRK2, parkin, DJ-1 and PINK1 [137]. α-syn and LRRK2 mutations are commonly found in patients with autosomal dominant PD and are mainly involved in the formation of intracellular protein inclusion bodies. While mutations in Parkin, DJ-1 and PINK1 are common in autosomal recessive and sporadic Parkinson's disease patients and are mainly involved in the regulation of mitochondrial and oxidative stress-related signaling pathways. DJ-1 is a common pathogenic gene in Parkinson's disease and has an important role in transcriptional regulation and resistance to oxidative stress [138]. The α-syn gene encodes a presynaptic protein, α-syn protein, which is widely expressed in the brain, mainly in presynaptic terminals of the central nervous system. The α-syn exists in solution as an irregularly coiled form and is a highly soluble protein in the neuronal cytoplasm. The α-syn mutations, overexpression, and abnormal aggregation of the protein may result in large aggregates of α-syn protein to form Lewy vesicles. The α-syn protein is present in the fibrils of the a-beta lamellar structure in the Lewy microsomes and binds to other proteins such as synphilin-1 and parkin to form insoluble aggregates [139]. In addition, because α-syn protein has a natural unfolded molecular conformation, it has a tendency to interact with homologous protein molecules, and high concentrations of α-syn can self-aggregate and form fibrillar structures, which have toxic effects on neurons [140, 141].

1.4.3.3 Oxidative stress/injury

Oxidative stress occurs because of an imbalance between the intracellular oxidative and antioxidant systems, leading to the accumulation of reactive oxygen species (ROS) clusters in cells, and when the production of these free radicals or their products exceeds antioxidant defense mechanisms, these endogenous reactive oxygen

species produce cytotoxic damage to cells. The excessive ROS produces damage such as cell membrane lipid peroxidation[142], altered lipid-protein interactions, enzyme inactivation, DNA and RNA breaks[143, 144], mitochondrial respiratory dysfunction[145], excitotoxicity leading to cell necrosis or apoptosis [146], then inhibiting glutamate uptake followed by release and intracellular calcium overload and activation of neuroinflammatory responses and apoptotic pathways[147, 148]. Some tissues of the body, especially brain tissue, are particularly sensitive to oxidative stress oxidative stress attack because of its high oxygen utilization, its high content of polyunsaturated fatty acids and multiple metal ions required for oxidative reduction reactions, and its relatively low antioxidant content in the brain, which makes it particularly vulnerable to oxidative stress [149, 150]. In the models of human AD and transgenic (tg) mice of AD, oxidative injury occurs prior to Aβ deposition, which further leads to OS and ND[151], and OS induces macroautophagy of Aβ proteins and leads to apoptosis[152]. The hippocampus is the earliest and most severe brain region where nitrated brain[153] proteins are seen in both the early and late stages of AD, and oxidative damage to DNA and RNA repair is particularly severe in the hippocampus.AD is accompanied by substantial free radical production and insufficient free radical scavenging capacity, and the imbalance between free radical production and scavenging is the main cause of neuropathological changes inducing AD. Other studies have shown that in Parkinson's disease patients there is a defect in the antioxidant system, with reduced activity of both reduced glutathione and glutathione peroxidase[154], as in the nigrostriatal reduced glutathione levels are significantly reduced. The DAergic neurons in the substantia nigra densa (SNc) of humans brain, recent proteomics has identified L-ferritin in neuromelanin granules, suggesting that it is an important player in the complex network controlling Fe homeostasis in human DA neurons[155]. For oxidative stress injury, antioxidants may protect neurons in AD and PD and reduce the risk of ND[156-158]. The picture below demonstrated the role of OS in neurodegenerative diseases. OS may not be a trigger for NND, but they may

exacerbate disease progression through oxidative damage and interactions with mitochondria[159].

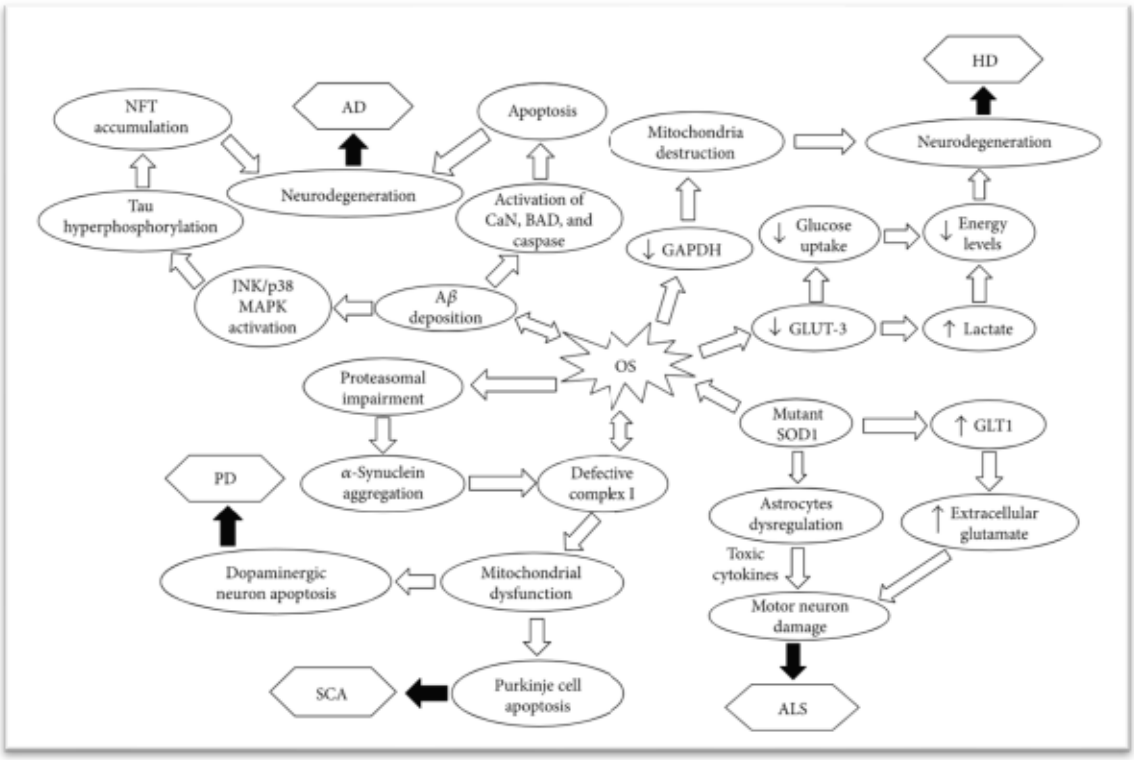

Figure 19. Schematic illustrating the key roles of OS in the development of AD, HD, PD, ALS, and SCA. (Zewen Liu, 2017）

1.4.3.4 Mitochondrial damage

Mitochondria are the main site of cellular energy production and play an important role in oxidative stress, and mitochondrial dysfunction can lead to cell death. Mitochondrial damage can lead to impaired energy demand of cells, such as impaired ATP production and increased oxygen radicals can induce mitochondria-dependent cell death. Through inhibiting mitochondrial function, the permeability of the membrane is increased, resulting in the release of cytochrome C and second mitochondrial activator of caspases (Smac), which are in turn to promote Aβ oligomerization, causing cellular damage [160]. Aβ binding alcohol dehydrogenase (ABAD) is located in the mitochondrial matrix and is the direct effector of Aβ-induced mitochondrial toxic damage [161]. It has also been found that overexpression of Tau protein in cultured cells can also cause increased Aβ production, resulting in mitochondrial damage [162,

163]. The mitochondria damaged and the affection of axonal transportation were described in chapter 1.2.2.2.

1.4.3.5 Cells death – apoptosis, autophagy and necroptosis

Programmed cell death (PCD) is the process by which nucleated cells end their lives on their own under certain conditions by initiating internal death mechanisms according to a specific genetic program. Neuronal cells are long-lived, non-recoverable, and non-differentiated cells that cannot be regenerated. When the body is exposed to persistent low levels of oxidative stress and brain injury, the neuronal cycle can be abnormal, with dysregulation of apoptosis-related gene expression, dysregulation of calcium homeostasis, oxidative damage, and low energy metabolism triggering the initiation of the apoptotic program, leading to a significant reduction in neuronal numbers and consequent brain dysfunction. PCD is classified into three major types: apoptosis (PCD type I), autophagy (PCD type II) and necroptosis (PCD type III) [164]. The main difference between PCD I and PCD III is that the former is dependent on the activation of caspases and can occur locally without damaging adjacent cells. The latter one is an unexpected and uncontrolled mode of cell death, triggered by OS[165], which exhibits rapid cell swelling and subsequent plasma membrane rupture, with DNA breakage also involved in the degradation process. Autophagy (PCD type II), known as the process by which molecules and organelles undergo lysosomal clearance/degradation to help maintain cellular homeostasis[166]. In the brain of AD patients, they first lose hippocampal neurons and as the disease progresses, the frontal cortex and other cortical/subcortical areas also experience neuronal loss[167, 168]. The death pathway involved may be apoptosis or necroptosis. Tau proteins can form neurogenic fiber tangles (NFTs) under disease conditions[169]and the formation of these aggregates is associated with DNA fragmentation. It suggests that they may be related to regulated neuronal death [170]. Besides, it has been shown that Tau is related to the re-entry of cells cycle and directs mature neurons towards death, which may also increase their susceptibility to cell death [171]. An in vitro study showed that neuronal

cell membrane elasticity decreases by 30% in short-term co-cultures of Aβ40 or Aβ42 with hippocampal neurons, and that these biomechanical changes may affect vesicular transport and ion channel activity, so that neurons are more susceptible to neuronal cell death [172]. In PD, there is a heavy loss of nigrostriatal neurons, and some studies suggest that necroptosis may also be involved in the death pathway in PD [173]. At the molecular level, it is not clear how α-synuclein induces neuronal death[174]. But its expression in dopaminergic neurons is related to mitochondrial dysfunction and oxidative stress. Overexpression of α-synuclein in vivo takes a long time to induce significant pathological changes and neuronal loss [175]. It has been shown that after co-culture of α-synuclein with DA neurons, cells were found to be susceptible to apoptosis in the presence of minimal levels of proteasomal toxins and cells exhibited nuclear fragmentation and caspases activation[176]. In another study, the authors found that when α-synaptic nucleoprotein aggregates entering cells via endocytosis, it leads to lysosomal membrane rupture and increases ROS levels[177], which leads to cell death. Overall, for these neurodegenerative diseases there is no evidence to fully distinguish the PSD type of neuronal cell death[178].

1.4.4 Current disease models

1.4.4.1 Animal models in vivo

In vivo animal models are usually used to simulate brain injury and lesions by some means such as chemical way or biological transgenesis. For example, animal models in PD often use 6-hydroxydopamine (6-OHDA) damaged rats and 1-methyl-4-phenyl-1,2,3,6-tetrahydropyridine (MPTP) poisoned non-human primates [179]. These models simulate neurochemical lesions in which loss of dopamine-producing cell bodies in the substantia nigra, so the levels of striatal dopamine decreased. Animal models of HD mainly employ some neurotoxins such as quinolinic acid (QA), itaconic acid (IA) or 3-nitropropionic acid (3-NP) to break the cortical striatal circuit. Based on studies of genetic loci involved in PD, transgenic rodents model modeling familial PD

disease have been created that partly recapitulates human neuropathology. More recently, in an attempt to substantiates the "prion like" spreading hypothesis of synuclein, intracerebral injection of Preformed Synuclein aggregates became a new animal model of PD [180-182]. Similarly in AD, animal models primarily mimic expression of human amyloid precursor protein (APP), and the most common rodent model of AD is the transgenic mouse model [183]. However, unlike humans, the tracer bound to β-amyloid deposits does not accumulate substantially in the brains of transgenic mice [184, 185].

The most commonly used imaging techniques in animal models in vivo are positron emission tomography (PET) and magnetic resonance imaging (MRI). The great advantage of in vivo imaging is that it allows the non-invasive study of biological processes, thus enabling the longitudinal follow-up of the same objects over time [186]. However, at the same time, there are many limitations like the instrument cost, difficult to go the molecular levels. All the chemical ways usually cannot control in a very precise condition, because it also impact by metabolism in different species. And some transgenic models also not very ideally for disease modelling.

1.4.4.2 Brain Slice culture in vitro

An intermediate process that lies between in vivo and in vitro models consists of slicing brains in thick samples to allow the study of intact networks in a in vitro paradigm. Usually, brain slices preserve the structural connections which exist in vivo. Two main systems are primarily used in neurosciences: Adult brain slice, that can be maintained alive for a couple of hours. While those are primarily used for [187] electrophysiological studies of neurons, and neural networks or synapses, like Sara [188] they do not allow long term studies as the networks starts to degenerates after a few hours ex vivo.

A second alternative consists in slicing embryonic brains which can be maintained in vitro for several weeks in air/liquid interface cell culture system. This allows to

preserve some anatomical pathways and study long term biological processes. Recently, mouse hippocampal organotypic brain slice has been used to study α-synuclein aggregation and inter-neuronal spreading initiated by microinjection of pre-formed α-synuclein fibrils (PFFs). But the drawback of organotypic slices is that few slices can be obtained per animal and their in vitro manipulation remains tedious [189]. Moreover, some studies have shown that keeping the slices in high (95%) O_2 conditions may lead to hyperoxia and progressive cell death and oxidative stress[190]. The traditional way and novel technic of culturing dissociated neurons in vitro.

1.4.4.3 The traditional way and novel technic of culturing the dissociated neurons in vitro

Traditional cell cultures, usually dissociated cells, are suitable for studying the function of neurons and synapses under pathological or pharmacological conditions at relatively higher throughput that in vivo or ex vivo methods. This type of model allows studies for long periods of time in vitro. In the neurodegeneration field, in vitro cultures of primary neurons are mostly used to decipher cell signalling pathways that are involved in cell autonomous molecular and cellular dysfunction. For example, Raiss et al studied the formation of intracellular α-synuclein protein inclusion bodies with and without the addition of low concentrations of fibrillated seeds in the neural extracellular matrix). [191]. Using this king of models, numerous evidences have been acquired that shows that that high concentrations of extracellularly added α-synuclein or aggregates leads to nucleation of host encoded synuclein, amplification of synuclein aggregates and progressive synaptic and mitochondrial dysfunction [192] [193] [194] [195] [196]. However, all these studies in traditional Petri dishes have certain limitations. First, neurons grown in traditional culture dishes form a semi-random network in complex state of connectivity that do not mimic ordered brain pathways and /or brain connectomics. Moreover, traditional "petri dishes" cultures do not permit to initiates cellular and molecular processes at a subcellular level, and are only used to study cell-autonomous processes were all neurons in the petri dishes are considered "equivalent".

While non-cell autonomous processes are classically used trough co-culture experiments, treatment of distinct cell populations cannot be performed separately. The differences between in vivo and in vitro tissue-cell-molecular responses thus do not permit modeling of human physiology or pathology at the neuronal network level and therefore create barriers to the discovery of therapeutic solutions. Traditional culture dish techniques have therefore been gradually replaced by emerging technologies [197-202]. For example, in recent years, neural networks have been cultured in microfluidic chips and achieved using 3D printing technology. In the next section, the emerging field of organ-on-a-chip will be specifically described as it encounters with neuroscience.

1.5 Brain on a chip

The European ORCHID (Organ-on-Chip development) defined that: "An Organ-on-Chip (OoC) is a fit for purpose fabricated microfluidic-based device, containing living engineered organ substructures in a controlled micro- or nano environment, that recapitulate one or more aspects of the dynamics, functionality and physiological response of an organ in vivo, in real-time monitoring mode." Theoretically theses OoC can be used for studying human organs physiology and disease in a dynamic and spatially controlled context and therefore allows to envision better biomarker and target identification, personalized medicine approaches (use of patient-specific cells), emulation of host-microbiome interaction, drug development process. The organoid research field progressively interacts with the "organ on chip" field, aiming at reconstructing organ through a top bottom approach by imposing directed evolution through the use of micro-technological approaches. This represents a challenge to create a microphysiological systems (MPS) which involved in identifying new material allowing to control cell-cell interaction and therefore creates advanced co-cultures platforms, interfacing with new physical and/or chemicals sensors, and control of cellular micro-environment and fluid circulation in micro-chips. The major aim of this field is to reconstructs, trough top bottom approaches, ordered minimalistic models of

human organs that could eventually leads to human body on a chip trough serial interfacing [203, 204].

The brain being a highly ordered organ with very complexes topological features, it represents a specific challenge in the field of organ on chip. In our labs, we are focusing on developing and using Brain-on-chip models to study the brain related disease processes. In the following section, I will therefore introduce the basic engineering process that underlies brain on chip platforms development.

1.5.1 Major micro-physiological systems for Brain-on-chips

1.5.1.1 2D spatially controlled technics - Micropatterning

Micropatterning is a 2D stamping technique which allows creation of spatially controlled adhesive pattern on a substratum and that has been widely used to control local adhesion and the geometry of living cells. The figure (Figure 20) illustrates some examples of geometric control of neuronal growth over rational patterns of adhesive polycations. Feinerman et al. [205] designed large triangle shaped patterns which allow neuronal cells bodies adhesion and axonal outgrowth toward other triangular areas. This permitted the creation of chain like directional networks and the creation of complex logical Boolean loops (Figure 20a). One major issue with micropatterning technique is that neurons often detach from the patterned areas. Copatterning of cell repulsive moieties has been explored by several laboratories to increase cell adhesion contrast. For example, Hardelauf et al.[206] printed poly-lysine with micro-structured network motif onto a PLL-g-PEG coated glass substrate that allowed reconstruction of a multi nodal neural network with good stability (Figure 20b). Using similar techniques Jang [207] also demonstrated the effect geometric constrains on initial neuritogenesis and axon guidance in 2D patterning methods. The Figure 20c shows the neurite escaping out of the geometric patterns followed a sharpest vertex. While numerous studies using micro-pattering to control axonal outgrowth have been published in the literature, the vast majority of those aims at studying the impact of initial constrains on neuronal

polarization and few studies use MP to model mature network's function and dysfunctions. This may be due to the fact that mature networks (trans neuronally connected) tend to collapse and detach from the patterned substratum due to important mechanical tension in axonal tracts that links neuronal patterned islands. Therefore, alternative methods that enforce neuronal polarity trough mechanical constrains have also been explored.

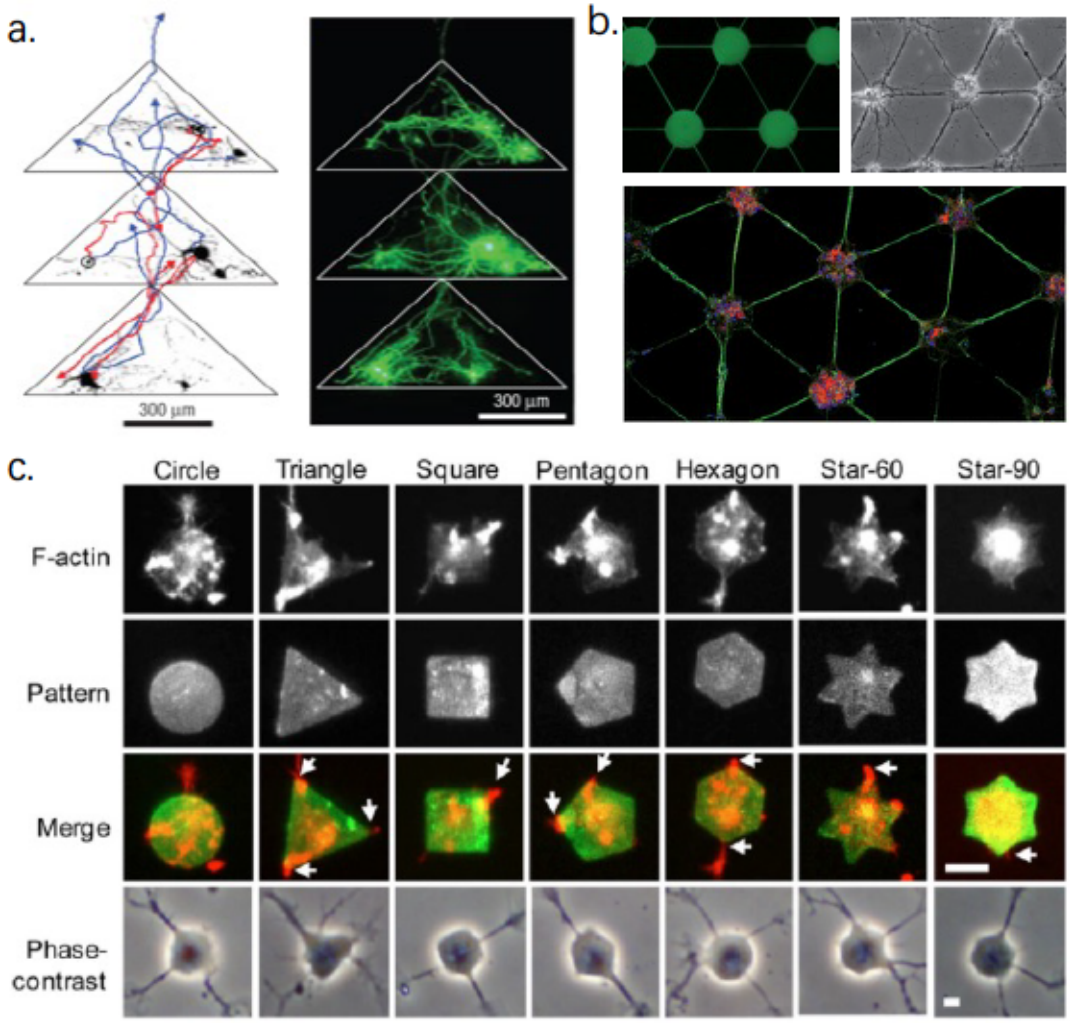

Figure 20. Micropatterning technics. (a) The axons can cross the triangle shape to form the network. (Ofer Feinerman, 2008) (b) Mini-network created on PLL-g-PEG coated glass substrate with poly-lysine pattern. (Heike Hardelauf, 2014) (c) Micropolygon motifs affect single neuron survival (Min Jee Jang, 2012).

1.5.1.2 2.5D or 3D architecture-based on compartmentalized system

Compartmentalized neuronal models are micro-systems that contain multiple culture chambers connected by microchannels. Microfluidics-based chips are usually

fabricated from PDMS using soft photolithography. The principle of these devices were originally designed by the group of Taylor et al [208, 209]. Inspired by the seminal work of R Campenot in the late 70's, PDMS compartmentalized chambers allows to guide some axons and dendrites originating from a primary neuronal culture toward a second chamber and therefore compartmentalize distal axons from somato-dendritic compartments (the length of micro-channel controlling whether or not dendrites from a specific neuronal subtype will reach the second compartments with the axons). Based on this principle, seeding different types in the axonal compartments allowed the creation of minimalistic models such as neuromuscular junctions, neuroimmune interface etc... One of the main advantages of compartmentalized platforms compared to MP approaches is first that axons cannot escape the guiding, tunnel like, microstructures and therefore allow long term culture and second that fluidic isolation between microfluidic chambers allows to control fluidic neuronal micro-environment. Many laboratories have cloned and further optimized that principle and demonstrated that guiding micro-channels allows to compartmentalize axons from all type of neurons. As shown in the figures (Figure 21 a and b) theoretically, this type of device is ideally suited for controlling connections between different types of neurons and therefore reconstructs small networks modules and compartmentalized systems have been particularly used for modelling neurodegenerative diseases related to axonal transport and synapse formation (see following chapters). Similarly to MP approaches such kind of devices can also be combined with MEA thus allowing recording of electrical signals propagation along neurons [210, 211]. Soscia et al. [212] created a compartmentalized device for precise placement of different cells on MEA substrate (Figure 21c). Kajtez et al. [213] also use 3D printed compartmentalized microfluidic device (Figure 21d). Ndyabawe et al. [214] used similar principle to reconstruct neural network by multicompartment microdevice (Figure 21e).

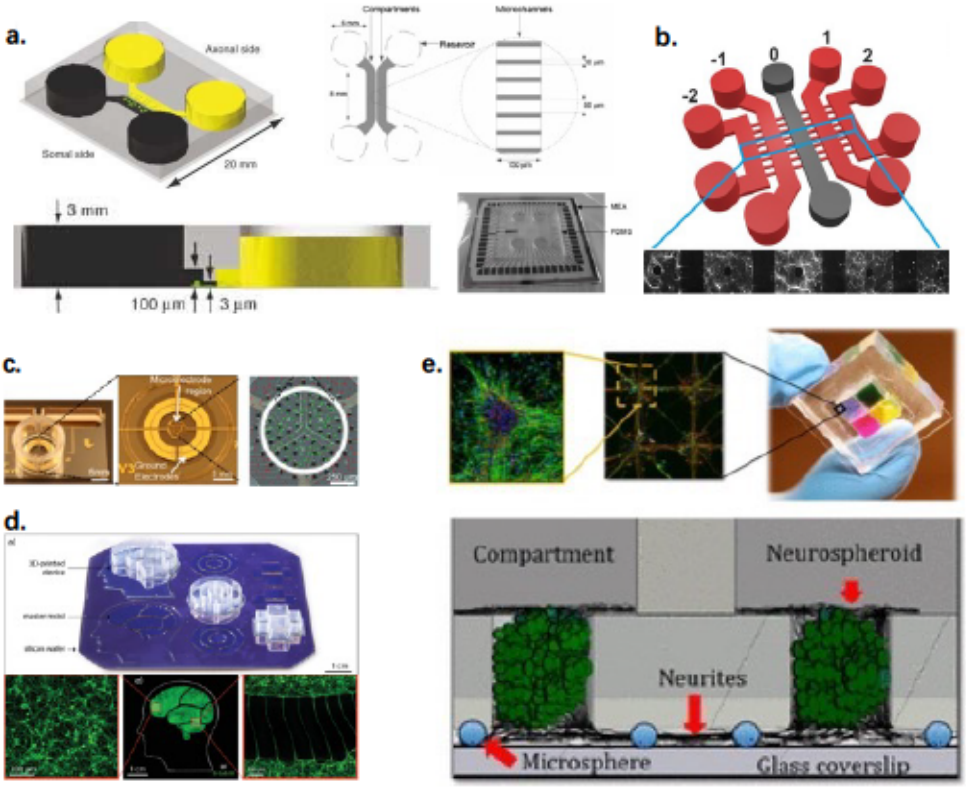

Figure 21. Compartmentalized systems. (a) Compartmentalized microfluidic device for neuron survival and axon guidance. Taylor, 2005. (b) Five parallel culture chambers device. Andrew J. Samson, 2016. (c) Cell positioning on MEA substrate. Soscia, 2017. (d) 3D printed compartmentalized microfluidic device. Kajtez, 2020. (e) Multicompartment microdevice. Kenneth, 2021.

1.5.1.3 Micro or macro scales neural spheroid on chip

Conventional compartmentalized platforms are also used to compartmentalize axons from brain explants; Park et al. [215] developed a three-dimensional (3D) neurospheroids system on chip that allows both the control of initial spheroid development and inter-spheroid connections. In that system which provides a constant flow of fluid, the neurospheroids were formed in concave microwell arrays interconnected to build a complex neural network (Figure 22a). Jeong et al.[216] also created a similar system with a deep hemispherical, microchannel-networked, concave array system and applied it to generate three-dimensional nerve-like neural bundles (Figure 22b). Kato-Negishi et al. [217] established a millimeter-sized 3D neural network by connecting neural building block composed of different neuronal subtypes. This technique allows the visualization of axonal extension, dendritic branching, and morphological changes of presynaptic components and synapses in real time (Figure

22c) between 2 tridimensional neuronal networks blocks.

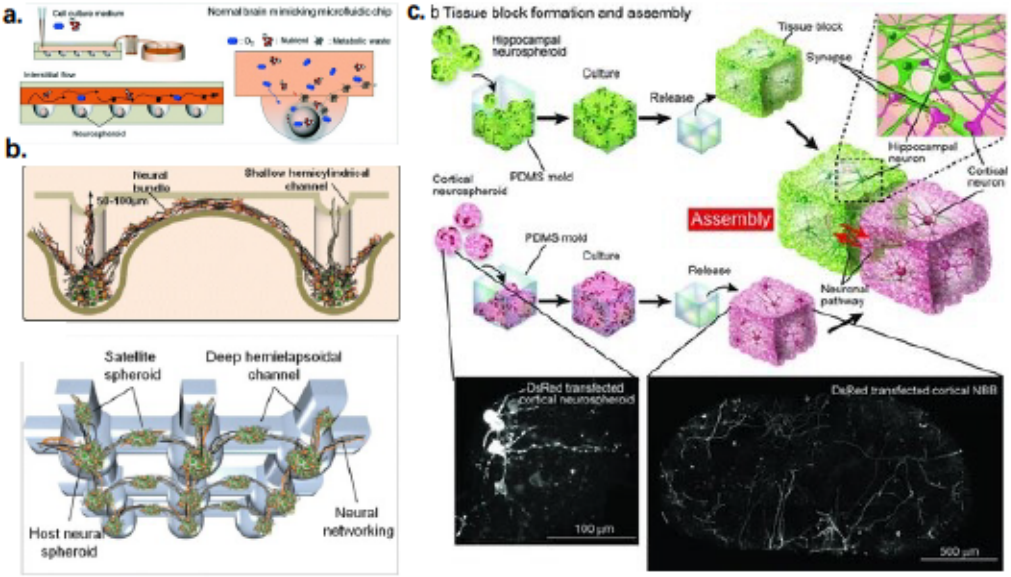

Figure 22. Neural spheroids. (a) Neurospheroids on chip. Park, 2015. (b) (c) A millimeter-sized 3D neural network. Midori,2013.

1.5.1.4 Material associated scaffold device

The figure below demonstrates a device based on three-dimensional (3D) scaffolds which fabricated by 3D laser writing (nanoprinted) [218]. Structurally, it enriches the extension of the neural network in Z-axis space, while more complex imaging problems should be considered and further applications are still some way off.

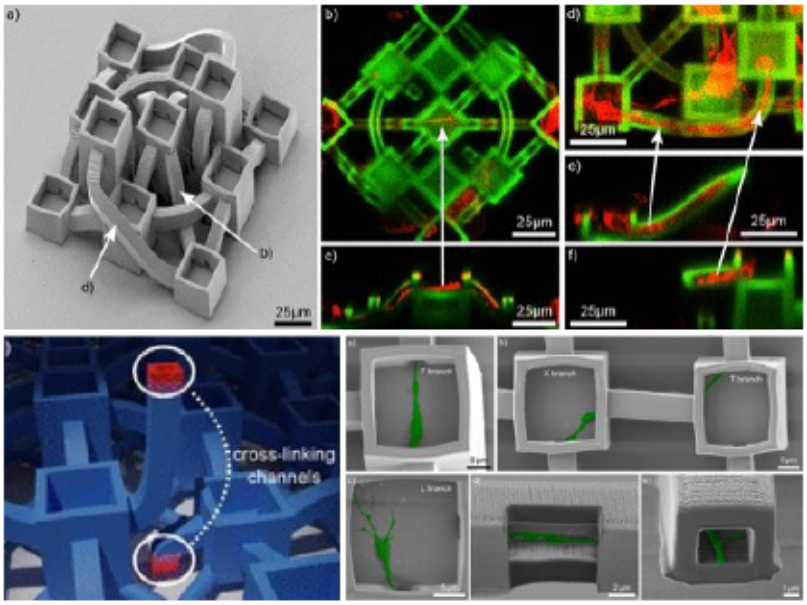

Figure 23. 3D scaffold devices (Harberts, 2020)

1.5.1.5 Integrating multiple physiological and functional system

Microfluidic technologies pave the way toward the reconstruction of modular elements of complex organs. Many groups are actually involved in trying to capture complex physiological features of organs through simple microfluidic platforms. For example, Booth et al. [219] developed a two-channel microfluidic device that contained a semipermeable membrane coated with brain endothelial cells on one side and astrocytes on the other. They implemented a transendothelial electrical resistance (TEER) assays on both sides of the membrane to evidence that they modeled a simple blood brain barrier (BBB) microchip. Similarly Kilic et al. [220] created a new multi-layer silicone elastomer device allowing interfacing of layer of human brain microvascular endothelial cells with neuronal-glial environment.. They used this device to model migration of human neural progenitors within a brain-tissue setting. Bang et al. [221] created a novel three-dimensional BBB platform which has one vascular channel connected to the inner lumen of the vascular network while the other supplies media to the neural cells channel.

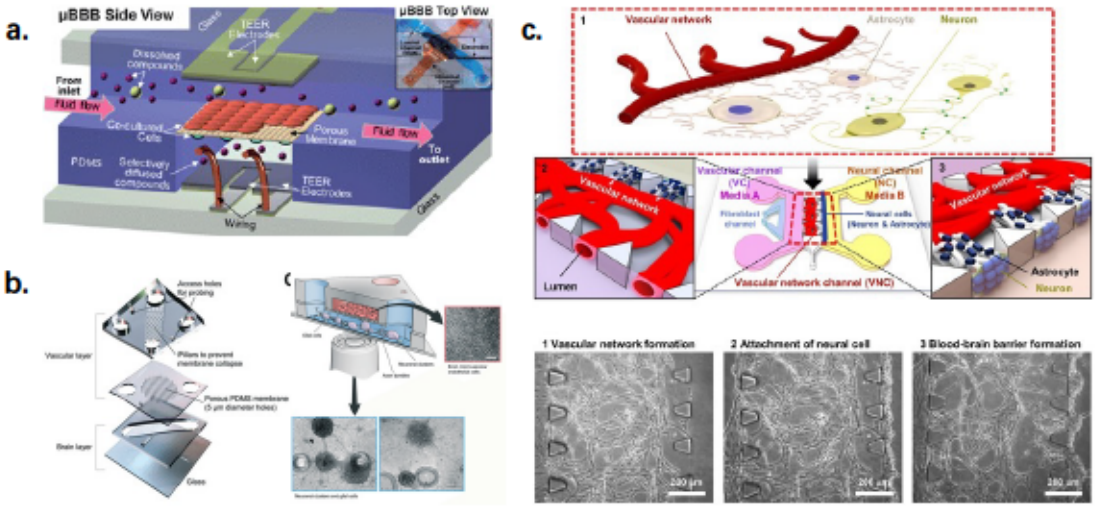

Figure 24. Integrating multiple physiological functions in one system. (a) Blood brain barrier on chip. Booth 2012. (b) Microvascular on chip. (Kilic,2016). (c) Neurovascular unit with blood-brain barrier on chip. (Seokyoung, 2017).

1.5.2 Consideration about physical cues in designing microfluidic chips to build neuronal networks.

Shear stress is defined as the stress created when a tangential force acts on a surface. The definition of shear stress applied to biology and microfluidics is the frictional force of a biological fluid flow acting on cells or tissues. The fluid flow does not have the same velocity at every point in the channel, creating a velocity distribution with a velocity profile that tends to be parabolic in most simple cases of laminar flow. Fluid velocity is the fastest at the center and slowest near the channel wall. The picture below showing the cell behavior changed under the shear stress (Figure 25). Viscous flow is a fluid defined as a substance that continues to exhibit strain when subjected to shear stress. The Reynolds number (Re) compares inertial effects with viscous effects, and the very low values for Re that are typical in microfluidics reveal that microscale flows are greatly dominated by viscous effects. The threshold between turbulent flow and laminar flow typically does not occur until Re is at least 10,000 times greater, so microchannel flow is clearly laminar. It's a good way to mimic flows found in veins and small arteries where the flow is usually unidirectional and laminar. Huber [222] reviewed how the hydrodynamics effects the cellular behavior, cell adhesion and deformation. In this field, the micro scale physical forces are a very important point.

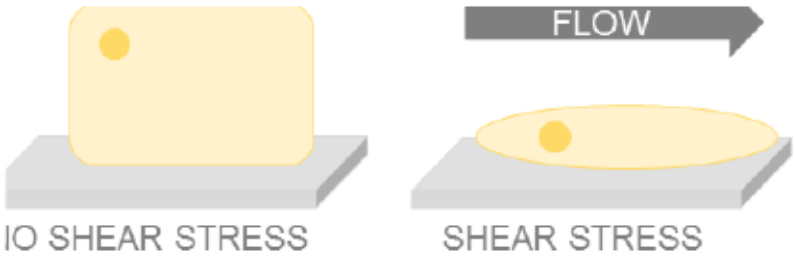

Figure 25. Cell behavior under shear stress (Copyright: Darwin-microfluidics https://darwin-microfluidics.com/blogs/reviews/shear-stress-in-microfluidic-devices)

1.5.3 The basic technics for microfluidics chips fabrication

The micron-sized structures of the basic building blocks of microfluidic chips requires that the environment must be carefully controlled during the preparation

process. The environmental indicators involved here typically include: air temperature, air humidity, air and particle density in the various media used in the preparation process. The higher environmental requirements for chip fabrication generally need to be achieved in a clean room. The success or failure of the microfluidic chip fabrication process is inextricably linked to cleanroom technology.

1.5.3.1 The principle and process of photolithography

In the previous subsection the importance of structures for organ-on-a-chip was mentioned, and how to construct these structures is one of the goals that are constantly being explored by researchers in this field. There are two broad categories of these methods. The first category is direct sculpting on the material, such as laser ablation, where micro-pores and micro-channels of different shapes and sizes are machined into materials such as metals, plastics and ceramics by precisely controlling the position of the laser in the X-Y direction, or direct moulding by 3D printing techniques. The advantages of these methods are that the resulting microfluidic chip structures are less damaged by heat, less dependent on the mask and more flexible. The disadvantages are lower productivity and the risk of operating in a standard laser laboratory during laser ablation and the high cost of UV lasers, which has limited the further development of laser ablation methods. Inspired by this technology, stencil-based chip fabrication has developed rapidly and photolithography based on photosensitizers has become mainstream. After obtaining an accurate mold, in addition to injection molding there is also hot embossing, which cures thermoplastic materials to quickly replicate the microstructure. In addition to the use of photosensitizers, molds can also be constructed from wire with a diameter of 50 μm or less. This method of manufacturing through a die allows for multiple use production with high efficiency.

Photolithography is the process for patterning the microstructure on the substrate, such as silicon or glass, by using light exposure and the photoresists chemical reactions. The photoresist used in photolithography is a photosensitive polymer material. After

light exposure it can undergo photo-crosslinking reactions, photo-polymerization reactions and photo-dissolution reactions.

In photolithography, a mask is used for light filtering. The microchannels are usually designed using standard CAD computer graphics software and the design graphics are transferred to a graphics file. Depending on the resolution required, different substrates are used to carry the different design. For example, plastic has a resolution of approximately 20um, but quartz can be used on a sub-micron scale. Then the pattern is printed on the substrate material using high resolution printing technology.

Photolithography begins by placing the silicon wafer on a spin coater, covering it with photoresist, then achieving the required thickness by controlling the rotation speed of the spin coater. The silicon wafer is then transferred on an aligner, where it will be put in contact with the mask, and illuminated. Thus, only the unmasked areas of the material are exposed to light. With positive photoresists, the photosensitive material is photodegraded and the developer dissolves the exposed areas, then leaving a coated surface where the opaque areas of the mask are placed. With negative photoresists, the photosensitive material is photo-enhanced (polymerized or cross-linked) and the developer only dissolves the unexposed areas. The mask has two types of structures (transparent and opaque) and the photoresist can be positive and negative, so there are four combinations of mask and photoresist. The mask pattern is finally transferred and the mold obtained after a. process of development.

The basic process of photolithography using the negative resist SU-8 is composed of some of the following processes: pre-treatment, coating, pre-baking, exposure, post-baking, development and checking, hard baking (Figure 26), and the Characterization of geometry of SU-8 master.

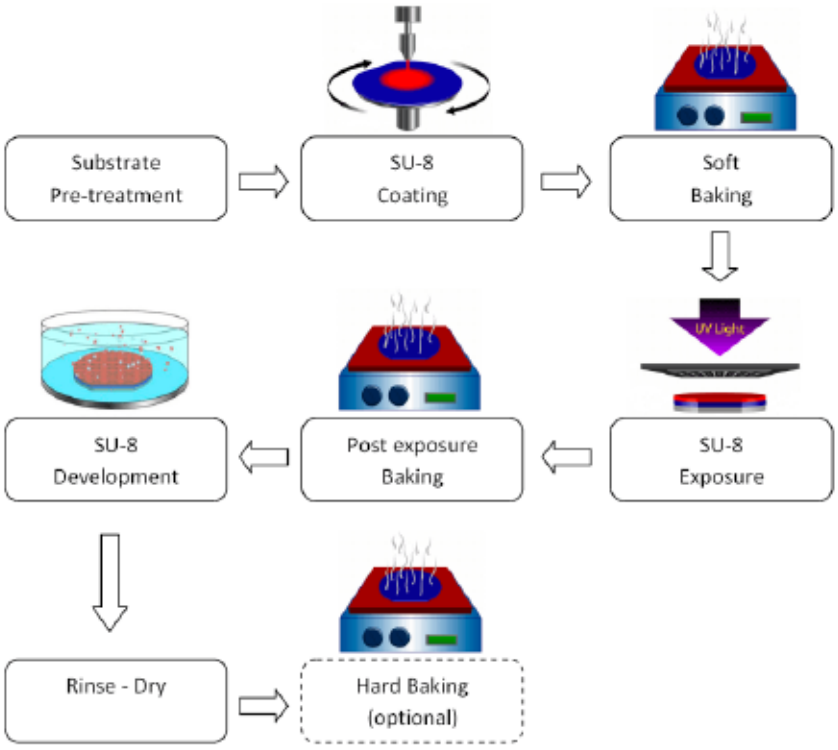

Figure 26. The process of SU-8 master fabrication. (Copyright: elveflow.com). 1) Wafer preparation. cleaning the surface of the substrate (wafer) is required to have a good adhesion of the photoresist with the surface of the substrate. 2) Spin coating of the negative SU-8 photoresist. The common method is the spin coating, using different molecular weight photoresist on a flat clean surface with different rotational speed, can get different thickness of the photosensitive adhesive layer, this thickness determines the height of the internal microstructure of the chip. In addition, there are brush coating method, dipping method, spraying method. 3) Soft baking (first baking of the photoresist). The solvent in the photoresist solution is evaporated by heat, which enhances the adhesion of the photoresist to the substrate. This solid state protects it from the effects of friction with the mask and ensures a sufficient photochemical reaction during the exposure. 4) UV exposure. The mask is placed between the light source, usually using a mercury lamp emitting at 300-500nm, and the photoresist. 5) Post baking (second baking of the photoresist). The patterned substrate is heated again to accelerate the rate of light-induced chemical reaction and to make the three-dimensional pattern stick tightly to the substrate. 6) Development. The developing solution washes away the unexposed photoresist, then remain the final patterns. 7) Hard baking. By further increasing the baking temperature, residual solvents are removed and the pattern cannot slip off. The final master is obtained.

1.5.3.2 The solidification process and PDMS soft lithography

One of the more widespread applications of soft lithography is based on PDMS. This technique uses an elastic mold instead of a hard mold in lithography to produce micro-structures and is known as soft lithography. The emergence of soft lithography and the large-scale application of PDMS materials is an important milestone in the

history of microfluidic chip development. As compared to conventional lithography, soft lithography is more flexible. It can create complex three-dimensional structures, even on irregular curved surfaces.

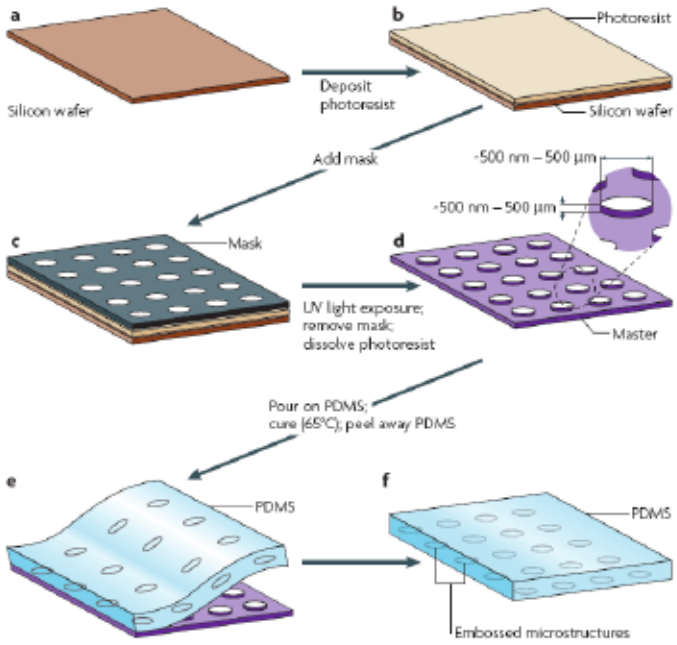

Figure 27. The process of soft lithography (Copyright: elveflow.com)

There are still some limitations in the application of soft lithography in microfabrication, such as the 1% shrinkage deformation of PDMS after curing, and there will be some expansion of the width-to-depth ratio in the presence of toluene and ethane. The elasticity and thermal expansion of PDMS makes it difficult to obtain high accuracy and also limits soft lithography in multifaceted microfabrication; as the elastic mode is too soft to obtain a large depth-to-depth ratio, too large or too small aspect ratio will result in deformation or distortion of the microstructure. However, these are not enough to stop PDMS being widely used in soft lithography, and it is believed that with further research, various ways will be found to compensate for these shortcomings.

1.5.3.3 Substrate bonding

There are many different polymer materials that can be used for microfluidic chip fabrication. The method of bonding is also different. The common bonding methods include hot pressing, thermal or photocatalytic adhesive bonding, organic solvent

bonding, automatic bonding, plasma oxidation bonding, UV irradiation and crosslinker conditioning.

PDMS is relatively well adherent and the micro structured PDMS substrate can be reversibly or irreversibly bonded to the same material or to a variety of different covering materials. If the surface of the PDMS substrate and coverslip is first treated with plasma oxidation or UV irradiation, the PDMS chip can be irreversibly bonded, allowing for a stronger and more durable bond. In addition, by changing the optimal ratio of PDMS polymer and crosslinker so that the ratio of PDMS polymer and crosslinker in the substrate and cover chip are slightly higher and lower, when the substrate and cover chip are bonded together, the polymer and crosslinker are better matched at the junction due to molecular diffusion, which can also improve the sealing solidity.

1.5.3.4 Others machining methods for chips fabrication.

Etching is the method of chemically or physically stripping off the etched material to obtain the desired pattern. The method using chemical etching is widely used for materials such as metals, glass and plastics, but the resolution is poor. In contrast, more precise etching can be achieved using high-energy particle beams, but the instruments are expensive and not commonly used for patterned construction.

1.5.4 The materials used in the field of microfluidics

The materials chosen for the bio-microfluidic chips need to be biocompatible and should have good electrical insulation and permeability to oxygen and carbon dioxide. The light transmission properties facilitate the monitoring of the inside of the chip. Materials commonly used to make microfluidic chips include glass and organic polymers such as polymethylmethacrylate (PMMA), polydimethylsiloxane (PDMS), polycarbonate (PC) and hydrogels. The wide range of polymers, the ease of processing and molding, and the low cost of raw materials make them ideal for high volume production at the laboratory scale and low material costs. There are three main types of

polymers used in microfluidic chip fabrication: thermoplastic polymers, cured polymers and solvent-volatile polymers. Thermoplastic polymers include PMMA, PC and polyethylene; cured polymers include PDMS, epoxy resins and polyurethanes, which are mixed with a curing agent and hardened over a period of time to give the chip. Solvent-volatile polymers such as acrylic, rubber and fluoroplastics are produced by dissolving them in a suitable solvent and then slowly evaporating the solvent to obtain the chip[223, 224].

PDMS material, also known as silicone rubber, is one of the most used polymers, with the following advantages: i) it can transmit ultraviolet and visible light above 250nm, ii) it is permeable to gas, iii) stable under repeated deformations and iv) it has a certain degree of chemical inertness. Moreover, the chip microchannel surface can be modified with a variety of coatings. Finally, PDMS can be molded to replicate the microfluidic chip with high fidelity, not only with itself reversibly, but also with glass, silicon, silica and oxidized polymers reversibly.

Hydrogels [225, 226] are a class of natural or synthetic polymeric materials that are microscopically composed of hydrophilic polymer chains in a three-dimensional lattice-like structure with gaps of typically a few to several hundred nanometers. Synthetic hydrogels are mostly named after their polymer composition. The most commonly used are polyacrylamide (PAAM), polyethylene glycol (PEG), polyvinyl alcohol (PVA) and polyhydroxy ethyl methacrylate (PHEMA). Typical natural hydrogels include agarose gels, gelatine, sodium alginate gels, hyaluronic acid gels, etc. Hydrogels have a range of bulk and surface properties that distinguish them from other materials. The special bulk properties include high water content, high permeability, structural stability and mechanical elasticity; in addition, some hydrogel materials also have good optical properties, such as transparency. The surface properties of hydrogels are mainly reflected in their overall hydrophilic nature. Some hydrogels can be synthesized from aqueous solutions of their monomers by UV or visible light-initiated radical reactions.

Quartz and glass have good electro-permeability and excellent optical properties, their surface adsorption and surface reactivity are conducive to surface modification, and microstructures can be etched onto quartz and glass using similar photolithography and etching techniques to silicon wafers [227]. The high UV transmission and stable surface properties of quartz make it easy to achieve surface modification and are particularly suitable for microfluidic chips for detection. However, due to its high price, it is not commonly used in the organ-on-a-chip field. Glass is often used as a substrate material in organ-on-a-chip. During the sealing process of the chip, the surface of these materials must reach a high level of cleanliness, which usually requires a rigorous chemical cleaning of the chip substrate and cover, and the cleaned chip should complete the bonding process in a clean room. The success of the chip bonding also depends to a large extent on the flatness (total thickness deviation) and roughness of the chip surface [228, 229].

1.5.5 Advances for neural network reconstruction on microfluidics chips

Brain networks topology is tremendously complex and although neuro-anatomy is an historical research field that started in the late 19th century, new neuronal pathways and connections modes between brain areas are still discovered these days primarily through the study of whole brain connectome [62, 67, 77]. The anatomical connectivity of the brain drives the impact of neural circuits on brain function [72]. While brain areas connections can be viewed at a macroscale level with nodes composed of specific neuronal subtypes linked by edges representing axonal tracts, each node is also highly ordered at a micro-connectome level [69]. And the projection of multiple regions in the brain is constructed in a way that cannot be achieved on traditional Petri dishes. Most in vitro studies of neural networks have been performed through the use of brain slicing techniques that allows to study intact networks at the electrophysiological level. However, brain slicing is susceptible to trigger cell death damage and adults slices survives only for a few hours in vitro, thus preventing the study of any chronic

biological process. Compartmentalized microfluidic chips are therefore an interesting complementary model that may allow construction of complex neural (physiological or non-physiological) minimalistic networks that survives for long period of time. Indeed, by compartmentalizing the cells which originate from different regions of the brain and connecting them through microchannels, it should therefore be possible to reconstruct functional network in vitro.

1.5.5.1 The binary neural network reconstruction in microfluidics device

Based on the seminal work of A Taylor and NL Jeon, several groups have been involved in trying to reconstruct networks by seeding 2 different neuronal populations in separates chambers of compartmentalizing devices. Using their initial design AM Taylor et al constructed a hippocampo-hippocampal device [230] to study hippocampal synaptic connectivity. This was progressively followed by the work of many other groups who created a variety of networks composed of different neuronal identities [197]. While this constitute a first step toward building of ordered networks the main drawback of those approaches is that, permitting selection of axons over dendrites, isotropic guiding micro-channels used in the initial Jeon's group allows connections between the 2 neuronal population in a bi-directional manner. An improvement was reached by seeding the 2 neuronal populations at different times or using specific patterning of proteins in the microfluidic chambers [255].

From the above construction of neural networks, it can be concluded that these bidirectional neural networks can respond to stimuli and achieve compartmentalized segmentation of neural networks. While many studies have demonstrated that cells and neurons survive for long term in microfluidic environment, controlling the projection direction of neurons is an absolute prerequisite to envision the construction of neuronal networks in vitro for the study of trans neuronal dialogue or any approach that envision to capture network properties.

1.5.5.2 The geometric strategies for neural projecting direction and the studies on unidirectional neural network

Cells sense their environment through integration of many different types of cues among which mechanical ones are increasingly studied. Decades of research on neuronal biology have evidenced that mechanical cues participate both in the control of neuronal migration and axonal outgrowth, while more recent evidences show that they also control neuronal differentiation. Therefore, geometrical features encoded by soft lithography are very interesting levers that can be used to enforce axonal outgrowth and ultimately permit building unidirectional the network. Compared to other approaches that could prove useful (protein patterning or flowing of chemo attractive or repulsive cues, use of electrical field etc..) the use of mechanical cues allows to encode guiding cues in rather static platforms that are easy to manipulate. Our lab first created an asymmetric axonal guidance "Diodes" that bridges two different neuronal populations. The principle being that axons originating from "emitting" neurons enters faster in the micro-channels than the one from the "receiving" population[231](Figure 28a). This allowed to generates oriented networks with an axonal selectivity of approximately 90%. Using this system, we built unidirectional cortico-striatal network [231-235]. Using that platform, the neurophysiological properties of cortico striatal networks were studied. We also demonstrated that this kind of platform could prove useful as a drug screen tool for evaluate the synaptic protection ability of candidate molecular in damaged neural network[232]. Furthermore, we found the axonal trauma, focal ischemia, or alteration of neuronal rhythms can initiate spreading of dysfunction along neuronal pathways [233]. In cortical-hippocamps networks, we found that β-amyloid [236] can cause presynaptic loss and evaluate the aSyn expression level and pSyn accumulation[193]. Progressively other research teams explored similar approaches to enforces axonal directivity to build modular oriented networks. For instance, Kamudzandu et al. [237] used "Diodes" built neuronal circuit which conclude cortical, substantia nigra (SN), globus pallidal (GP) and striatal neurons.

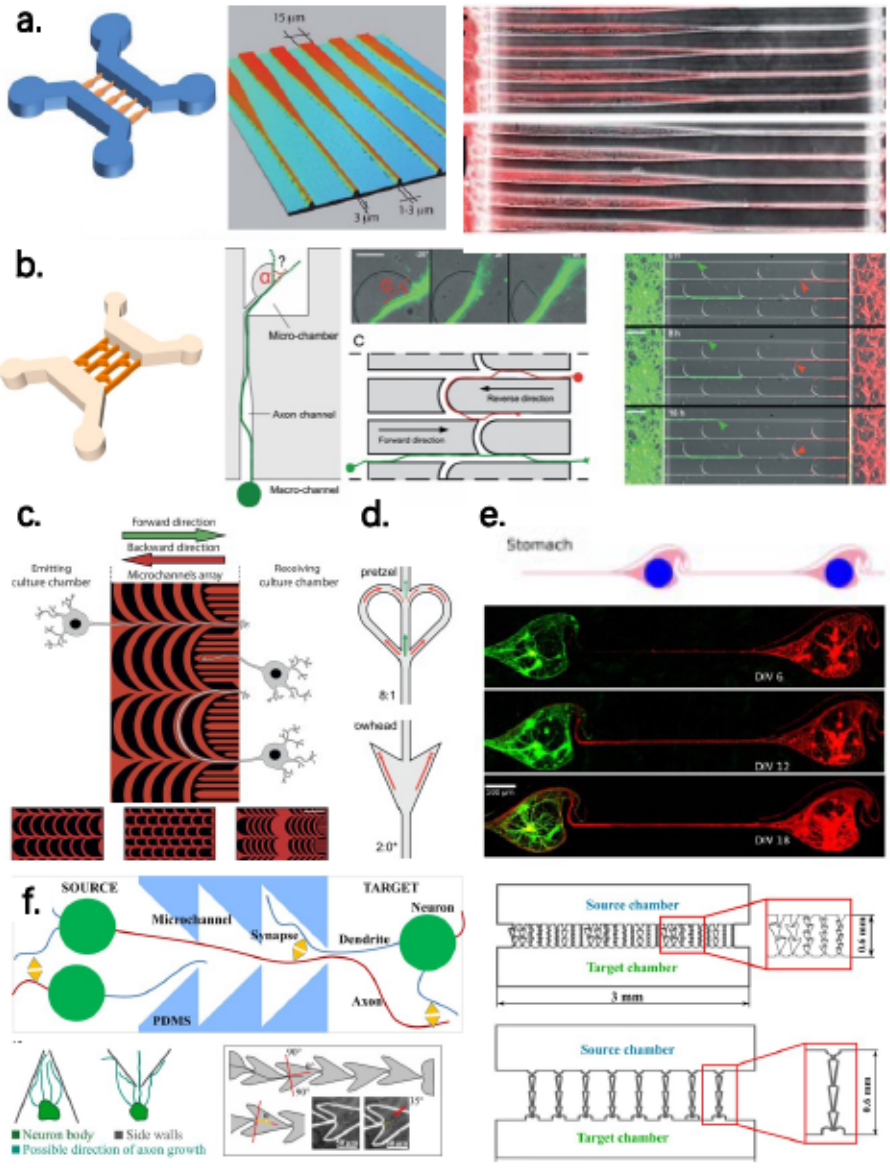

Figure 28. The geometric strategies for building unidirectional neural network. (a) Diodes (Peyrin, 2011). (b-c) Arches (Renault, 2016; Courte, 2018). (d) Arches-like structure (Holloway, 2019). (e) Stomach shape (Forró, 2018). (f) Triangle (Gladkov, 2017).

While "Axonal diodes" were the first demonstration that encoding anisotropic guiding structures could be interesting, extensive biological experiments with different neuronal subtypes showed that the funneling micro-channel shape exhibited limits. Especially for long-term cultures were axons from the receiving population progressively invaded the emitting chambers or with the use of neurons which extends very long axons (e.g. human neurons). In search of alternatives and improvement our labs created another asymmetric geometry enforcing unidirectional guidance in two

chamber microfluidics chips named "Arches" [238](Figure 28b), the principle being that growing axons follow walls and edges and have a tendency to be guided by the direction of the microstructures once they leave it. Therefore encoding "arche" like structures allows axons to cross the structures in one direction while they are deflected back in the other direction. Although the principle differs from the one of the "diode", similar filtration results were obtained. A further improvement was proposed[239] (Figure 28c) that allows full control (100%) of axon directionality and therefore the reconstruction of fully oriented networks [240, 241]. As followed, Holloway et al. used arches-like structure guided the axons growth of primary hippocampus cells in vitro two weeks [242](Figure 28d). Based on improved "Arch" system, we tested the aSyn spreading level in unidirectional hippocampal network [240].

Using a similar philosophy, Forró et al. designed "stomach shape" guiding microstructures for hippocampal axonal guidance[243] (Figure 28e). In their system, they also used MEA to record neural activity of the networks. They proved the unidirectional hippocampal network have highly information transmission. Gladkov et al. designed " Triangle " geometry [210] (Figure 28f), they also built hippocampal network and used MEA to validate the neural activities.

1.5.6 The strategy of neurological disease modelling on microfluidics chips

1.5.6.1 Alzheimer's disease modeling on chips

In the previous sections I mentioned that prion-like mechanism is an important hypothesis in neurodegenerative diseases. The studies of Alzheimer's disease modeling on chip have focused on the spreading of tau and Aβ in network. Microfluidic platforms are being increasingly used by the community of researcher involved in studying neurodegenerative syndromes and their associated molecular mechanisms dysfunctions. Using conventional microfluidics, tau aggregates have been shown to be taken up by neurons and can be axonally transported both in an anterograde and retrograde

manner[244-246]. While Tau oligomers also induce aggregation and phosphorylation they cause neurosynaptic retraction, synaptic loss, abnormal calcium homeostasis and imbalance in neurotransmitter release [244]. Using reconstructed networks in conventional microfluidic platforms tau antibody have been proposed to effectively block Tau uptake, aggregation and trans-neuronal diffusion[247]. For the mechanism of tau transmission, it has been suggested that synaptic activities can enhance the tau transmission to connected neurons via synapses [248, 249] [246, 248], while non-synaptic mechanisms such as exosome release have also been proposed to take part in prionoid spreading [249] [250].

Aβ has been similarly shown to be taken up and to have axonal transport processes [251], and exposure to Aβ can cause neuronal atrophy [252]. Deleglise et al.[236] observed that Aβ induces death and synaptic changes in presynaptic neurons and phosphorylate Tau occurred post-synaptic neurons in reconstructed networks. In addition, Aβ can affect morphological changes in microglia in a co-culture system [253], and it can indirectly triggers astrocytes play a detrimental role on neurons[254].

1.5.6.2 Parkinson disease modeling on chips

Similar approaches have been published to study the "prion like" properties of alpha synuclein. For example, exogenous misfolded α-syn and α-syn fibrillar form have been shown to be transported cis and retrograde in axons[255, 256]. Both forms of α-syn, fibrils and ribbons, were shown to be transported between neurons and could trigger endogenous α-syn aggregation, disrupting synaptic integrity and mitochondrial morphology [257] α-syn oligomers have similarly been shown to have the same toxicity [258]. The mechanism studies of a-syn propagation in neural networks can be found in chapter 4 of my thesis.

Quite surprisingly, neuronal networks reconstructed in microfluidic platforms have been mostly studied to probe "Prion like" propagation of protein aggregated and/or viral spread between neurons. Yet, care should be taken in the interpretation of

some results published with classical (straight channels) microchips as bidirectional connection occurs at various level in these networks therefore mitigating the trans neuronal spread "evidence" that are sometime commented [240, 241].

1.5.6.3 Huntington's disease modelling on chips

Microchip have also been used to model Huntington Disease processes, which etiology (100% genetic) differs from the one of AD and PD (90% Sporadic) [259]. Importantly, Huntingtin, the main protein involved in HD forms intracellular aggregates, is not supposed to hold an efficient "prion like" amplification capacity and therefore do not behave like an amplifying infectious agent. This limits the technical problem raised in the previous chapter (possibility that receiving neurons send some axons in the emitting chamber) therefore making the results obtained through the use of "conventional" microfluidic chips more reliable. Virlogeux et al. [260] used a binary device and reconstructed a Htt diseased corticostriatal network,

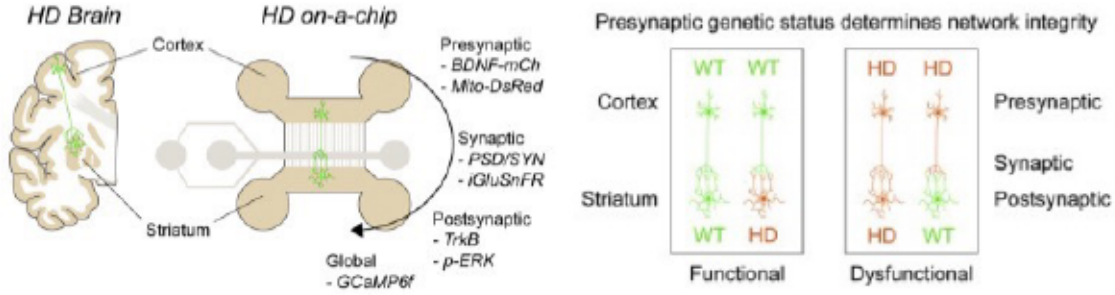

Figure 29. Binary corticostriatal network for Huntington's Disease studies (Virlogeux, 2018)

The modelling of other diseases of the nervous system on MPS or chips is usually based on similar principles as mentioned previously. For example, modelling of micro strokes through the use of chips allowing precise control in time and space of oxygen levels[259]. Increasing numbers of studies also demonstrates the interest of MPS for the study of brain cancer cells dynamic and migration issues [261]. Overall, microfluidic chips and other MPS that enable precise control of the microenvironment, precise arrangement of cells using spatial structure, and powerful integration capabilities have tremendous room for development in neurological disease modelling.

2 Using in-mold patterning technique to reconstruct cortico-striatal neural network and controlling synaptic connectivity *in vitro*

2.1 Introduction

As global ageing of population increases, the prevalence of neurodegenerative diseases arises. The complexity of neural networks in the human brain, which links brain cells in a highly deterministic manner, underlies the diversity of research on neurodegenerative diseases. The main hypotheses regarding the cellular and molecular mechanisms underlying neurodegeneration studies include progressive protein aggregation, cumulative oxidative injury, impaired bioenergetics and mitochondrial dysfunction, disruption of cellular/axonal transport, axonal and synaptic collapse etc. [164]. Notably, most of the molecular scenario being drawn from both cellular and animal models describes cell autonomous processes leading to progressive neuronal death. While non cell autonomous dysfunction is gaining more attention, they mainly focus on neuronal/non neuronal crosstalk dysfunctions. Only a few approaches aim at studying non cell autonomous dysfunction between neurons. This is primarily due to lack of adequate in vitro system. For the study of neurodegenerative diseases, experimental models include animal models, brain slice cultures, and in vitro cell cultures. Animal models preserve anatomical structures but limit experiments at the cellular level. Brain slice culture preserves the structure and cellular level to a certain extent. Still, the slicing procedures can easily damage networks and do not allow for long term culture experiments. While permitting the precise interference and study of molecular scenario, conventional in vitro neuronal culture allows reconstructing random networks which do not model the orderly and deterministic architecture of brain networks. Therefore, techniques that enable the control of connection between isolated neurons to mimic the reconstruction of neural networks have become a hot issue in this field.

Over the past two decades, techniques to manipulate neuronal differentiation in vitro have been expanding. Both micropatterning[262] and microfluidic techniques [263, 264] were shown to be powerful tools to allow the growth of primary neurons in

a constrained environment and control their complex topology. Biochemical constraints like microcontact printing to print substrates with cell adhesive poly-lysine patterns have been used to guide the neurite extension and control the connections of neurons[205, 265, 266]. This has been successfully used to build ordered networks consisting of single neurons on flat and open substrates. Microfluidic chip with precise structure has also been developed as a tool allowing mechanical confinement of axonal growth. Inspired by the "Campenot chamber" developed in the late 70's, the principle of microfluidic cell culture chamber for neurons which allows physical separation of axons terminal from the somatic compartment was first demonstrated in the laboratory of NL Jeon in 2003 [208, 209]. In these studies, 2 cell cultures chambers separated by an array of micro-channels which size is inferior to neuronal somas allows neurons seeded in the first chamber to send their axons along the straight microchannels to the second cell culture chamber. The laminar flow in cell culture chamber and hydrostatic pressure encoded by the microchannels allows selective perfusion by over pressurization of one of the 2 chambers. This innovative design has been rapidly adopted by many neuroscience laboratories and optimized by several laboratories involved in microfabrication. Indeed, besides the advantages of these microfluidic chips allowing somatic and axonal separation, these chips are relatively easy to construct in a highly reproducible manner, allowing the conception of simple or complex multilayer channel systems. Most of the chips being fabricated with a silicon-elastic material PDMS (more detail with this material in chapter1.5.4), they exhibited excellent biocompatibility, optical quality and gas permeation.

The microfluidic device reported in [208] provided the foundation for the development of brain on a chip technology, and more research based on the principles of this chip has emerged over the years. A major issue with the initial design from the Jeon's group relates to the control of neural connection between 2 distinct populations as 2 cell population seeded in the 2 opposed chambers will connect in a bidirectional manner. Mimicking brain pathways requires controlling the directional growth of axons

to obtain unidirectional networks. Not only this would permit to construct deterministic networks capturing some of their in vivo properties but this would prove useful for molecular and cellular studies exploring neurotropic viruses and "prion-like" propagation along nerve pathways (see 1.4.3.1). The design and reconstruction of unidirectional neuronal networks can be suitable for studying how information flows from one neuron to the other (neurophysiology) or eventually the way various key proteins involved in ND syndromes propagate along the neural network (please see more related knowledge in 1.2.2). Our lab has published the first strategy allowing to easily control network topology in vitro. The initial system, called "axonal diode" system (Figure 30a) allows to promotes to some extend unidirectional connectivity of neurons by using funnel-like asymmetrical microchannels to selectively filter axon growth [231]. The principle relies on the increased probability that neurons seeded on the wide parts of microchannels send their axons to the opposite chamber compared to neurons seeded in front of the narrow part of the microchannels. These techniques have been successfully used in in vitro studies aiming at studying neuronal network development and dysfunctions [193, 236, 267, 268], thus paving the way for modelling neurodegenerative syndromes on a chip.

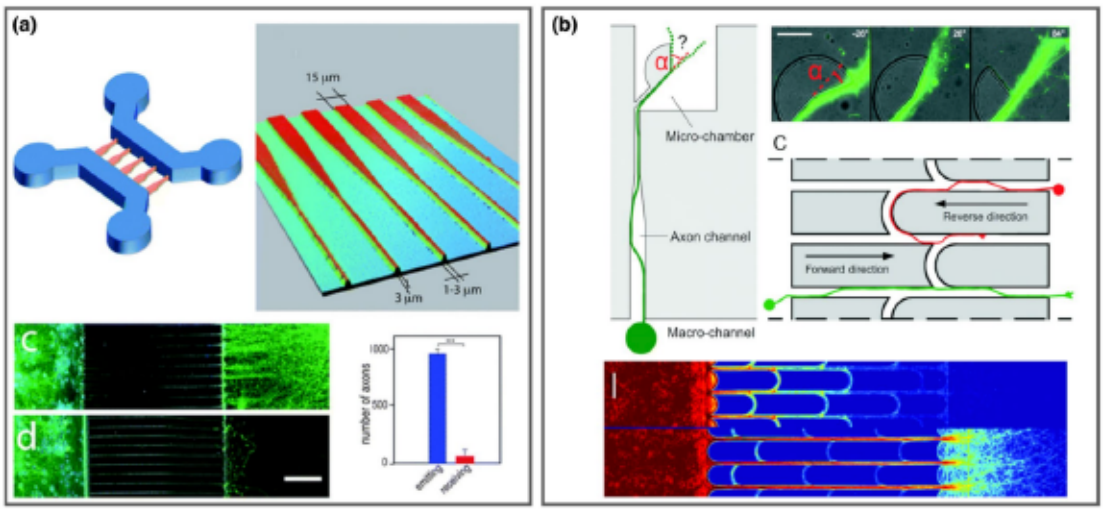

Figure 30. Methods for mechanical axon guidance in compartmentalized microfluidic and construction of unidirectional networks. (a) Peyrin et al. use funnel shaped axonal outgrowth channels to preferentially guide axons from one chamber to the other (Peyrin et al., 2011). (b) Renault et al. exploit an arch shape structure to guide the axon growth and promotes a "return" to sender affect (Renault et al., 2016).

While "axonal diode" structures enable to enhance directional connectivity in, they do not allow to enforce full directionality of the reconstructed networks. Indeed, while initial axonal directionality approximates 90% in forward growth from emitting to receiving chambers, with increasing time of cultures, axons from neurons seeded in the "non permissive" compartment can reach to emitting chambers then leading to a 10% to 20% backward growth.

In order to improve that bias, studying how axons grow when encountering a physical obstacle, our teams described that axon, which tends to follow walls, can be either deflected or guided by an obstacle depending on the contact angle between the axon and the obstacle. Based on this principle, the teams developed a curved channel-shaped structure, named "Arches" structure. (Figure 30 b) [238]. Using the arch structure between the chambers, it is possible for axons from the transmitting chamber to reach the receiving chamber smoothly, while axons from the receiving chamber encounter the guidance of the arch structure, it will fold back into the receiving chamber, thus achieving a higher unidirectional guidance rate than the original "axonal diode" system. Further improvement of the filtrating micro structured barrier by a trial and error procedure led to the generation of a microsystem allowing full unidirectional construction of neural network [239].

While allowing studies requiring the absolute control of axonal directions [240] the "conventional" microfluidic platforms used for brain chip modelling have shown some limitations for the building of complex neural networks that would be composed of several (>2) "nodes". In conventional chip fabrication, the entire surface of the incubation zones, including the microchannels and chambers, were coated with adhesive molecules (usually poly-lysine). Due to the usual width of, neuron chambers (a few hundred of microns), only a low proportion of "emitting" neurons will be able to send their axons to the (asymmetric or not) microchannels and connect to the receiving chambers. This results in a low ratio (5%) of connections between the emitting and receiving chambers, thus impairing efficient and controlled multi nodal

networks to be reconstructed. Hence, how to efficiently guide the majority of axons in the emitting chambers to connect with neurons in the receiving chamber, and how to segment areas where neurons adhere to achieve a higher degree of node-network structure, are further challenges for the construction of neural networks.

Years ago, our labs developed a technique called "in-mold patterning" (iMP) [269] (Figure 31), which incorporates both micropatterning and microgrooves/micro pockets. iMP allows patterning of poly-lysine specifically inside the grooved structure therefore allowing controlled axonal guidance trough chemical and physical constraints. Compared to conventional micropatterning of the poly-lysine alone on flat substratum on the one hand and mechanical constrains provided by the groove alone on the other hand, IMP provides a better axonal constraint on the long term with much less axonal escape from the guides. Yet, in the original study, this technique has not been used to build neural networks. We therefore attempted to use this technique in association with arches structure to reconstruct unidirectional, highly nodal connected neuronal networks in vitro.

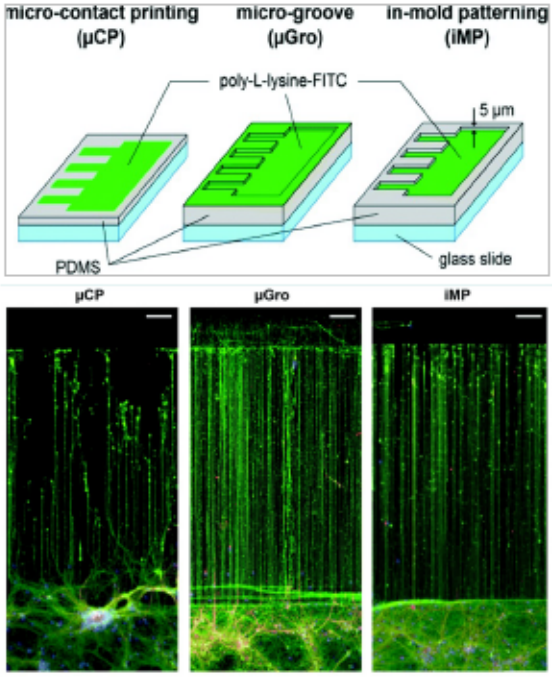

Figure 31. in-Mold patterning (IMP) techniques allows to encodes both mechanical and chemical cues to guide axons in open areas. IMP outperforms classical micro contact printing or mechanical guidance in maintaining axons in specific location for long period of time (from Yamada et al 2016) .

First, we designed a theoretical motif that would allow to control the connection (or not) of 2 nodes composed of 2 distinct neuronal populations in a directional manner with help of guiding structures enforcing exit of the axons from the first node toward the second node. At the microfabrication level, the optimal platform shall comprise a bottom layer encoding the neuronal circuitry through the iMP technique (Figure 32c) and an upper layer allowing fluidic isolation between the nodes (Figure 32b). In Figure 32a, the theoretical motif depicted in darker blue color are the cell trapping areas and axonal grooves coated with poly-lysine while the lighter blue areas represent flat, uncoated PDMS. The white color presents the walls of the three separate cultures chambers corresponding to the 3D representation shown in Figure 32b and e. The only connections between two chambers are the microchannels encoded in the IMP layer.

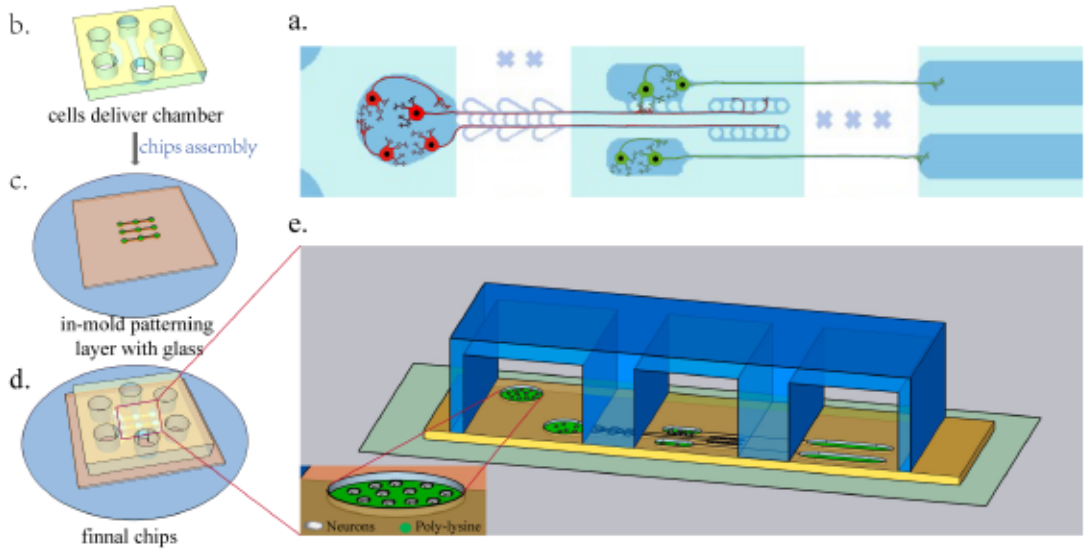

Figure 32. Principle and important structures of the "2 node" in-mold patterning micro-chips. (a) The intersection point between "fins" structures (middle chamber with neurons in green) and straight axonal micro-grooves shall allow physical contact between cortical axons (in red) and striatal dendrite (in green). In principle, these two types of neurons should establish synaptic connectivity around the vicinity of "fins" structure. The purpose of arches-like structures and longer crooked channels is to decrease striatal neurons backward growth. Cortical axons will terminate in the coiled structures. The striatal axon will through straight channel reach the right chamber. (b) Global view of the upper part of the device, which has three compartments. (c) In-mold patterning layer and glass coverslip as substrates for cell adhesion and guidance. (d) The final appearance of the device. (e) 3D Drawing of cross-section of final chips.

Each microchips encodes five 2 nodes networks and four microchips are arranged in one large microfluidic chip, thus allowing replicated experiments. The chips

fabrication follows the process depicted in Figure 33.

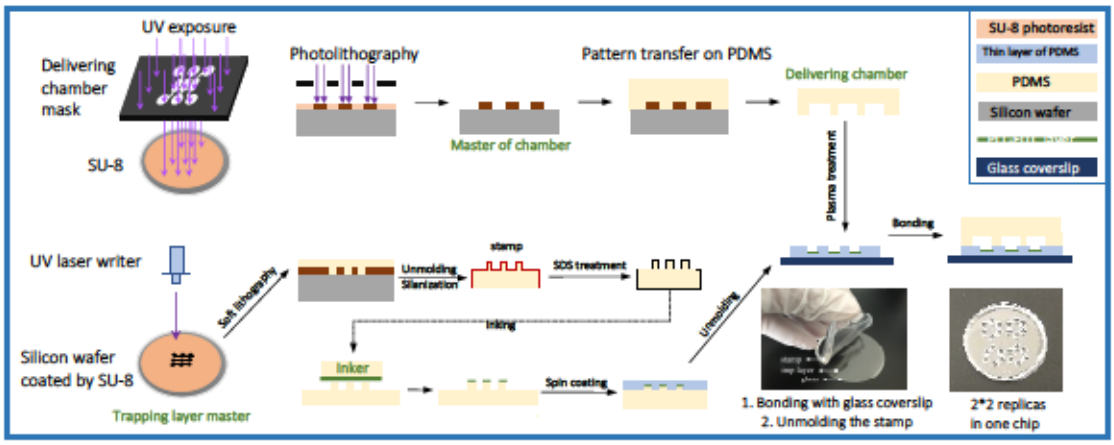

Figure 33. Microfabrication process of 2 nodes chips. Upper part: A silicon wafer encoding the macrochamber was produced by photolithography followed by PDMS soft lithography to produce the upper chambers. Lower part: The in-mold patterning motifs were designed by laser writer allowing to produce a stamp. The stamp was then inked with a solution of poly-lysine to promotes PLL adhesion on the areas of interest. Next, uncured PDMS was spincoated on top of the inked stamp and let at RT until PDMS is cured. The resulting hybrid layer was bonded on top of a glass coverslip and the stamp was removed by peeling, letting the final, coated iMP layer bonded to the glass coverslip. Finally, the macrochamber (treated by plasma) was aligned and bonded with the iMP substratum.

Using the technology presented here, we were able to reconstruct Cortico-Striatal network where small populations of cortical axons are unidirectionally connected, or not, to pockets of striatal neurons which itself send their axons in a third, fluidically isolated, chamber. A simple functional neural network was thus reconstructed. The establishment of this neural network may provide an effective model for subsequent studies of the propagation of abnormally folded proteins in neural networks, mimicking the mechanisms of disease and providing potential drug screening functions.

2.2 Methods and Materials

2.2.1 Structure and principle of the in-mold patterning chips

The chip includes multiple independent nodes in the same microfluidic chamber (both emitting and receiving), each emitting node being connected to a receiving one. The upper layer consists of a large chamber used for cell delivery and compartmentalized media renewal. The lower layer consists of a glass substratum on

top of which a thin layer (75µm) of PDMS encoding the IMP design (5µm depth) is bonded.

The microchip designs capitalize on previous studies showing that i) both axons and dendrites can travel in microchannels and grooves, cortical dendrites not being able to grow more than 400µm. ii) Axons are guided by walls of microgroove or channels and follows walls which deflection angle is not more than 40°.

The nodes in a given chamber are independent and do not connect to each other, only sharing the same culture medium. The nodes in different chambers are connected by microchannels in the bottom thin layer. Thanks to fluidic isolation there is no liquid exchange between the two chambers, thus allowing cell culture medium compartmentalization. Axons from neurons seeded in the emitting chambers will extend in the cell traps and find the arche-like guiding microgrooves which reach the second "receiving" chamber, pass by pockets of striatal neurons and ultimately reach an "infinite" circular loop. Oval shaped cell pockets in the second cell culture chambers have 2 microgroove exits. The first one shall allow striatal neurons to send their axon in a third cell culture chamber. The second one is constituted of small microgrooves connecting the cortical axons microgroove tracts. Cortico-striatal connection occurring in fins structure, this shall allow Striatal dendrites to extend to the cortical axons' tracts.

In addition, independent nodes in the emitting chamber not being linked to any microgroove guiding tracts have been positioned. They shall enable more "independent" data acquisition and observation and increase number of neurons seeded in the emitting chamber thus improving cortical neurons survival by allowing cell culture media conditioning by neuron derived pro survival factors.

2.2.2 Micro-Chips Fabrication

The designs of each layer chip patterns were drawn using Clewin5 software. The plastic masks with high resolution of the delivery chamber were printed at IPGG Microfluidic platform.

2.2.3 The process of in-mold patterning chips fabrication

2.2.3.1 The silicon wafer for macro-chamber fabrication.

A 4-inch silicon wafer was spin-coated with 4ml negative photoresist SU-8 2050 (MicroChem) at 3000 rpm for the 30s, then soft-baked for 1min at 65°C and followed by 6min at 95°C. After the wafer cooling down to room temperature, it was exposed 14s under UV light (MJB4 Mask Aligner, wavelength: 365nm, energy: 16.8mW/cm2) through the delivery chamber photomask. And then baked for 2min at 65°C and followed by 7min at 95°C. The master was developed in PGMEA at 60 rpm for the 6min and dried with pressurized nitrogen. A final "hard bake" was performed for 5 mins at 200°C.

2.2.3.2 The silicon wafer of IMP trapping layer

A 4-inch silicon wafer was spin-coated with SU-8 2005 (MicroChem) at 2500 rpm for 30s, then soft-baked for 2 mins at 95°C. After cooling down to room temperature, the wafer was loaded in a UV Laser Writer (Heidelberg μPG 101) to promotes local SU8 polymerization according to the chips blueprints. The resulting master was post-baked for 3 mins at 95°C followed by development in PGMEA under 60 rpm agitation for 45s and finally dried with pressurized nitrogen. A final hard bake was performed for 5 mins at 200°C.

All above masters' dimension were characterized by an optical profilometer (Veeco Wyko NT9100).

2.2.3.3 Soft Lithography of the (upper) cell delivery macrochamber and IMP stamp fabrication

Polydimethylsiloxane (PDMS, Sylgard 184, Ellsworth Adhesives) base was mixed with its curing agent as ratio of 10:1, and degassed under vacuum. The mixture was poured on the silicon master surrounded by aluminium and incubated at 70 °C， 3h for the macrochamber and 2h for the stamp. After unmolding, using the 4mm dimeter

punch to make the wells on delivery chamber, and cleaning it very well to keep for chips assembly.

2.2.3.4 The PLL-FITC Inker preparation

7-8ml of the mixed polydimethylsiloxane were poured in a 5cm petri dish, baked into an oven at 70 °C for 10 hours, and further cooled down to the room temperature. The PDMS was incubated with 10% sodium dodecyl sulfate (SDS) solution for 15mins, rinsed with water and further incubated with a 100µg/ml PLL-FITC solution for 1h. The inked PDMS was then dried with pressurized nitrogen. The dried inker was sliced in 5mm*5mm small square blocks.

2.2.3.5 The stamp fabrication of trapping substrate

The stamp was placed in O_2 plasma machine (FEMTO, science, CYTE) with pattern side above (exposed to plasma). After plasma treatments, the stamp was silanized using (Tridecafluoro-1,1,2,2-tetrahydrooctyl) trichlorosilane (AB111444, abcr) for 30mins.

2.2.3.6 IMP layer trapping substrate fabrication

The stamp was immersed into 10% SDS solution for 30min, rinsed and dried with pressurized nitrogen. Next, the stamp was inked with poly-lysine by gently contact with the dried inker without any pressure. Then the inked stamp was spin coated with fresh PDMS at 1000rpm for 45s, and baked at 70°C for 75mins to promote PDMS curing.

Glass coverslip were cleaned with iso-propanol, treated with plasma and attached to the IMP stamp. After 5mins of contact, the stamp was peeled off, generating a final IMP bottom layer ready for further assembly with the top delivery chamber.

2.2.3.7 Chips assembly

The cell delivery macrochamber was treated in a plasma oven and immediately (not more than 10s) manually aligned and bonded with the IMP layer, and pressed for

bonding for approximately 30s. Final micro-chips were then immediately filled with PBS through the punched reservoirs (appropriate liquid flow in chamber is monitored by eyes thus ensuring the device hydrophily is adequate for further biological experiments. The final microchips are kept in 5cm petri dish, sterilized with UV illumination, covered and sealed for storage in a fridge until use.

2.2.4 The preparation of primary neurons cell suspension

E14 Pregnant WT Swiss mice were purchased from Janvier Lab (Le Genest Saint Isle, France) and sacrificed the day of delivery for neuronal cultures. The C57BL/6J tdTomato and GFP mouse lines were supplied by Institut Curie animal facility. The study was carried out in accordance with European Community guidelines on the care and use of laboratory animals: 86/609/EEC, and the standard ethical guidelines of local institutions at Sorbonne University.

Cortical and striatal regions of E14 embryos of WT SWISS mouse (Janvier Labs), C57BL/6J tdTomato mouse and GFP mouse were micro-dissected under the microscope in the cold Gey's balanced salt solution (GBSS) supplemented with 0.1% glucose (w/v). Cortical and striatal dissected structures were separately rinced 2 times with GBSS. Cortices were incubated at 37 °C with 5ml of 5mg/ mL papain (Sigma 76220) in Dulbecco's Modified Eagle Medium (DMEM, Thermofisher 31966 021) supplemented with 100 units/mL penicillin-streptomycin for 8 min. Papain was then inactivated by adding 500µl of Fetal Bovine Serum (FBS, GE Healthcare), followed by 2 mins incubation at room temperature. Brain tissue was allowed to sediment and dissociation medium was removed and replaced by 5ml of fresh DMEM containing 20ul of deoxyribonuclease (DNAse, Sigma D5025). The tissue was mechanically dissociated by pipetting. Following a similar procedure, striatal tissue was incubated with 2ml GBSS supplemented with 1mL of Trypsin-EDTA at room temperature for 10mins. Trypsin was then inactivated by adding 1ml DMEM, 300ul FBS and 20ul DNAse. The striata were then mechanically dissociated by pipetting. Cortical and

striatal neurons were recovered by centrifugation (80 g, 7 min) and counted with a Malassez counting device. Neurons were resuspended at final concentration in Neurobasal complete culture medium containing 5% FBS and 2% B27 neural supplemented (Invitrogen). Final concentration for Cortical cell suspensions was 30 million cells per milliliter, and the striatal cells suspensions was 20M/ml.

2.2.5 Cell seeding and culturing

The micro-chips were sterilized by UV light (15mins) before took to cell culture room. PBS was removed from micro-chips reservoirs. 6µl of cortical neurons cell suspension were introduced in the upper wells of emitting (left) chamber. 6ul of striatal neurons cell suspension were introduced in the upper wells of the middle chamber, and the right chambers were filled with 6µl of culture media with no cells. The seeded cells flow into the cell culture chamber from upper to lower well and rapidly settled on the cell culture (IMP) substratum. Seeded suspension let to settle for 25 mins permit strong adhesion to the IMP PLL area, the non-adherent cells were removed by flowing fresh cell culture medium in the devices. After filling the microchips reservoir with complete medium, chips were placed in an incubator at 37 °C with 5% CO2 for long term culture. In order to avoid evaporation of media from the reservoir, water was placed in the 6 cm holding petri dishes. 24 hours after seeding, initial cell culture media was replaced by FBS free Neural basal medium containing 2%B27. The medium was half-changed every 6-7days.

2.2.6 Live-Imaging of Calcium activity

Cortico Striatal networks were recorded for calcium transients after 12 to 14 days of culture. To start calcium live-imaging recording, two buffer should be prepared before experiments [235]. Recording (rinsing) buffer preparation composed of NaCl 116 mM, KCl 5.4 mM, MgSO4 0.8 mM, CaCl2 1.8 mM, NaH2PO4 1.3 mM, Glucose 10 mM, Hepes 10 mM, bicarbonate 25 mM, glycine 10 µM dissolved in sterile water. Loading buffer preparation: recording buffer supplemented with 2 µM Fluo-4 calcium

indicators and 1/1000 dilution of a 20% pluronic F68 acid dissolved in sterile water. The loading buffer should be freshly made for each experiment.

When the cell cultures are mature for recording cell culture medium was gently removed with a pipette, and networks were washed with rinsing buffer. Networks were then incubated with loading buffer for 10mins at 37 °C, 5% CO2 environment. Networks were then washed with recording buffer, and recorded under an inverted epifluorescence microscope (Zeiss Axio-observer, 5X or 20X objective, Coolsnap HQ CDD camera). Areas of interest were selected with a 5x objective and time laps imaging was recorded at a 500ms frame rate (0.5 Hz) with a 200ms acquisition time. Movies were acquired so that both emitting and receiving chambers could be recorded at the same time allowing further analysis for intra node synchronous activity.

2.2.7 Calcium activity analysis by FluoroSNNAP software

The data (images stacks) were processed under MATLAB environment by using Fluorescence Single Neuron and Network Analysis Package (FluoroSNNAP, Tapan Patel, University of Pennsylvania) [270]. Following the FluoroSNNAP user guide. Briefly R.O.I's representing entire nodes were automatically selected and variation in Fluo4 fluorescent signal intensity was quantified over time. This generated raw calcium traces that were further normalized through the use of FluoroSNAPP internal dF/F0 internal functions. Bursting peaks were then isolated by selecting up states that were higher than 3 standard deviations over noise, allowing raster plot representation.

2.2.8 Immunofluorescence staining and imaging

Cell culture medium was removed and replaced by 4% paraformaldehyde (PFA, Electron Microscopy Science) and 4% sucrose (Sigma) dissolved in phosphate buffered saline (PBS, Thermo Fisher) for 15mins at room temperature. After rinsing with PBS, the chips incubated with 1% bovine serum albumin (BSA, Sigma) and 0.2% Triton X-100 (Sigma) PBS solution for 45mins to allow both saturation and permeabilization. After removing the saturation solution primary antibodies diluted (1/500 in 1% BSA

PBS solution was introduced. These primary antibodies were anti-microtubule associated protein 2 (MAP2, IgG1, sigma, M4403), anti-β-Tubulin Isotype III (TUBB3, IgG2b, sigma, T5076), Bassoon (IgG2a, Abcam, SAP7F407), Homer1(IgG1, Synaptic System,160011), VGLUT1 (Rabbit, Sala El Mestikawi's lab), and Phospho-p44/42 MAPK (Erk1/2, Rabbit, Cell Signalling Technology, 4370). Chips were covered with aluminium foil and incubated at (4°C) overnight. Micro chips were then washed with a PBS rinsing step and further incubated with species specific secondary antibodies diluted at 1/500 in 1% BSA PBS solution for 45min at RT. These secondary antibodies are corresponding with isotype of primary antibodies, which conjunct to Alexa Fluor 365, 488, 555 or 633 (Thermo Fisher). In order to probe cell nuclei, Hoechst (Sigma, 33342) can be added to secondary antibodies solution with 1/5000 dilution. After rinsing by DPBS, the chips were imaged by an Axio-observer Z1 (Zeiss) fluorescence microscope, which equipped with a CCD camera (CoolsnapHQ2, Ropert Scientific) through a 5X, 20x, and 63x objectives and was controlled via Metamorph software. All imaging data were processed using Fiji[271] Imaging software. The chips were stored at 4°C in PBS solution containing 0.1% azide before eventual analysis.

2.3 Results

2.3.1 The PLL-FITC inking and cell trapping performance

2.3.1.1 The poly-lysine patterning of the IMP cell trapping layer and cell capture in the initial 2 hours

To study the results of microfabrication process and IMP patterning efficiency, we used fluorescently labelled PLLs during the IMP layer fabrication. After full chip assembly, microscope imaging showed the distribution of PLL patterns in the chips (Figure 34). A long trial and error optimization process of the IMP patterning technique led to the validation of stable protocol allowing reproducible production of microchips. The results demonstrated that the patterns are well defined and are also intact for relatively narrow microchannels. The complexity of the optimization is underlined by

the fact that resolution of patterns ranges from 5µm (microgrooves) to 3000µm (some large cell culture pockets) and that several independent networks are patterned in a single micro-chip (Figure 34d). Figure 34 shows representative image of chips produced with optimized protocol. Overall, our IMP patterning protocol allows good and homogenous PLL patterning in all the area of interest with barely no interruption of the PLL pattern. Due to some amount of PLL was insert into PDMS by spinning coating process, thus FITC-PLL signal intensity was not measured. Figure 34e and f show cortical neurons and striatal neurons seeding 2 hours after seeding primary neuronal cells in chips.

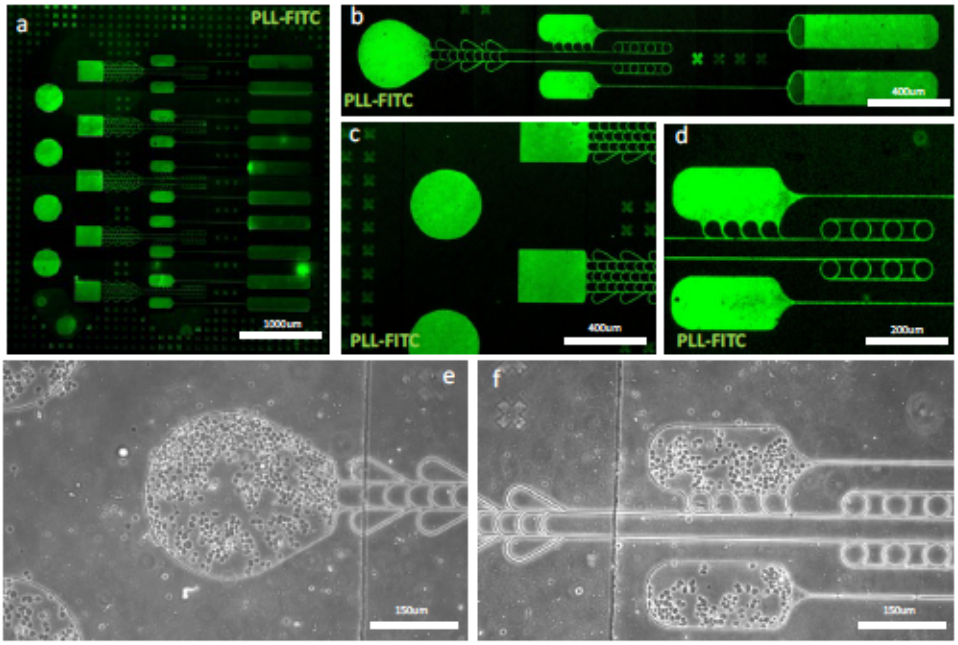

Figure 34. IMP layer Fluorescent PLL Pattern and Cell trapping efficiency. (a) Micrograph of a complete microchip encoding 5 minimalistic networks. (b) Higher magnification picture of a single minimalistic iMP network (c-d) Left, magnification of emitting nodes. Right, Magnification of Receiving nodes, the upper one being connected to the axonal grooves originating from the emitting node. (e) Freshly dissociated cortical neurons seeded in the emitting chamber after 2 hours. (f) Freshly dissociated striatal neurons seeded in the receiving chamber after 2 hours.

2.3.1.2 Cells trapping efficiency and final cell density in emitting and receiving chambers.

In order to estimate the efficiency of IMP protocol on local cell trapping in the areas of interest, the number of cells which adhered in the emitting and receiving

chambers were quantified after seeding with neural primary cells for 2 hours. Each micro-chip contained 11 individual cortical traps (6 non connected and 5 connected) and 10 striatal pockets, constituting 5 individual minimalistic cortico-striatal networks (each cortical pockets linking or not 2 striatal pockets). We therefore quantified the trapping efficiency in each single node. The efficiency of cells being captured for cortical and striatal neurons were 86.36% and 87.8% respectively (Figure 35a) (>10 independent experiments). In routine experiments a mean of 260 (round-like traps) and 220 (square traps) cortical neurons were seeded in each trap while a mean of 223 striatal cells adhered in the pair of receiving chambers (Figure 35b). The final trapped cell density was correlated with the initial seeding concentration. Hence, for further use, the seeding concentrations were fixed at 30 million/ml for emitting chamber (corresponding to 33 cells per 1 $\times 10^4$ μm^2 of round-like traps and 35 cells per 1 $\times 10^4$ μm^2 of square traps), and 20 million/ml for receiving chamber (35 cells per 10000μm^2 of ellipsoidal traps) (Figure 35c).

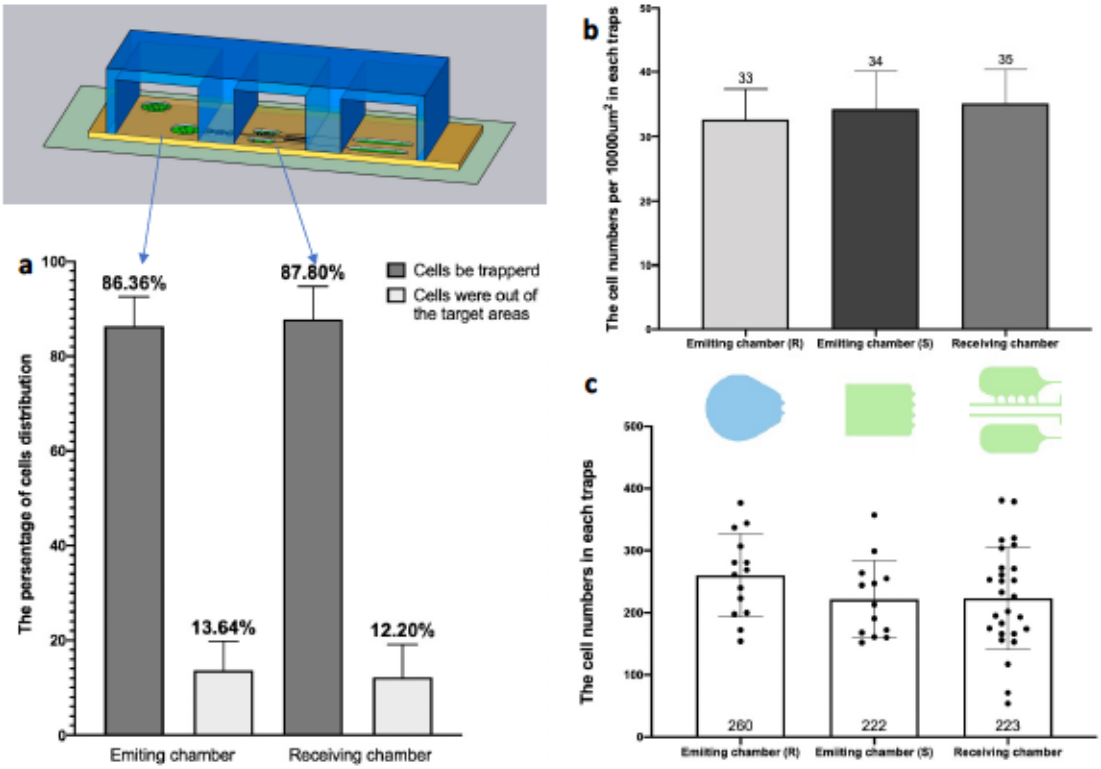

Figure 35. Cell trapping quantification and cell density in each chamber 2 hours after seeding. (a) Percentage of brain cells trapped inside PLL coated areas (dark grey) versus outside the PLL areas (light

grey). (b-c) Quantification of final cell density (b) and cell number/trap (c) in traps located in both emitting and receiving chambers.

2.3.2 Topographical control of reconstructed neural network

2.3.2.1 Axon guidance and tracing

After 3 to 4 days in vitro, neurons positioned in the traps and have extended dendrites and growing axons. In order to visualize the whole neuronal architecture of the reconstructed networks, cortical and striatal neurons from fluorescent Tomato transgenic mice were seeded in their respective chambers. As shown in Figure 36 both neurons and growing axon are well confined by the traps and that axons tends to follow the walls/edge of the cell culture traps. Neurites finally entered to the exiting microgrooves. Importantly no axon escaped also from the traps and guiding micro-grooves. The fins structure in the receiving chamber encodes a curved microgroove that links striatal pockets to cortical axonal grooves. As shown in Figure 36c the curved "fins" efficiently guides the striatal neurite to the axonal grooves. The second exit of striatal pockets is a straight microgroove that reach the 3thd cell culture chamber which is progressively invaded by the extending neurites from the striatal neurons (Figure 36d).

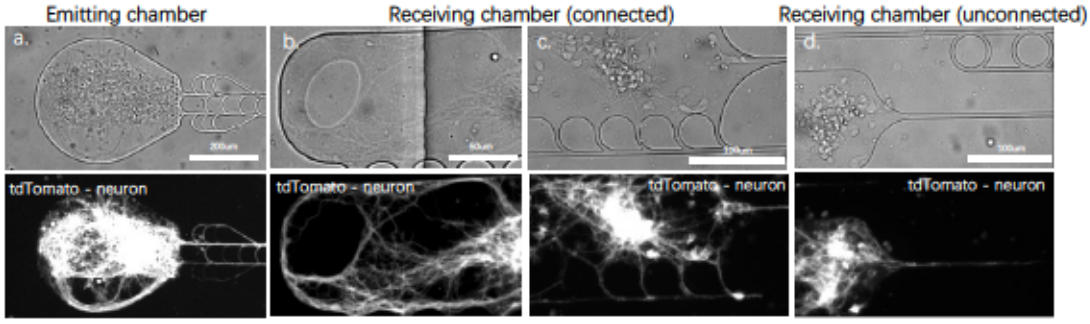

Figure 36. Representative image of tdTomato fluorescent cortical neurons seeded in the emitting nodes (a); and tdTomato fluorescent striatal neurons seeded in the receiving nodes after 6DIV (b, c, d). Note that neurites are strictly confined in the traps of emitting (a) and receiving chambers (b) with neurites being guided by "fin" structures (c) and axonal tracts (d).

2.3.2.2 The encounter of two groups of neurons

We recorded axonal outgrowth between 4 days and 6 days in vitro. Starting from

5 DIV, arch structures are progressively invaded by axons originating from the cortical pockets (Figure 37) with barely no escape of cortical axons from their initial pocket. After 6 DIV cortical axons bundles constrained in the microgrooves reach the area of striatal pockets after which they pass by that area and keep growing toward the circular "infinite" wrapping area. Analysis of several networks seeded with Td Tomato transgenic neurons shows excellent axonal confinement in the axonal grooves with not escape up to 2 weeks in vitro. On the other hand, striatal neurons are well confined in the striatal pockets and efficiently send neurites to the axonal grooves as well as axons (>400µm length) in the 3thd cell culture chamber.

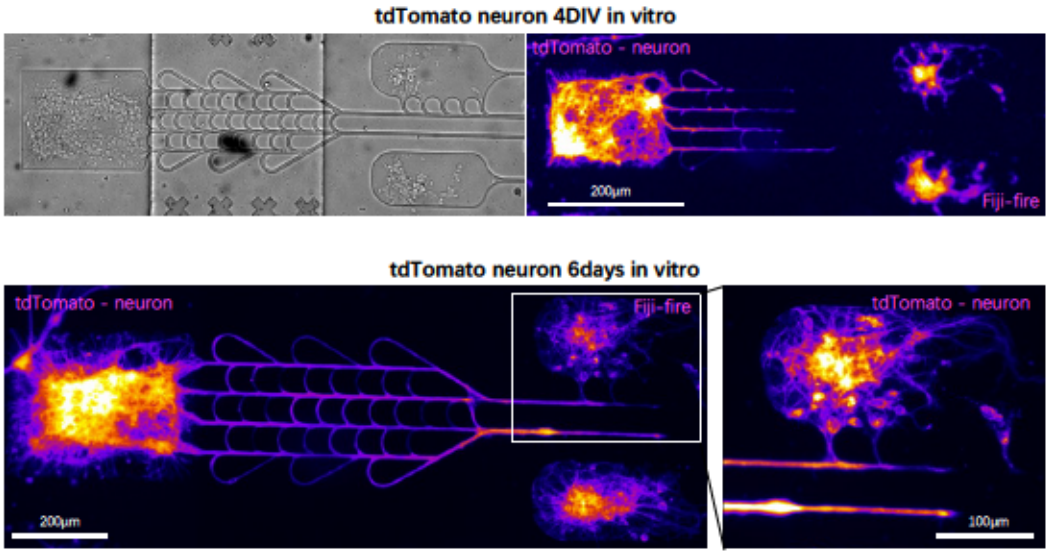

Figure 37. Progressive axonal invasion of tdTomato fluorescent cortical axons trough "arch" guiding structures between DIV4 (upper) and DIV 6 (lower).

2.3.2.3 The topography of axon confinement in mature network

错误!未找到引用源。 below shows several micro-networks grown in the same chips after 13 days in Vitro. Networks were stained with β-III-tubulin, highlighting the axonal compartments.

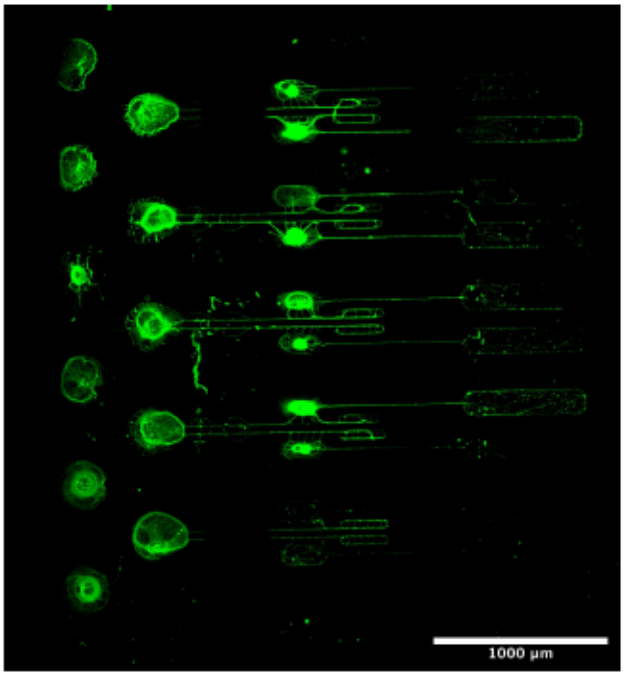

Figure 38. Representative image of a full scan of a single device encoding 5 minimalistic networks seeded with GFP fluorescent cortical and striatal neurons after 13 DIV.

2.3.2.4 Quantification of topographical distribution of neuritic extensions in various areas of the microchips

For a two-node neural network, the unidirectionality of the neural network is an important aspect. We therefore undertook single-chamber seeding to evaluate the paths distribution of cortical and striatal extensions in the guiding tracks, and therefore assess the effectiveness of the pattern in guiding axon growth to their expected location.

Quantification of Anterograde Cortical shooting toward striatal pockets. After two weeks of cultures, a time by which cortical axons have reached the circular "infinite" loop, cortical neurons seeded in the emitting chamber were fixed and stained. As described earlier, before reaching the final loop area, each cortical path passes by 2 pockets of striatal neurons one connected through "fins" structure to axonal groove and one unconnected receiving trap. Quantification of cortical axonal location at the vicinity of the striatal traps connected to through "fins" to the striatal traps shows that 23.33% of striatal traps were invaded by cortical axons and 76.67% of them did not contain any cortical material, with cortical axons being confined in their grooves up to the twining

in circle loops (Figure 39). No cortical axons were able to reach the striatal pocket in absence of "fins" connecting structures (Fig40), cortical axons being confined to their tracts and "infinite" loops.

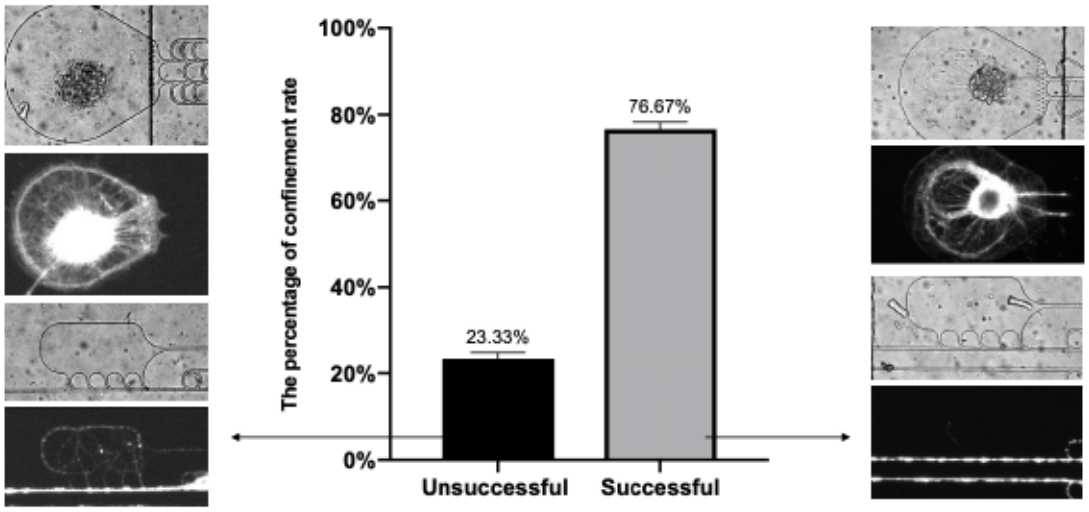

Figure 39. At DIV12, cortical axons from GFP neurons exhibit 2 behaviors at the vicinity of striatal pockets by invading (left) or not (right) the striatal pocket through the connecting "fins" microstructures. (center) quantification of percentage of striatal traps exhibiting cortical axons (unsuccessful) or not (successful). Data from 3 Independent experiments (one experiment=4 chips ; One chip=5 mini networks.

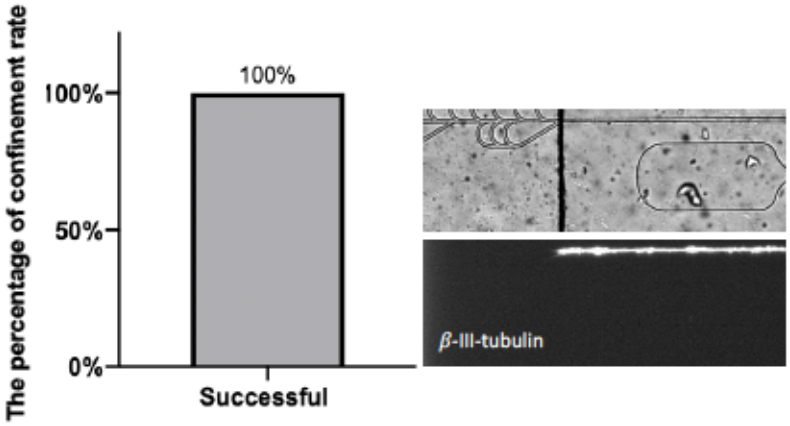

Figure 40. Cortical axons from GFP neurons forward growth toward striatal pockets containing no "fin" strictures at DIV12. Cortical axons are confined in their guiding tracts and do not invade the striatal pockets. Data from 3 Independent experiments (one experiment=4 chips; One chip=5 mini networks).

These experiments demonstrates that cortical neurons are efficiently guided toward the striatal pockets and that IMP allow exquisite axonal confinement in the guiding tracts. Communication between the cortical axons and striatal pocket is efficiently controlled by the presence of "fins" connecting micro-structures.

Quantification of Retrograde Striatal shooting toward cortical pockets. We next assessed the potential retrograde shooting of striatal neurons back to the cortical chambers. Under the same experimental conditions, the chips were seeded with primary cells in the receiving chamber and analyzed after 2 weeks of culture (Figure 41). We analyzed the distribution of striatal neurons according to two main criteria 1) "Forward" Axonal invasion of the cortical axonal tract (from "fins" to circular loop) and 2) Retrograde striatal axon invasion of the cortical pockets, in both the "connected (trough "fins" or not connected configuration.

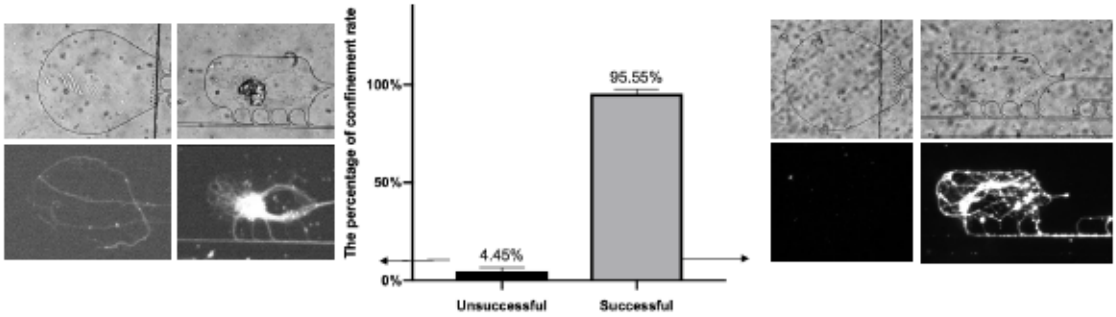

Figure 41. Behaviors of axon from neurons seeded in the pockets from receiving "fin" connected or chambers; (Left) axons invading the emitting chamber, (Right) axons invading the forward cortical axonal tracts. (Center) quantification of backward growth from "fin" connected receiving chamber to the emitting chamber. 4.45% of the emitting chambers evidenced one or more axons originating from the receiving chambers. Data from 3 different experiments. (One experiment=3 chips; One chip=5 mini network)

As shown in Fig41, 4.45% of the neural networks exhibited striatal axons that reach retrogradely the emitting chamber despites the presence of arch-like structures. This shows that the filtering efficiency of the fins and arches structure for unidirectional axon guidance reaches 95.55%. Likewise, no axons from neurons seeded in receiving (striatal) chambers that were not connected through "fins" were able to reach the emitting chamber (Figure 42).

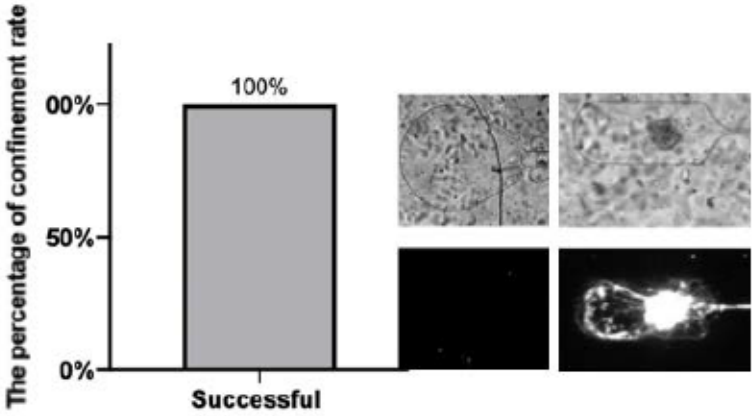

Figure 42. Quantification of backward growth of axons from neurons seeded in the unconnected receiving chambers; virtually no network exhibited retrograde axonal growth in such conditions. Data from 3 different experiments (one experiment=3 chips; One chip=5 mini networks).

Overall, after 2 weeks of culture; the minimalistic networks exhibited good topological control of inter node connections. For forward growth axons from emitting chambers were efficiently guided toward receiving pockets. Out of the successful (good survival) networks, at striatal pocket vicinity, 76.67% exhibited intact cortical axons confined on the cortical tracks while; 23.33% of the networks exhibited slight invasion of the receiving pocket. Regarding retrograde (unwanted) shooting from the receiving chambers back to emitting ones only 4.45% of the reconstructed networks exhibited emitting chamber invasion. We therefore conclude that approximately 90% of the seeded minimalistic networks exhibit the appropriate "anterograde" topology.

2.3.3 The survival behaviour of neurons and synaptic connectivity.

After 6 days in vitro, networks were stained for assessing integrity of axonal, dendritic and nuclear compartments (**错误!未找到引用源。**). Neurons trapped in both the cortical and striatal pockets shows good differentiation with intact dendritic and nuclear compartments. Importantly, the image shown in Figure 43 is representative of "healthy" networks (as determined with phase contrast microscopy). The survival of reconstructed networks was generally homogeneous in a single chip, but some variability occurred between the chips of the same fabrication batch. This variability

arose mostly from chip leaking and incorrect initial cell seeding density.

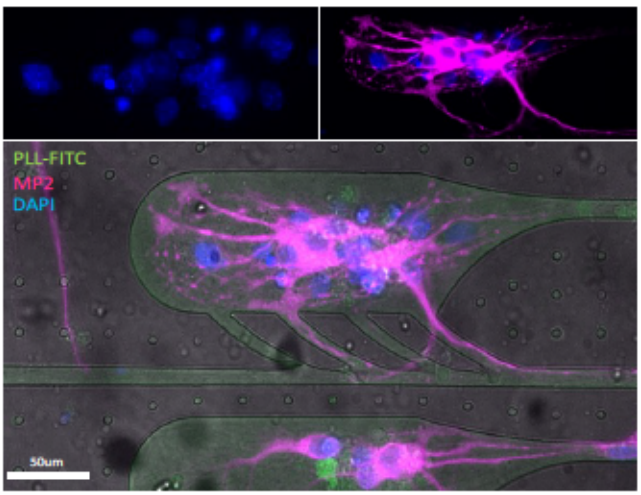

Figure 43. Striatal neurons differentiation in receiving chambers after 6DIV. Striatal neurons growing on FITC labelled PLL, were stained with MAP2 (dendrites) and DAPI (nuclei). Note that Striatal dendrites invades the whole striatal pockets with some dendrites invading the cortical axonal tracks.

We next assessed survival and differentiation at longer time of culture. As shown on Figure 44, 14 days neuronal cultures seeded at low density shows exhibited excellent neuronal survival both in both cortical and striatal nodes with no signs of spontaneous axonal degeneration. Staining the networks with bassoon (pre synaptic marker) and Homer1 (post synaptic marker) antibodies allows to evidence pre and post synaptic puncta in the cortical and striatal nodes. Interestingly strong synaptic puncta were evidenced at the junction between striatal dendrites and cortical axons tracts, suggesting that pre and post synaptic connections occurs between both neuronal types in the minimalistic networks.

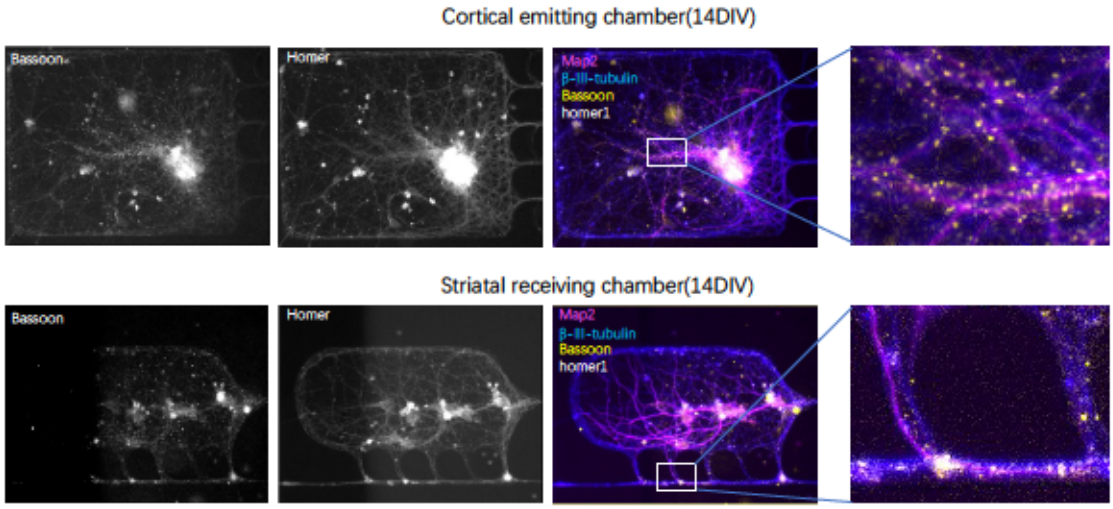

Figure 44. Representative immunofluorescence of axonal and dendritic arbours and synaptic markers of 14 DIV cortico-striatal network. Neurons from both emitting (upper lane) and receiving (lower lane) pockets were stained for axonal β3 tubulin (blue), dendritic MAP2 (red), pre-synaptic Bassoon compartment (yellow) and post synaptic homer compartment (white). Note the strong pre and post synaptic clusters in the "fin" structures at the vicinity of theoretical contact zone between striatal dendrites and cortical axons.

2.3.4 Ca^{2+} activity analysis for estimating synaptic connectivity.

In neurons, propagation of action potential leads to transient modification of Ca^{2+} ions influxes, a process that can be monitored by dynamic imaging using calcium probes indicators (fluorescent molecules) which reversibly chelates Ca^{2+} ions. In dissociated cell cultures, cortical neuron exhibit calcium oscillation patterns which evolves with maturation time. This is linked to the progressive connection of Glutamatergic pyramidal cortical neurons and GABAergic cortical interneurons. The activity goes from spontaneous sparse activity in single neurons to massive inter-neurons synchronisation events up to 50% of cortical neurons exhibiting synchronous activity. The emergence and amplitude of these patterns depends on the Excitatory/Inhibitory (E/I) balance of the cultures and the final density of cortical neurons[272] .On the other hand, striatal neurons, which are GABAergic inhibitory neurons and only connect to themselves do not show any signs of synchronous calcium activity in culture. We previously showed that striatal neurons connected to cortical neurons in conventional microfluidic chips exhibited synchronous oscillatory behaviour with cortical neurons, a process driven by striatal NR2B signaling [231, 235].

Here, after 2 weeks of culture, we therefore loaded our minimalistic networks with fluo-4 indicator and recorded the signals with 2Hz frame rate. Activity patterns being analyzed with FluoroSNNAP MATLAB plugin [270].

2.3.4.1 Spontaneous calcium activity of individual cortical cluster in emitting chamber

In preliminary experiments we noticed that emergence of cortical neurons synchronous oscillation was highly dependent on the initial cell seeding densities. Cortical pockets seeded with low density exhibiting no synchronous activity. We therefore proceeded to high density seeding of the cortical neurons, which after 2 weeks in vitro promotes the formation of cortical cluster/spheroids. Using 5X imaging we first recorded calcium signals from neuronal clusters in the emitting cortical chamber. Figure 45 shows the fluorescence traces of each cluster in different traps; 2 clusters show robust oscillatory synchronous activity while one shows modest activity.

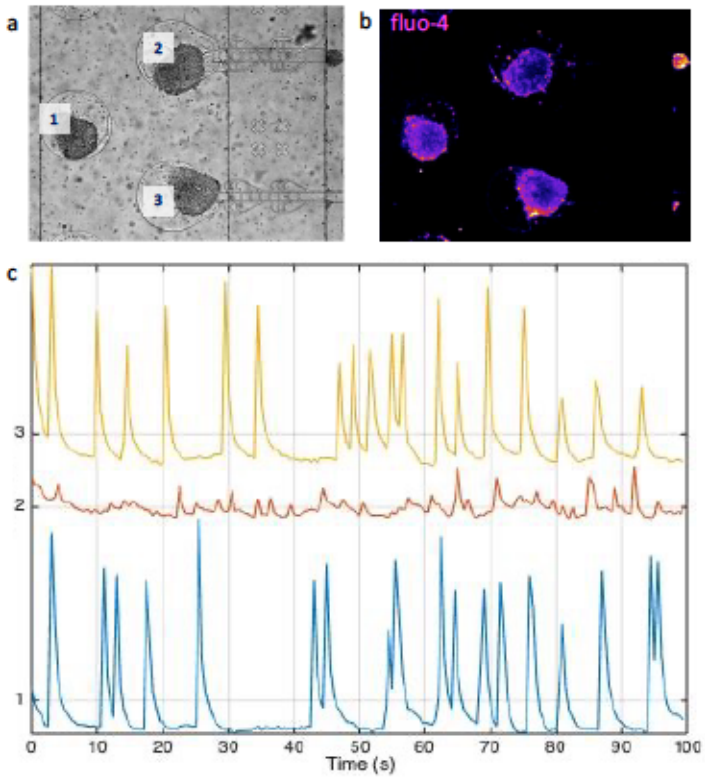

Figure 45. Representative data of spontaneous activity of three cortical clusters in emitting chamber at 19 DIV. (a) phase image, (b) Fluo-4 staining (show in fire color type). (c) ΔF/F0 Fluo-trace of Neuron cluster bursting. Representative Image from experiments conducted in 3 independent dissections with

several networks per condition.

FluoroSNNAP analysis of calcium traces through Raster Plot representation allows to detect synchronous oscillatory events.

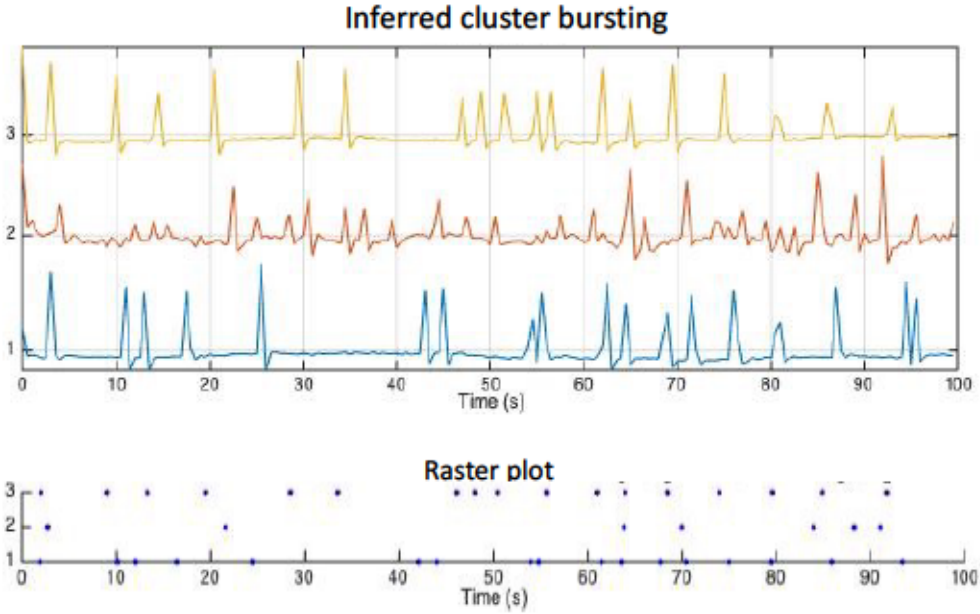

Figure 46. Ratser plot representation from data obtained in Fig45.

As shown in 错误!未找到引用源。, during the sampling time, trap N°1 and N°3 fired 17 times in total and no. 2 fired 7 times. Overall, the average bursting frequency is about 0.19 s^{-1}. Comparison of the cortical nodes two by two evidences no inter node synchronicity suggesting no functional connection between the nodes. The Raster plot is representative of what was observed in several independent experiments yet the spontaneous bursting frequency and amplitude changed from on chip to the other, a process linked to the stochasticity of calcium transient emergence in in vitro models.

2.3.4.2 Synaptic activity of Cortical - Striatum connective cluster in compartmental chambers

Ca^{2+} signal in the neural network were next monitored in connected vs unconnected cortico-striatal minimalistic networks. In these configurations, each cortical axon tract was surrounded by 2 striatal nodes, one connected to cortical axon channel through small curvilinear grooves "fins", one not connected lying 30µm away

from the axonal grooves. Representative calcium traces are depicted in Figure 47. In those representative experiments, among the 4 ROIs that were sampled, cluster 1 and cluster 4 are connected via "fins" microchannels, cluster 3 serves as a control as the striatal neurons are not connected to the cluster 1, and cluster 2 is a cluster of cells incidentally adhering to the outside of the trap.

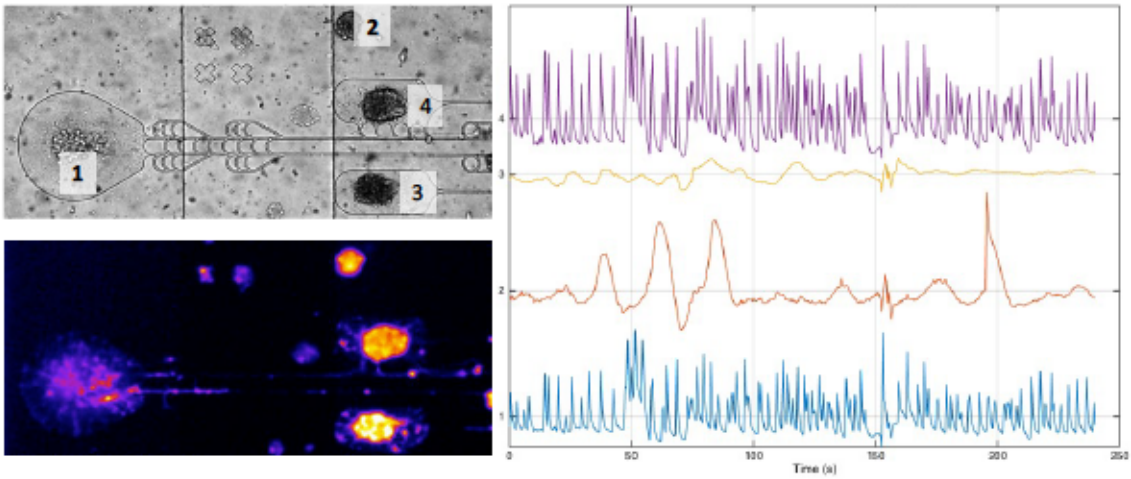

Figure 47. Spontaneous activity of two nodes networks. (a) neuron cluster survival 19days. (b) Fluo-4 as Ca^{2+} indicator to estimate calcium activity (show in fire color type). (c) Neuron cluster bursting signal analysis - fluorescence trace (Δ F/F0 traces). We observed this phenomenon in survival chips, and choosing one or two chips from each experiment to record the data.

In the calcium imaging results, clusters 1 and 4 fired 64 and 67 times, respectively, with a firing frequency around 0.23 Hz, in which the same inferred peaks were found 63 times. This means that about 94% of the firing activity of cluster 4 is synchronizing to cluster 1, while 98% of the peaks in cluster 1 can find a corresponding signal in cluster 4. The striatal cluster 3 and cluster 2, which were not connected to the cortical network, fired 11 and 17 times, respectively, and only once at the same time as cluster 1. Thus, the percentage of synchrony between cluster 1 and the other clusters was only 1.5% (Figure 48). Importantly Calcium traces of unconnected striatal neurons exhibit very broad bands reminiscent of intra node non synchronous calcium transient events. In comparison connected striatal neurons exhibit sharp and fast oscillatory behaviour mimicking conventional cortical rhythms. The Raster plot is representative of what was observed in several independent experiments yet the spontaneous bursting frequency

and amplitude changed from on chip to the other, a process linked to the stochasticity of calcium transient emergence in in vitro models.

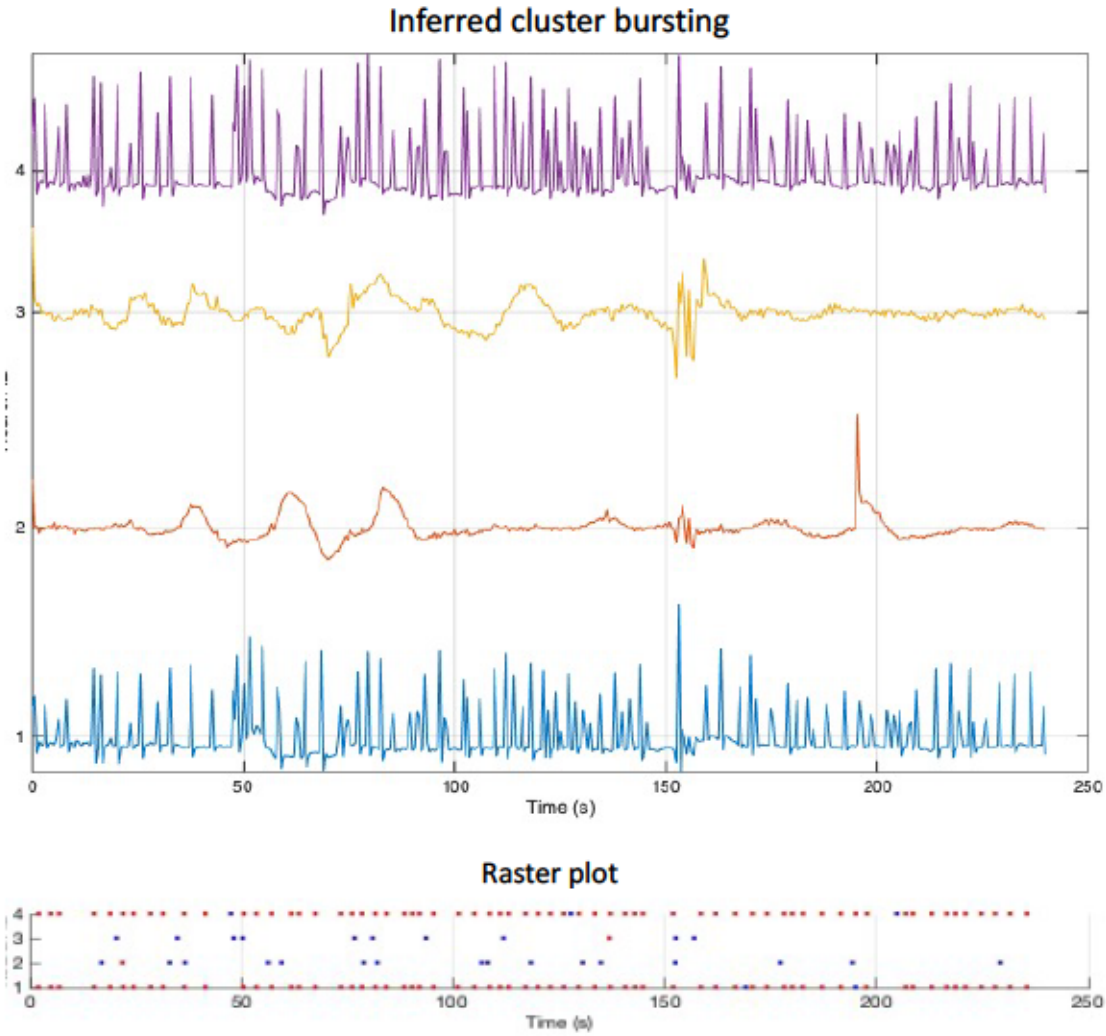

Figure 48. The interred network cluster and correspond raster plot

The conclusion is that cortical neurons spheroids exhibiting spontaneous activity efficiently transmit action potential toward the connected striatal pockets and not to the unconnected one that lies 30µm away from the cortical axonal bundles. This is reminiscent of efficient synaptic contact establishing between striatal neurites and cortical axons.

2.3.4.3 Effect of KCL stimulation of Cortical nodes

In order to further validate the coupling of cortical and striatal neurons, we also stimulated cortical neurons with 50mM potassium Chloride (KCl) to enhance cluster

activity. 错误!未找到引用源。 shows calcium traces before and after (red line) stimulation of the cortical nodes with KCl. After KCl stimulation node 1 in the emitting chamber starts to oscillate synchronously, together with node 2 and 4 (connected striatal pockets). Raster plot analysis shows high coincident bursting between node 1 (cortex) 2 and 4 suggesting efficient coupling in the networks. While node 3 that is not connected through node one, shows no sign of bursting, surprisingly, node 5 (an incidental striatal cluster growing outside of the striatal pockets) shows increase in calcium frequency.

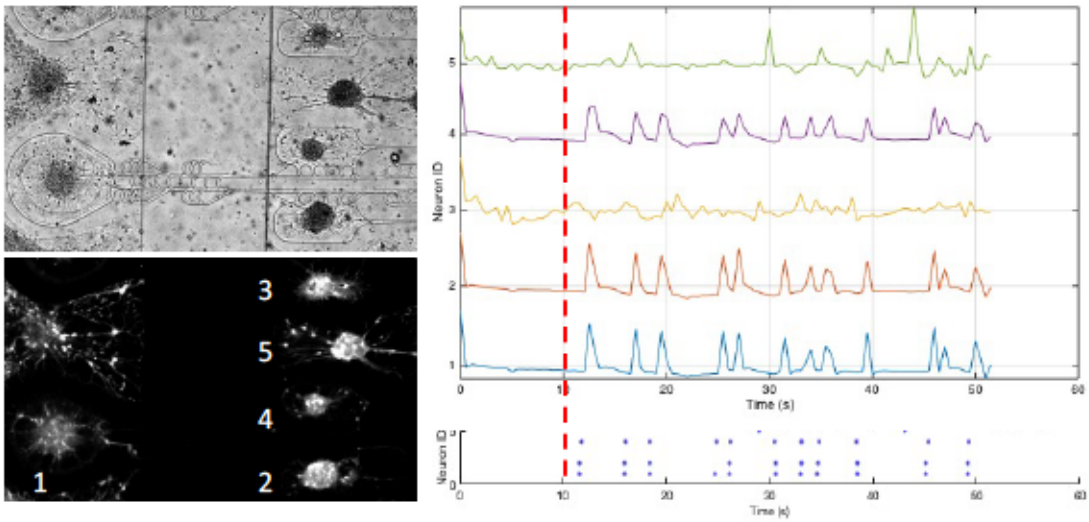

Figure 49. KCL stimulation of Cortical nodes and impact on Striatal oscillations. (Left) : phase and Fluo 4 images. (Right) raster plot analysis of extracted DF/F traces. Preliminary experiment performed once.

2.3.5 Activation of striatal Erk signaling pathway in reconstructed networks

We previously showed that cortically induced striatal oscillation leads to activation of Erk signaling pathway in striatal neurons [231, 273].Having shown that calcium oscillation only occurred in the connected striatal pockets we therefore assessed whether cortical activity would trigger changes in Erk phosphorylation in connected or unconnected striatal nodes. First, the emitting chamber of mature (>>14 DIV) networks were treated with Bicuculline, a competitive $GABA_A$ receptor antagonist that leads to increase excitability of cortical neuronal culture, or TTX an inhibitory stimulus that

abolishes cortical rhythms. As shown by our preliminary results depicted in Figure 50, striatal neurons seeded in the trap connected to the emitting chamber have higher pERK signal than the control (unconnected) chamber (Figure 50). As shown in Figure 51, analysis at higher microscope magnification to evidence Erk nuclear translocation at the single cell level, was rendered difficult by the clumping of neurons into spheroids. Shall these results being reproduced this would further substantiates our results showing that cortico-striatal connectivity can be finely tuned in our minimalistic IMP platforms.

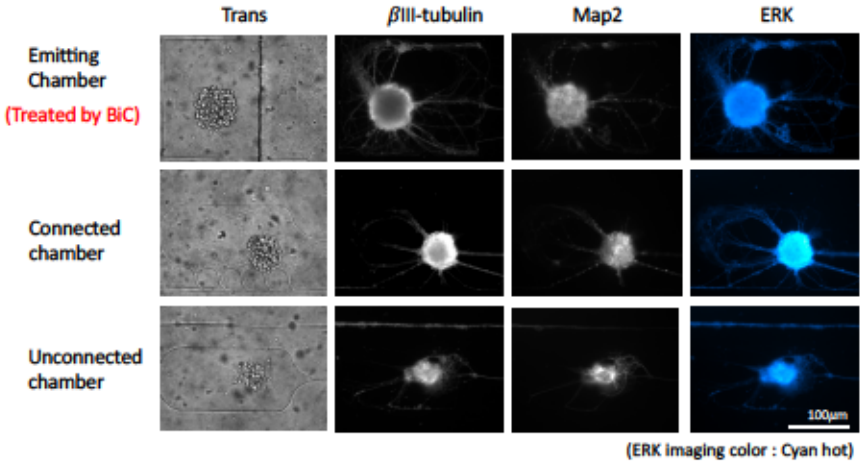

Figure 50. The pERK signals in BiC treated neural network.

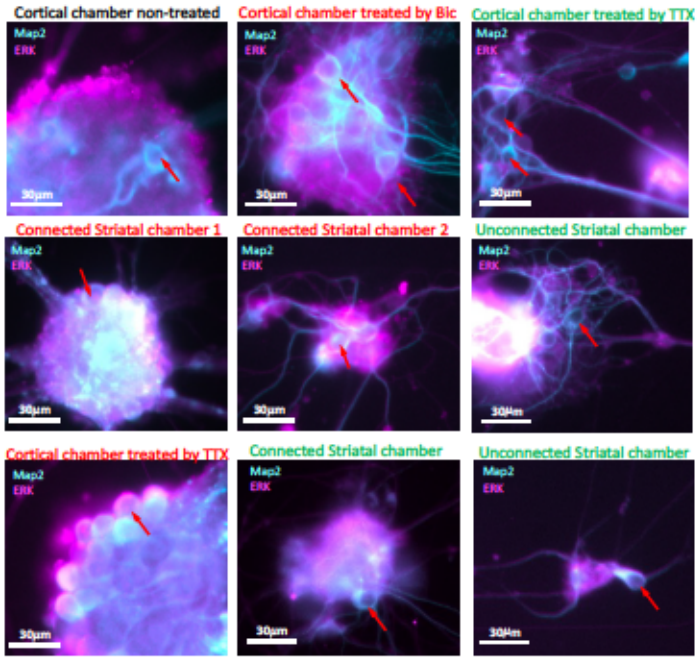

Figure 51. The ERK signal in cortico-striatal neural network. First row, emitting chambers. Second

row, BiC treated network. Third row, TTX treated network. The title with red color, it may have pErk signals. The title with green color, it shows no pErk signal.

2.4 Discussion

Using "In Mold Patterning" that allows to impose both mechanical and chemical guidance to growing neurons, we designed a microfluidic platform that allows to construct minimalistic oriented 2 nodes networks with a control of synaptic connectivity. Starting from conventional microfluidic platforms our initial aims were to achieve 3 goals: 1) Encode a platform were all the neurons seeded in the first node send their axons toward the second node. 2) Compartmentalize axons from the second nodes away from the ones of the first node. 3) Allow to control synaptic connectivity between the first and the second node. These goals rooted in biological requirement that were 1) permit the future construction of multi-nodal networks such as feedforward A→B→C networks in which C Neurons are indirectly connected to A. 2) allows the study of retrograde propagation signals from B axons toward A neurons without targeting A axons. 3) Allows the study of the role of synaptic contact in age matched networks. At the technological level, while some of these goals could have been achieved using classical micro-patterning approaches we reasoned that this would have been impaired by the fact that first networks tends to detach from their patterned substratum once they mature due to strong tensile strength between connected neurons; second, implementing micro-patterning on flat substratum requires micro alignment with funneling microfluidic channels that serves both as guides and fluidic compartmentation barrier. "In Mold Patterning" that was previously developed in our laboratories initially demonstrated that it allowed the construction of "mono-nodal" networks with exquisite stability over time. "In Mold Patterning" technique is a demanding approach that required many technological optimization steps to obtain reproducible patterning in the groove and pockets, efficient neuronal survival at relatively low cell culture densities and good maintain stability of network topology.

2.4.1 Micro-fabrication process and micro-chips production.

Efficient, homogeneous and reproducible patterning of poly-lysine inside the traps and grooves was an absolute prerequisite for enabling the chip to capture cells and confine neuritis.

This turned out to be a challenging issue as the designs encodes surface dimensions encompassing 3 orders of magnitudes; the smallest resolution of design for axonal guidance being a few microns wide, while the scale of the whole chip neural network can reach several thousand microns. The most important parameter to control therefore relied on the way of stamping and imprinting PLL, a complex issue. since poly-lysine faces two transfers steps, one classical micro contact printing and one imprinting/embedding in the bulk of reticulating PDMS. For this reason, through extensive trial and error empirical processes encompassing variation of PLL quantities, coating of PDMS stamps with various amounts of SDS, modification in PDMS stiffness (variation of % curing agents, variation in T° and curing time.), prevention of collapse during the IMP patterning (creating unwanted pattern zones) with distribution of supporting micro-pillars. we renovated the whole initial process to make such complex chips. Overall, by the end of the optimization process, this permitted the production of 6-10 overall mold replica leading to 40 independent chips, therefore 200 mini networks per batch of microfabrication session with a fabrication rate of success (according to fluorescent PLL deposition) being >80%. Sometimes, we lost some chips due to misalignment, but we still at least have 120 mini networks for each trial. That fabrication success rates were then challenged by the biological functional properties of the chips. At the microfabrication process level, IMP therefore turns as a feasible process to constructs serialized microfluidic chips. Yet we envision further adaptations to simplify the fabrication process, which limiting steps stands in the patterning/molding of the bottom layer. Moreover, in depth cell biological experiments led us to pin point some specific limitation of the IMP process in controlling cell clustering through PLL bioavaibility. Indeed, IMP process most probably triggers

partial embedding of the biochemical cues that are patterned, the proportion of which is unknown. The exact quantity of PLL adsorption on 2D surface for optimal neuronal "gluing" is not known, as for neuronal attachment on 2D substratum the optimal PLL concentration is mostly inferred through empirical observation in the biological labs. Yet, modification in the quantity of PLL during the fabrication process did not lead to significant changes in the cell culture outcomes. As mentioned in Chapter 5, this promoted us to explore alternative ways to promote controlled local PLL deposition in microstructures areas.

2.4.2 Microenvironment systems for cell culturing and survival.

In order to promote survival on the reconstructed mini networks, I had to modify some cell culture parameters. We thus have tried different cell culture media formulation. Among them, DMEM and Neurobasal are our common formulations and we have tried to adjust the ratio of serum. We found that DMEM with 5% serum supported better neuronal survival than Neurobasal for hippocampal cells, while for cortical and striatal cells, there was no significant difference. As far as the results of the current experiment, we believe that the engineering parameters underlying the chip assembly process (volume and geometry of cell culture macro-chambers holding the pockets, control of PLL quantity, final initial cell density) have a more pronounced effect on cell survival than basic culture medium formulation. Yet unexplored strategies such as supplementation with neurotrophic growth factors, use of astrocytic conditioned media or rational co-culture with glial cells to the system could be tried to enhance stabilize the survival outcomes.

2.4.3 The topology of the pattern controls the direction of axonal growth and neural network connections.

The control of connections between cell populations is mostly influenced by topographical factors and surface adherence, and it is also related to the concentration of cells seeding. During the reconstruction of neural networks process, we noticed that

the efficiency of neurons seeded in the two chambers to form network connections dependencies is highly impacted by the initial cell seeding densities. Too few neurons don't allow to form connections because of impaired cell survival, too many cells induce cell clumping and formation of spheroids. Overall, our experiments showed that once seeded at relatively low densities the IMP synaptic chips work as predicted, allowing to establishes fully oriented synaptic contacts between cortical pockets and striatal ones. Importantly these devices allow for the first time to 1) study the role of synaptic contact in a specific biological question (e.g. prion like spreading) in age matched networks and 2) study genuine retrograde propagation toward cortical neurons of any biological or biophysical entities introduced specifically in striatal axons. We believe our platform is on the few one allowing to such a controlled process in vitro.

Calcium imaging experiments demonstrated that spontaneous oscillation from the cortical pockets arose only in clustered spheroids. While this permitted to demonstrate the unidirectional, anterograde, propagation of cortical influxes toward striatal connected micro-pockets, this came at the cost of loss of topography, especially for striatal neurons. The control of unidirectional connection of neural populations was enforced by the classical "arch" structure, while this allowed to enforce anterograde topology, arches proved not always efficient to control striatal shoot backs when seeded at too high densities. Indeed, striatal clumping led striatal axon fasciculation and tension, detachment from their guiding microgrooves and erroneous connections with cortical material. Control of these drawbacks could theoretically be enforced by microfabrication procedures rather than biological adaptation of the system. This mainly encompass: 1) implementing more stringent arch/diode like structures such as the described in Courte et al 2018 [239]; 2) increasing the PDMS wall surface to minimize the "open" (fluidically accessible) groove areas in the macro-chambers; 3) modifying the fabrication process so that PLL quantities are more controlled. Therefore, the final cell seeding density was set around 30-40 per 10^4 µm2.

2.5 Conclusion

In this work, we demonstrated the interest of using both mechanical and chemical cues to control the reconstruction of oriented minimalistic two-node neural network allowing 1) control of synaptic contacts un age matched cultures 2) post synaptic neurons axonal compartment allowing genuine retrograde transport studies between connected neurons 3) enforcement of anterograde connection between nodes compared to conventional microfluidic designs. Through experimental iteration/optimization of the fabrication process we achieved serial construction of the IMP microchips, a process that requires further simplification to be fully operational. Culture of low-density networks demonstrated that deterministic networks can be obtained in a reliable manner thus paving the way for biological studies based on axonal transport or synaptic connection establishment. The IMP protocol only showed its limits when high density neuronal nodes were required, mostly to permit the arising of spontaneous collective neuronal activity. We envision that that specific point requires alternative ways to control local deposition of cell adhesive cues in micro-pockets, a process we started to evaluate by the end of the PhD works (Chapter 5).

2.6 Supplementary data

2.6.1 Final chips design and geometry

During the work aiming at reconstructing minimalistic cortico-striatal networks with controllable synaptic connectivity, we assessed the efficiency of several designs in order to obtain microchips allowing reproducible seeding, neuronal survival and topological control of axonal outgrowth.

2.6.1.1 The whole chips design map

Figure 52 depicts the different geometries that were finally chosen for the two-node cortico-striatal chip. The geometry of the chip has also been optimized several times to overcome problems such as microfluidic flow dynamics caused by

hydrophobic surfaces that could arise in PLL free PDMS areas, cell survival, chip assembly and production efficiency. More discussion on the manufacturing aspects of the organ-on-a-chip domain can be found in Chapter 6.

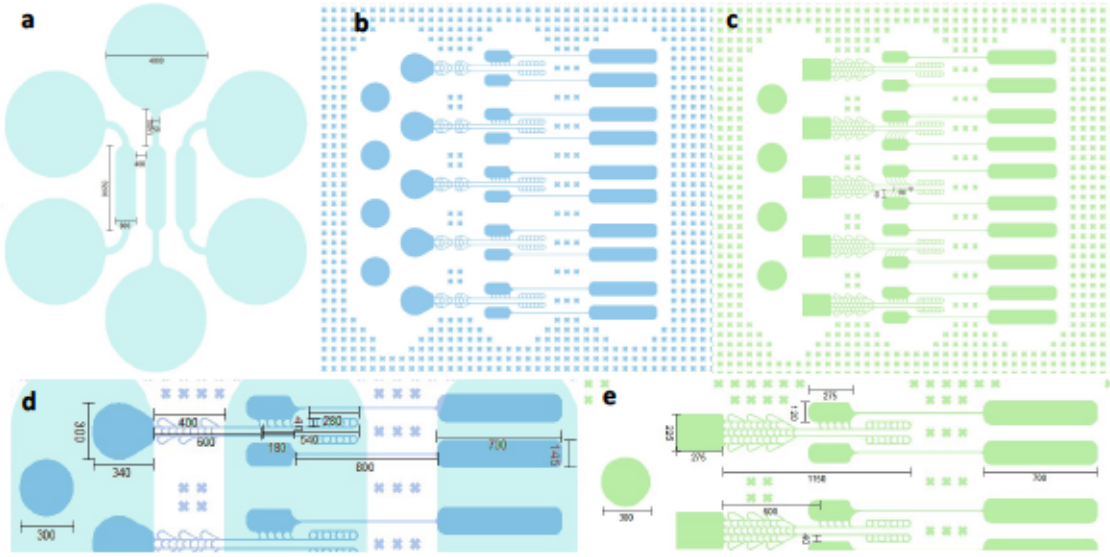

Figure 52. The whole chips design map. (a) Cell delivery chamber. (b) The trapping pattern with round grove in emitting chamber. (c) The trapping pattern with square grove in emitting chamber. (e-f) The optimized size of chip patterns.

2.6.1.2 The details of each design parameter and their purpose

In the emitting chamber, the size of the cell trap is about 300μm in width (diameter), and the area of the round trap (the area marked as 1 in the Figure 53) is about 1.2 times larger than the square one, where the individual trap on the left side (the area marked as 2 in the Figure 53) is used to enhance the survival of cortical neuronal cells by increasing the cell numbers in the whole chamber (Figure 53).

According to the experimental results of the type A chip of the screening system, the selection of the interval of 200μm-400μm as the size of the cell trap can take into account the spatial structure of the chip and the survival of the cells. The area of a single receiving trap is approximately equal to the area of a circle with a diameter of 200μm. In two-nodes chips, the area of emitting traps is approximately equal to a pair of receiving traps.

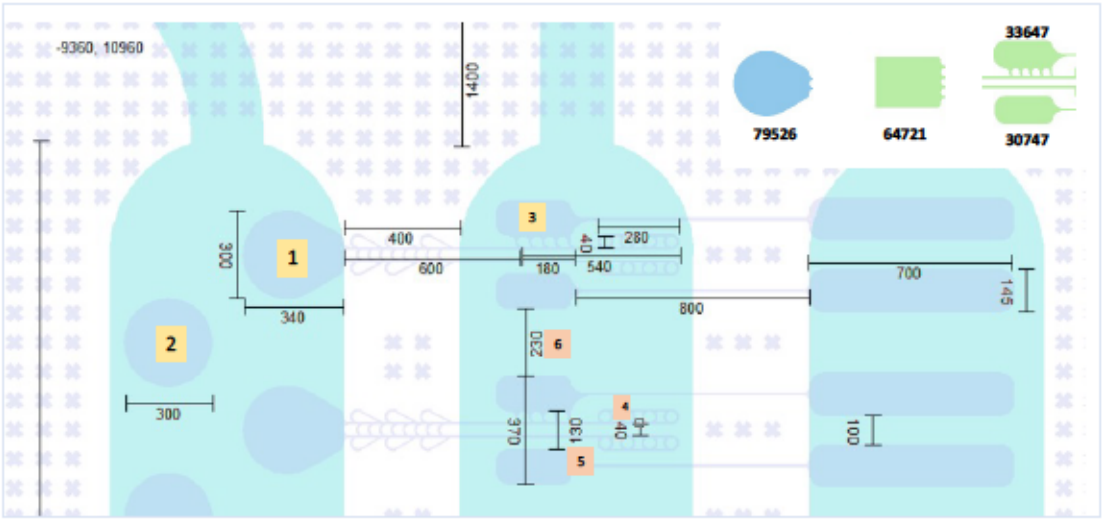

Figure 53. The geometry size of two-nodes system. The size of each emitting trap is around 300μm, and the distance between traps is at least 130μm, and between two group networks, the distance is around 230μm. The number of the right corner above are the aera of each part, the unit is μm^2.

The distance between cell traps accommodates the one of the Class E chip (chapter 3) of the screening system. In a group of neural networks, the spacing between two receiving groove is 130μm, where the spacing between parallel channels is a minimum of 40μm, and the spacing between the receiving chambers of two groups of neural networks is 230μm, to minimize the probability of unwanted connection between these nodes. In cell culturing, except for a very small number of experiments chips in which cell seeding overload caused unwanted connections, these spacing dimensions worked properly. The emitting chambers being independent of each other no connection occurred between them.

During our experiments were both compartments were seeded to obtain cortico-striatal networks we noticed that the cell seeding density is the most important parameter to control. In the two-node chip, after several adjustments of the seeding scheme, the cell density can be controlled around 35 cells per 1×10^4 μm^2, when seeding 6ul of cortical cells with a concentration of 30 million/ml in the emitting chamber and 6ul of 20 million/ml striatal cells in the receiving chamber.

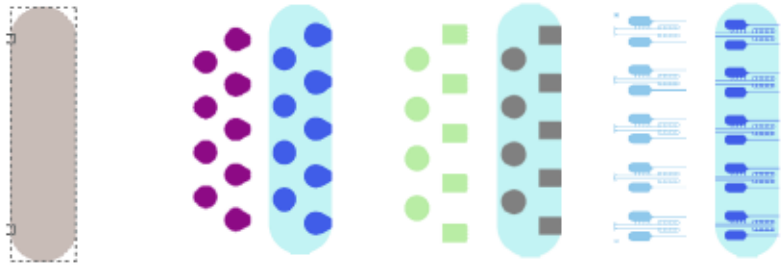

	Whole chamber	Emitting chamber (Rd.)	Emitting chamber (Sq.)	Receiving chamber
Surface area	2432147	678806	605885	386290
Pattern rate	0%	28%	25%	16%

Figure 54. The percentage of trapping area occupy all chamber surface

In conclusion, for neural network chips, designing the pattern of the chip relies on biological data, microfluidic hydrodynamic calculations, and a sense of architectural spatial structure. And a large amount of statistical data can help guide further chip design.

2.6.2 Characterization of chips geometry

The wafers for fabricating the pattern master were characterized by an optical surface instrument. The results show that the height of the cell delivery chamber is about 50µm (Figure 55) and the depth of the cell traps is 5µm (Figure 56).

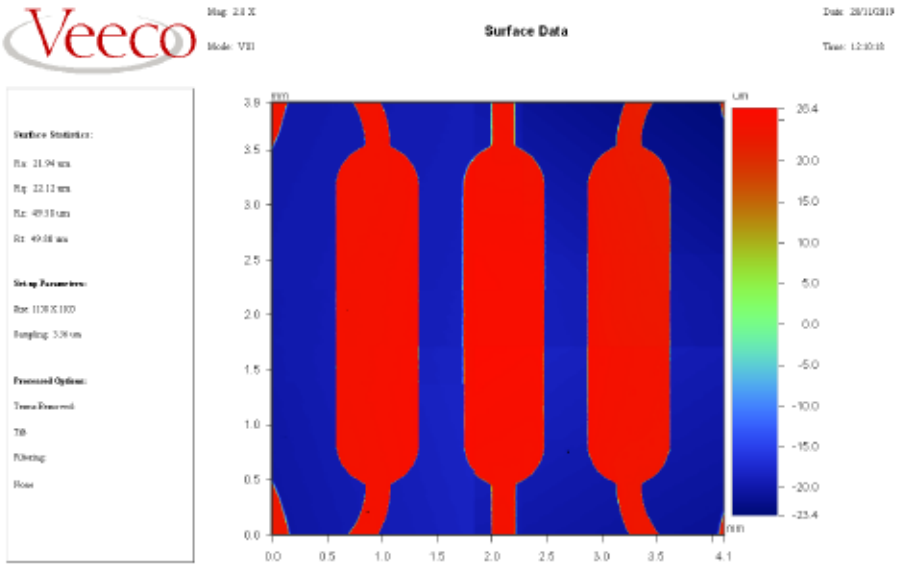

Figure 55. The master of cell delivery chamber characterizing by optical profilometer

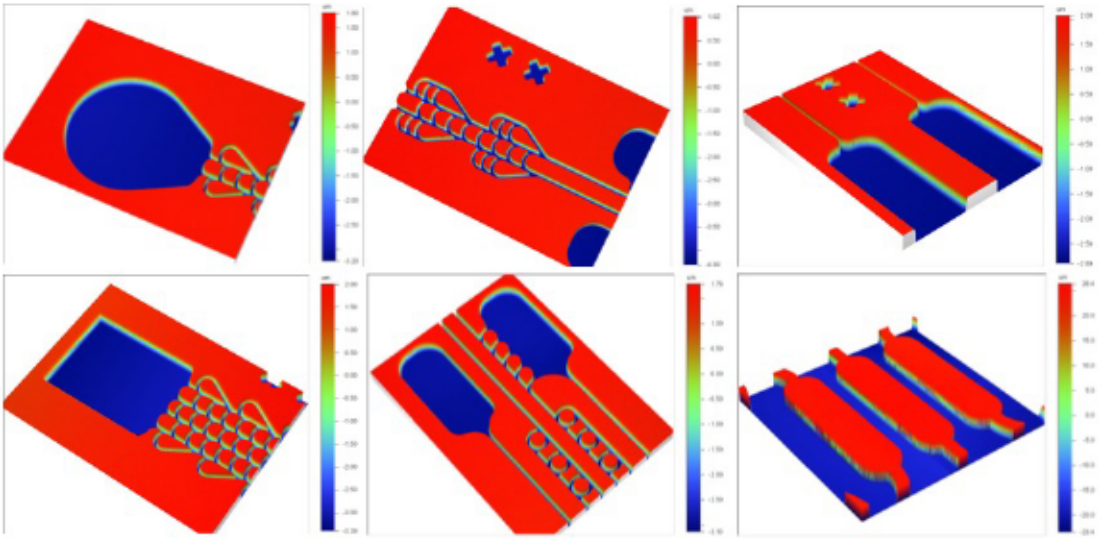

Figure 56. The master of cell traps layer characterizing by optical profilometer

2.6.3 Evaluation of various "Arches" pattern to guides axonal outgrowth direction.

A variety of arch-like channels were produced and assessed for their ability 1) to promotes good anterograde axonal outgrowth from emitting chambers while 2) diminishing retrograde axonal outgrowth from the receiving chambers. They capitalize on the principle that 1) axon growth in contact with edges of microgroove or walls of micro-channels 2) that bundled axons that were guided by walls keep growing in straight direction when they are not guided anymore or when the walls/grooves deflect abruptly [238]. The following figure (Figure 57) shows axon from GPF expressing neurons invading several of the tested patterns. The arch-like channels can serve to guide the axons forward growth (Figure 57 a and b) and turn to backward growth (Figure 57c and d). Hearth shape pattern were also assessed, giving less reliable results.

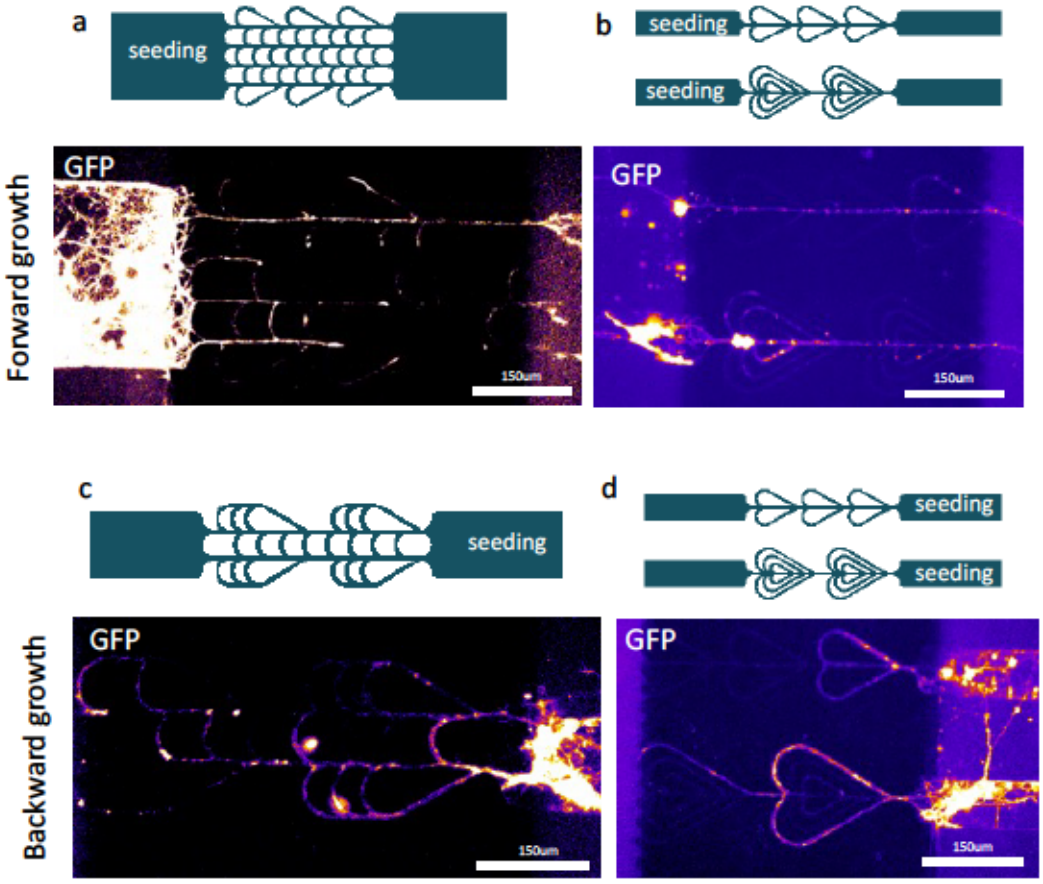

Figure 57. Some selected arches patterning working on axon guidance which tracking by GFP neurons survival 5 days in vitro. (a-b) The cells seeded in emitting chambers. (c-d) The cells seeded in receiving chambers.

2.6.4 Ca^{2+} imaging movies from cortico-striatal minimalistic networks.

2.6.4.1 Spontaneous calcium activity of individual cortical cluster in emitting chamber

chapter2_spon_activity_emiting.avi

2.6.4.2 Synaptic activity of Cortical - Striatum connective cluster in compartmental chambers

chapter2_spon_activity_networks.avi

2.6.4.3 Stimulating connective network by chemicals- Potassium chloride

chapter2_stimulating_KCl.avi

3 Reconstructing compartmentalized multi-nodal neural network on microfluidic chips

3.1 Introduction

In section 1.3.3, I elaborated on the relationship between hubs and nodes in neural connectomics. Connectomics stems in the study of fundamental networks theories [65, 67]. It mainly consists in identifying specific neuronal networks topologies both at the macro scale and micron-scale levels. The core theory is that, at the macroscale level, brain networks depict generic topologies that are shared by all kind of networks. Indeed, brain macro connectome is organized as a "small world" network (were each neurons is close to anyone else) and specific regions (eg. hippocampus) in the brains encodes structures such as hubs. Besides classical neuro anatomical description, brain networks can therefore be described by network theories properties such as centrality, hubness, robustness etc. Besides the description of the brain basic architecture, an increasing number of studies now aim at describing the change of the connectome during acute or progressive neurological syndromes with specific topologies being targeted earlier.

In the previous chapter, we demonstrated that IMP allows generation of finely tuned 2 nodes networks composed of distinct neuronal identities. Here, inspired by the theory of neural connectomics, using IMP approaches, we aimed at building more complex neural networks encoding some generic network properties. In our initial idea, we limited the scale size of neuronal networks roughly to the milli-micrometer level. After assessing optimal node size and spatial spacing between nodes to permit good neuronal survival our goal was to generate a microsystem allowing to control inter node connectivity in order to build multi-nodal topologies with 1) control of unidirectional vs bidirectional inter node connections and 2) specific fluidic access to the nodes. We used the IMP technique for these goals.

A matrix composed of nodes can serve as an ideal model for building different architectures of inter-node connections. We therefore designed multiple matrices of traps (i.e. defining nodes) ， which can first be of different sizes and have different spacing. In order to provide homogeneous conditions for cell delivery, we designed a

parallel multichannel delivery system, which together with a matrix of traps made using IMP technology constitutes the structure shown in the figures (Figure 58, I).

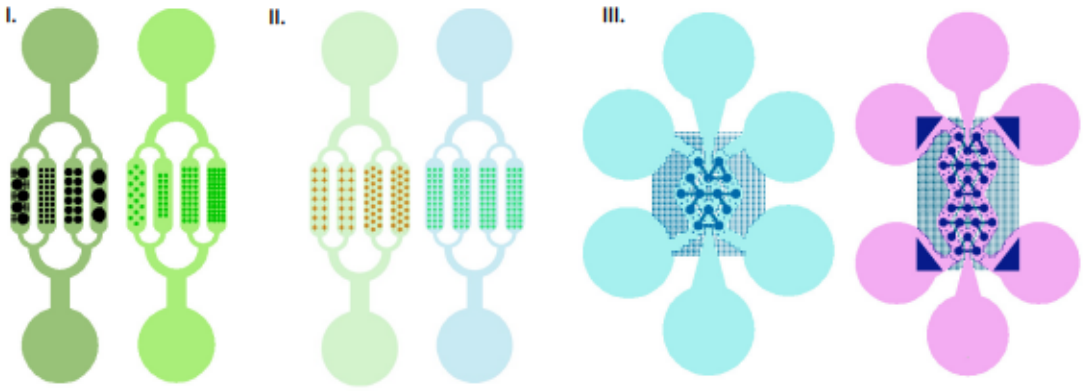

Figure 58. The two types of connection in multi nodes array. (I) The screen system (II) The multi-nodes with internal connection. (III) The multi-nodes with external connection.

The working principle of this system is that when the cell suspension enters the main seeding channel, they are evenly distributed into four identical macro-chambers enclosing round traps. The cells fill these traps by sedimentation. Each macro-chambers encodes different IMP patterns thus allowing cell trapping and survival comparisons for the same seeding conditions system. While we assessed several node shapes some networks were encoded with an "internal" connectivity linking the nodes of the same chamber together (Figure 58, II).

Beyond neuronal survival in the nodes, a critical aspect relies on how to build controlled external connections between the nodes in a platform allowing fluidic isolation between some of the nodes. This was followed by the optimization of microfluidic geometries allowing to enforce connectivity between arrays of nodes located in sperate microfluidic cell culture chambers while limiting the topological problems of encoding too long inter node distance. Consequently, we designed a wave-shaped cell delivery chamber, similar to the flower bud structure that solves the topological problem.

With such an optimized design, we evaluated several networks motifs encompassing ring-like (feedback) connection, linear (feedforward) connection,

(Figure 58, III) that may potentially encode properties that may impact neurodegenerative traits such as Prion Like elements spreading.

3.2 Design and patterns of multi-nodes array

3.2.1 Isolated traps to study cell survival conditions

The survival of cells and the formation of network structures are related to a variety of factors encompassing neuronal density, cell surface attachment area, geometrical shape and surface/volume ratio of the macro-chambers.

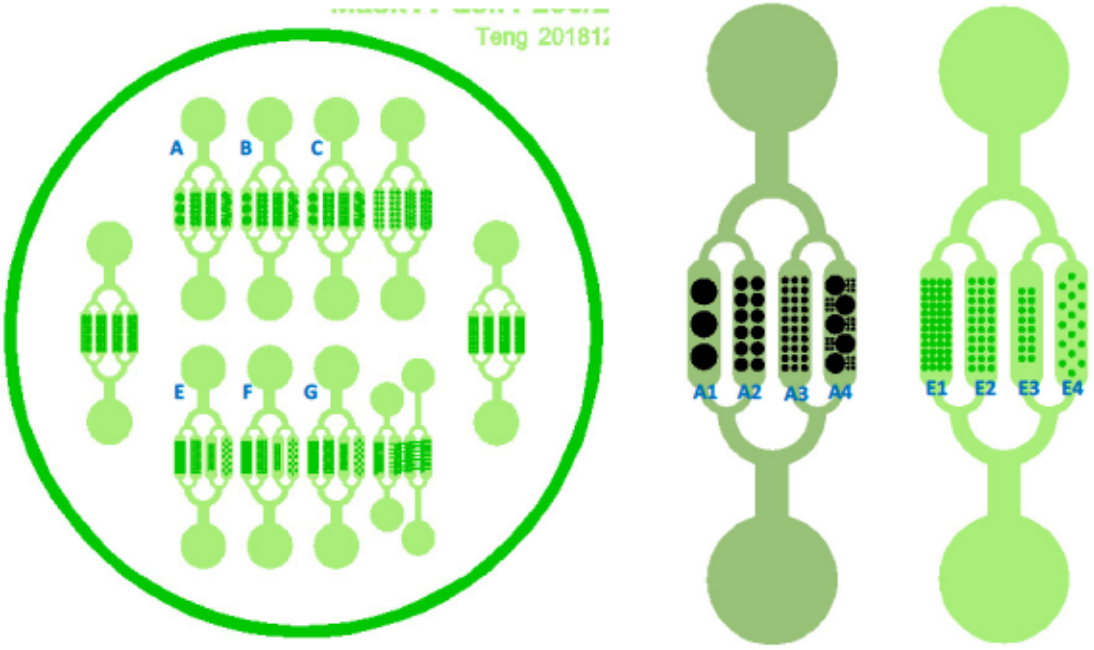

Figure 59. Design of a "screening" device allowing to assess optimal node size, internode distance and shape. (Left) design of a SU8 wafer encoding 10 different micro-chips encompassing several IMP patterns. (Right) Each micro-chips encode 4 distinct chambers that can be interfaced with an IMP layer encoding several node size, shape and inter node distance.

In order to explore some of these parameters, we first designed a split-flow parallel channel chip for homogeneous cell distribution and seeding in the macro-chambers. This allowed to measure the optimal parameters of cell trap interval, size, and seeding density. Figure 59 shows the design of wafer exhibiting several independent chips (A, B, C, E, F, and G) each of those being composed of 4 macro-chambers named A1, A2, A3, and A4. When the cell suspension was seeded in the inlets, due to capillary force and hydrodynamic channel properties, cells flew rapidly and homogeneously in the four

macro-chambers, thus creating a completely parallel seeding and incubation environment. B and C are copies of A. E1 to E4 have the same diameter of cell traps but with 40µm to 240µm intervals. F and G are copies of E. In that 5cm diameter chip, we integrated 10 such small chips to improve the productivity.

3.2.2 Multi-nodes mono-chamber devices

We designed a second type of mold (Figure 60). They are divided in two types, depending on the shape of the nodes. The left image of Figure 60 shows the connected and unconnected star-like dot arrays, where the corners of each star are expected to provide neurite guiding properties. The right figure shows a circular dot array, connected by straight lines. The different types of connections are implemented in the same seeding chamber. Therefore, we define these chips as "Multi-nodes mono-chamber" devices.

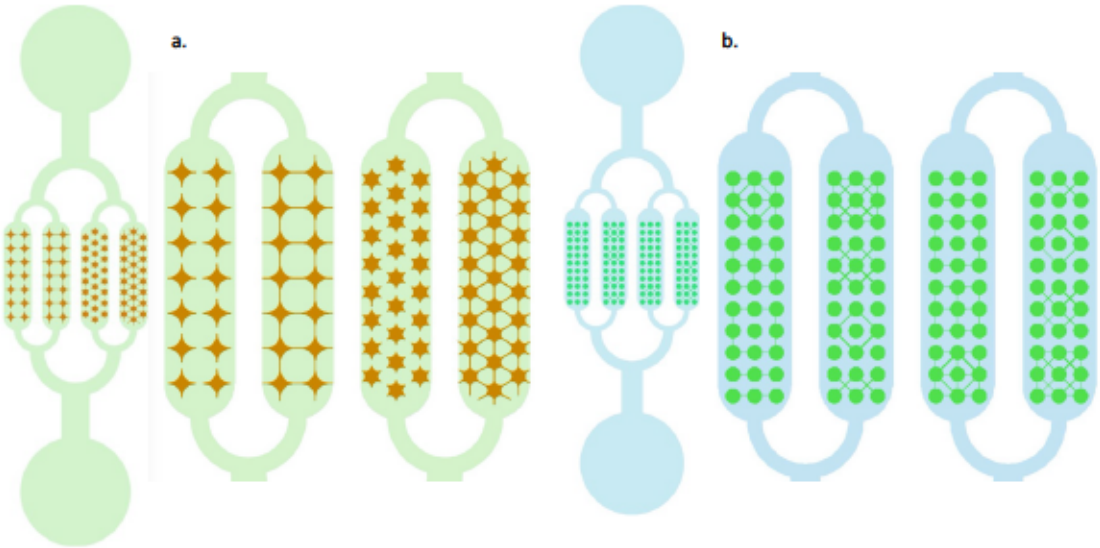

Figure 60. Example of IMP patterns encoding variation of node shape and internal connectivity. (a) Star-like connected array and unconnected array. (b) Round multi-nodes arrays with internal connection.

3.2.3 Multi-nodes multi-chamber devices

The following figure (Figure 61) shows the design of "multi-nodes multi-chamber" devices. For the precise design of this system, we took advantage of the results of cell survival in isolated traps, leading to an optimized diameter of 400µm and trap intervals of at least 400µm when located in the same chamber. The different chambers are

connected by unidirectional arches, or straight channels, with a length (inter node distance) of about 500µm. They have a height of 50µm and a width of 600µm.

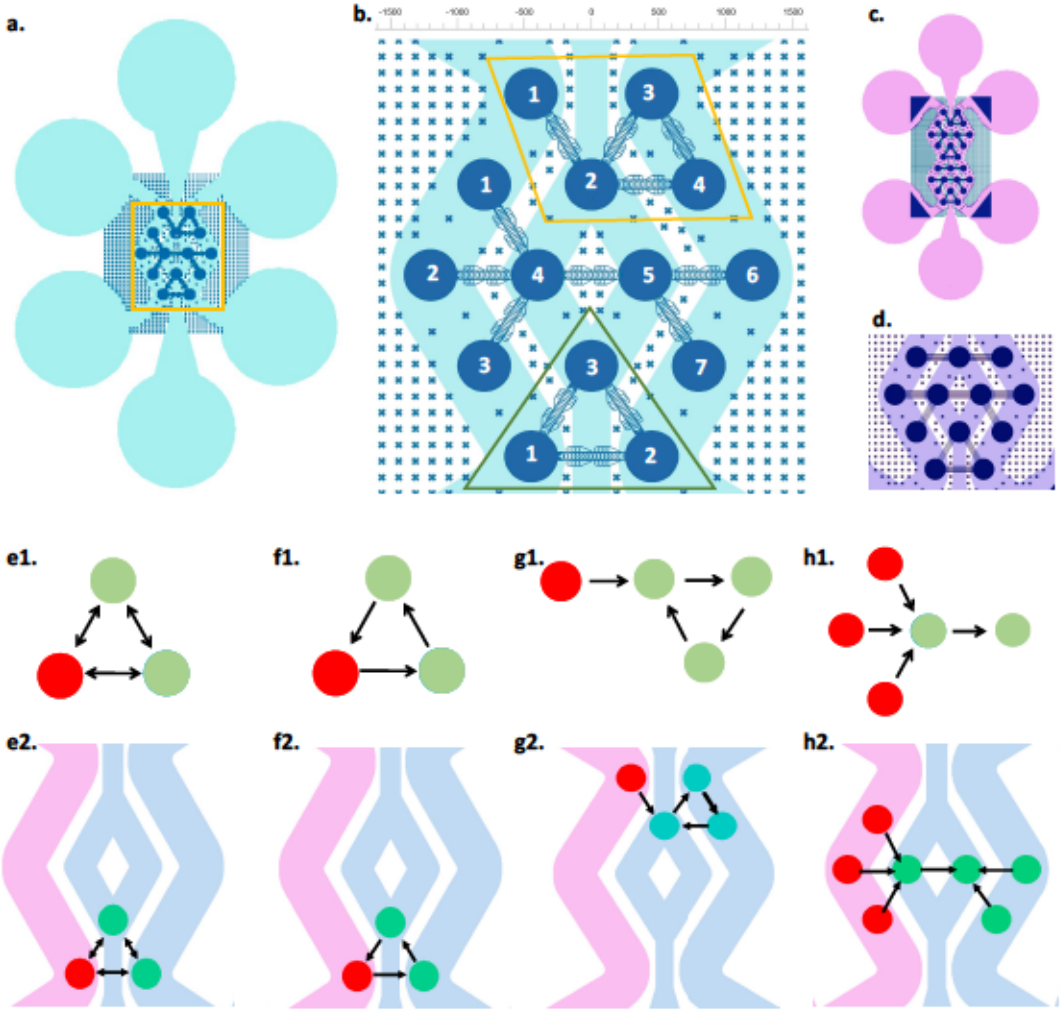

Figure 61. The design of multi-nodes network system with external connections. (a) The whole chips. (b) The central pattern of chips. (c) Some other version of design. (d) The design of binary direction multi-nodes with straight channels (e1, e2) The concept motif of binary direction multi-nodes and corresponding location in chips. (f1, f2) The loop motif of unidirectional multi-nodes and corresponding location in chips. (g1, g2) The second loop motif type. (h1, h2) The multi-nodes network with multiplier emitting traps motif and corresponding location in chips.

3.3 Methods

3.3.1 Chips fabrication and assembly.

Chips fabrication process is similar to the one described in chapter 2.

3.3.2 The preparation of primary cell suspension

E14 Pregnant WT Swiss mouse were purchased from Janvier Lab, and cortical neuronal suspensions were generated using similar procedure as the one described in Chap2. Studies followed the standard ethical guidelines.

3.3.3 Cell seeding and culturing

The Cell seeding and culture condition are similar as the one described in chapter 2.

3.3.4 Immunofluorescence staining and image acquisition

The staining and imaging process using similar process as described in chapter 2.

3.4 Results

3.4.1 Impact of node size on neuronal survival and clumping

3.4.1.1 The relationship between the size of traps and cell survival status

The diameters of the traps encoded on the IMP layers in the four channels were 800µm, 400µm, 200µm, and a combination of 600µm and 100µm, respectively.

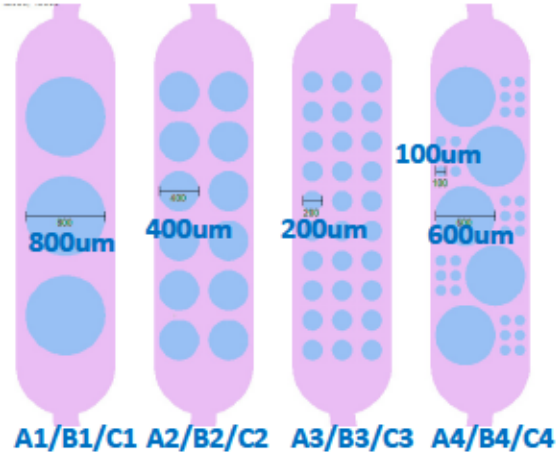

Figure 62. Internal Nodes array with 4 parallel delivery chamber named screen chips for choosing the ideal size of cell traps

After 8 days of culture followed by immunostaining, cell survival and differentiation were assessed by ranking the mini networks formed in the traps in four

distinct states. 1) Nodes exhibiting good survival (little DAPI nuclear condensation, limited β3 tubulin axonal fragmentation) and homogeneous neuronal spreading in the traps. 2) Good survival (same criterion as above) with cell clumping in spheroids. 3) Un-clumped nodes showing signs of degeneration with fragmented axons and dendrites and condensed nucleus. 4) Incomplete network with very low density.

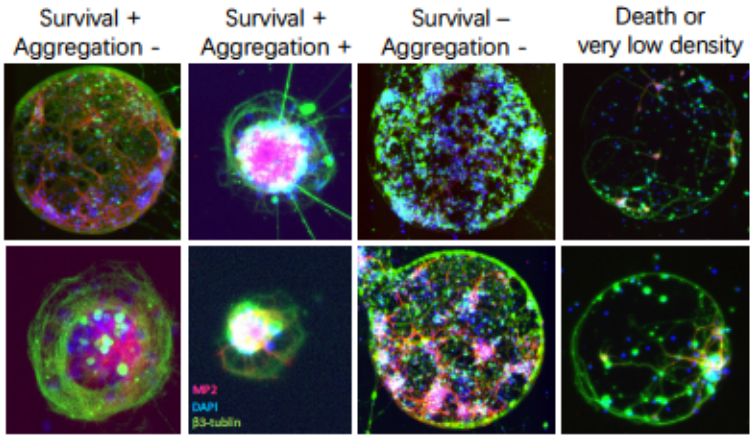

Figure 63. Illustration of the 4 classes of nodes after 8 DIV stained for MAP2 (red), β3 tubulin (Green) and DAPI (blue). (The images are mainly used to show the state of the cells and are extracted from multi-scale, so the scale bar is not shown here.)

Analysis of "network topology and survival" showed that the percentage of traps with network clustering increased as the trap size decreased, while signs of neuro-degeneration shows an inverse variation (Figure 64).

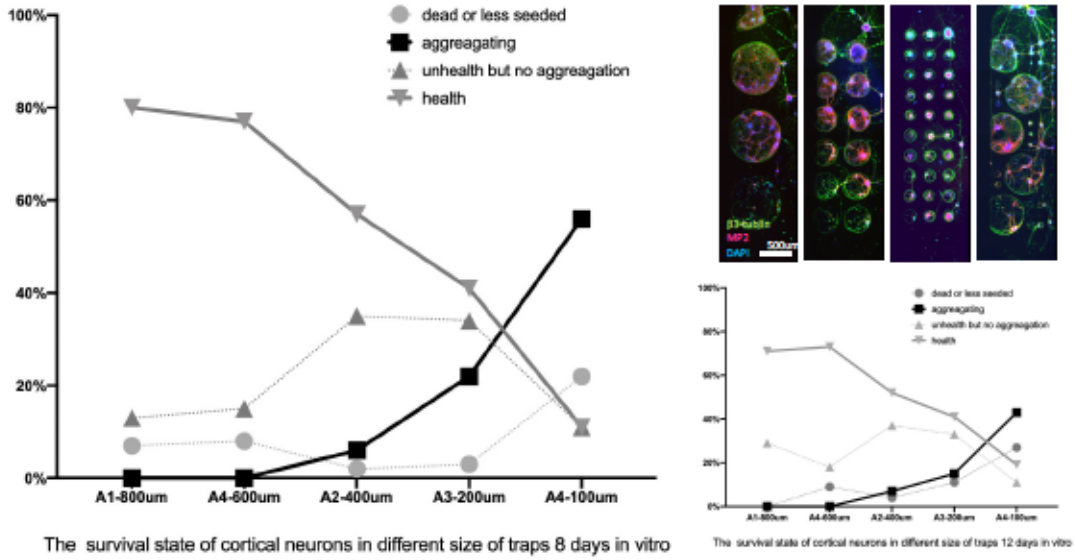

Figure 64. Survival rate of cortical neurons in different size of traps, after 8 and 12 days in vitro. Percentage of nodes exhibiting type 1 ("Health"), 2 ("Aggregating", good survival with sign of node

clumping), 3 (Unhealth but no aggregation") and 4 ("dead or less density") behaviors, as a relationship with node size. Experiments were performed in 2 separate (cell seeding) experiments.

The trend of the two curves depicting "healthy" (grey triangles) and clumped (black squares) nodes have further been used as a criterion for the upcoming design patterns in the future. From these preliminary studies we concluded that for a chip which should accommodate as many nodes as possible to improve the connection efficiency, a trap size of 600 µm diameter should be the upper limit of the design, while the trap diameter for cell survival should not be smaller than 200µm. They correspond to areas of 12.56 $\times 10^4$ µm^2 and 3.14 $\times 10^4$ µm^2, respectively. As shown in Figure 65, after 8 days in vitro, the seeding density in the nodes where the cells exhibited good survival, was about 20-30 per 10^4 µm^2. When the density reached 40 per 10^4 µm^2, the cells started to clump. When the seeding density was higher, the cells neurons exhibited clear signs of degeneration, (axonal fragmentation and dendritic blebbing). Below 8 per 10^4 µm^2, neurons degenerated quickly.

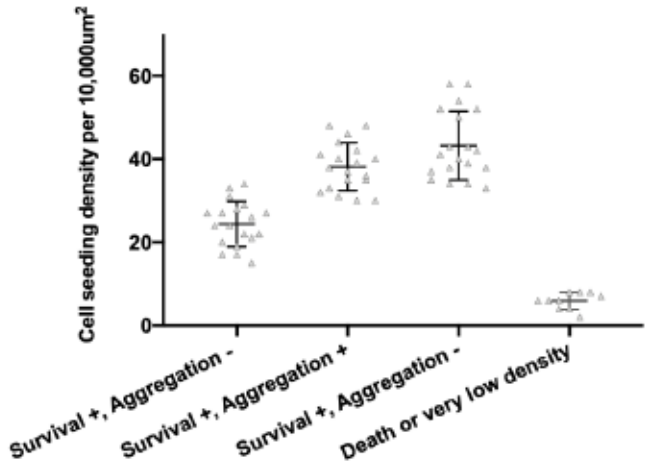

Figure 65. Relationship between cell density and cell survival states.

Interestingly, 90% data of node exhibited clumped spheroids states arose from 200um traps indicating a threshold between initial cell seeding densities / area of cell adhesion and formation of spheroids. Considering that 600 µm diameter nodes traps thousands of cells are systematically associated with node clumping and spheroid

formation, we finally choose 200 to 400µm node size for further experiments.

3.4.1.2 *Intra Node axonal outgrowth topography as a function of cell density.*

Axons, which can grow over long distances, were confined in isolated cell seeding traps. Interestingly, the distribution of axonal bundles in the traps seemed to be correlated with the seeding density. In 200µm traps, axons often circled endlessly along the node walls (Type I). When a certain boundary condition is reached, some of these axons will detach from the wall and retract toward the nodes center (Type II & III). Also, a few nodes have no axons visible (Type IV). Numeration of the number of neurons per trap shows that axons detachment from the wall borders is directly correlated with number of neurons, suggesting that cell clumping causes strong axonal tension and relocation of axons in the spheroids.

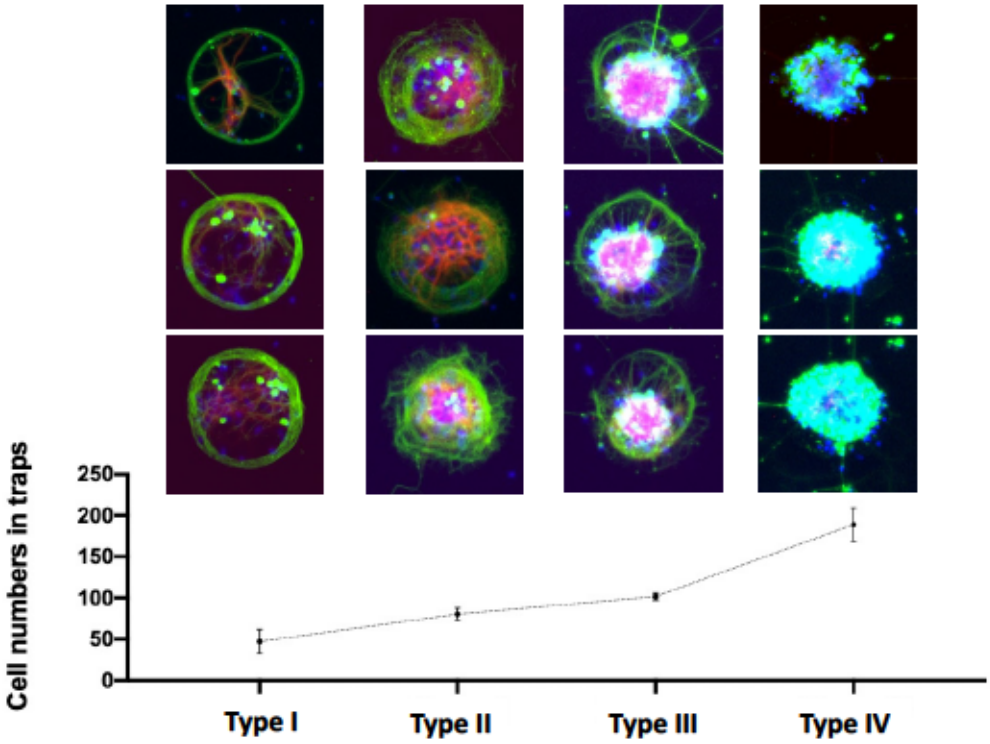

Figure 66. Relationship between cell number, axon circling and clumping behaviour in 200µm nodes.

Indeed, in nodes showing between 30 to 60 neurons (trap size 200µm), axons consistently circle around the edge of the traps for more than 8 DIV. However, when cell density reached 80-100 neurons per 200µm trap soma started to clump and axons

to detach from the edges. At higher densities nodes formed spheroids which survival rate was difficult to assess; only a few axonal projections were evidenced out of these spheroids.

3.4.1.3 Influence of inter node distance on unwanted inter node connections

Our second chip pattern was designed to assess the distance between traps and the occurrence of "unwanted" axonal connection that sometimes occurs between nodes despites no adhesive cues linking the nodes being encoded. In this pattern design, the channels of E1, E2, E3, and E4 are laid with round trap matrices with different spacing. Among them, the shortest distance and the longest distance exist between adjacent trap boundaries. As showed by Figure 67, each macro-chamber of the same chip accommodates several inter nodes spacing for the same node surface.

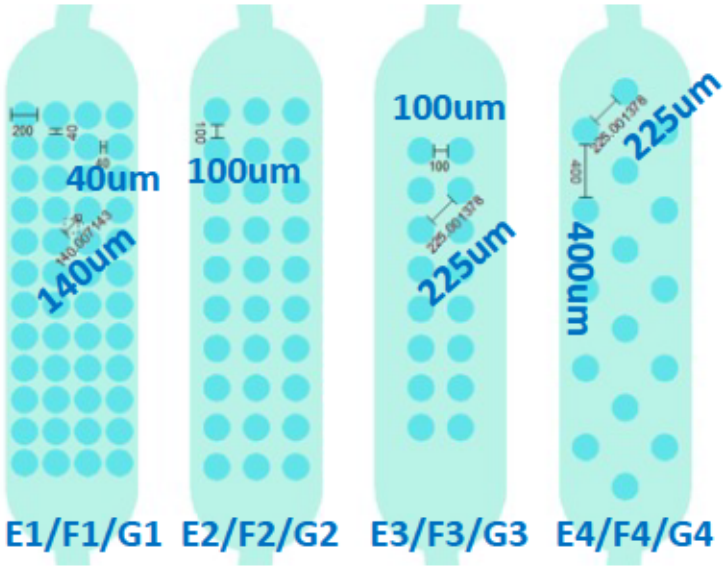

Figure 67. Four channel microfluidic chips encompassing 4 type of IMP layers encoding various inter node distances.

Cortical neuronal cells were seeded, grown and stained after 8 or 12 days of culture in the chips (Figure 68).

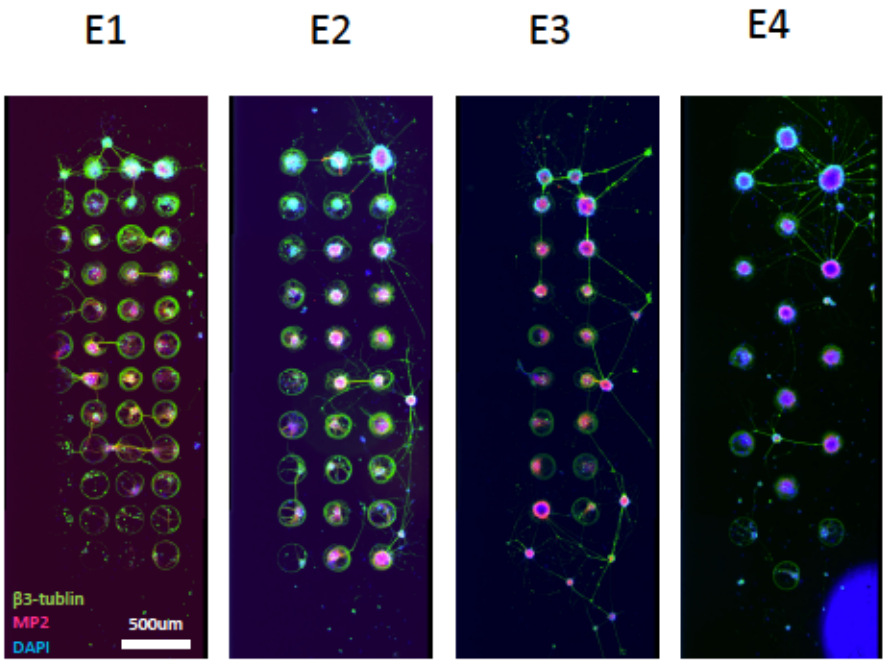

Figure 68. Illustration of unwanted connections between Cortical nodes at 8DIV. Neurons were stained for axons (β3 tubulin), dendrites (MAP2) an nucleus (DAPI)

We estimated the proportion of nodes that tend to be inter connected by counting the number of connections established between two traps and compared it with the number of connectable connections that theoretically exist in whole chamber. The picture below (Figure 69) depicts a portion of the E1 channel, i.e. a 3×4 matrix of nodes. If axons are crossing each other to connect nodes, 17 connections with a spacing of 100µm (red line), and 12 connections with a spacing of 140µm (black line) can occur.

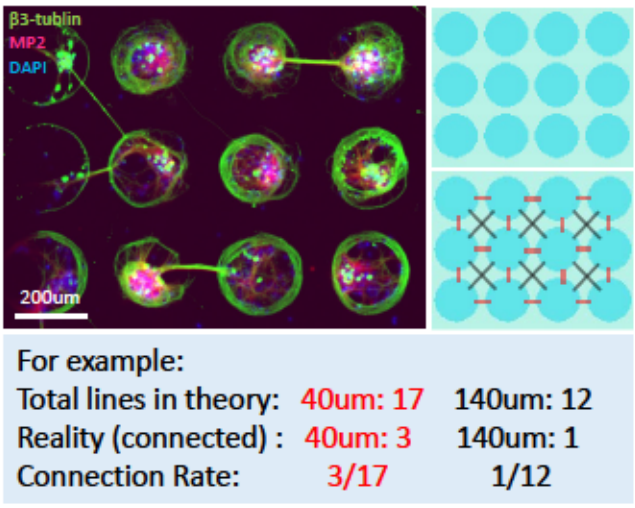

Figure 69. Illustration of the quantification method of "unwanted" internode connections on chip encoding 40 and 140µm internode distance.

After 8 DIV, the "unwanted" inter trap connection rate for 40µm spacing was 21.54% a percentage that dropped at 4% for a 140µm spacing (see Figure 70).

chamber name	EFG1	EFG1	EFG2	EFG2	EFG3	EFG3	EFG4	EFG4
distance (um)	40	140	100	225	100	225	225	400
porket number	48	48	30	30	16	16	16	16
possibly links	77	66	45	36	25	14	20	18
The percentage of unwanted connections happened	21.54%	4.15%	16.06%	3.72%	14.51%	9.37%	11.58%	5.87%

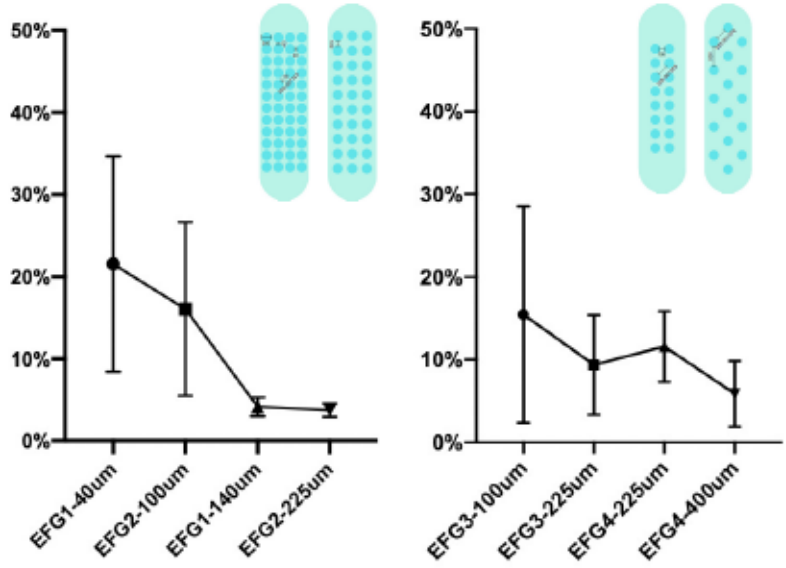

Figure 70. Quantification of the proportion of unwanted inter node connections as a function of inter node distance. Experiments were conducted in 3 separates experiments (cell seeding).

Based on the above experimental results, we thus obtained a variety of data that helped us to optimized both 2 nodes networks (Chapter 2) and multi nodal platforms. First, the diameter of the optimal node traps size should be between 200µm and 400µm for good survival, the spacing between traps should not be below 140µm to prevent unwanted inter node connections, and when seeding cells, the final seeding density of cells should be controlled at 20-40 cells per 10^4 µm^2 to mitigate spontaneous neuronal clumping and keep axons in the borders of the nodes These concepts were implemented in the last versions of the two-node cortico-striatal neural network chip shown in chapter 2 : the diameter of the emitting chamber trap is around 300µm, with an area of about 7×10^4 µm^2, and the area of the receiving chamber trap connected (or not) to the emitting chamber through a microchannel is about 3×10^4 µm^2 (refer to Figure 53 for

specific dimensions). The distance between receiving traps should be at least 140µm and 300µm between two mini networks. We also controlled the seeding density followed the results in this chapter. Also, all these size parameters were used for building and designing new multi nodal chips.

3.4.2 Study of the multinodes mono-chamber microfluidic devices

3.4.2.1 The preference of neural node connection

In addition to circular shaped nodes, we tested other hypotheses that aimed at optimizing axonal bundles exit from cell traps. Based on the observation that axonal bundles follow walls, as illustrated in the Figure 71, we assessed several pocket shapes that could impact axon guiding. We used the curvature of the star corner to induce the direction of axon growth. We encoded both connected and unconnected cell traps to monitor 1) the escape rate of axons in unconnected states and 2) the efficiency in inter nodal connection through connections. Interestingly, although the results stayed preliminary, star shaped pockets seemed to decrease the unwanted inter node connections. Comparing both connected to un-connected patterns seemed to indicate that axonal connections promote higher survival rates in the nodes, these results requiring further reproduction.

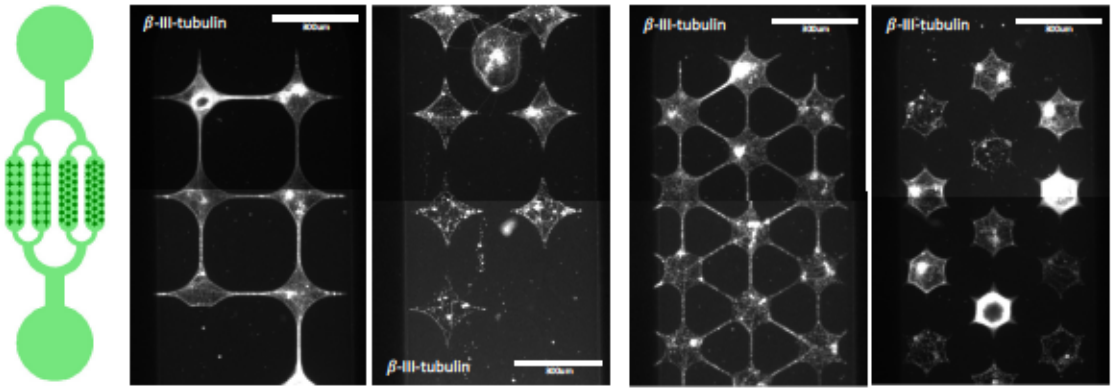

Figure 71. Cortical neurons seeded in star traps nodes with connected or unconnected patterns. 8DIV neurons were stained for β-III-3 tubulin.

Interestingly, the experiments performed with linked multi nodes shows that "unwanted" inter node connections decrease with the number of "wanted" node

connectivity. This suggests that promoting axonal exit from the nodes trough adhesive tracts strongly diminishes "unwanted" axonal escapes on non-cell adhesive areas (Figure 72). Although not tested here, we can infer that the depth of the IMP trap should also affects the behaviour of axonal escape over the wall. Due to engineering limitations, we did not test that parameter for now, and the trap depth were controlled to 5µm depth in this work.

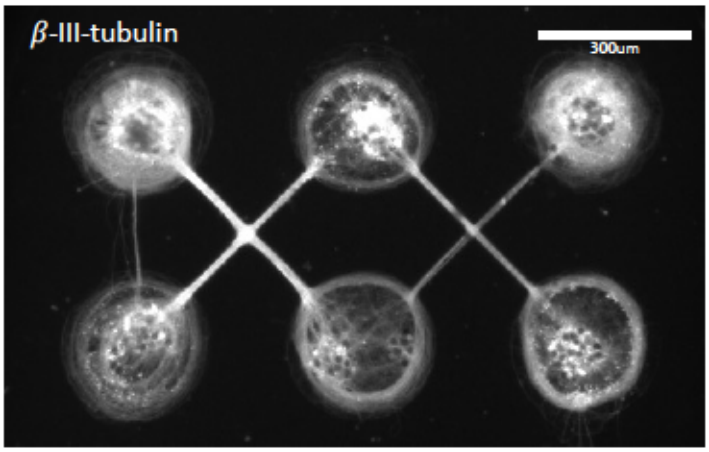

Figure 72. Neural node connection in 12 DIV cortical neural networks in vitro. Neurons were stained for β3 tubulin.

3.4.2.2 The survival of cell in multi-nodes network with internal connection

After 12 days in vitro, networks were stained by MAP2 (dendrites), and β-III-tubulin (axons). Figure 73 shows efficient neurites confinement and topographic control. In this multi-nodal network, all the cortical neurons in each nodes share the same culture environment. No cell nuclei were evidenced outside the traps and guiding tracts were mostly populated by axonal material, although some dendrites were able to reach neighboring nodes. This is due to the fact that cortical dendrites have been shown to grow up to 400 µm long in vitro, a limiting distance used in micro-channels of classical microfluidic chips to select axons and dendrites.

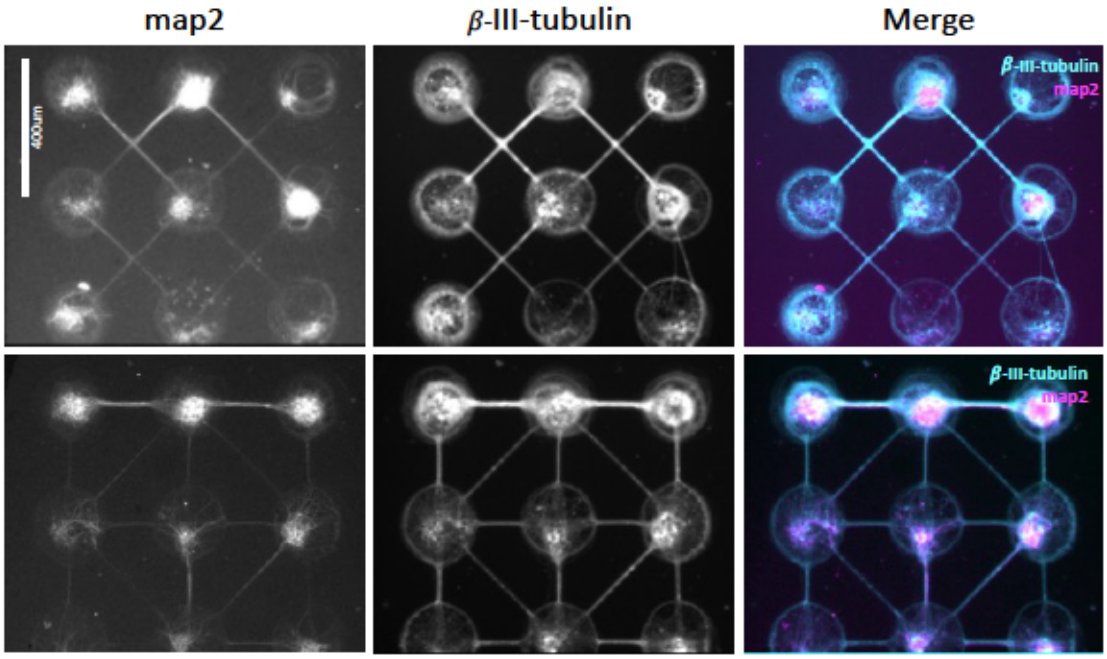

Figure 73. Distribution of Axons (β-III-tubulin) and dendrites (MAP2) of cortical neurons in multi-nodes system after 12DIV. (Horizontal distance between node's edge: 100um. Diagonal distance between node's edge: 225um).

3.4.3 Study of the multi-nodes multi-chamber devices

In the previous paragraph we described some critical parameters allowing multi-nodal networks reconstruction seeded in a single microfluidic cell culture chamber. Here, we wanted to implement axonal guiding tracts to connect nodes that are located in distinct microfluidic chamber, thus bridging the gap between conventional microfluidic and multi nodal positioning. We therefore designed microfluidic chips as described in Figure 61 which encodes different chambers (Z shaped) connected by unidirectional arches, or straight channels, with a length (inter node distance) of about 500µm. The cell delivery chambers having a height of 50µm and a width of 600µm.

3.4.3.1 Cortical neurons survival

Due to the length and geometry of the microfluidic seeding chamber, seeding volumes were adapted to obtain relatively homogeneous seeding along the flow axis. The microchips were first seeded with primary cortical or hippocampal neurons to study the parameters of progressive internode connections. In that new multi-nodal system,

we found that axons grew accordingly to what we initially observed in non-connected multi nodal chips and that they progressively invaded the axonal guiding tracts linking the nodes. Crossing of the microchannel and reaching of the distant node occurred around 5 to 6 days in vitro (Figure 74 a). As the figures shown below the more axons in the microchannel, the quicker they reach the other chamber (Figure 74 b).

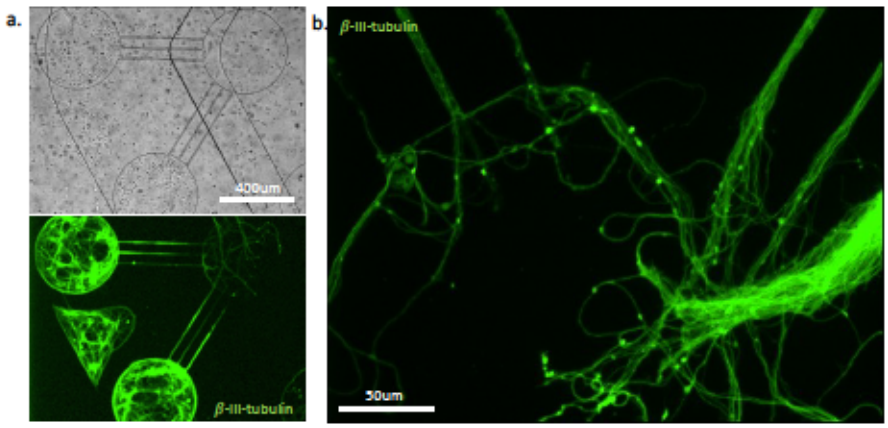

Figure 74. Axonal projection in compartmentalized multi nodal chips encoding straight inter chamber linking micro-grooves after 6 DIV. (a) Phase contrast and fluorescent images (β-III tubulin staining) showing axonal trajectory between nodes. (b) Axonal invasion of a non-seeded node.

The networks were stained to assess neuronal survival axons vs dendrite outgrowth (0). As described earlier, axons followed the edge of traps and finally entered the straight microchannel, and showed no sign of degeneration (0 a). The unidirectional arches microstructures majored anterograde growth (0b) while limiting the retrograde one (0 c). Due to the fact that some parts of the microgrooves or arches are exposed in the fluidic chambers and not fully covered by the PDMS walls of the macro-chambers few cells were found captured into the arch's channels (0 b). However, that problem can be further solved by optimizing the pattern design and alignment process in a future study.

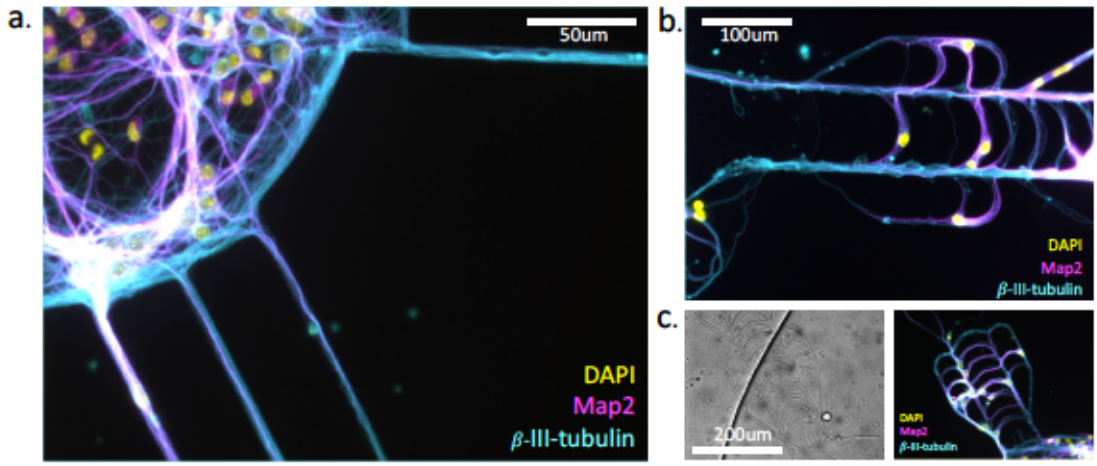

Axonal (β-III-tubulin) and dendritic (MAP2) growth in compartmentalized multi nodes chips encoding (a) Straight microchannel or (b-c) Arches as a directional guidance for neurites.

3.4.3.2 Establishment of compartmentalized multi-nodal cortical networks

After 6 days in vitro, the nodes from the cortical network starts to link and therefore establish a multi nodal platform either in unidirectional or bidirectional configuration (Figure 75). Overall, we succeeded in establishing intact compartmentalized multi-nodal cortical network that survived adequately for more than a week in vitro. Assessing further ageing of these networks showed that intact networks could be maintained for longer time of cultures but as described earlier, cortical clumping occurred progressively leading to loss in single cell study resolution. Clumping also induces high neurite tension leading to detachment of cells in the open (non PDMS covered) areas of the guiding microstructures. We tried to address this drawback in the following chapter.

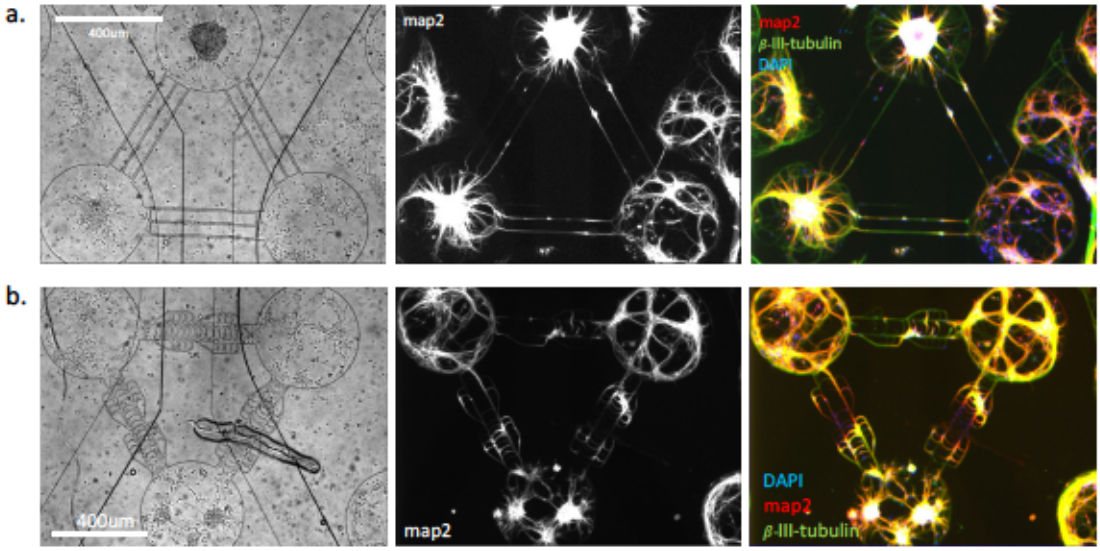

Figure 75. 6 days cortical neural network seeded in compartmentalized multi nodal platforms. Cortical network encoding 3-nodes looped, bidirectional (a) or unidirectional (b) motifs. (Left) phase image, (Center) MAP2 staining, (Right) overlay of MAP2, β-III-tubulin and DAPI staining. Each node being individually fluidically accessible it can be seeded with distinct neuronal subpopulations and/or challenged with distinct fluidic conditions.

3.5 Discussion

The purpose of this work was to build a multi-nodal platform allowing control of axonal outgrowth directionality and microfluidic compartmentalization. As a proof of principle, we used the IMP technique to pattern nodes and guiding tracts to build several theoretical motifs that encode feedforward, recurrent and "synaptic weight" topologies. These topologies being potentially interesting for studying how Prion-like element spreads along neuronal networks. Importantly in our final design each node being independently fluidically accessible. This shall permit both 1) seeding with distinct neuronal subpopulations allowing to construct complex neuro anatomical loops such as the basal ganglia loop; and/or 2) challenging of the nodes with distinct fluidic conditions and therefore initiation of diseases on one node to study disease progression according to the connectome grid.

The most demanding part of the work consisted in optimizing the critical parameters for node size and distance, as well as neuronal density to allow 1) good

neuronal survival and differentiation and 2) controlled axonal shooting toward the target nodes, after which we successfully encoded compartmentalized interconnected neuronal grids that survives for a week in vitro.

3.5.1 Geometric features as a dominant factor in OoC system

3.5.1.1 The geometry and master fabrication

Geometrical considerations to achieves microdevices that allows neuronal culture, axonal guidance and control of synaptic contacts requires the production of micro-systems that encompass a range of 2 orders of magnitude in the dimensions of their building elements. When producing the master of the design, some thin structure of the microchannel will be limited by the thickness of the coated photoresist, and too small width-to-height ratio will lead to the failure of the photolithography process. The MJB4 is a common photolithography machine, and the power of its light source is easily influenced by the laboratory conditions. It cannot expose a homogenous large area such as the one needed for cell trapping substrate. Therefore, I used microPG UV laser to directly engrave the iMP master, and achieved good performance. However, there is a limit of depth that can be patterned by this machine. Currently, the more mature experimental condition in our lab is to use SU 8 2005, leading to about 5µm in-depth structures after development. But good quality patterns might be obtained for thicker photoresists. It might thus be possible to limit the escape of cell axons by exploring the production of traps with a depth of about 6-8 µm.

3.5.1.2 Geometry and hydrophobicity issues

In both 2 nodes and multi-nodal designs (Figure 64, Figure 68), cell seeding along the flow axis presents a gradient of cell density distribution in the traps. Besides the cell suspension being progressively depleted from cells when they adhere to the target areas, a nonexclusive explanation could be that this is caused or majored by the fact that the bottom (IMP) layer of the chip is a rather hydrophobic surface with only the traps being hydrophilic due to PLL printing. When the cell suspension enters the chamber, the

hydrophobic surface slows down the fluid flow. The easiest way to solve that problem would be to extend the width of delivery channels to decrease flow resistance. Having noticed at the early stage of the processes that cells almost cannot enter "classical" rectangular flow chamber, this is why in a second generation of devices I encoded the size of entrance and exit of the flow chamber.

In addition, the cell suspension flow inside the chambers highly depends on the ratio between the seeding cell volume and the total volume of the flow chamber. A too high cell seeding volume (>10µl) would lead to such a flow rate that it would prevent cells to touch and adhere to the target areas. Inversely, a too low volume would lead the flow to stop inside the flow chamber. I therefore had to adjust an optimal seeding volume for a good compromise between hydrophobicity, cell adhesion and homogeneous seeding along the flow axis.

The attention to the features of hydrophobicity and hydrophilicity in IMP system is due to the microfabrication process that differs from the one of conventional microfluidic chips. Indeed, once generated, the patterned IMP layered cannot be processed with a plasma generator that will enhances hydrophily of PDMS, as this will destroyed the PLL patterned areas. Alternative methods solving that problem could be to use copatterning approaches of the non PLL areas to enhance substratum hydrophily (see chapter 5) or eventually to consider an alternative, more hydrophilic material as a substratum for IMP (thermoplastics). Yet this would require a complete re adaptation of the IMP process to study whether or not molecules such as PLL could locally be deposited in grooves and traps for example in hot embossing protocols. While not addressing that specific issue, the alternative methods I describes in Chap5 may be compatible with the use of hot embossed thermoplastics.

3.5.1.3 Chip geometry and cell survival

The geometry of the nodes in the chip also affects the cell survival and indirectly axon confinement. In the multi-nodes array, the internal structure encoded different

diameters of circular traps, and its purpose was to screen the smallest area that is suitable for neurons survival. The size of the traps clearly had a direct impact on the number of captured cells and that to some extend also depends on the density of the cell suspension. Yet we did not find a significant linear relationship between the area at the bottom of the trap and the cell density after seeding. This observation should deserve further exploration in the future. Therefore, the topology of the chip is not only important for the creation of appropriate connection distances between axons and dendrites to form the synapse between the different cell populations: the size of the chip determines whether the cell populations can be healthy and survive for a long time.

To sum up, the topology and size of the chip design are core elements for brain on a chip device. For the reconstruction of neural networks based on network connectomics, it is even more important to control the space inside the chip in order to accommodate as many nodes as possible and separate the nodes from each other to create an individual microenvironment, thus that chip can be used to study and mimic how neurodegeneration propagates in the neural network.

3.5.2 The network connection and open/further questions

Although we have explored the optimal distance to prevent axonal escape using Class E chip experiments, there are still some issues that are worth discussing and investigating. The clumped (high density) networks established internode links at a much higher distance that low density networks. The cut off for low density networks being around 100µm while clumped high density networks being able to send projections at 250µm distance. The reason why highly packed, spheroid neurons send "off target" axons more efficiently than low density networks remain obscure. This could be due to better adhesion of individual axons within axon bundles compared to a PLL substrate. Similarly, to a laminin substrate (known to accelerate axonal elongation), axons could promote the elongation of other axons, resulting in increased collective growth.

The figure below displays some interesting phenomena. In 77a, a clustered neural network forms a connection with the low density one. In 77b, nodes occupied by spheroids are interconnected. In Figure 76 d, close clustered nodes don't connect, while in c the long distance between the high-density nodes does not prevent connection. These observations lead to many very interesting questions about the dynamics of axonal path finding above non-adhesive surfaces, and how it is modulated by the properties of the region from which they emerge.

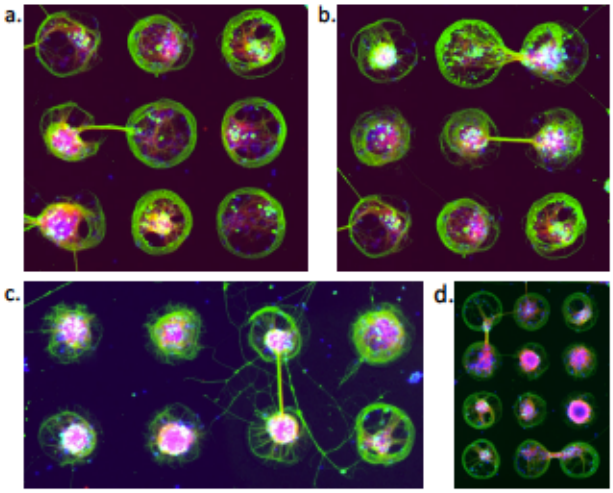

Figure 76. Illustration of unexplained unwanted connections. The diameter of traps size is 200um, and trapping distance is 100um in c, others are 40um.

3.6 Conclusion

In this chapter, I generated three types of multi-nodal neuron arrays. The optimization of various kind of microfluidic devices led to the generation of a new platform that would allow to study the role of topological features on networks behaviour. While these platforms could prove useful to decipher basic properties of information flow in structured networks our initial goals were to use these platforms to study some specific aspects of neurodegenerative syndromes, more specifically, the way prion like elements flows in neuronal networks. This is the topic of a next chapter.

4 α-synuclein spreading in cortico-striatal two-nodes neural network and hippocampus multi-nodes network

4.1 Introduction

Progressive degeneration of neurons in the brain, showing multiregional sequential chronic lesions over time, accompanied by deposition of pathological plaques of abnormal protein aggregates are pathological features of neurodegenerative diseases [274]. In Parkinson's disease, for example, the pathway by which Lewy bodies, of which a-syn aggregates are the main component, appear in the brain starts from the vagus nerve to the brainstem, the midbrain and then the cerebral cortex [275, 276]. The propagation mechanism of neurodegenerative diseases was then investigated [277-279]. In chapter 1.4.3, I reviewed various hypotheses of neurodegenerative diseases, among which the prion-like hypothesis attributes the disease mechanism to a variety of toxic proteins exhibiting prion-like propagation capabilities e.g. a-syn, tau, Aβ (also suggested in the literature as prioniods [280, 281]). Prion-like propagation encompass several rate limiting steps including 1) spread between cells (fit vs unable to spread between individuals) 2) seeding induced misfolding and aggregation, and 3 loss of neuronal structure and function and death, leading to this degenerative pathology [282]. These prionoids, especially exogenous seeds can propagate between cells by unknown mechanisms. In contrast, prions cannot be amplified in cells without an endogenous template [283, 284].

In the last decades, many studies have validated the concept of the transmission of pathological proteins between cells [285, 286]. The potential mechanisms are shown in the figure below (Figure 77). The main potential vectors of transmissions might be 1) Synaptic vesicles and exosomes, which are related to endocytosis and exocytosis process. The prionoids can be released from donor neuron by vesicles or exosome [250, 287-289]. Once in the extracellular space, these seeds can be uptaken by receiving neurons or other cells through several pathways [286, 290], including penetrating into plasma membrane and fluid-phase endocytosis [280, 291], synaptic vesicles endocytosis and fusion of plasma-exosomal membranes [24, 292-295]. Also, there is a

study [296] showing that pathological α-synuclein fibril transmission maybe receptor mediated. 2) Tunnelling nanotubes (TNTs). TNTs are also a kind of mechanism for cells communication, and these dynamic membranous tubes can create direct transient cytoplasmic continuity between cells [297]. Several studies shown TNT may mediate the prionoids transfer [298-301]. 3) Phagocytosis. The phagocytosis usually do not occur between neuron to neuron, but between neurons and glial cells [182, 302]. Microglial cells and astrocytes can endocytosis α-synuclein as a role in clearance [291].

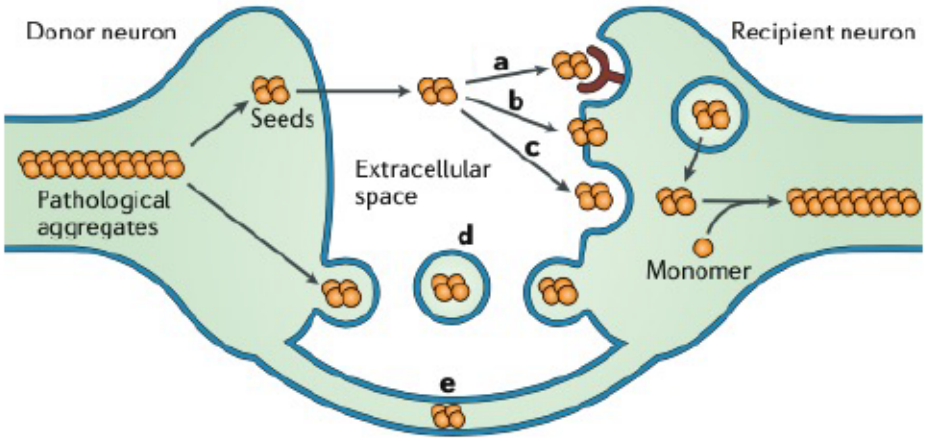

Figure 77. Potential mechanisms for the transmission of pathological proteins between cells. (a) Receptor-mediated endocytosis. (b) Penetrating into plasma membrane. (c) Fluid-phase endocytosis. (d) Synaptic vesicles or exosomes. (e) Tunnelling nanotubes. (Chao PENG, 2020).

To sum up, various exogenous prionoids are mostly introduced in these research models and the triggering and propagation of these proteins can be observed through the uptake of these seeds by cells. In in vitro studies, it is difficult to track its transmission process by traditional petri-dish culture. Thanks to microfluidic chip with fluid isolation [208, 209], it is possible to compartmentalize not only the neuronal soma and axon in different fluid environments, but also different populations of neuronal cells in different chambers through specific architectural designs. This means that it is possible to achieve a single chamber exposed to the seeds while the other chambers are not affected. It provides a very ideal model for studying the propagation mechanism of prionoids.

Microfluidic devices were successfully used for studying the intracellular transportation of pathogenic tau, aSyn, Aβ and HTT. The anterograde and retrograde axonal transportation of these prions was demonstrated [245, 255-257].

Our team and collaborators using conventional microfluidic chips validated that α-Syn strains trigger sustained nucleation of host-encoded neuronal α-Syn and associated neuronal dysfunctions. pSyn aggregates accumulate progressively in hiPSC-derived Corticocortical neuronal network [257]. In addition, they also concluded that mouse primary neurons exposed to fibrillar aSyn, exogenous aSyn were similar uptaken by neuronal cells from distinct brain regions but differed greatly in their seeding amplification capacities mainly because of their endogenous physiological aSyn expression levels [193]. Regarding the aSyn spreading in 100% oriented reconstructed neural networks made of different neuron population, the data from my colleagues shown that the inter neuronal transfer efficiency was very low [240]. From these results, they inferred that the prionoids spreading maybe impaired by intact synaptic structures. However, in the microfluidic devices they used (large chambers), most of axons stays in the same compartment as their soma. In other terms, only a weak proportion of axons cross the microchannels and contacted the post-synaptic neurons raising the question of impact of synaptic weight on prionoid inter-neuronal transfer. Moreover, due to absence of separation between axons from presynaptic neurons and post synaptic neurons it was not possible to assess retrograde trans neuronal capacities of prionoids. But in the iMP systems developed in this work, the connection rate between two chambers was extremely improved. We therefore wished to ask again the question of the modalities of synaptic transmission using this new experimental setting.

In this chapter, using our IMP microchips, the propagation mechanism of prionoids between neurons was explored. I first reconstructed the cortico-striatal neural network in a two-node chip in vitro (more information about cortico-striatal neural pathways and neurodegenerative diseases, please refer to 1.3.1.1), and treated the emitting chamber with exogenous recombinant aSyn aggregates. A disconnected node was

settled up in the receiving chamber in order to explore whether this propagation is synaptic dependent. The same treatment was also applied to the third chamber to explore the retrograde propagation in the neural network. Further, I performed experiments in a multi-node neural network as well. Multiple motifs in multi-node neural networks have been studied for specific purposes. It will be shown in the following subsections.

4.2 Methods

4.2.1 Chips fabrication and assembly.

Chips fabrication process as chapter 2.

4.2.2 Preparation of primary cell suspension

WT Swiss E14 pregnant mice were purchased from Janvier Lab, and studies all followed the standard ethical guidelines. The preparations of cortical and striatal and primary suspension are same as described in above chapters.

For hippocampal cultures, the hippocampal region of E16 embryos of WT SWISS mouse (Janvier Labs) were micro-dissected under the microscope in the cold Gey's balanced salt solution (GBSS) supplemented with 0.1% glucose (w/v). The hippocampal structures were rinsed by GBSS two times，then the falcon contained hippocampal pieces were incubated at 37 °C with 5ml of 10mg/ mL papain in DMEM supplemented with 100 units/mL penicillin-streptomycin for 8 min. Then papain was inactivated by adding 500µl of FBS and incubation at room temperature for 2 mins. After removing the medium and replacing it by fresh 5ml DMEM with 20ul of DNAse, the cells were mechanically dissociated by pipetting. After centrifugation (80 g, 7 min) of the cell suspension, the upper medium was removed, and DMEM used to suspend the cells. The cells were counted using Malassez counting device. The cell suspension was centrifuged again then removed the upper medium, followed by mixed in Neural basal complete culture medium (5% FBS and 2% B27) and controlled to 25 million

cells per millilitre as final concentration of hippocampal suspensions.

4.2.3 Cell seeding and culturing

The Cell seeding and culturing of cortical-striatal and hippocampal networks are same as above chapters.

4.2.4 α-Synuclein treatments

4.2.4.1 Treatments in the mature (around 2 weeks) neural network

After around two weeks of in vitro cultures, we first removed the medium from reservoirs of cortical chamber and transfer it to an eppendorf where it is mixed with α-synuclein Fibrils (Ronald Melki's Lab) labelled with a 633nm fluorescent dye. Then filled 30ul of α-synuclein medium solution back to wells, knowing that the final treatment concentration should be 200nM. After 48 hours, remove all medium and replace it by neural basal complete medium without phenol red. All procedures were performed under the PSM in L2 laboratory, and all containers or surfaces which touched with α-synuclein are all inactivated by a 2% sodium dodecyl sulphate solution. Then the chips were imaged under the fluorescent microscope. The same treatment was performed also in the central chamber of the device for studying the retrograde transmission.

4.2.4.2 Treatments in the hippocampus multi-nodes network (1 week) for p-syn nucleation

After one week of in vitro cultures, we first removed all mediums from the two reservoirs of the emitting chamber, and keeping half volume of old medium in the other reservoirs, then filled 40ul of fresh medium to wells except emitting chambers. The 30ul of 200nM α-synuclein Fibrils (Ronald Melki's Lab) labelled with 633nm fluorescent dye which well diluted in neuronal cell culture medium was added in each reservoir of emitting chamber. All procedures were performed under the PSM in L2 laboratory, and all containers or surfaces that had been in contact with α-synuclein were

inactivated by a 2% sodium dodecyl sulphate solution. After one week, cell culture medium was replaced by fresh one. Just before imaging, the cell culture media was replaced by Neurobasal medium without phenol red and microchips were imaged under an inverted microscope.

4.2.5 Immunofluorescence staining and imaging

Imaging acquisition and data processing are already described in the previous chapters. The primary antibody used (pSyn, Rabbit, Abcam, 51253) only detects alpha synuclein phosphorylated on Ser129. It shows no staining in human hippocampus normal brain but label human Parkinson substantia nigra tissue as expected.

4.3 Results of synuclein spread in two nodes system

4.3.1 α-synuclein propagation in two nodes cortico-striatal network

4.3.1.1 The anterograde propagating of α-synuclein in two nodes network

Cortico-striatal networks were reconstructed in 2 nodes iMP platforms according to the procedure described in Chap 2. Axons from one cortical node grew to the vicinity of 2 striatal nodes that were either connected or not to the cortical axons.

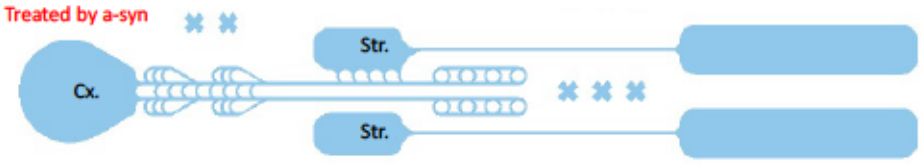

Figure 78. Schematic of chip pattern and treatment nodes. The left node was seeded with cortical cells and treated using aSyn. Middle nodes: the upper one is "Str. Connected" and bottom one is "Str. Isolated", non-treated. The right nodes have no cells but are filled with medium.

After 16 days of in vitro culture, networks were selected for good viability an appropriate connectivity (no off target nodes and axons) in phase contrast microscopy and cortical nodes in the emitting chamber were exposed to 200nM of exogenous fluorescently labelled recombinant alpha synuclein seeding aggregates [303] for 48 hours. Representative images of cortical and striatal nodes are shown in Figure 79.

While cortical nodes exhibited strong aSyn uptakes and dispersion of in axonal compartments, faints yet significant signal of aSyn appears in the striatal trap that were connected to the cortical neurons. This is reminiscent of a recent study conducted by our groups showing that strict anterograde transfer of aSyn aggregates from pre to post synaptic neurons is a limited process. Importantly no aSyn signal was evidenced in striatal nodes that were not connected to the cortical axonal grooves.

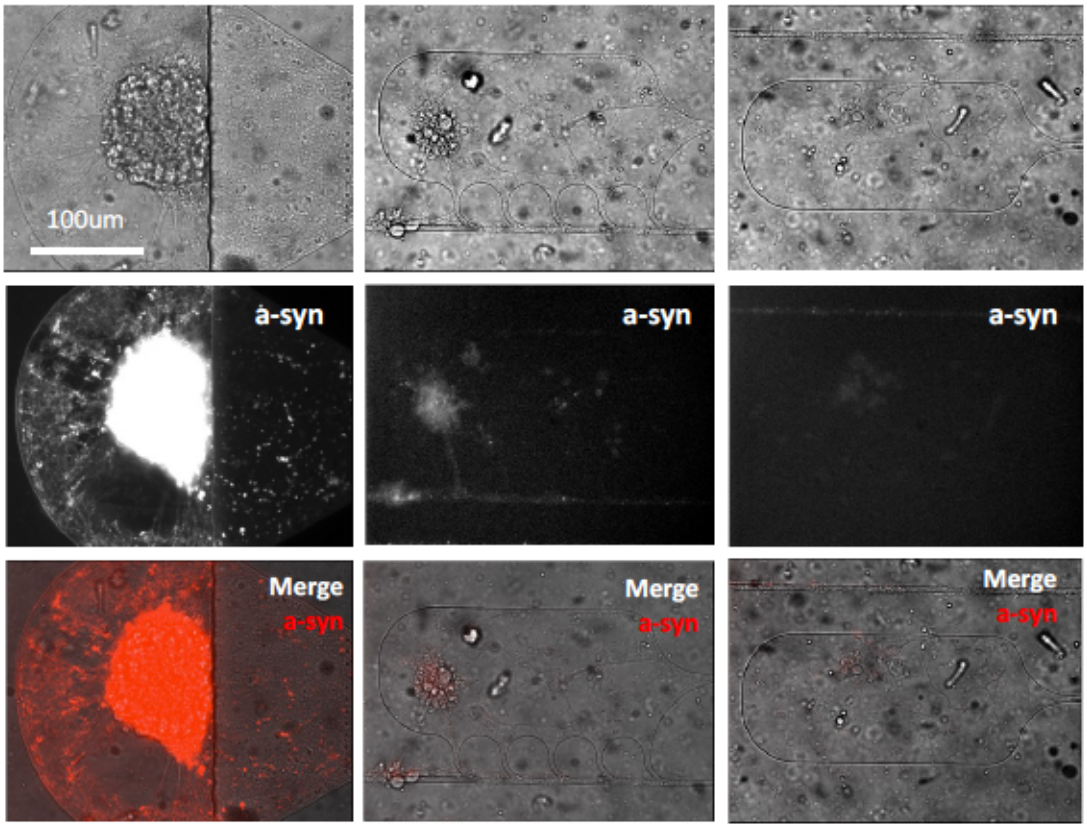

Figure 79. Results of the neural network being treated with aSyn for 48 hours after forward propagation. The first column in the figure shows the emitting chamber, the second column shows the connected receiving chamber, and the third column shows the unconnected receiving chamber. The images of aSyn in the figure were acquired at the same imaging exposure time and are presented at the same brightness and contrast.

Although I cannot completely rule out that the receiving (striatal) nodes shoots axons back to the emitting (cortical) chamber, this is rather unlikely. Indeed, in Chapter 2, I evaluated the that only 7.4% of all striatal nodes shoots a few axons back toward the cortical ones. During aSyn propagation experiments we found 3 connected receptive chambers with aSyn signals in 5 miniature networks of one chip, while none of isolated traps showed aSyn signals. Other chips from the same batch also had 1 to 3 mini

networks showing aSyn signals in connected receiving traps. In addition to this, We also observed that the intensity of the signals in receiving traps is weaker compared to the emitting chambers as we previously observed [240]. These observations suggests that aSyn spreading in our experiments occurred mostly through anterograde propagation. Further quantification and tracking of aSyn signals and higher resolution imaging results could better confirm this hypothesis. However, since the cells in the chip are mostly like spheroid which makes quantification difficult, and the thickness of the substrate of the chip is close to 200um (glass120 to 170um + PDMS layer 50 to 75um), which reaches the threshold for high resolution imaging. So, the quantification data will not be presented in my PhD thesis. Acknowledging that the experiments should be reproduced to permit statistical analysis, our results suggest that ASyn trans-neuronal spreading only occurs when synaptic contacts are established between pre and post synaptic neurons and do not majorly occur through humoral, diffusible (i.e. exosomal), spreads of protein aggregates. This would constitute a new finding in the field of prion like research.

4.3.1.2 Study of the retrograde propagation of α-synuclein in two-nodes network

Previous, published, studies have shown that both active anterograde and retrograde transport occurs in one's neuronal cytoplasm when aSyn seeds are introduced either on somatic or distal axonal compartments. Yet whether or not aSyn can spread in a retrograde manner between neurons has never been assessed. Using our platforms, we therefore investigated whether aSyn can backward propagates in a retrograde manner across neurons. In order to assess retrograde propagation, the third (axonal) chamber of the neural network was also treated with 200nM of fluorescent aSyn aggregates. The third chamber being mostly composed of striatal axons. The figure below shows the location of aSyn treatment in the neural network.

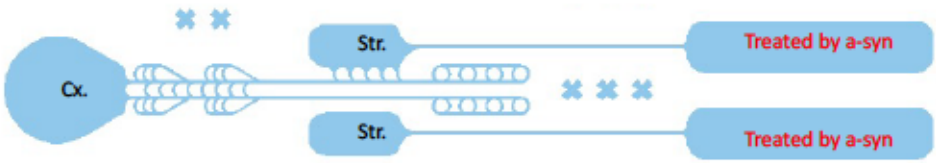

Figure 80. The schematic of chip pattern and treatment traps. (Fins could have different design version, all these designs will demonstrate in appendix.)

After 16.5 days of in vitro culture, the third chamber, containing striatal axons only, was treated with aSyn. The Figure 81 shows the aSyn signals are strongly detected in the striatal axon compartment while fluorescent aggregates could be detected in the striatal pocket, evidencing efficient retrograde transport from striatal axons terminal to their cell bodies. Although preliminary, interestingly, we found an aSyn signal in the cortical, emitting, chamber.

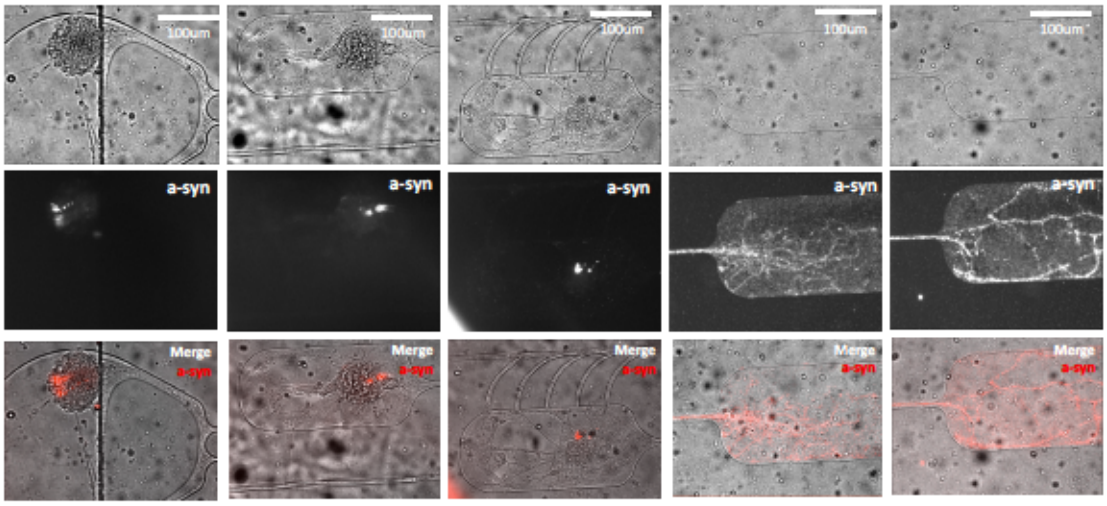

Figure 81. Results of retrograde propagation of fluorescent aSyn aggregates. aSyn was loaded on the striatal axon compartment (right images), and fluorescence spreading to the striatal nodes (center) and cortical nodes (Left images) was monitored.

After live experiments, networks were fixed and assessed for synaptic connectivity. As shown in Figure 82, cortical axons expressed strong VGLUT1 labelling with faint VGLUT1 staining along striatal MAP dendrites thus suggesting efficient synaptic contacts in the networks that exhibited aSyn retrograde propagation.

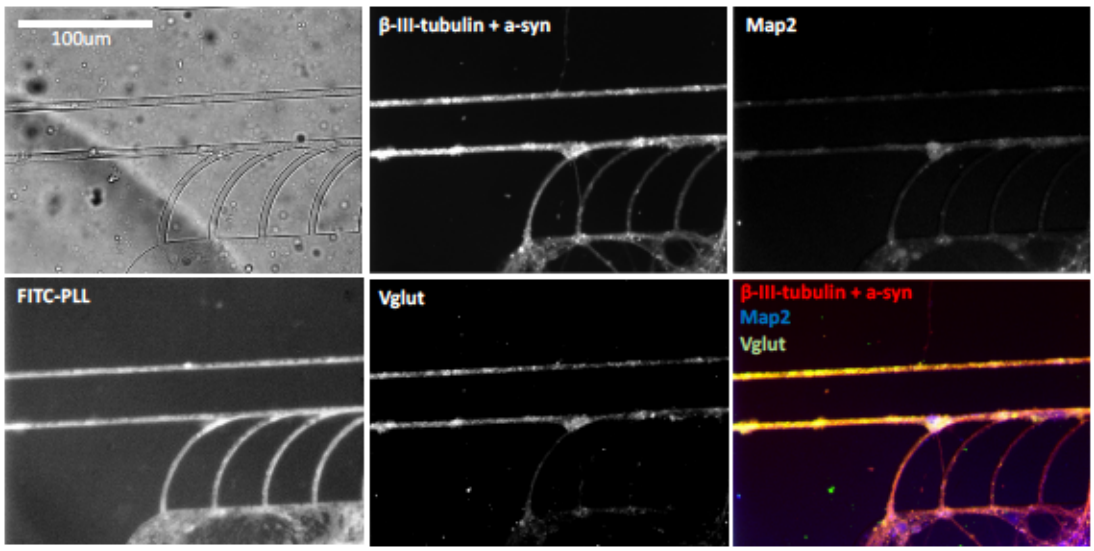

Figure 82. Synaptic connection between cortical and striatal nodes in the retrograde spreading study. After aSyn imaging, neurons were fixed and stained for MAP2, β-III-tubulin and VGLUT1.

In Chapter 2, I showed that axons from the emitting chamber are mostly confined inside the serial roller structure. However, axons from the emitting chamber were still found in 26.8% of the receptive chambers, and these axons cannot reach the third chamber 14DIV. But we observed here 18 days cultures, the possibility that axons from the emitting chamber have crossed the whole chip to reach the last compartment is not completely excluded. Based on the above results, it is clear that striatal neurons can uptake aSyn from axon terminals and transport it back to the soma in a retrograde way. However, although unlikely, it remains possible that the presence of aSyn signal in the transmitting chamber is due to the fact that axons from the transmitting chamber in a small number of receiving chambers launch into the third chamber to absorb aSyn and transport it to soma, or whether aSyn may also somehow travel across neurons in reverse to upstream neurons. This requires further study in the future.

4.4 Discussion about of few atypical cases that occurred during the aSyn spreading experiments

4.4.1 No cortical connections due to the misalignment chips

In the above experiments, we mentioned that neural networks with aSyn signals in

the post synaptic chambers accounts for about half of their total number. However, this proportion is also influenced by the chip fabrication process. It is difficult to avoid misalignment in the fabrication of the chip, such that some channels may be completely blocked when bonding is achieved (Figure 83, red arrow), while some will not. This affects the number of statistics on the mini networks that appear aSyn. In addition to this, there are accidents such as a random unequal seeding of cells.

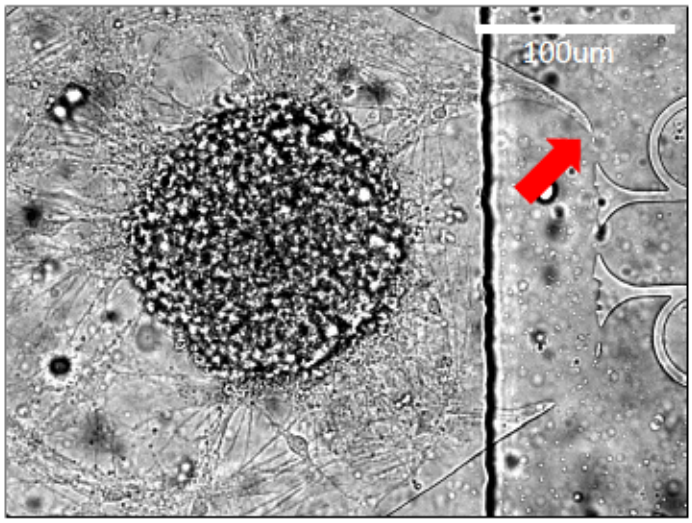

Figure 83. The connection cut down by misalignment.

4.5 α-Synuclein propagation in multi-nodes system

In the above study we showed that aSyn propagates from one neuron to the other only if synaptic contacts can be established between neurons. Reminiscent with one of our previous studies [240] anterograde spreading of aSyn aggregates is a limited process. One pending question is whether or not the number of synapses linking pre and post synaptic neurons is an important factor and whether or not a threshold of axonal connectivity for triggering the process of aSyn transfer exists. Therefore, in preliminary experiments, we assessed aSyn spreading in the multi nodal platforms that encoded 3 distinct motifs. The platforms were seeded with hippocampal neurons that grows at low density and most importantly have 2 important features that may impact prion like spreading in the multimodal context. 1) Hippocampal neurons express high level of endogenous synuclein and are therefore fast Synuclein amplifier trough

molecular seeding [303]. 2) Hippocampal neurons forms autapses both in vivo and in vitro and thus can form feedback loops.

First a "cluster" motif (Figure 84 b) was designed, which consisted in a group of 7 nodes connected through unidirectional arches microgrooves (Identifier: N7a, nodes-7-arches), among which 3 nodes in the emitting chamber (left transmitting chamber) and 3 nodes in the level 2nd grade nodes (one node in the left side of the middle transmitting chamber, and 2nd nodes in the right emitting chamber. This Ph.D. thesis will not discuss the 2nd emitting case, just focusing on the 5 nodes in the Figure 84b). The purpose of this motif pattern was to test the influence of the number of synapses between emitting and receiving nodes on the aSyn transfer capacities.

Moreover, hippocampal neurons being able to form autapses and feedback connection with themselves, I designed a 3-node unidirectional loop (Figure 84c), and a bidirectional loop as a control (Figure 84a) to assess the influence of feedback connection on aSyn spatial dispersion. Last, to study retrograde propagation and isolate the treatment nodes, I also designed a loop with an exit node (Figure 84d).

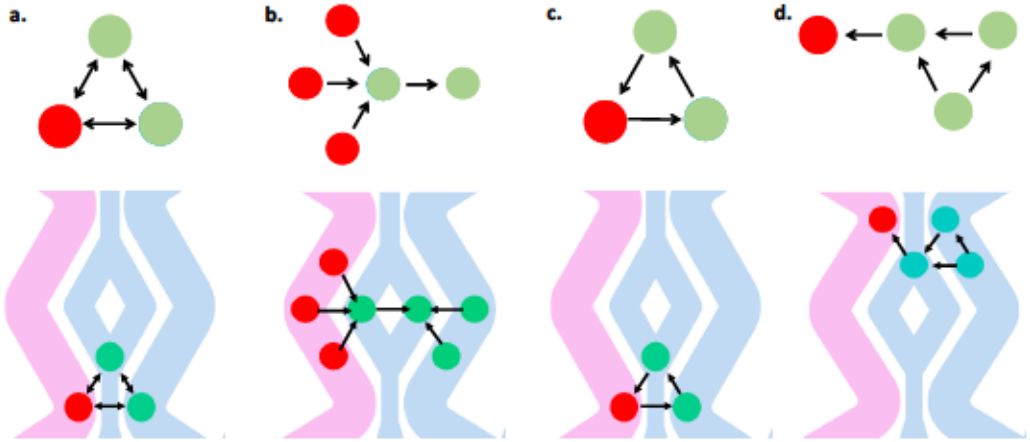

Figure 84. The main four kinds of motif in multi-nodes system. (a) Binary loop motif. Identifier: N3s, nodes-3-straight. (b) Clustering motif. Identifier: N7a，nodes-7-arches. (c) Unidirectional loop motif. Identifier: N3a, nodes-3-arches. (d) The loop with a tail motif. Identifier: N4a，nodes-4-arches. The aSyn were injected in left chamber (red color).

aSyn transneuronal propagation occurring in 2 sequential steps 1) fast transfer of protein seeds between neurons, 2) slow Syn aggregate amplification through a

nucleation process of host encodes synuclein; in these multi-node neural networks, aSyn aggregates were introduced in two different ways. The first one corresponds to a treatment of the emitting chamber of 2 weeks old network and a treatment time of about 48 hours to evaluates transneuronal transfer of fluorescent seeds. The other paradigm uses 1 week old network that were treated for a full week to assess synuclein aggregates amplification trough nucleation. The seeding induced amplification of endogenous syn was observed with pSyn antibody which is known as a reliable marker to visualize endogenous synuclein aggregation [303].

4.5.1 α-synuclein spreading in "clustering" motif

4.5.1.1 Transfer of fluorescent aSyn seeds in hippocampal topologies.

Hippocampal neural network was grown for 13 DIV and emitting nodes were challenged with 200nM of recombinant fluorescently labelled aSyn aggregates. Networks were imaged after 48hours. As shown by preliminary results in Figure 84b, emitting nodes were strongly labelled with aSyn aggregates evidencing strong hippocampal uptakes of the seeds. Interestingly detectable aSyn signal were evidenced in the second order nodes that received 3 inputs from the emitting chamber. No signal was detected in the downward nodes. Empirical observation gave the impression that aSyn signal in receiving first ode were stronger than the one observed in the 2 nodes systems.

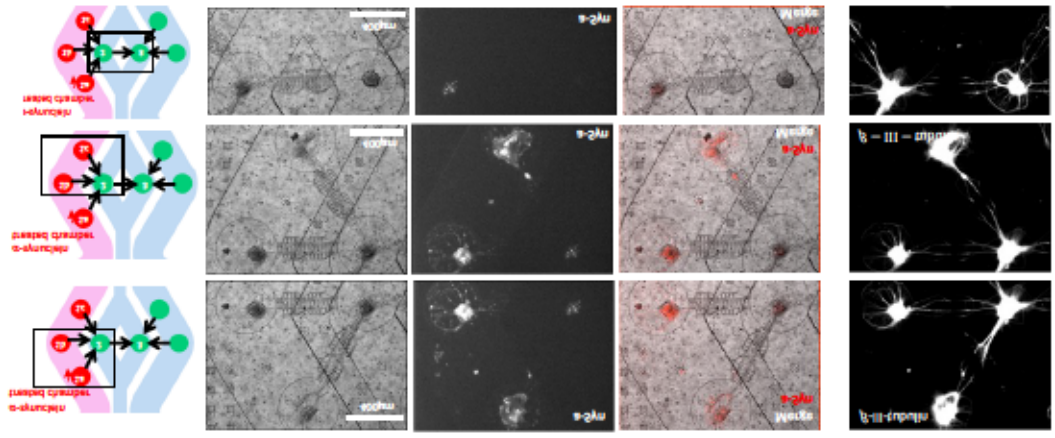

Figure 85. The cluster motif of hippocampal neural network treated by α-synuclein start at 13rd days and lasting 48 hours. Fixation at 15DIV, then staining by β-III-tubulin.

4.5.1.2 *Spatial dispersion of aSyn Nucleation in hippocampal topologies*

Using a lower seeding density, we treated the chips with aSyn at 7DIV. At DIV15, the signal of fluorescently labelled aSyn seeds in the emitting chamber was faint, and was even weaker in the second receptive trap in the next node, and not visible in the third node (Figure 86), evidencing transfer of recombinant seeds from node 1 to 2. However, p-syn staining (endogenous syn aggregated by the recombinant seeds) shows detectable phosphorylated aSyn in the second node with faint staining in the 3rd one This shows that recombinant seeds introduced in the first nodes leads to transfer and nucleation activity in the second nodes with an eventual transfer to the 3thd one that remains ambiguous as pSyn signal in the 3thd node could be due to staining of axons of the 2nd node neurons.

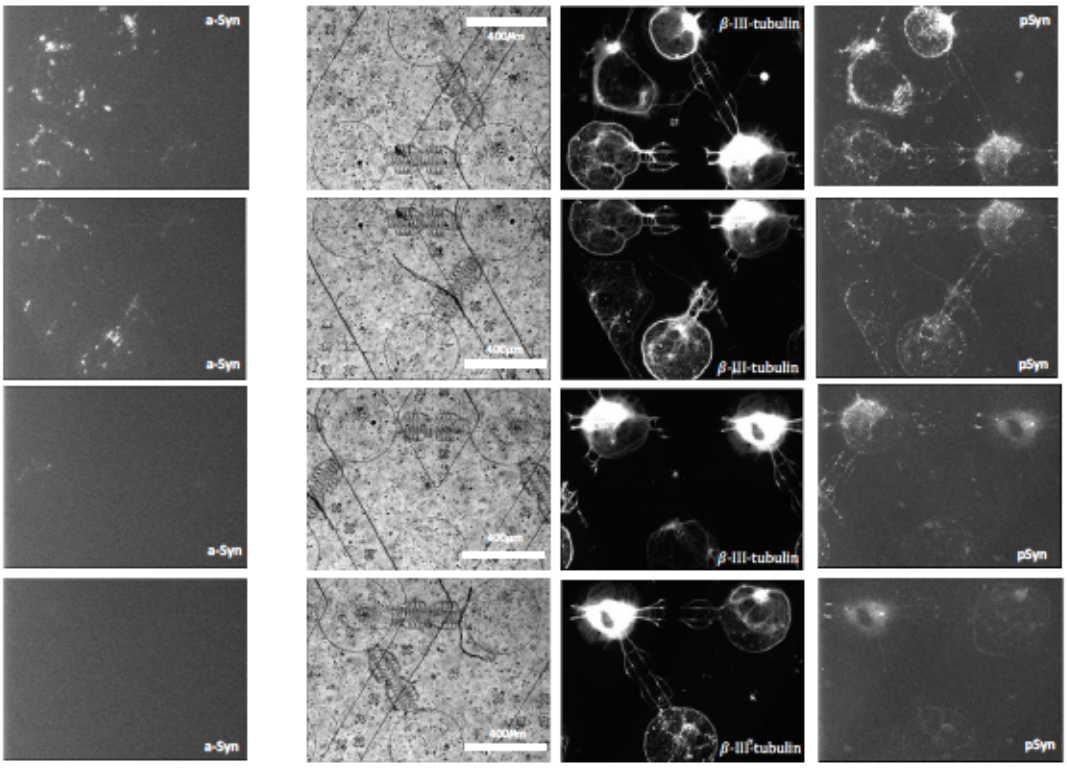

Figure 86. Images of a hippocampal neural network formed in a cluster motif after α-synuclein treatment at 7DIV. Fixation at 15DIV, then staining by b-III-tubulin and p-syn.

4.5.1.3 *Spatial dispersion of aSyn Nucleation in hippocampal topologies, late time points*

Nucleation of endogenous synuclein by recombinant seeds occurring

progressively over days of cultures, in order to try to observe higher aSyn and p-syn signals in networks, we extended the culture duration up to 21DIV. A more intense signal of phosphorylated aSyn was observed in the second node thus evidencing progressive amplification of Synuclein Prions.

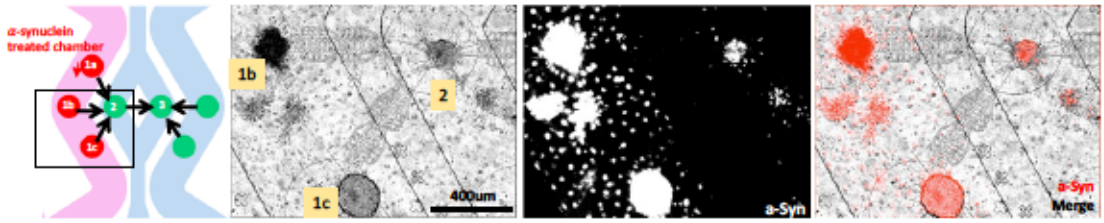

Figure 87. Images of a hippocampal neural network formed in a cluster motif after α-synuclein treatment at 7DIV. Fixation at 21DIV, then staining by b-III-tubulin and p-syn.

4.5.2 α-synuclein propagating in looped motif

4.5.2.1 α-Synuclein spreading in bi-directional loop motif, treated 7DIV, fixed 15DIV.

The following Figure 88 shows the propagation of aSyn and phosphorylated synuclein in a two-way loop. The propagation seems significantly less efficient due to the small number of neurons seeded in two nodes.

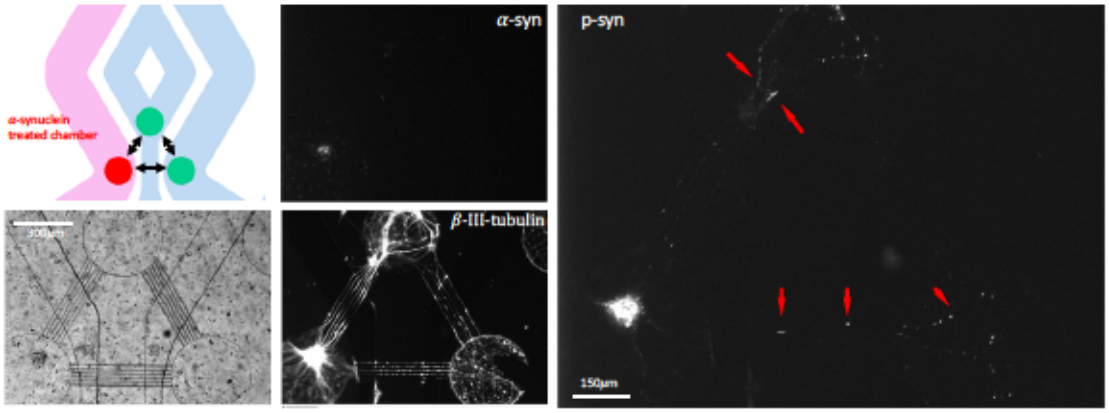

Figure 88. α-synuclein spreading in a bi-directional looped network. Red arrows show pSyn labeling.

4.5.2.2 α-Synuclein spreading in unidirectional loop motif, treated 7DIV, fixed 21DIV.

The Figure 89 shows the propagation of aSyn in a unidirectional loop motif at 21DIV. As seen in the figure the signal of aSyn decreases from 1st to 3rd grade step by step, as does phosphorylate synuclein.

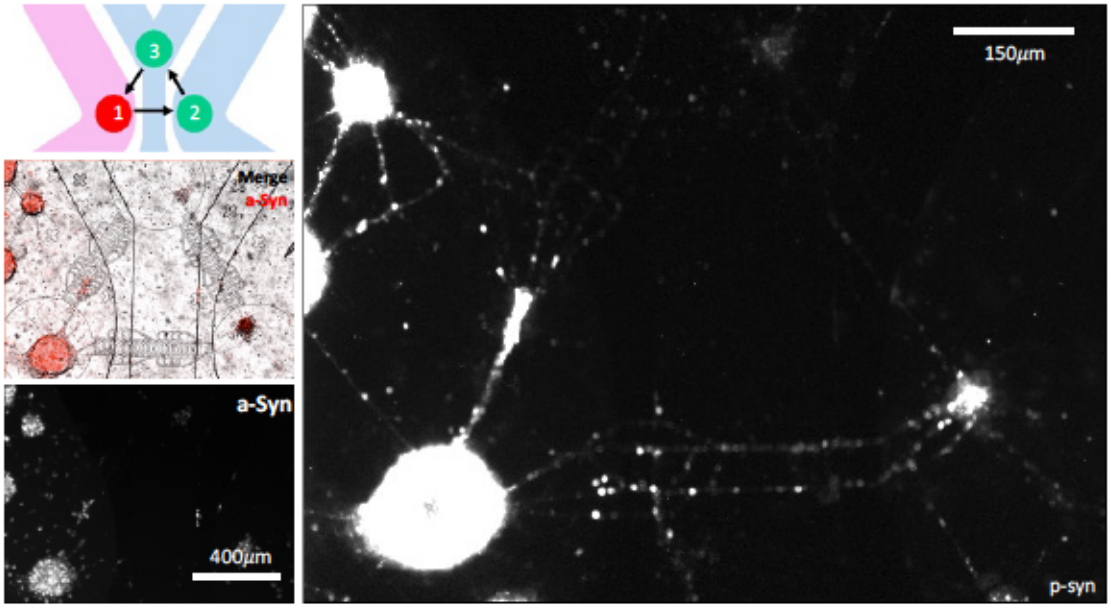

Figure 89. α-Synuclein spreads in unidirectional loop motif after 3 weeks culture.

Overall, the experiments of aSyn spatial dispersion in multi nodal networks encoding specific topologies remains preliminary. Unfortunately, due to the COVID pandemic episode the multimodal experiments were delayed. We were not able to proceed through a formal comparison between receiving nodes that were connected to 1, 2 and 3 nodes or statistical analysis. We therefore cannot draw any conclusion from our preliminary observations about the role of synaptic weight and topological features in the spreading of Prionoid elements. Yet, this demonstrates that the multimodal platforms are ready for such experiments.

4.6 Discussion

4.6.1 Forward propagation of exogenous aSyn

In this chapter, we tested the interest of multi nodal platform in modeling aSyn spreading in neuronal networks. The results depicted in that paragraph remains preliminary and more experiments should be done to obtain robust data allowing to correlate network topological features with aSyn prionoid spreading. Yet I observed several trends that may be of interest. I first constructed a linear two-node cortical-striatal neural network and treated the emitting node with exogenous α-syn. Exogenous aSyn was first uptake by soma then anterogradely transported to axon terminals located

in the receiving chamber. In connected traps, we observed that exogenous aSyn propagates in the neural network thanks to synaptic connection, while unconnected traps are free of aSyn signals. We therefore speculated that the cross-neuronal propagation of exogenous aSyn may be synapse-dependent and/or that paracrine secretion (i.e., exosome) of aSyn aggregates does not significantly participates in prionoid transfer between neurons. The anterograde transport of exogenous aSyn in axons has been reported in several studies[255, 257]. But the mechanisms of propagation across neurons still constitute an open question [239].

4.6.2 Retrograde axonal transport and backward propagation of exogenous aSyn

After treatment of the 2 nodes cortico-striatal neural network with exogenous α-syn in the striatal axonal compartment, aSyn was efficiently uptaken at the axon terminal and retrotranslocated to the striatal soma located in a separated node. Such a retrograde axonal transportation phenomenon has been consistently reported in the literature both on propose [304] and inadvertently in non-directional microfluidic chips used by groups (see Courte et al. [240] or chapter 1.5.5) studying neuronal transfer. More interestingly, we observed exogenous aSyn signals in the soma of upstream cortical neurons at a faint level, suggesting efficient retrograde transfer between neurons. Taken together our results suggests that aSyn seeds are transferred in both anterograde and retrograde manner along neuronal networks.

4.6.3 Increasing the number of emitting nodes is more likely to trigger enhanced-cell propagation of Synuclein.

In a previous study, using fully oriented neuronal networks [240] we identified that aSyn trans-neuronal transfer was a limited process involving molecular sieving of large size Synuclein aggregates. Yet, in these microfluidic chips, enforcing 100% axonal directionality was permitted at the cost of decreasing the number of synapses between the pre and post synaptic chambers. The multi nodal platforms allowed to rise

the proportion of first order neurons sending their axons toward the second nodes while permitting to increase the number of emitting nodes connected toward a secondary one. This, in theory should allow to control the "synaptic weight" between first and second order neurons. To understand the difference in the propagation efficiency of exogenous aSyn in the two nodes chips compared with conventional microfluidic chips, we made the hypothesis that this increased efficiency is due to an increase number of connecting axons. Following this hypothesis, we speculated that increasing the number of emitting chambers can trigger the propagation of aSyn more easily. Therefore, we designed the clustering motif in a multi-node neural network, and the results show a clear propagation of aSyn in three-week neural network, and the signal of aSyn can be extended across up to the next node.

Besides, we observed the accumulation of pSyn in the neural network, which indicates that exogenous aSyn triggers the aggregation of endogenous phosphorylated synuclein. pSyn's signal can even span 2 nodes. In contrast, exogenous aSyn recombinant seeds can propagate only to the next node. Our results remaining preliminary we still noticed a trend that showed that aSyn phosphorylation (aggregation) of endogenous synuclein of the nodes seems more efficient when multiple emitting nodes connect a single receiving one thus furthering the further study on the role of synaptic weight in prionoid element transfer.

4.6.4 Retrograde axonal transport in multi-node neural networks

4.7 Summary of disease modelling on chips

I successfully observed the forward propagation of aSyn across neurons in multi-nodes neural networks forming synaptic connections. We can draw preliminary conclusions from the set of experiments presented in this chapter. aSyn propagation across neurons in the forward direction may occur through synaptic connections. The mechanism of the retrograde transneuronal propagation of aSyn is not clear, but we speculate that it may be related to the production of exosomes.

When aSyn is uptaken by neuronal cells, endogenous aSyn expression is observed, phosphorylation and nucleation can be induced, manifesting as propagation in a prion-like way to the downstream neural network. Neurons on iMP devices have a tendency to aggregate, which constitutes an obstacle to quantification. To solve this problem, I have developed novel approaches to improve cell adhesion, so that the above experiments can be replicated and neural networks can be more easily tracked and quantified. The next chapter shows the two new methods I have developed.

5 New Methodologies of patterning poly-lysine on PDMS surface for improving cells adhesion and survivals on microfluidic chips

5.1 Introduction

In the previous chapters, using the "In mold patterning" technique, I demonstrate the conception of two types and multi-node neural networks encoding distinct topological features. In the two-node microfluidic chips, a cortico-striatal neural network was constructed that allows the control of functional connectivity between cortical axons and striatal neurons at the synaptic level. In Multi node platforms I achieved construction of complexes topologies networks composed of the same type of neurons. These experimental platforms allowed reproducible experiments when growing networks nodes composed of limited number of neurons thus permitting preliminary experiments on alpha synuclein aggregates trans neuronal spreading. However, while trying to increase the duration of cell culture and the number of neurons/nodes, two variable that controls the emergence of spontaneous neuronal network activity, I noticed that groups of neurons had a tendency to forms clumps after several days of culture. This had two main impacts on the efficiency of our platform: First, this decreased the capacity to track subtle fluorescent signals (e.g. pERK nuclear translocation) as the cells organized in spheroids; Second and most importantly, axons tracts linking the two nodes had a tendency to escape the guiding tracks after internode connections. In addition, I noticed that in some multi-node brain chips, the survival of hippocampal cells was highly variable thus increasing noise in our experiments.

In this chapter, I therefore assessed alternative strategies that could help stabilizing the reliability of our platform. I postulated that cell clumping at higher density and long-term toxicity may be linked to the uncontrolled quantity of PLL linked by the IMP fabrication process (unknown % of PLL embedded in PDMS bulk, and uncontrolled PLL desorption on long term cultures). Hence, I explore alternative strategies that would allow growing neurons using both mechanical and chemical constrains with more controlled PLL deposition.

It has been shown that both the behaviour and the survival of cells seeded on top

of artificial substratum are strongly related to the interface of their adhesion and the properties of different material interfaces [305-308]. Currently, besides polycarbonate and glass, the main material used in microfluidic organ chips is PDMS which mechanical properties varies according to the reticulation process. Park et al. used varying ratios between PDMS and crosslinker agent mixture to change the stiffness of the PDMS surface. When the crosslinker concentration ratio was raised from 10% to 20%, the survival rate of fibroblast cells was higher. However, for neurons, Chen[309], Cheng[310] and Lantoine [311] et al. studied the effect of PDMS surface stiffness on the growth of various brain cell types (hippocampal, dorsal root ganglion neurons, and cortical neurons, as well as glial cells). In Wei-Hsin Chen's and Joséphine Lantoine's studies, the growth rate of axon outgrowth was accelerated with a softer substrate that is obtained through the use of lower curing agent quantity. In contrast, in Chao-Min Cheng's study, the effect of PDMS stiffness on neuronal cells was not linearly related and already showed a bimodal response of neurite extensions at lower ratio of crosslinker. Considering that the stiffness threshold for the mechanosensitivity of neuronal cells is much below the lowest rigidity achieved by lowering the proportion of curing agent, the changes in growth behavior reported above might be the result of a change in the availability of adhesive molecules at the PDMS surface. Besides by adjustment of the crosslinker proportion of PDMS mixture, some studies focused on chemical modifications of PDMS surface [312-314]. However, in our attempt to modify PDMS stiffness, I found that modification of PDMS and adjustment of the stiffness affects the quality of surface bonding leading to liquid leaks at PDMS/PDMS interfaces. I therefore discarded that approaches that furthermore would have not solved the potential PLL bioavailability issue.

I therefore explored an alternative strategy that would allow more controlled PLL deposition in the areas of interest. I hope to change both the long-term survival and adhesion of the neurons by enhancing the polycationic attractive force of the substrate toward the neurons.

Unlike non neuronal cells such as Human mammary epithelial cells that can survive without adhesive proteins on PDMS as mentioned in Chung's study [308], the adsorption of cell adhesive proteins that are coated on the substrate surface are essential for neurons. Neuronal growth and neural network formation rely on both interaction with a polycationic molecules which "sticks" neurons to the substratum and allows 2D neurite extension, and extracellular matrix (ECM) proteins coating, such as laminin [315], fibronectin and collagen [316] which enhances neuronal survival and can acts as neurite elongating factors [266, 317] [318] and neurexin-1β[319]. As a source of polycations PDL and PLL are the most commonly used. I therefore created two new methods to promotes PLL local deposition in pock and grooves. I evaluated the potency of these two new methods compared to IMP technique, which all promotes local deposition of PLL in embossed areas of the chips.

(Note: The results shown in this chapter were obtained from three independent neuronal dissection and seeded in two batches of chip, each batch of chips were created in parallel and under the same time and same environmental conditions.)

5.2 Methodology I: Co-patterning microfluidics chips

In-mold patterning technique is achieved through a two-step pattern transfer process. Therefore poly-lysine transfer efficiency can be suboptimal compared to classical micro contact printing. In order to reduce pattern efficiency and transfer times, cell adhesion outside of patterned areas, we decided to evaluate a co-patterning strategy. PEG and PEG derivatives being commonly used to prevent cell spreading outside micro-patterned areas [320-322]. I thus tried to use the stamp-off technique[323] combined with IMP to achieve co-patterning PLL and PEG/PLL in the chips. I evaluated two strategies to fabricate the co-patterned chips that are illustrated in Figure 90.

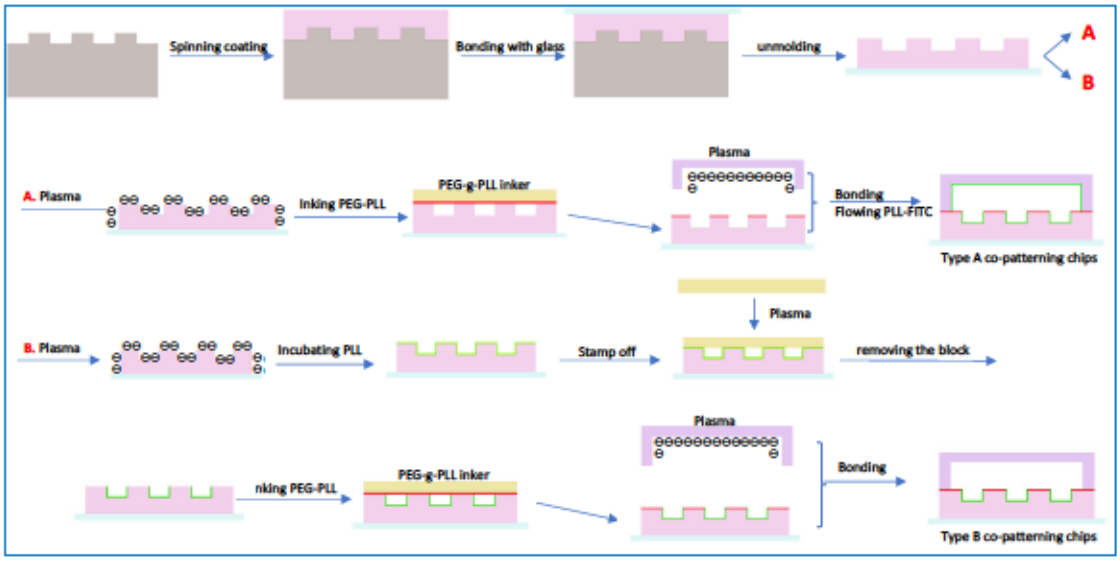

Figure 90. Two alternatives (A and B) for co-patterning PLL and PEG-PLL on microchips chips. PEG-g-PLL is represented in red, PLL in green.

5.2.1 Methods for PEG-g-PLL and PLL-FITC co-patterning chips fabrication

The design of the microfluidic patterns was obtained with Clewin5 software. High resolution photo-lithographic plastic mask of the upper chamber and extra fluidic chamber are printed at IPGG Microfluidic platform, while masks encoding the bottom layer are printed by microPG direct laser writer.

5.2.1.1 The cell delivery macro chamber and the stamp for trapping layers

The process is the same with chapter 2.2.3.1 to 2.2.3.3 and 2.2.3.5.

5.2.1.2 The PEG-g-PLL Inker preparation

7-8ml of polydimethylsiloxane are poured in a 5cm petri dish. The PDMS is then baked for 10 hours at 70 °C in a dry oven, and further allowed to cool down to the room temperature. The surface of the PDMS inker is incubated with a 100µg/ml PEG-g-PLL solution for 1h and then dyed with pressurized nitrogen. The inker is cut in 6mm*6mm small square blocks.

5.2.1.3 Route A: The fabrication of trapping layers and chips assembly

Su8 mold were spin coated with PDMS at 1000rpm for 45s, then baked into the

oven at 70°C for 75mins. Clean a glass coverslip with iso-propanol, perform plasma bonding on the surface of spincoated PDMS. After peeling off the PDMS from the mold, treat it with O_2 plasma, then ink it using the PEG-g-PLL stamp. Removing the stamp, bond and align the PDMS with the macrochamber, then fill with 10μg/ml PLL-FITC and incubate for 4h, rinse by deionized water followed by PBS. Type A of co-patterned chips achieved.

5.2.1.4 Route B: The fabrication of trapping layers and the chips assembly

Spin coat the Su8 mold with PDMS at 1000rpm for 45s, then put the resulting covered mold into the oven at 70°C for 75mins. Clean a glass coverslip with iso-propanol, then perform plasma bonding on the surface of spincoated PDMS. After peeling off the PDMS from the mold, treat it with O_2 plasma and incubated the surface in 10μg/ml PLL-FITC solution for 4h, rinsed by PBS and deionized water. Then using a block whished treated by plasma attached on the surface to remove the poly-lysine, then inked with the PEG-g-PLL. After removed the inker, bonded and aligned the trapping layers with the microchamber, Type B of co-patterned chips is achieved.

5.2.1.5 Cells seeding and culturing

The hippocampal cell suspension was prepared and cultured using similar process as described in chapter 4.2.2.

5.2.1.6 Immunofluorescence staining

After cell culture, cells were fixed with a 4% paraformaldehyde (PFA, Electron Microscopy Science) 4% sucrose (Sigma) phosphate buffered saline (PBS, Thermo Fisher) solution also contained for 15mins at room temperature. After rinse with PBS, chips were incubated with a 1% bovine serum albumin (BSA, Sigma) and 0.2% Triton X-100 (Sigma) PBS solution for 45mins at RT. Fixed and permeabilized cells were sequentially incubated for 1h with primary and secondary antibodies diluted in 1% BSA PBS solution.

The primary antibodies used in that study were, anti-microtubule associated protein 2 (MAP2, IgG1, sigma, M4403), anti-β-Tubulin Isotype III (TUBB3, IgG2b, sigma, T5076). Hoechst (Sigma, 33342). Secondary antibodies are Alexa labelled diluted at 1/500 in PBS 1% BSA.

5.2.1.7 Image Acquisition

After rinsing with DPBS, the chips were imaged using an Axio-observer Z1 (Zeiss) epi-fluorescence microscope, equipped with a CCD camera (CoolsnapHQ2, Ropert Scientific), 5X, 20x, and 63x objectives and controlled with Metamorph software (BioImaging). All imaging data were processing using Fiji [271] software. After imaging, the chips were filled with PBS containing 0.1% azide (Sigma) and placed at 4°C for long term storage.

5.2.2 Results

5.2.2.1 The patterning results of two ways of co-patterning chips

Two co-patterning approaches are shown here, type A and type B obtained respectively by route A and B in Figure 90. The main difference between them is the process order of PEG-g-PLL inker and PLL solution coating. From the literature I know that PEG-g-PLL has a repelling effect on cell adhesion[324], I therefore used PEG-g-PLL labeled TRIC (red fluorescence in Figure 91) and PLL-FITC (green fluorescence in Figure 91) to visualize co-patterning efficiency. In route A, I used PEG-g-PLL as an inker to imprint the plasma-treated PDMS surface. After assembly, the microchips were incubated with PLL-FITC, the cell trapping area had a clear pattern representation. The apparent homogeneous FITC-PLL staining is due to the fact that the entire chamber being perfused with PLL-FITC: both the ceiling and walls of the chamber are also coated with FITC-PLL. Yet careful examination of trapping areas that are outside the macro-chambers shows that target cell seeding areas were properly patterned (white arrow, Figure 91 left). Moreover, PEG-g-PLL was appropriately counter-patterned on the bottom layer, outside the cell trapping areas (The red fluorescent channel shows the

complete patterning of the non-cellular adhesion zone). As the patterned area of interest usually encodes thin-lines, most of the flat areas that will ultimately encode PLL free areas, require small pillars to support the weight of the inker and to prevent collapse and unwanted transfer of PLL (if the pillars and thin lines cannot stand the inking force, it tends to collapse). In route B, I have used PEG-g-PLL to cover undesired cell adhesion regions on the fully coated PLL-FITC surface. The images shown a clear patterning of trapping regions and unwanted-trapping regions coated with PEG-g-PLL and PLL-FITC respectively. The results show that both methods of co-patterning present a good co-pattern of partitioned adsorbed proteins regions.

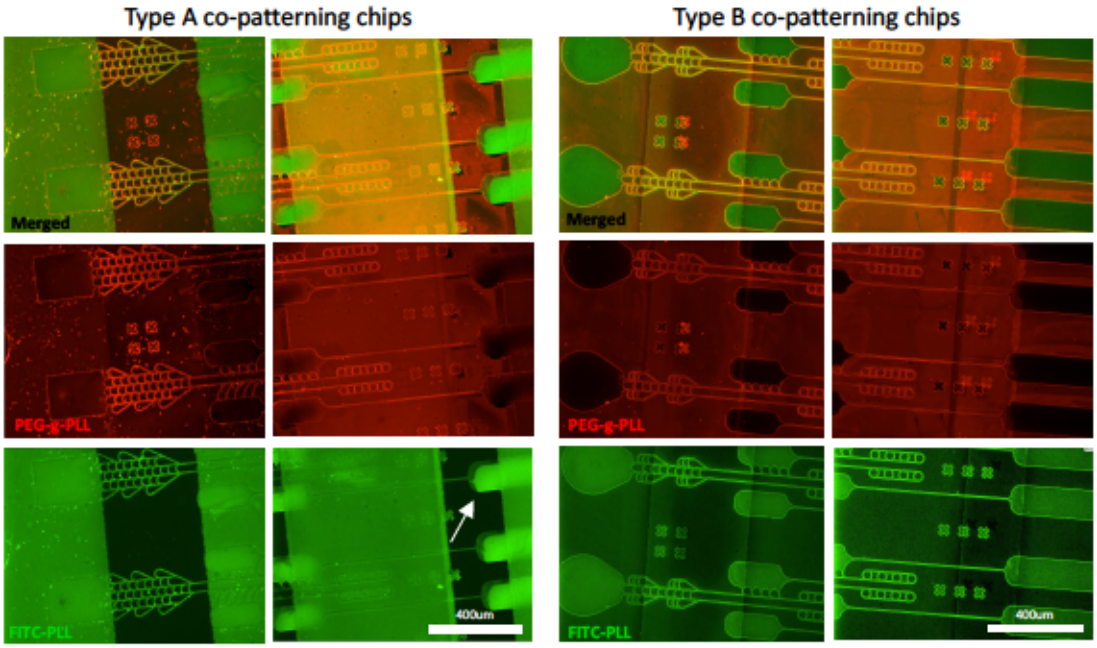

Figure 91. Co-Patterning of PLL-FITC and PEG-g-PLL on in-mold patterning chips: the red color corresponds to TRITC labelled PEG-g-PLL and the green color corresponds to FITC labelled PLL. The white arrow shown the overlapping shadows from the ceiling of chamber.

5.2.2.2 Cell behaviours on co-patterning chips

I imaged the distribution of three different cell types in the type A chips after 6 days. The results showed (Figure 92) that although the adhesive contrast was present, the cells were distributed over almost all areas, suggesting that although good apparent co-deposition, PEG-g-PLL did not prevented cell adhesion efficiently.

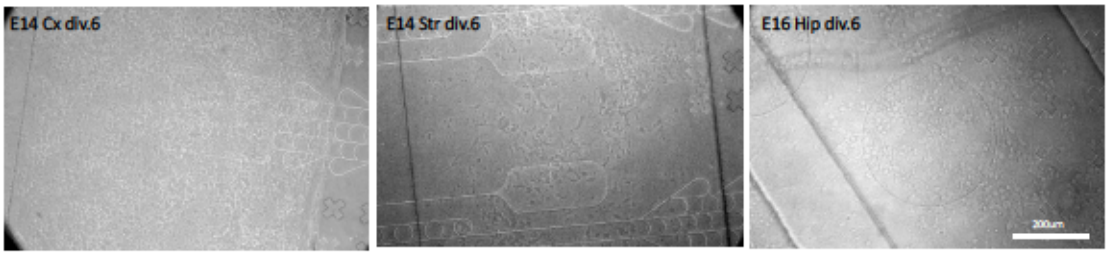

Figure 92. Three neuronal subtypes (Cx : cortical, Str : Striatal, Hip : Hippocampal) seeded in a two nodes network chips fabricated by route A co-pattering techniques. Note that adhesions "contrast" is poor with many cells growing on PEG-PLL areas.

Based on the results of cell adhesion, we can infer that small molecule such as PLL may enter in-between the chains of PEG-g-PLL: the PLL head of PLL-FITC is positively charged and could be adsorbed within PEG chains [325] thus leading to non-conclusive results.

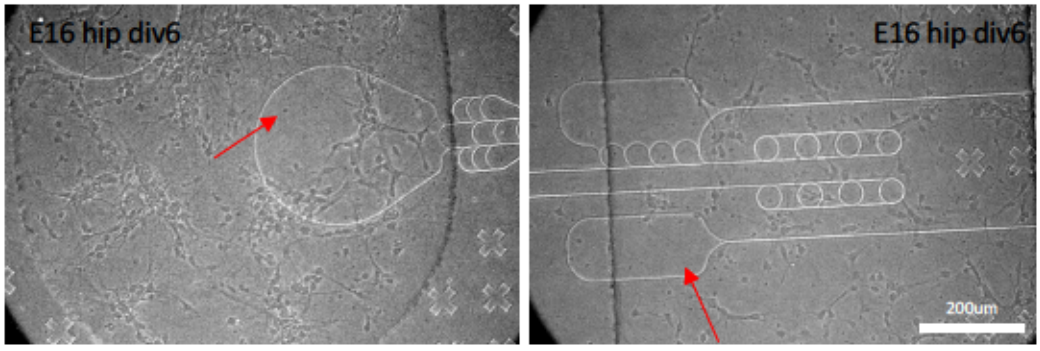

Figure 93. Hippocampal primary neurons seeded in two nodes network chips which produced by route B co-pattering techniques. Note that adhesions "contrast" is poor with many cells growing on PEG-PLL areas.

5.2.2.3 Cell survival in co-patterning chips

Interestingly, after I immuno-stained some of the micro-chips, I found that neurons exhibited good survivals on the PEG-g-PLL surface after 8 days of culture (Figure 94).

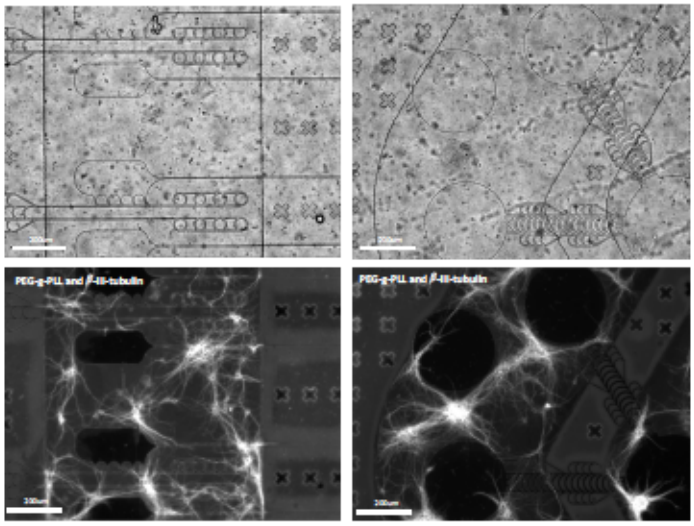

Figure 94. Neuronal differentiation on co-patterned (route B) chips at 8 DIV. Note that neurons primarily grow outside the area of interest.

5.3 Methodology II: Extra-flowing patterning chips

Second, an alternative method to promote local PLL deposition in the pockets and grooves of the substratum through microflow patterning was evaluated. That approach relies on the use of 3 specific layer, 1) a thin (50µm) bottom layer encoding cell traps and axonal grooves, 2) a transiently (reversible bonding) bonded microfluidic flow chamber encoding channels targeting the cell trapping areas, 3) a microfluidic cell seeding/feeding layer that encodes several cell cultures macro chambers that is ultimately bonded on top of the flow patterned textured bottom layer. The transient microfluidic layer partially matches the cell seeding areas of the bottom layer. After treatment of the bottom layer with oxygen plasma, the flowing layer is immediately contacted with the bottom layer and PLL is flown through the channels of the microfluidic layer. Plasma activation of the bottom layer allows minute PLL grafting in the exposed areas. After a few hours of contact, this top microfluidic chamber is removed. Due to the specific structure of the flowing interface, the poly-lysine will only follow the desired channel in the cell traps, thus allowing coating only in specific area of interest (Figure 95). Upon upper, fluidic, chamber removal, the final cell delivery microfluidic is assembled on top of the bottom layer. The fabrication method of this chip requires one step more than IMP, but it should provide stronger adsorption of PLL

in the areas of interest and therefore, compared to the physical transfer of IMP, and therefore allows better adhesion of neurons on the substratum.

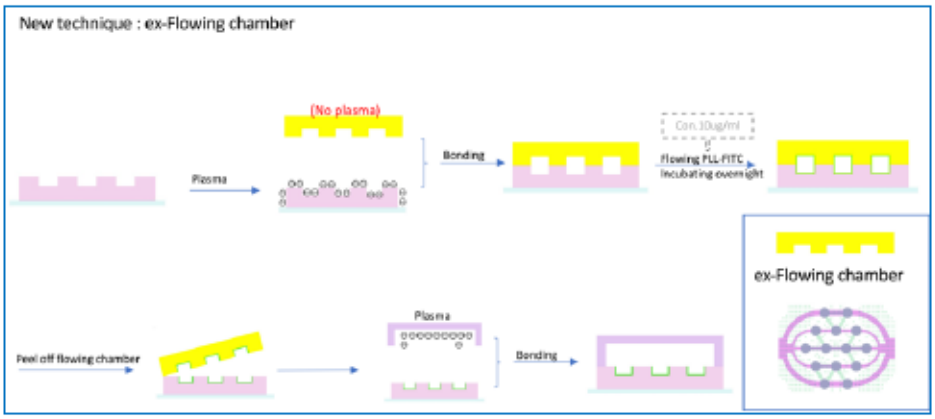

Figure 95. Design and Fabrication process of ex-flowing chips: An uncoated thin PDMS layer encoding grooves and traps is produced. A transient microfluidic interface targeting nodes of the PDMS layer is contacted with the PDMS membrane and PLL is flown. Extra flow in pockets and grooves. The transient microfluidic interface is removed and a Cell culture microfluidic interface is bonded on the locally coated PDMS layer.

In this chapter, I compare the efficiency if the 3 methods (IMP; Co-patterning IMP; flow patterned chambers) by seeding hippocampal neurons and assessing their survival rate at different stages.

5.3.1 Methods for Extra-flowing patterning chips fabrication

5.3.1.1 The master of cell delivery chamber, ex-flowing chambers and trapping layers fabrication.

Fabrication of the cell delivery chamber and the trapping layers are similar to the process described in 2.2.3.1. The master encoding the ex-flowing transient chambers was fabricated by spin coating SU-8 2075 at 3000 rpm on top of a silicon wafer, then soft-baked for 2min at 65°C and followed by 8min at 95°C. After cooling down at room temperature, the wafer was exposed 17s under a UV light through the ex-flowing chamber photomask. It was further baked for 3min at 65°C and followed by 9min at 95°C. The master was then developed in PGMEA at 60 rpm for the 7min and dried with pressurized nitrogen. A final hard baking was performed for 5 mins at 200°C.

5.3.1.2 *The soft lithograph for cell delivery chamber and ex-flowing chambers*

Polydimethylsiloxane (PDMS, Sylgard 184, Ellsworth Adhesives) was mixed with its curing agent at a of ratio of 10:1, then degassed under vacuum. PDMS was then poured on top of the silicon master surrounded by aluminums and incubated at 70 °C for 3h (chamber and ex-flowing chambers were produced at thicknesses around 4-5mm). After unmolding, reservoirs were pinched in specific areas with 4mm biopsy punches.

5.3.1.3 *The fabrication of stamp for trapping substrate*

The stamp was placed in O_2 plasma generator (FEMTO, science, CYTE), with pattern facing up (exposed to plasma). After plasma treatment, the stamp was silanized for 30 mins with (Tridecafluoro-1,1,2,2-tetrahydrooctyl) trichlorosilane (AB111444, abcr). PDMS was then spin coated on top of the silanized stamp for 45s at 1000rpm and further baked for 75 min at 70°C in a dry oven.

5.3.1.4 *The fabrication of trapping layers*

5cm glass coverslip were cleaned with iso-propanol, then plasma bonded with the surface of the coated stamp. After peeling off of the stamp, the substrate layer treated with O_2 plasma, was contacted with the ex-flowing chamber (which is non-plasma treated). 10μg/ml PLL-FITC solution was then flown in the circuitry and incubated for 4h, followed by rinsing with PBS and deionized water. The ex-flowing chamber, was then dried with pressurized nitrogen.

5.3.1.5 *The chips assembly*

Finally, the PLL patterned trapping substrates was aligned and bonded with the cell seeding micro-chamber producing the final micro-chip ready for cell seeding. Chips were sealed and stored at 4°C until use (max 1 week after fabrication).

5.3.1.6 *Cells seeding, culturing, staining and Image Acquisition*

The process is the same with above section.

5.3.2 Results of ex-flow chips

5.3.2.1 Patterning in two nodes system

As I mentioned, in IMP techniques the poly-lysine coating is obtained first through micro-contact inking on the stamp, then from transfer by the spin coating process. It is thus unknown how much PLL is left on the groove surface. Therefore, I created a method to avoid any pattern transfer by adding a temporary chamber bonded with a plasma active trapping layer. The role of this temporary chamber is to flow the poly-lysine solution. This chamber will be removed after completion of the patterning. The challenge here is to align two times properly the textured substrate with the temporary "flowing" chamber then the final culture macrochamber.

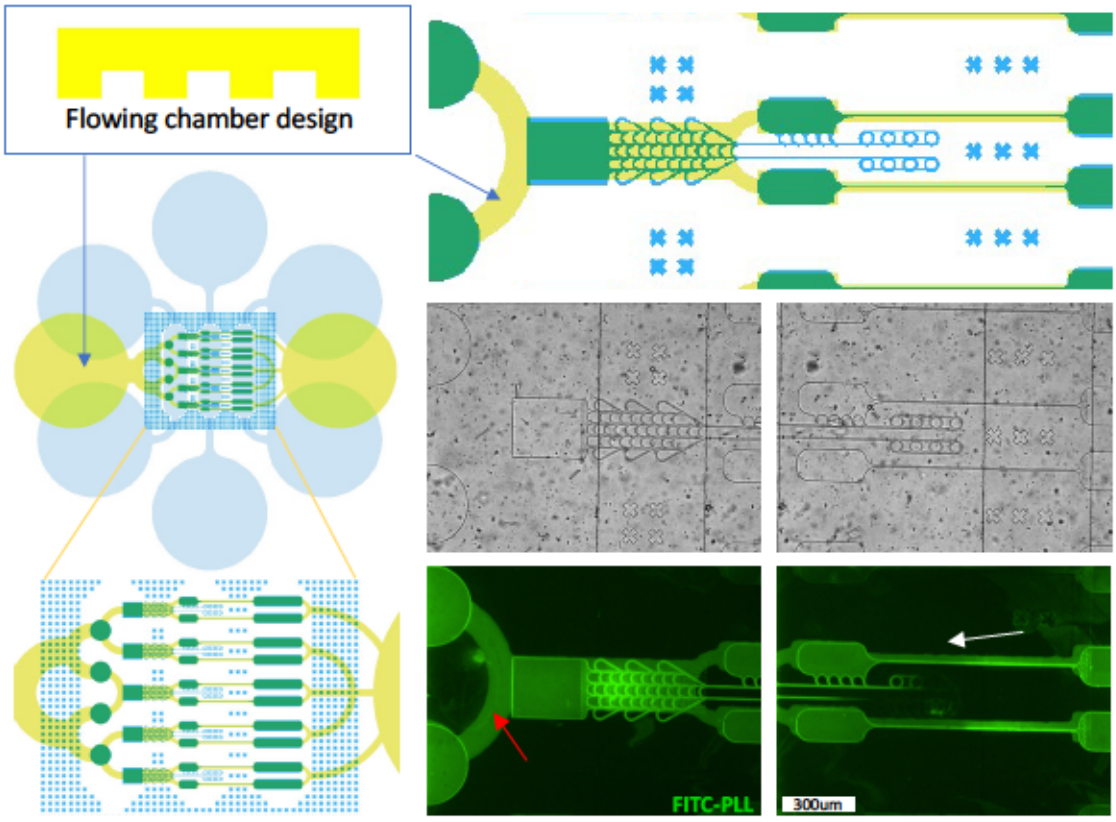

Figure 96. Illustration of "ex-flow" microchips design. The yellow device corresponds to the transient microfluidic flow chamber. Yellow area corresponds to the areas of the PDMS membrane that will be coated with PLL. (Right, center): Phase contrast image of an ex-flow chip. Note that PDMS walls of the final microfluidic cell culture layer are located on top of the arche like micro-grooves. (Right, bottom): Fluorescent image of a final ex-flow microchip coated with FITC labelled PLL. Note that because of the design of the transient microfluidic flow chamber not matching the one of the final cell culture layers,

some PLL is deposited in unwanted areas. A important part of the design work consist in minimizing these areas.

The figures (Figure 96) show the design pattern of this extra device, that we will from now name the "ex-flowing chamber", positioned on top of the substrate with groove structures. It will be attached to its substrate only reversibly, thanks to the plasma activation of only its surface and not that of the substrate, and filled with PLL. As a result, the 5um deep traps will be coated with PLL-FITC. This ex-flowing chamber was designed to cover the connections between traps arranged along each parallel neuronal circuit (red arrow). It is important to note that the traps belonging to different circuits remain unconnected. It is clearly seen that the ex-flowing chamber can create precise patterning areas. A few areas that do not constitute a connection are be coated (white arrows), creating the desired adhesive contrast.

5.3.2.2 Cell behaviour in two nodes system during two weeks in vitro

During the two weeks of growth of hippocampal cells in the chip, I recorded the distribution and survivals of cells at 15 minutes, 7 days and 14 days after seeding (Figure 97). It can be seen in the figure that although in the initial state just after seeding there are some cells distributed all over the surface of the substrate as the time passes most of the cell survival and growth occur on the poly-lysine coated areas (red arrows). Moreover, it is obvious that when the positioning of the ex-flowing chamber matches perfectly with the cell traps pattern, the wall of the traps has a well-assisted guide to axon growth (blue arrows).

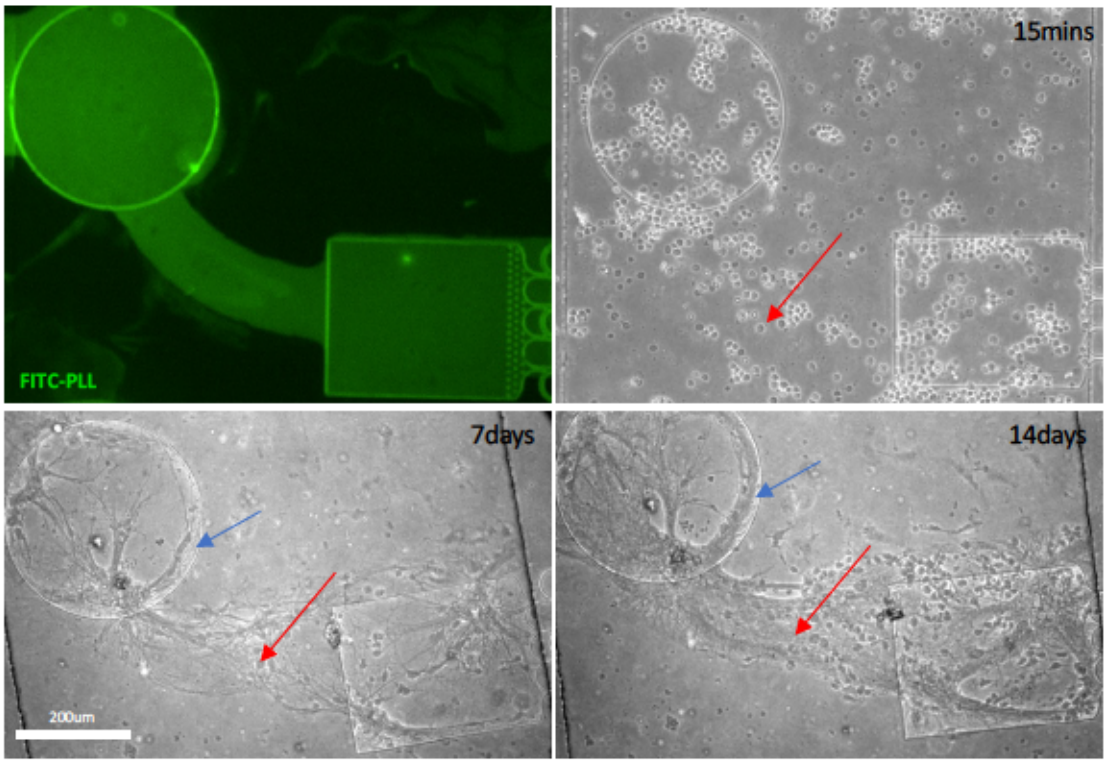

Figure 97. 14 DIV Hippocampal neurons survival in a two nodes network chips produced trough by ex-flow patterning. (Left, up) : FITCC PLL deposition in square and round node. Note that unwanted PLL patterning link the 2 nodes. Phase contrast images of hippocampal neurons seeded after 15 min, 7 DIV or 14DIV. Note that neurons grow only in PLL patterned areas and that both nodes are linked by growing neurons.

5.3.2.3 Patterning in multi-nodes system

I have used this new technique in the multi-node network configuration. The Figure 98 contains two designs of ex-flowing devices. The first design passes through almost all the traps, and even most of the microchannels (blue pattern). The second design aimed to reduce the hydrodynamic resistance of the ex-flowing device and does not pass through most of the microchannels (purple pattern). Coating of the micro-channels will occur instead through the diffusion of the PLL solution in-between the arms of the ex-flowing device. The purpose of these experiments is to verify how microchannels and traps can be selectively coated with poly-lysine in each condition. This will guide the optimization of the next generation of designs.

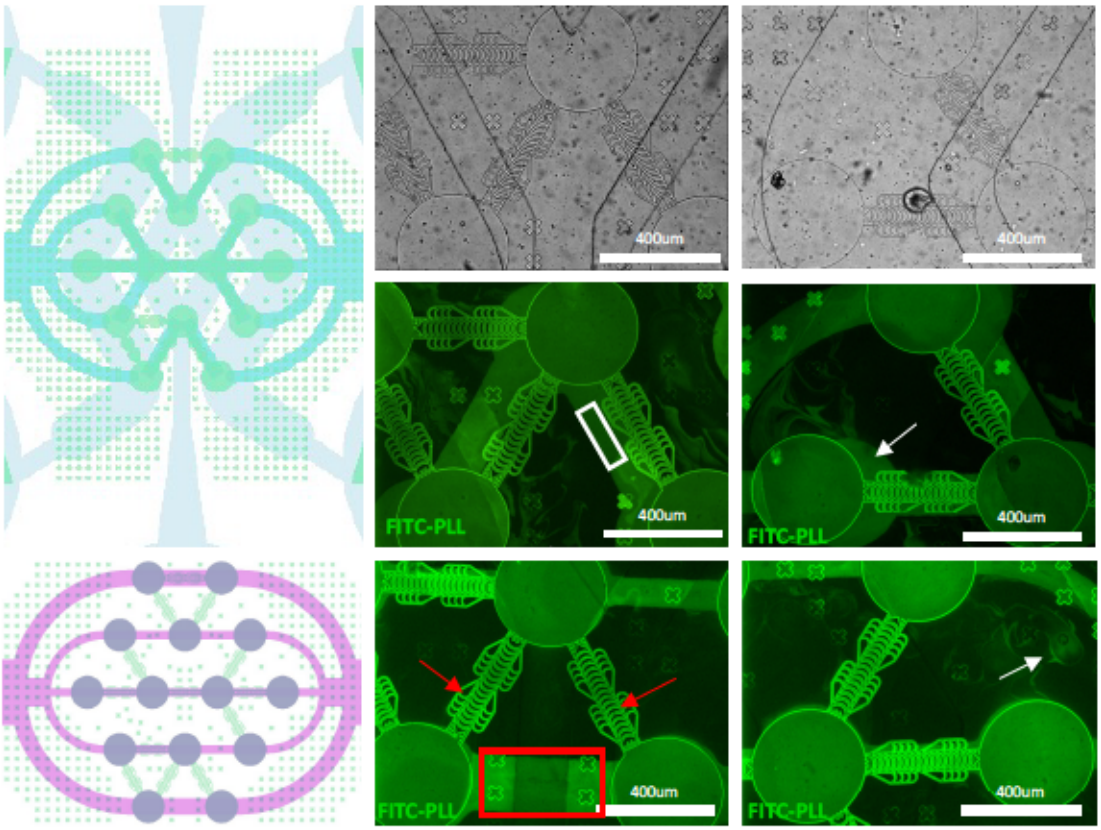

Figure 98. Design of a multi-nodal ex-flow chamber. Schemes: (Up, blue): Methods 1 Design of a transient microfluidic flow chamber that allow PLL flowing on both the nodes and grooves of the PDMS layer. (Bottom, Pink) Methods 2 Design of a transient microfluidic flow chamber that allow PLL flowing only on the nodes of the PDMS layer. In this latter design, the PLL solution flows from the traps inside the microchannels. Each methods produce specific drawbacks, due their specific design unwanted PLL overflow are depicted in white or red rectangle. Methods 1 respects the trap while methods 2 respects the groove. (Right) phase contrast image (upper lane) and fluorescent images (Center and bottom lane) of fluorescent PLL deposition using Method 1 (center row) or Method 2 (bottom row). White arrow and white and red box depict "off target" PLL deposition due to the flow chamber design limitations. Red arrow depicts perfect coating of microgrooves trough Methods 2.

The first issue to solve with the ex-flowing chamber is to avoid to coat with PLL the areas which should not be populated by neurons. Examples of such unwanted coatings are indicated by the arrows and rectangle in the Figure 98: in white for type A ex-flowing devices (top scheme with the ex-flowing in blue), and red for type B (bottom scheme with the ex-flowing in purple). The white square in the picture shows where poly-lysine remains when the ex-flowing chamber is opened. It is due to the fact that the whole alignment and bonding process has to be done in 10 seconds, so there is sometimes a chance of misalignment. White arrows show infiltration of PLL solution

below the PDMS from type A ex-flowing channels. The red arrows also point the success of the type B ex-flowing device in terms of micro-channel coating, even though these micro grooves are 5um high. (Thus, suggesting that narrower flow channel could have been encoded to join the trap areas and reduce unwanted PLL between traps in Methods2).

As shown in Figure 99(same image as Figure 98 but with enhanced phase contrast), the cell seeding microfluidic layer encodes walls that actually separates the node and therefore compensate the default of the second as most of inter-node unwanted PLL is covered by the cell seeding chamber walls.

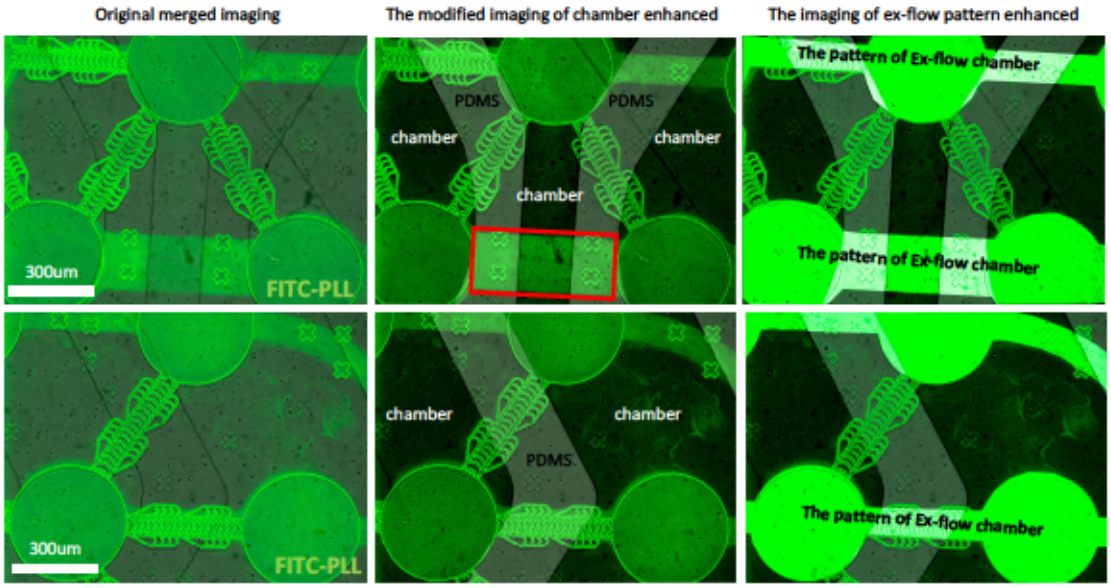

Figure 99. Optimized Methods 2 ex flow patterning of node and grooves of a multi-nodal microchip. The columns represent the same pictures with different contrasting methods to help visualization of the patterning process. (Left column): Original images showing perfect node and groove patterning an area of 'off target" PLL deposition linking 2 nodes is present. (Middle columns): same images with different contrast allowing to visualize the PDMS walls of the final microfluidic interface. Note that, thanks to careful design and alignment, the PDMS walls intersects both the microgrooves areas and the "off target" PLL deposition (red rectangle). (Right columns) Same image with enhanced green contrast allowing to visualize details of PLL patterning.

5.3.2.4 *The Cell adhesion and survival behaviors in 3 weeks*

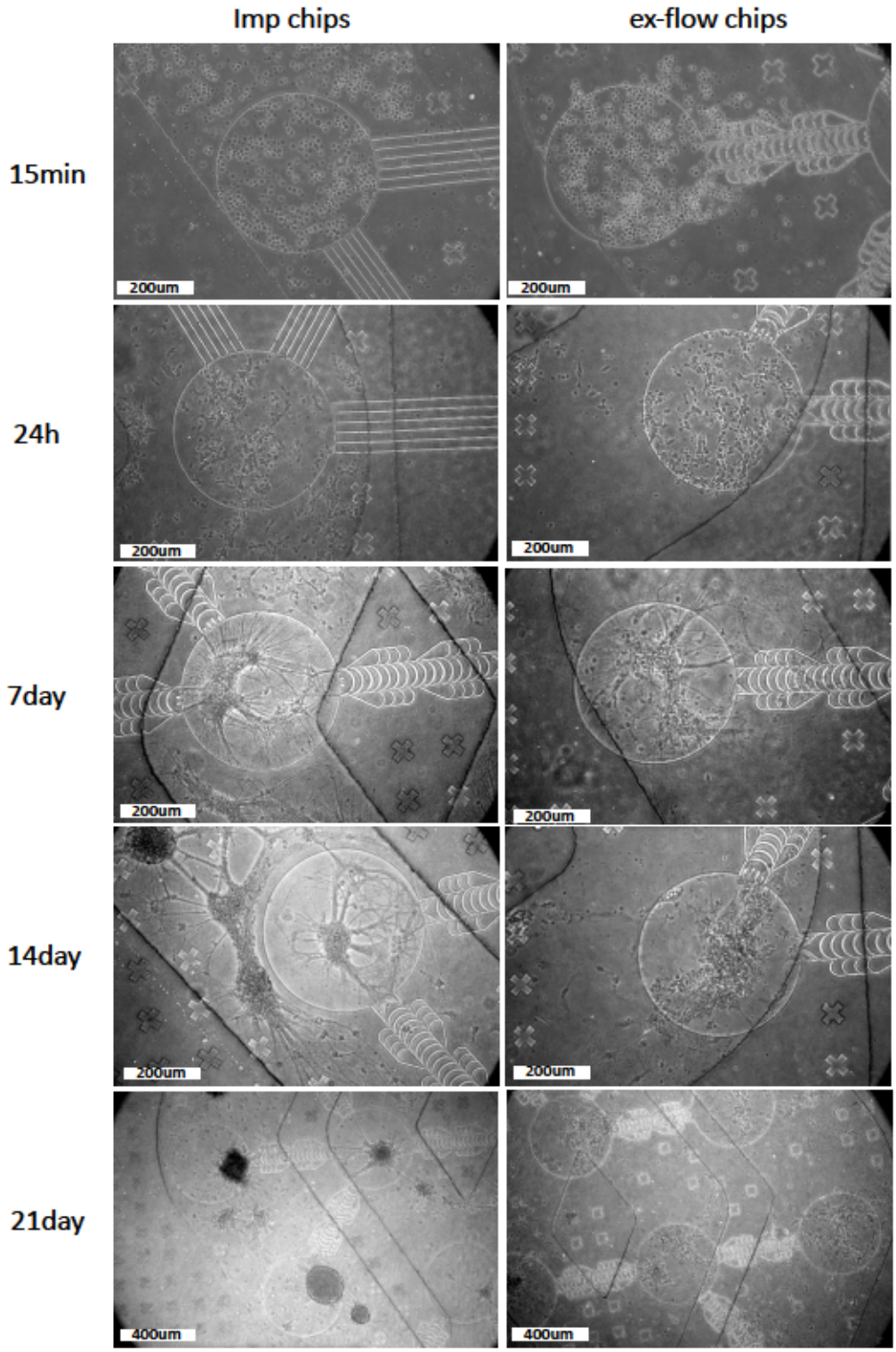

Figure 100. Comparison between IMP and Ex-flow Methods for neuronal growth. Hippocampal neurons seeded in both IMP and exflow systems and monitored for 15min, 24h, 7, 14 and 21 DIV. Note that hippocampal neurons seeded in the exflow chamber exhibit less clumping behaviour.

In order to estimate whether new methods increase the poly-lysine and improve

the cell survival behavior, I compared it with IMP chips. The adhesion and survival status of cells were recorded at 15 min, 24hours, 7 days, two weeks and three weeks after seeded hippocampus neurons in three different chips. Comparing the extra-flowing coating chips with in-mold pattern chips, I found, that after one week, the cells in IMP chips tend to aggregate and clump. On the contrary, in ex-flowing chips, initial adhesion of cell seems better and neurons do no clump in aggregates, a process that is stable until 3 weeks of culture. To sum up, Ex-flow chamber methods allows the deposition of a better controlled cell adhesive substratum.

5.3.2.5 Neuronal survival in IMP and ex-flowing chips

After 21 days of in vitro culture, the dendrites, axons and nuclei of the neurons in the IMP and ex-flowing chip were stained with Map2, β-III-Tubulin, and DAPI, respectively.

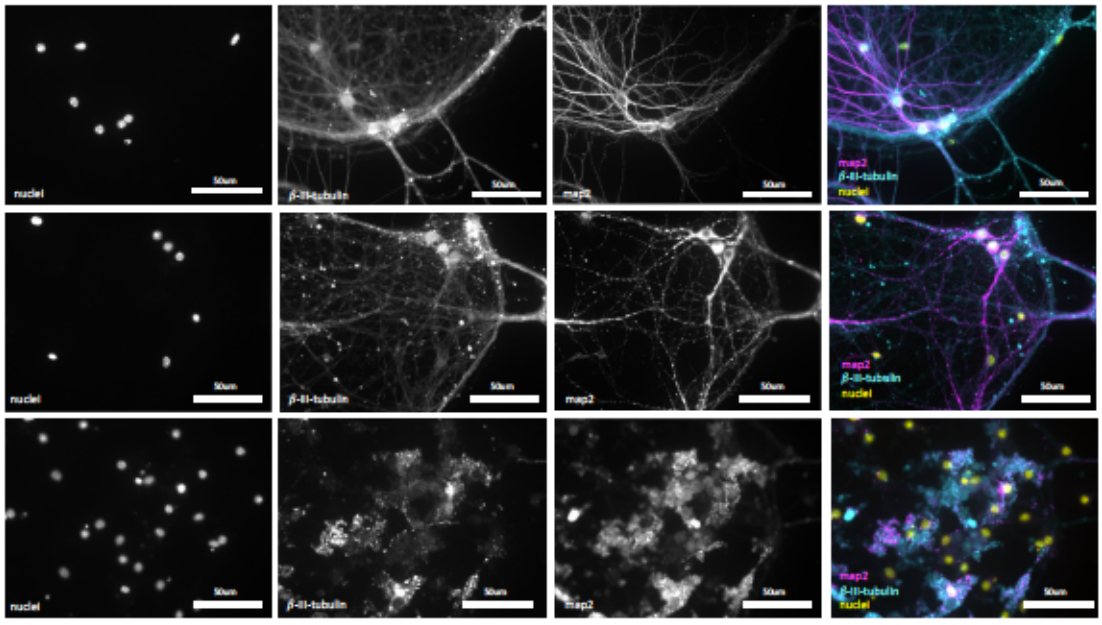

Figure 101. Immunofluorescence staining of hippocampal neurons seeded in multi-nodes IMP chips after 21DIV. Each row corresponds to one node images from a different chip. Neurons were stained for nuclei (DAPI, left columns), Axons (β-III-tubulin, second column), dendrites (MAP2, third column) and merge (4th column, right). Note that row 2 and 3 shows poor survival.

The multi-node IMP chip shows few surviving cells with only a small number of hippocampal cells surviving for 21 days in the multi-nodal chips (Figure 101).

Surviving neurons shows signs of degeneration, as evidenced by axonal and dendritic blebbing and fragmentation.

In the ex-flowing chips (Figure 102), axons and dendrites are clearer and unbroken. There were more samples that were able to survive for 21 days and chips were divided of large degenerating areas as sometime seen in some IMP chips

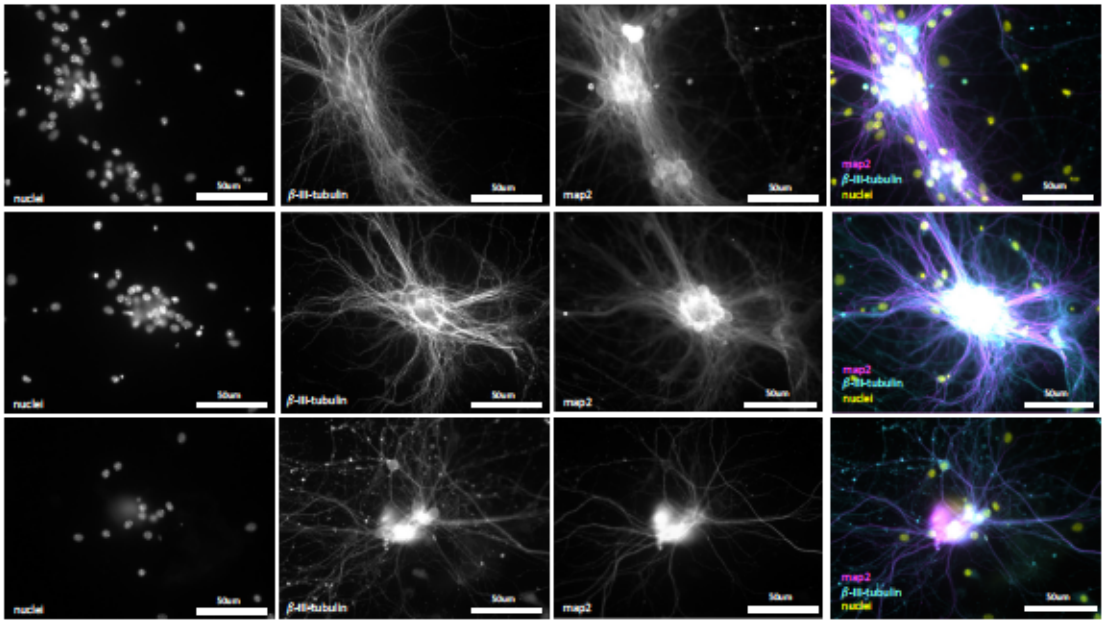

Figure 102. Immunofluorescence staining of hippocampal neurons seeded in multi-nodes IMP chips after 21DIV. Each row corresponds to one node images from a different chip. Neurons were stained for nuclei (Dapi, left columns), Axons ((β-III-tubulin, second column), dendrites (MAP2, third column) and merge (4th column, right). Note excellent differentiation and survival in all nodes.

Regarding the relationship between the number of cells and viability, in the multi-nodes IMP chips, the neurites present a degenerative state in the traps with lower cell numbers. The regions with a higher number of cells did not show a survival benefit. It is difficult to quantify the exact survival in IMP chip because of the limited samples at 21 days of culture and neurons forming spheroids which are difficult to image at the single cell level. However, in general, it is obvious that cells in ex-flowing survived to a better extend in the challenging condition of 3 weeks of cell culture.

5.3.2.6 Axon guidance and escaping in ex-flowing chips

Although the ex-flowing chips shows cell survival benefits, attention should be

paid to the axon guidance and confinement properties. In our first design and experiment, I experienced some defect with alignment, so the flowing chamber showed slight mislocation between the trapping pockets and areas of PLL deposition (Figure 103, red arrow). As seen in the Figure 103, walls of cell traps restricted axonal escape from the traps, even though there may be poly-lysine outside the trap (Figure 103, white arrow), thus evidencing the interest of joining mechanical constrains with chemical ones.

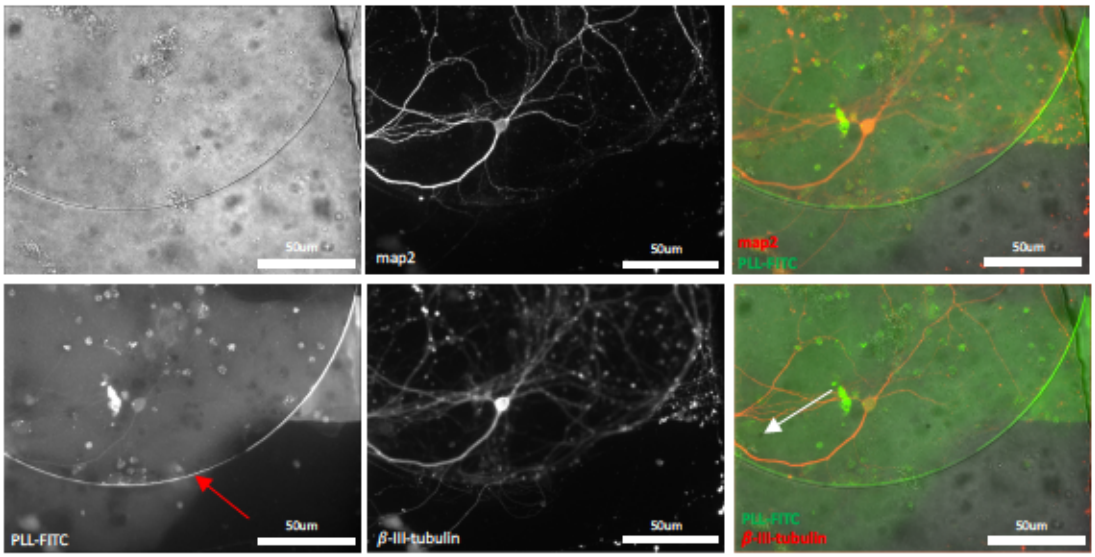

Figure 103. Guidance of axons by pockets walls in an exflow microchips. Hippocampal neurons after 10DIV stained for β-III-tubulin. Note that the axons follow the border of the ex-flow patterned node although some PLL has been patterned outside.

For traps with more cells, most of the axons grow along the wall of the trap (错误!未找到引用源。, white arrow), but there are still a small number of axons and dendrites that can escape across the 5um height of the trap wall and travels along the area covered with "unwanted" poly-lysine (Figure 104, black arrow). As seen in the IMP chip, when poly-lysine is usually distributed on the surface of the traps, the wall can serve as a good trapping and guiding role, besides the risk of possible collapse. If the poly-lysine in the ex-flowing chip flows according to the established position, no mislocation of alignment occurs and it will it may provide the same constraining effect as IMP chips.

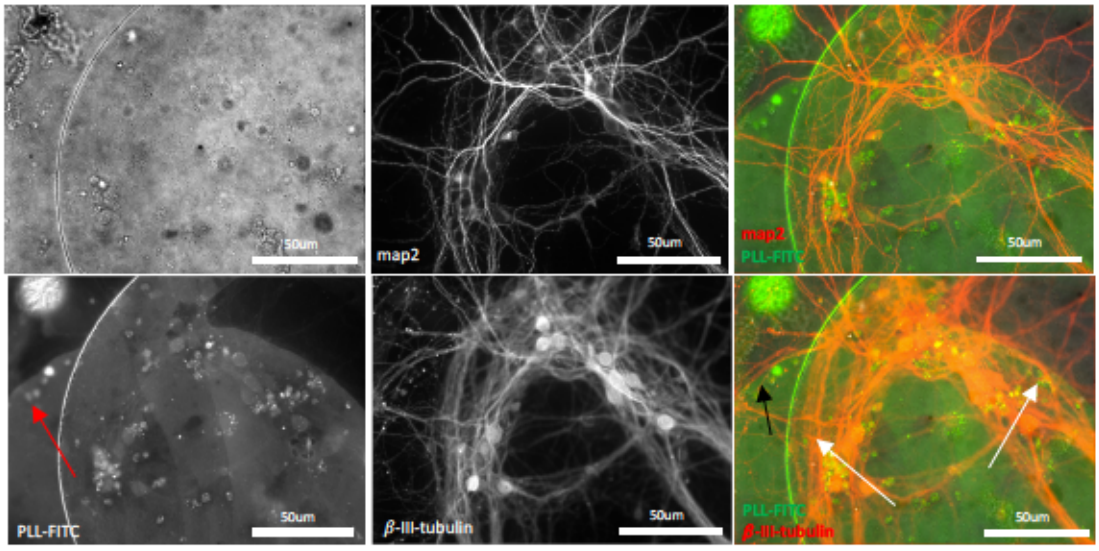

Figure 104. Guidance of axons and dendrites by pockets walls in an exflow microchips. Hippocampal neurons after 10DIV stained for β-III-tubulin and MAP2. Note that the axons escape the border of the ex-flow patterned node although some PLL has been patterned outside.

5.4 Discussion

In that part of my work, I tried to develop 2 alternative methods that compensate the default I have observed with IMP patterning technique (cell clumping of high-density networks and loss of axonal guidance in the microgrooves due to high density). I explored to distinct methods. The First one, co-patterning of PEG PLL cell repellent moieties, aimed primarily at avoiding axons to grow outside the grooved areas and respect the guiding principle we have designed. The second methods, PLL flowing, aimed at better controlling the surface concentration of PLL in the area of interest and therefore enforce neuronal adhesively in the pockets and grooves. Overall, while co-patterning methods proved ineffective (and even counter effective), the ex-flow approaches proved very promising in term of maintaining neurons at the right place and preventing cell clumping.

5.4.1 The issues and inspiration from co-patterning

In the new methods of co-patterning, I have assessed to compensate the default of IMP chips (clumping of neurons for high density networks), PEG-g-PLL showed no positive results as cells adhered in PEG PLL areas. This may arise from the possibility

that PEG may have adsorbed PLL, there suggesting an inker problem. According to the product chemical formula (Figure 105), PEG-g-PLL has a positively charged PLL head that should lies at the bottom and being covered by the PEG moieties. During the transfer from the surface of the inker to the trapping layer of the inker, the head and tail of the molecule may have shifted leading to the inversion of the pattern topology. It leads to the fact that in route B, the PEG head of PEG-g-PLL on the inker surface is on top and then upon contact with PLL-FITC, the other end of the PLL head of PEG-g-PLL is exposed to become a surface adhesive protein that can attach to the cells. Another, non-exclusive, hypothesis, may be related to a suboptimal concentration of PEG-g-PLL not being sufficient to counteract the adsorption capacity of PLL-FITC. Therefore, there are still many details to be explored in the technique of co-patterning, such as the self-assembly of molecules in the process of patterning, the behaviour of cellular repulsion, and the relationships between concentration of various proteins and cell adhesion.

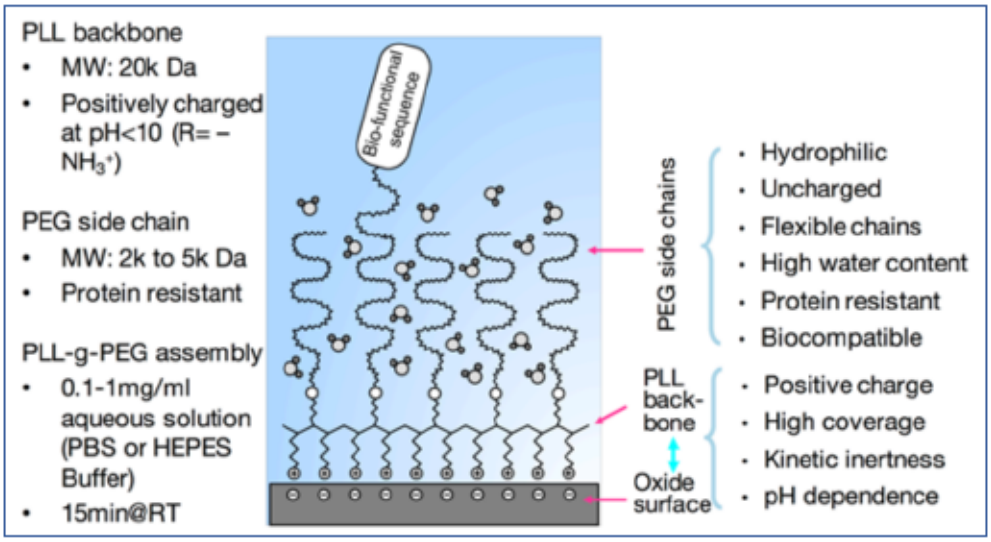

Figure 105. Principle of PEG-g-PLL as cell repellent (https://susos.com/beschichtungstechnologien/pll-g-peg-polymere/)

In the sequel of repeated experiments, I found that this phenomenon is not a coincidental situation. The survival and adhesion of neurons in two-nodes and multi-nodes are shown in Figure 94. The two regions in which co-patterning produces a clear difference in cell distribution. In particular, surprisingly, there is no cell adhesion in the traps. Checking the poly-lysine coating there were no poly-lysine inside groove,

possibly because adsorption of liquid PLL in the tiny 5µm grooves may have been impaired by small hydrophobic tracts of PDMS Although such results are contrary to expectations, but they have important inspiration for the development of future chips, for the new idea please see the perspective section (Figure 106).

5.4.2 Poly-lysine, Patterning techniques and cells adhesion behaviors

Any subtle structural engineering changes in the system can cause effects on cell survival morphology. In IMP system, however, the transfer of poly-lysine occurs by contact inking process, and this transfer is influenced by a variety of factors that result in low amounts of poly-lysine on its surface. When the adhesion capacity is insufficient, the cells tend to clump and to form aggregates. Although the cells still survive, in the earlier stage (2 weeks) it proved unfavorable for long term cultures (>3 weeks) and most importantly, due to axonal fasciculation and tension, escape from the guiding groves and therefore loss of constrains on network topology.

However, in this chapter, the second methodologies, ex-flow patterning, that allows to flow controlled quantities of cell adhesive cues in the grooves and pockets allowed very good neuronal adhesion and prevented neuronal clumping at higher densities. Compared to the physical patterns transfer of PLL by inking, the attachment ability is much stronger. This step is difficult to implement in the fabrication process of IMP chips. In fact, the concentration of poly-lysine in IMP chips has been increased up to 100ug/ml for preparing the inkers without noticeable improvement while the poly-lysine consumption used for this process is very high. In the ex-flowing chip, the fluid concentration is only 10ug/ml, and the total volume is only one third of that of IMP. That consumption difference is almost 30 times, it shown the ex-flowing chips have a great advantage in cost. The advantages of ex-flow methods arise at the cost of a drawback: patterning of PLL outside the pockets due to the necessity of creating linking channels between nodes to allow PLL flowing during the ex-flow process. Yet, the efficiency of PLL flowing in the tiny microgrooves to reach distant cells pockets and

achieve good cell adhesivity allows us to foresee refinement in the design of the transient flow chamber that the next version of the design will achieve a better patterning.

5.4.3 The Biocompatibility of Materials and the survivals of different cell type

When cells are delivered into a microfluidic culture channel, cells attach to the substratum through electrostatic attraction (or bind to proteins on the channel surface via receptor-protein binding). Once the cells attached, they differentiates and ultimately secrete extracellular matrix (ECM) proteins, that in turns may trigger signals that regulate cell differentiation, cell cycle, cell migration, and cell survival [326]. The flow in the cell culture channel exerts a shear force on cells that competes with the adhesion between cells and their extracellular matrix [327].

Therefore, as material surface also affect both the cell adhesion and survival, I also tested some material-related experiments. The PDMS has good biocompatibility, and other materials or mixed PDMS materials will not be described in detail here because of unsuccessful chips assembly process. For slightly adjusting the amount of curing agent in PDMS and culturing neuronal cells on flat PDMS membranes, we found that the adhesion and survival of neurons was a little better when the concentration of curing agent was at 15% compared to 5%. However, this modification raised issues such as stamp surface after silanization, spin coating with PDMS and unmolding efficiency. Moreover, the results of several experiments were not consistent, so finally we kept the concentration of curing agents at the initial 10% concentration as for the top chamber. In addition, I also found that the different populations of cells have different reliance on surface properties and poly-lysine concentration. Especially, hippocampal cells were more challenging to manage than cortical or striatal ones. The survival of hippocampal cells in a multi-node chip was sometimes disappointing, and it turns out difficult to obtain perfectly homogeneous seeding in chips with hippocampal cells in all traps. This

also may be due to the complex cell delivery circuitry that enhance cell density gradient formation due to the ratio of cell suspension seeding volume and the volume of the seeding chamber. Further fluidic optimization in the cell delivery chamber may be envisioned. The influence of the surface of the material used to make organ-on-a-chip on the survival of neurons is still a worthy field for exploration. Importantly, the ex-flow process is compatible with the use of non PDMS substratum. For example the use of thermoplastic elastomers which shows excellent biocompatibility and that can very easily be mechanically embossed (hot embossing) and patterned with polycation could be an interesting alternative for the fabrication of the bottom, textured, layer. .

To sum up, the experimental results indicates that although the co-patterning technique allows excellent printing of the adhesive/repellent patterns, the cell behavior is unsatisfactory, suggesting further optimization of the technique. The flow patterning approach allows excellent pattern deposition in the area of interest and promotes better hippocampal neurons adhesion and survival than IMP chips. Optimization of PLL quantity may allow further improvement to tune homogeneous cell seeding, survival and constrained topology.

5.5 Perspective

In this chapter, both the experiments and the design of the new method are in their initial stages. Fortunately, they are all feasible in terms of method principles. So, the next step will be to further optimize the pattern design and fabrication steps of the chip.

For co-patterning techniques, although the chips have unexpected results for cell adhesion, it was not without gain. Instead, these failures inspired me to come up with new ideas for chips design. The figure below shows a preliminary idea of the structure and principle of the new chip (Figure 106). That idea is to confine neurons at the surface of poly-lysine coated islands instead at the bottom of traps. A macrochamber on top will then block the connections between the islands and define connecting microchannels. That structural assembly can also have the same functions to achieve

isolation of the cells in small group in big seeding chamber and making an individual connection between two cell population chambers. The detailed description of the production method will not be shown here and belongs to the perspective of my PhD.

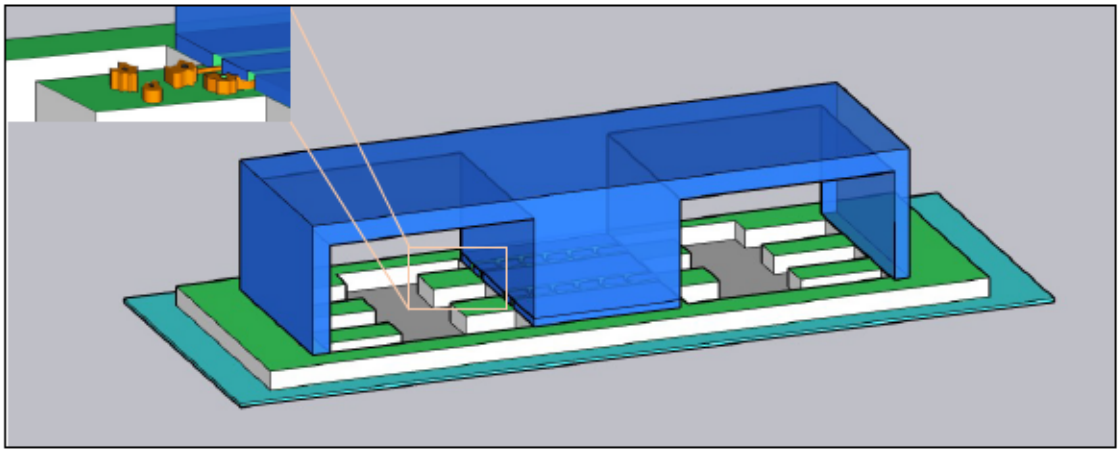

Figure 106. The new chips' structure inspired from the co-patterning results. Neurons (in orange) attach on PLL (green) inked islands. A macrochamber (in blue) is aligned on top define the microchannels connecting the islands.

6 Discussion and perspective

6.1 Considerations on Brain on chips design

In previous chapters, I developed two methods for fabricating brain-on-chips platforms and illustrated their potential interest trough two applications cases. These studies illustrates that that building an appropriates platform requires a constant cycling / adaptation process through trials and error approaches to reach and acceptable and operational device. The whole device creation contains several steps that each requires incremental optimization and that encompass chips theoretical design, chips fabrication processes, cell seeding and culturing in the microfluidic devices, neurons growing to form neural networks, and disease modelling (Figure 107), which could ultimately be used for drug screening in the future (no attempt is carried out in this thesis). Therefore, brain chips which can be used for disease modelling need to be iteratively developed, challenged and refined.

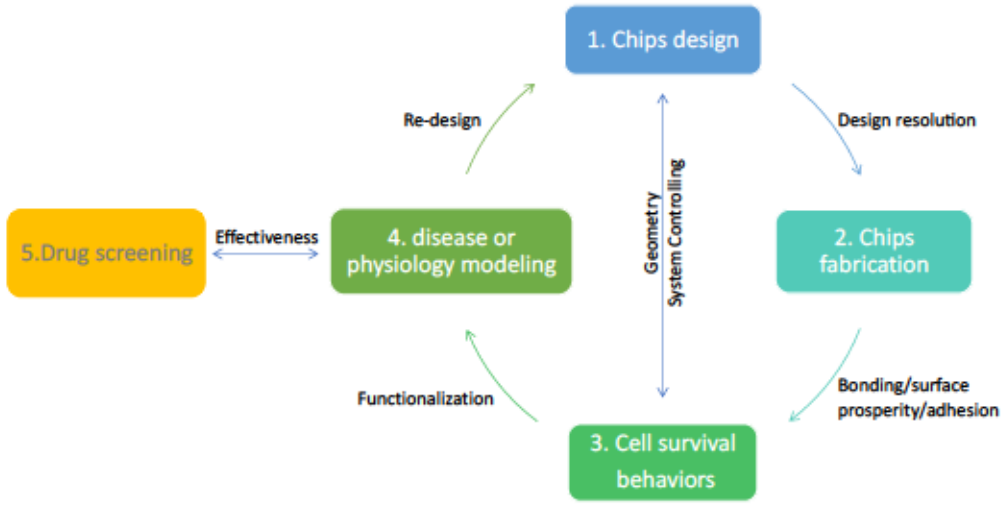

Figure 107. Mind map of the creation process of a brain on chip platform.

In the very first steps of my work, starting from the initial proof of concept from Yamada et al. [269] that IMP could prove useful to guide axons with a higher "cell contrast" level than conventional micropatterning, I optimized the whole "In Mold Patterning" fabrication process of the chip to be able to obtains several microchips per fabrication session, while comparing the effects of different culture environments on cell survival. Overall, after several round of microfabrication optimization process, I

was able to produce IMP patterned networks platforms at a reasonable working throughput by fabricating 30 to 40 devices per working session (devices being grouped 4 by 4 on a single microfluidic tab), 60% of which proved operational for cell culture. One of the main bottlenecks I encountered during the fabrication process was linked to poly-lysine patterning, in one batch of chips, some of them could have a bad poly-lysine transfer during the inking process. At a cell biological level, the main problem I encountered was linked to the relationship between substratum adhesively (related to PLL availability) and initial cell seeding density. Indeed, the topology and stability of the seeded neural network was highly controlled and reproducible for low density networks (10 neurons per $10^4 um^2$). The main issue arose from network seeded at higher density (>30 neurons per $10^4 um^2$) and that spontaneously formed neural spheroids after a week of culture. In those case, while the spheroids remained alive, the topology of the inter spheroid connection turned out to be less controlled than the one of now density networks, neuritic bundles sometimes detaching from the grooves due to high tensile force.

The environment in which brain cells survive in vivo is different in many ways from that in vitro. The substrates used in vitro usually have a high mechanical stiffness, and these properties can affect cell differentiation and migration, and even phenotype [328] [329]. In contrast with classical compartmentalized microfluidic platforms, the glass is routinely used as a substratum, in our study PDMS was used as a cell culture substratum a process that could affect axon outgrowth parameters as the micromechanical environment differs, with factors such as viscoelasticity, stress and stiffness [330]. Brain being one of the softest organs in mammalian bodies, this is especially true for brain derived cells which exhibit specific and complex behavior in response of stiffness variation. Several studies have shown that neurons initially extend longer axons on higher stiffness material [331] but tends to sense stiffness gradient and are further guided toward lower stiffness areas [332] a process that can be used to tune neuronal functions and growth cone navigation[333]. Similarly, substrates stiffness

modify astrocytic proliferation, migration and activation[334-336]. Therefore, while the "gold standard" for growing neuronal networks in vitro is high stiffness substratum (glass, or PC petri dishes) design of brain chips platforms also need to take substrates stiffness in account and requires investing in more fundamental research for optimal tuning and control of network connectivity.

6.2 Survival and differentiation of Neural network on chips

Neuronal adhesion and interaction with cell cultures substratum controls both the initial network typology and it's differentiation. In response to the problems encountered in the two-node network (progressive cell clumping on high density seeding), I show in Chapter 3 that a "screening system" allowing to study adhesive surface/cell density ratio is useful to explore the effect of suitable geometric factors on neuronal survival and network stability. I explored the effect of the growth area and spacing of neurons of different sizes on neuronal survival and axonal escape, and the control of cell seeding density with respect to topology. Problems of substrate hydrophobicity of the chip was addressed by optimizing geometric design. This allowed multi-nodal neural networks constructions where independent nodes are placed in the same fluidic chamber and connected nodes are placed in separates chambers. This permitted efficient inter node connection at low densities while allowing good neuronal survival trough paracrine effects in the same fluidic chambers.

The source of the cells used to construct the brain-on-a-chip was also an important factor and determined the function that the model can achieve. Cell sources used in brain-on-a-chip studies are neuronal cell lines, primary neuronal cells, embryonic stem cells (ESCs), induced pluripotent stem cells (iPSCs) and mesenchymal stem cells[337, 338].

In our studies I only used primary rodent neurons extracted from several brain areas. From these experiments it clear that different neuronal subtypes behaved differently in the IMP chips. It is well documented that optimal cell survival density

depends on neuronal subtypes, with cortical neurons requiring relative high densities for survival and hippocampal ones being able to grow as single neurons. This has been previously attributed to the intrinsic connectivity of neuronal subtypes, cortical neurons requiring the establishment of minimal network to trigger collective "pro survival" activity while Hamon's Horn Hippocampal neurons being able to survive as single cells due to their capacity to form high number of autapses and axo-axonal synapses[339, 340]. Another aspect impacting network survival and topology stability was that axonal fasciculation depended on the neuronal subtypes with cortical neurons exhibiting fasciculated axonal bundles at a much higher extend than striatal or hippocampal ones a process that also highly depends on seeding density. This impacted network "stability" over time as fasciculated axonal bundles tended to detaches more easily from PLL areas than non fasciculated ones and that mechanical tension in turn control axonal fasciculation [错误!超链接引用无效。]. A last aspect was that neuronal subtypes exhibit different total axonal length. In our experiments this did not significantly impact our cell culture parameters (survival and stability of topology), yet some preliminary experiments I have conducted with human derived iPSC cortical neurons the situation suggested that this could be a problem as human neurons differentiate over a very long time in vitro (several weeks) and extends much longer axons in vitro than rodent one. This suggest than platform for Neuronal network reconstruction may also need to take in account neuronal subtypes and specie specificities to reach an optimal design.

In 1.5.5, I reviewed the studies that have been performed over the last decade on the in vitro reconstruction of neural networks based on compartmentalized microfluidic technology. In summary, there are two features: the majority of studies have used primary cells from mouse cortical, hippocampal, and striatal regions. In a more long-term perspective, there can be many more types of cells can be used for reconstructing the neural networks. In particular, some cell recourse of genetic mutations, as well as multiple subtypes of primary cells. In recent years, it has been found that microglia are involved in the mechanism of neurodegeneration, therefore microglia in the system, are

also worth to be considered. Second, most of the reconstructed neural networks do not have unidirectional neural network connectivity. Although many studies have used techniques such as calcium imaging and MEA to demonstrate the connectivity of neural networks, such connectivity is extremely limited. However, such connections are extremely limited and do not have the physiological functionality to mimic real brain connections. For example, the glutamatergic, dopaminergic and GABAergic neural pathways in the brain are unidirectionally connected by specific regions of nerve cells in a certain way, and the neural signaling is ordered, as demonstrated in neurophysiological studies. Therefore, in vitro reconstruction of neural network for the study of neural function needs to take in account the unidirectional nature of neural networks. Both the two-node neural network and the multi-node system demonstrated in my PhD thesis are characterized by unidirectional connectivity. Therefore, there are certain advantages in simulating neural networks. In future research we plan to increase the variety of cells in the expectation of being able to construct multiple neural pathways for use in the study of disease models.

6.3 The development of NDD modelling on chips

6.3.1 The prionoids spreading mechanism of NDD

The mechanisms of transmission of neurodegenerative diseases in the brain have been studied mainly by prionoids hypothesis. Compartmentalized microfluidic chips have the ability to isolate soma and axons and are therefore ideal for studying protein propagation problems. However, conventional chips have a large emitting chamber that can accommodate approximately 8000 neuronal cells. The axons of these nerve cells have a relatively free growth area(800um*1000um), and only about 5% to 10% of the axons can cross the microchannel. We have therefore divided this relatively large chamber into small traps, each trap capturing approximately 400 nerve cells and allowing the axons of these cells to be guided into the microchannel only after encircling the trap, thus greatly increasing the efficiency of the interchamber

connections. With the use of unidirectional microchannel structures, the neural network we have built could allow control of both the initial start of the disease process and the direction it flew. This is difficult to achieve with conventional chips. The connections of these neural networks simulate the projections of some regions of the brain. During my PhD work, I used a-syn aggregates as an exogenous seed to initiate disease in specific neuronal nodes to monitor their spreading in remotes connected nodes of the neural network. The propagation efficiency and pathways of a-syn showed better results compared to conventional chips. My preliminary results obtained with the "2 nodes" network, suggest that trans-neuronal flow of protein aggregates requires neurons to neurons contact and synaptic connectivity rather than "humoral" like diffusion of proteins between neurons. Moreover, the few experiments I have been able to conduct with the multimodal platforms shows that our experimental platform allows aggregates transfer and seeding studies and may suggest that the number of inter-neuronal contacts may account for trans neuronal spreading of protein aggregates. Yet these results remain to be reproduced. Indeed, in terms of quantification, we found that the neurospherical morphology that appeared upon high density seeding and time of cultures hindered the tracking of a-syn spreading, thus requiring further experiments to substantiates our observations.

In the disease modelling, beyond the existing successfully reconstructed network of Parkinson's cortical-striatal network, the next step could be the reconstruction of a cortical-hippocampal circuit for the study of Alzheimer's disease. For the assessment of the "prion like" behaviour of proteins such as beta amyloid and Tau can be tested in those minimalistic "performant pathway" network as well as in the multi nodal platforms. This is something that can be foreseen in the short term and realized soon.

6.3.2 Synapse to nucleus signal modelling for studying NDD

From a disease modelling perspective, previous studies (Chapter 1.5.6), have focused mainly on the mechanisms of transmission of prionoids. Our team also believed

that the "synapse to nucleus" signaling pathway that integrates synaptic transmission into survival/death information is another entry point for studying NDD on chip. For now only few studies have tried to tackle that process in microfluidic reconstructed networks[236, 342, 343]. Therefore, we demonstrated our preliminary results in chapter 错误!未找到引用源。. Overall, there is still a long way to go to study cellular signaling pathways using microfluidic chips, and this path is bright and challenging and highly promising.

6.4 The perspective for future Brain on a chip

The current multi nodes chips are well suited to realistic needs. In fact, this arrangement and chamber innovation can achieve more switching connections and multiple configurations, which is an ideal platform for studying neural networks. Therefore, in addition to improving the stability of the chip, future devices will need to focus more on interfacing and integrating more advanced function and tools, such as MEA to records specific nodes, molecular sensor to monitors signaling pathways in a dynamic manner. Going further, the brain chip would also benefit from implementation of more physiological functional units. In addition to the construction of neural networks, the integration of physiological functions such as the BBB and cerebral vasculature may allow the simulated brain chip platform to further approximate the physiological functions of the brain.

In addition to this, the fabrication of chips often takes an important amount of time, so the implementation of a standard fabrication process for chips and industrial mass production shall facilitate spreading of such platforms in conventional biological research. This needs more scientists and engineers to get involved to tickles such a challenging goal aiming at reconstructing minimalistic organs in vitro. It will help to achieve the goal of human body-on-a chip, as we believe, it could eventually replace animal models.

Materials

Microfabrication and cell culturing

Photoresist SU-8 2050 (MicroChem Corporation, Westborough, MA, USA),

Propylene glycol monomethyl ether acetate (PGMEA，Sigma，484431),

Polydimethylsiloxane (PDMS, Sylgard 184, Ellsworth Adhesives),

Tridecafluoro-1,1,2,2-tetrahydrooctyl) trichlorosilane (AB111444, abcr),

Gey's balanced salt solution (GBSS, Sigma G9779),

Papain (Sigma 76220),

Dulbecco's Modified Eagle Medium (DMEM, Thermofisher 31966021),

Fetal Bovine Serum (FBS, GE Healthcare),

Eoxyribonuclease (DNAse, Sigma D5025),

Phosphate buffered saline (PBS, Thermo Fisher),

Bovine serum albumin (BSA, Sigma A7030),

PLL-FITC (Sigma, P3543),

PEG-g-PLL (SuSoS AG, Switzerland).

Immunofluorescent staining

MAP2, anti-microtubule associated protein 2 (IgG1, sigma, M4403),

Anti-β-Tubulin Isotype III (IgG2b, sigma, T5076),

Bassoon (IgG2a, Abcam, SAP7F407),

Homer1(IgG1, Synaptic System,160011),

VGLUT1 (Rabbit, Sala El Mestikawi's lab),

Phospho-p44/42 MAPK (Erk1/2, Rabbit, Cell Signalling Technology, 4370).

Hoechst (Sigma, 33342)

Alexa Fluor 365, 488, 555 or 633 (Thermo Fisher).

List of Figures

Reference

1. Paridaen, J.T.M.L. and W.B. Huttner, Neurogenesis during development of the vertebrate central nervous system. EMBO reports, 2014. 15(4): p. 351-364.
2. Dickson, D.W., et al., Microglia and cytokines in neurological disease, with special reference to AIDS and Alzheimer's disease. Glia, 1993. 7(1): p. 75-83.
3. Minagar, A., et al., The role of macrophage/microglia and astrocytes in the pathogenesis of three neurologic disorders: HIV-associated dementia, Alzheimer disease, and multiple sclerosis. Journal of the Neurological Sciences, 2002. 202(1): p. 13-23.
4. Streit, W.J., et al., Microglial pathology. Acta Neuropathologica Communications, 2014. 2(1): p. 142.
5. Walter, L. and H. Neumann, Role of microglia in neuronal degeneration and regeneration. Seminars in Immunopathology, 2009. 31(4): p. 513-525.
6. MacMahon Copas, A.N., et al., The Pathogenesis of Parkinson's Disease: A Complex Interplay Between Astrocytes, Microglia, and T Lymphocytes? Frontiers in neurology, 2021. 12: p. 666737-666737.
7. Nelson, P.T., L.A. Soma, and E. Lavi, Microglia in diseases of the central nervous system. Annals of Medicine, 2002. 34(7): p. 491-500.
8. Wang, Q., Y. Liu, and J. Zhou, Neuroinflammation in Parkinson's disease and its potential as therapeutic target. Transl Neurodegener, 2015. 4: p. 19.
9. Guedes-Dias, P. and E.L.F. Holzbaur, Axonal transport: Driving synaptic function. Science, 2019. 366(6462): p. eaaw9997.
10. Ballatore, C., V.M.Y. Lee, and J.Q. Trojanowski, Tau-mediated neurodegeneration in Alzheimer's disease and related disorders. Nature Reviews Neuroscience, 2007. 8(9): p. 663-672.
11. Spillantini, M.G., et al., α-Synuclein in Lewy bodies. Nature, 1997. 388(6645): p. 839-840.
12. Xiao, S., J. McLean, and J. Robertson, Neuronal intermediate filaments and ALS: A new look at an old question. Biochimica et Biophysica Acta (BBA) - Molecular Basis of Disease, 2006. 1762(11): p. 1001-1012.
13. Vos, K.J.D., et al., Role of Axonal Transport in Neurodegenerative Diseases. Annual Review of Neuroscience, 2008. 31(1): p. 151-173.
14. Hirokawa, N. and R. Takemura, Molecular motors and mechanisms of directional transport in neurons. Nature Reviews Neuroscience, 2005. 6(3): p. 201-214.
15. Lazarov, O., et al., Impairments in Fast Axonal Transport and Motor Neuron Deficits in Transgenic Mice Expressing Familial Alzheimer's Disease-Linked Mutant Presenilin 1. The Journal of Neuroscience, 2007. 27(26): p. 7011.

16. Pigino, G., et al., Alzheimer's presenilin 1 mutations impair kinesin-based axonal transport. Journal of Neuroscience, 2003. 23(11): p. 4499-4508.

17. Millecamps, S. and J.-P. Julien, Axonal transport deficits and neurodegenerative diseases. Nature Reviews Neuroscience, 2013. 14(3): p. 161-176.

18. De Vos, K.J., et al., Role of axonal transport in neurodegenerative diseases. Annu Rev Neurosci, 2008. 31: p. 151-73.

19. Miller, C.C., et al., The X11 proteins, Abeta production and Alzheimer's disease. Trends Neurosci, 2006. 29(5): p. 280-5.

20. Stokin, G.B., et al., Axonopathy and Transport Deficits Early in the Pathogenesis of Alzheimer's Disease. Science, 2005. 307(5713): p. 1282-1288.

21. Goldsbury, C., et al., Inhibition of APP Trafficking by Tau Protein Does Not Increase the Generation of Amyloid-β Peptides. Traffic, 2006. 7(7): p. 873-888.

22. Konecna, A., et al., Calsyntenin-1 Docks Vesicular Cargo to Kinesin-1. Molecular Biology of the Cell, 2006. 17(8): p. 3651-3663.

23. Lazarov, O., et al., Axonal Transport, Amyloid Precursor Protein, Kinesin-1, and the Processing Apparatus: Revisited. The Journal of Neuroscience, 2005. 25(9): p. 2386-2395.

24. Ngolab, J., et al., Brain-derived exosomes from dementia with Lewy bodies propagate α-synuclein pathology. Acta Neuropathologica Communications, 2017. 5(1): p. 46.

25. Xia, X., et al., Exosome: A novel neurotransmission modulator or non-canonical neurotransmitter? Ageing Research Reviews, 2022. 74: p. 101558.

26. Fauré, J., et al., Exosomes are released by cultured cortical neurones. Molecular and Cellular Neuroscience, 2006. 31(4): p. 642-648.

27. Ludwig, A.-K. and B. Giebel, Exosomes: Small vesicles participating in intercellular communication. The International Journal of Biochemistry & Cell Biology, 2012. 44(1): p. 11-15.

28. Pchitskaya, E., E. Popugaeva, and I. Bezprozvanny, Calcium signaling and molecular mechanisms underlying neurodegenerative diseases. Cell Calcium, 2018. 70: p. 87-94.

29. Berridge, M.J., Neuronal calcium signaling. Neuron, 1998. 21(1): p. 13-26.

30. Clapham, D.E., Calcium Signaling. Cell, 2007. 131(6): p. 1047-1058.

31. Brini, M., et al., Neuronal calcium signaling: function and dysfunction. Cellular and Molecular Life Sciences, 2014. 71(15): p. 2787-2814.

32. Bezprozvanny, I., Calcium signaling and neurodegenerative diseases. Trends in Molecular Medicine, 2009. 15(3): p. 89-100.

33. Texidó, L., et al., Amyloid β peptide oligomers directly activate NMDA receptors. Cell Calcium, 2011. 49(3): p. 184-190.

34. Lacor, P.N., et al., Aβ Oligomer-Induced Aberrations in Synapse Composition, Shape, and Density Provide a Molecular Basis for Loss of Connectivity in Alzheimer's Disease. The Journal of Neuroscience, 2007. 27(4): p. 796-807.

35. Foster, T.C., C. Kyritsopoulos, and A. Kumar, Central role for NMDA receptors in redox mediated impairment of synaptic function during aging and Alzheimer's disease. Behavioural Brain Research, 2017. 322: p. 223-232.

36. Mota, S.I., I.L. Ferreira, and A.C. Rego, Dysfunctional synapse in Alzheimer's disease – A focus on NMDA receptors. Neuropharmacology, 2014. 76: p. 16-26.

37. Zaichick, S.V., K.M. McGrath, and G. Caraveo, The role of Ca2+ signaling in Parkinson's disease. Disease Models & Mechanisms, 2017. 10(5): p. 519-535.

38. Calì, T., D. Ottolini, and M. Brini, Calcium signaling in Parkinson's disease. Cell and Tissue Research, 2014. 357(2): p. 439-454.

39. Grienberger, C. and A. Konnerth, Imaging calcium in neurons. Neuron, 2012. 73(5): p. 862-85.

40. Tsien, R.Y., A non-disruptive technique for loading calcium buffers and indicators into cells. Nature, 1981. 290(5806): p. 527-528.

41. Tsien, R.Y., T. Pozzan, and T.J. Rink, Calcium homeostasis in intact lymphocytes: cytoplasmic free calcium monitored with a new, intracellularly trapped fluorescent indicator. J Cell Biol, 1982. 94(2): p. 325-34.

42. Paredes, R.M., et al., Chemical calcium indicators. Methods, 2008. 46(3): p. 143-151.

43. Svoboda, K. and R. Yasuda, Principles of Two-Photon Excitation Microscopy and Its Applications to Neuroscience. Neuron, 2006. 50(6): p. 823-839.

44. Helmchen, F. and W. Denk, Deep tissue two-photon microscopy. Nature Methods, 2005. 2(12): p. 932-940.

45. Miyata, T., et al., Mechanisms that regulate the number of neurons during mouse neocortical development. Current Opinion in Neurobiology, 2010. 20(1): p. 22-28.

46. Pauly, M.-C., et al., Restoration of the striatal circuitry: from developmental aspects toward clinical applications. Frontiers in Cellular Neuroscience, 2012. 6.

47. Spalding, K.L., et al., Retrospective Birth Dating of Cells in Humans. Cell, 2005. 122(1): p. 133-143.

48. Shepherd, G.M.G., Corticostriatal connectivity and its role in disease. Nature reviews. Neuroscience, 2013. 14(4): p. 278-291.

49. Barth, C., A. Villringer, and J. Sacher, Sex hormones affect neurotransmitters and shape the adult female brain during hormonal transition periods. Frontiers in Neuroscience, 2015. 9.

50. Schwartz, T., S. Sachdeva, and S. Stahl, Glutamate Neurocircuitry: Theoretical Underpinnings in

Schizophrenia. Frontiers in Pharmacology, 2012. 3.

51. Conway, M.E., Alzheimer's disease: targeting the glutamatergic system. Biogerontology, 2020. 21(3): p. 257-274.

52. Francis, P.T., Glutamatergic systems in Alzheimer's disease. International Journal of Geriatric Psychiatry, 2003. 18(S1): p. S15-S21.

53. Enna, S.J., The GABA Receptors, in The GABA Receptors, S.J. Enna and H. Möhler, Editors. 2007, Humana Press: Totowa, NJ. p. 1-21.

54. Johnston, G.A.R., Unsaturated Analogues of the Neurotransmitter GABA: trans-4-Aminocrotonic, cis-4-Aminocrotonic and 4-Aminotetrolic Acids. Neurochemical Research, 2016. 41(3): p. 476-480.

55. Ochoa-de la Paz, L.D., et al., The role of GABA neurotransmitter in the human central nervous system, physiology, and pathophysiology. Revista mexicana de neurociencia, 2021. 22: p. 67-76.

56. Fino, E. and L. Venance, Spike-timing dependent plasticity in the striatum. Frontiers in Synaptic Neuroscience, 2010. 2.

57. Hensch, T.K., et al., Local GABA circuit control of experience-dependent plasticity in developing visual cortex. Science, 1998. 282(5393): p. 1504-8.

58. Rubenstein, J.L.R. and M.M. Merzenich, Model of autism: increased ratio of excitation/inhibition in key neural systems. Genes, brain, and behavior, 2003. 2(5): p. 255-267.

59. Chu, H.-Y., Synaptic and cellular plasticity in Parkinson's disease. Acta Pharmacologica Sinica, 2020. 41(4): p. 447-452.

60. Surmeier, D.J., S.M. Graves, and W. Shen, Dopaminergic modulation of striatal networks in health and Parkinson's disease. Current Opinion in Neurobiology, 2014. 29: p. 109-117.

61. Sporns, O. and R. Kotter, Motifs in brain networks. PLoS Biol, 2004. 2(11): p. e369.

62. van den Heuvel, M.P. and O. Sporns, Network hubs in the human brain. Trends Cogn Sci, 2013. 17(12): p. 683-96.

63. Bassett, D.S. and O. Sporns, Network neuroscience. Nat Neurosci, 2017. 20(3): p. 353-364.

64. Sporns, O., Connectome Networks: From Cells to Systems, in Micro-, Meso- and Macro-Connectomics of the Brain, H. Kennedy, D.C. Van Essen, and Y. Christen, Editors. 2016: Cham (CH). p. 107-127.

65. Sporns, O., The human connectome: origins and challenges. Neuroimage, 2013. 80: p. 53-61.

66. Schroter, M., O. Paulsen, and E.T. Bullmore, Micro-connectomics: probing the organization of neuronal networks at the cellular scale. Nat Rev Neurosci, 2017. 18(3): p. 131-146.

67. Sporns, O., The human connectome: a complex network. Ann N Y Acad Sci, 2011. 1224: p. 109-125.

68. Rothschild, G. and A. Mizrahi, Global order and local disorder in brain maps. Annu Rev Neurosci, 2015. 38: p. 247-68.

69. Devor, A., et al., The Challenge of Connecting the Dots in the B.R.A.I.N. Neuron, 2013. 80(2): p. 270-274.

70. Alagapan, S., et al., Structure, Function, and Propagation of Information across Living Two, Four, and Eight Node Degree Topologies. Front Bioeng Biotechnol, 2016. 4: p. 15.

71. Ju, H. and D.S. Bassett, Dynamic representations in networked neural systems. Nat Neurosci, 2020. 23(8): p. 908-917.

72. Pievani, M., et al., Brain connectivity in neurodegenerative diseases--from phenotype to proteinopathy. Nat Rev Neurol, 2014. 10(11): p. 620-33.

73. Ahrens, M.B., et al., Whole-brain functional imaging at cellular resolution using light-sheet microscopy. Nature Methods, 2013. 10(5): p. 413-420.

74. Portugues, R., et al., Whole-Brain Activity Maps Reveal Stereotyped, Distributed Networks for Visuomotor Behavior. Neuron, 2014. 81(6): p. 1328-1343.

75. Mechling, A.E., et al., Fine-grained mapping of mouse brain functional connectivity with resting-state fMRI. NeuroImage, 2014. 96: p. 203-215.

76. Oh, S.W., et al., A mesoscale connectome of the mouse brain. Nature, 2014. 508(7495): p. 207-214.

77. Wang, Z., et al., The Relationship of Anatomical and Functional Connectivity to Resting-State Connectivity in Primate Somatosensory Cortex. Neuron, 2013. 78(6): p. 1116-1126.

78. Kaiser, M., et al., Simulation of robustness against lesions of cortical networks. European Journal of Neuroscience, 2007. 25(10): p. 3185-3192.

79. Aerts, H., et al., Brain networks under attack: robustness properties and the impact of lesions. Brain, 2016. 139(12): p. 3063-3083.

80. Gao, J., B. Barzel, and A.-L. Barabási, Universal resilience patterns in complex networks. Nature, 2016. 530(7590): p. 307-312.

81. Peraza, L.R., J.-P. Taylor, and M. Kaiser, Divergent brain functional network alterations in dementia with Lewy bodies and Alzheimer's disease. Neurobiology of Aging, 2015. 36(9): p. 2458-2467.

82. Corey-Bloom, J., et al., Diagnosis and evaluation of dementia. Neurology, 1995. 45(2): p. 211-218.

83. Tune, L., Treatments for dementia. A Guide to Treatments that Work, 2007: p. 105-143.

84. Knopman, D.S., et al., Practice parameter: Diagnosis of dementia (an evidence-based review). Report of the Quality Standards Subcommittee of the American Academy of Neurology, 2001. 56(9): p. 1143-1153.

85. Song, Y. and J. Wang, Overview of Chinese research on senile dementia in mainland China. Ageing Research Reviews, 2010. 9: p. S6-S12.

86. Folstein, M.F., L.N. Robins, and J.E. Helzer, The mini-mental state examination. Archives of general psychiatry, 1983. 40(7): p. 812-812.

87. Blennow, K. and H. Zetterberg, The past and the future of Alzheimer's disease CSF biomarkers—a journey toward validated biochemical tests covering the whole spectrum of molecular events. Frontiers in Neuroscience, 2015. 9.

88. Stoiljkovic, M., T.L. Horvath, and M. Hajós, Therapy for Alzheimer's disease: Missing targets and functional markers? Ageing Research Reviews, 2021. 68: p. 101318.

89. Long, J.M. and D.M. Holtzman, Alzheimer disease: an update on pathobiology and treatment strategies. Cell, 2019. 179(2): p. 312-339.

90. Tariot, P.N. and H.J. Federoff, Current treatment for Alzheimer disease and future prospects. Alzheimer disease & associated disorders, 2003. 17: p. S105-S113.

91. Fisher, A., Therapeutic strategies in Alzheimer's disease: M1 muscarinic agonists. The Japanese Journal of Pharmacology, 2000. 84(2): p. 101-112.

92. Wilcock, G., et al., A long-term comparison of galantamine and donepezil in the treatment of Alzheimer's disease. Drugs & aging, 2003. 20(10): p. 777-789.

93. Sun, X., L. Jin, and P. Ling, Review of drugs for Alzheimer's disease. Drug discoveries & therapeutics, 2012. 6(6): p. 285-290.

94. Wright, T.M., Tramiprosate. Drugs of today (Barcelona, Spain: 1998), 2006. 42(5): p. 291-298.

95. Feng, Y. and X. Wang, Antioxidant therapies for Alzheimer's disease. Oxidative medicine and cellular longevity, 2012. 2012.

96. Fahn, S., Description of Parkinson's disease as a clinical syndrome. Annals of the New York Academy of Sciences, 2003. 991(1): p. 1-14.

97. Dickson, D.W., Neuropathology of Parkinson disease. Parkinsonism & related disorders, 2018. 46: p. S30-S33.

98. Lu, R., et al., Evaluation of wearable sensor devices in Parkinson's disease: A review of current status and future prospects. Parkinson's Disease, 2020. 2020.

99. Abdo, W.F., et al., The clinical approach to movement disorders. Nature Reviews Neurology, 2010. 6(1): p. 29-37.

100. Gallagher, D.A. and A. Schrag, Impact of newer pharmacological treatments on quality of life in patients with Parkinson's disease. CNS drugs, 2008. 22(7): p. 563-586.

101. Katzenschlager, R. and A.J. Lees, Treatment of Parkinson's disease: levodopa as the first choice. Journal of neurology, 2002. 249(2): p. ii19-ii24.

102. Djaldetti, R. and E. Melamed, Levodopa ethylester: a novel rescue therapy for response fluctuations in Parkinson's disease. Annals of Neurology: Official Journal of the American Neurological

Association and the Child Neurology Society, 1996. 39(3): p. 400-404.

103. Brooks, D., Dopamine agonists: their role in the treatment of Parkinson's disease. Journal of neurology, neurosurgery & psychiatry, 2000. 68(6): p. 685-689.

104. Kim, S.U., H.J. Lee, and Y.B. Kim, Neural stem cell-based treatment for neurodegenerative diseases. Neuropathology, 2013. 33(5): p. 491-504.

105. Marsh, S.E. and M. Blurton-Jones, Neural stem cell therapy for neurodegenerative disorders: the role of neurotrophic support. Neurochemistry international, 2017. 106: p. 94-100.

106. Ecroyd, H. and J.A. Carver, Unraveling the mysteries of protein folding and misfolding. IUBMB Life, 2008. 60(12): p. 769-774.

107. Schwartz, A.L. and A. Ciechanover, Targeting Proteins for Destruction by the Ubiquitin System: Implications for Human Pathobiology. Annual Review of Pharmacology and Toxicology, 2009. 49(1): p. 73-96.

108. Hartl, F.U. and M. Hayer-Hartl, Converging concepts of protein folding in vitro and in vivo. Nature Structural & Molecular Biology, 2009. 16(6): p. 574-581.

109. Palop, J.J., J. Chin, and L. Mucke, A network dysfunction perspective on neurodegenerative diseases. Nature, 2006. 443(7113): p. 768-773.

110. Seeley, W.W., et al., Neurodegenerative Diseases Target Large-Scale Human Brain Networks. Neuron, 2009. 62(1): p. 42-52.

111. Acquatella-Tran Van Ba, I., T. Imberdis, and V. Perrier, From Prion Diseases to Prion-Like Propagation Mechanisms of Neurodegenerative Diseases. International Journal of Cell Biology, 2013. 2013: p. 975832.

112. Kahle, P.J., et al., Subcellular Localization of Wild-Type and Parkinson's Disease-Associated Mutant α-Synuclein in Human and Transgenic Mouse Brain. The Journal of Neuroscience, 2000. 20(17): p. 6365-6373.

113. Davidson, W.S., et al., Stabilization of alpha-synuclein secondary structure upon binding to synthetic membranes. J Biol Chem, 1998. 273(16): p. 9443-9.

114. Ghosh, P., et al., Determination of critical nucleation number for a single nucleation amyloid-β aggregation model. Mathematical Biosciences, 2016. 273: p. 70-79.

115. Goedert, M., et al., Multiple isoforms of human microtubule-associated protein tau: sequences and localization in neurofibrillary tangles of Alzheimer's disease. Neuron, 1989. 3(4): p. 519-526.

116. Hanger, D.P., et al., Novel phosphorylation sites in tau from Alzheimer brain support a role for casein kinase 1 in disease pathogenesis. J Biol Chem, 2007. 282(32): p. 23645-54.

117. Iqbal, K., et al., Mechanisms of tau-induced neurodegeneration. Acta neuropathologica, 2009. 118(1): p. 53-69.

118. Mudher, A., et al., What is the evidence that tau pathology spreads through prion-like propagation? Acta Neuropathologica Communications, 2017. 5(1): p. 99.

119. Ling, Y., K. Morgan, and N. Kalsheker, Amyloid precursor protein (APP) and the biology of proteolytic processing: relevance to Alzheimer's disease. Int J Biochem Cell Biol, 2003. 35(11): p. 1505-35.

120. Breen, K.C., M. Bruce, and B.H. Anderton, Beta amyloid precursor protein mediates neuronal cell-cell and cell-surface adhesion. J Neurosci Res, 1991. 28(1): p. 90-100.

121. Herms, J., et al., Cortical dysplasia resembling human type 2 lissencephaly in mice lacking all three APP family members. The EMBO Journal, 2004. 23(20): p. 4106-4115.

122. Masters, C.L. and D.J. Selkoe, Biochemistry of Amyloid β-Protein and Amyloid Deposits in Alzheimer Disease. Cold Spring Harbor Perspectives in Medicine, 2012. 2(6).

123. Roher, A.E., et al., APP/Aβ structural diversity and Alzheimer's disease pathogenesis. Neurochemistry International, 2017. 110: p. 1-13.

124. Morishima-Kawashima, M., et al., Hyperphosphorylation of Tau in PHF. Neurobiology of Aging, 1995. 16(3): p. 365-371.

125. Hoenicka, J., Genes in Alzheimer's disease. Revista de neurologia, 2006. 42(5): p. 302-305.

126. Giri, M., M. Zhang, and Y. Lü, Genes associated with Alzheimer's disease: an overview and current status. Clinical interventions in aging, 2016. 11: p. 665-681.

127. Karch, C.M., C. Cruchaga, and A.M. Goate, Alzheimer's disease genetics: from the bench to the clinic. Neuron, 2014. 83(1): p. 11-26.

128. Dorszewska, J., et al., Molecular Basis of Familial and Sporadic Alzheimer's Disease. Curr Alzheimer Res, 2016. 13(9): p. 952-63.

129. Dourlen, P., et al., The new genetic landscape of Alzheimer's disease: from amyloid cascade to genetically driven synaptic failure hypothesis? Acta Neuropathol, 2019. 138(2): p. 221-236.

130. Bellenguez, C., B. Grenier-Boley, and J.C. Lambert, Genetics of Alzheimer's disease: where we are, and where we are going. Curr Opin Neurobiol, 2020. 61: p. 40-48.

131. Wirths, O., et al., Reelin in plaques of β-amyloid precursor protein and presenilin-1 double-transgenic mice. Neuroscience Letters, 2001. 316(3): p. 145-148.

132. Nizzari, M., et al., Neurodegeneration in Alzheimer Disease: Role of Amyloid Precursor Protein and Presenilin 1 Intracellular Signaling. Journal of Toxicology, 2012. 2012: p. 187297.

133. Wolozin, B., P. Alexander, and J. Palacino, Regulation of Apoptosis by Presenilin 1. Neurobiology of Aging, 1998. 19(1, Supplement 1): p. S23-S27.

134. Stanga, S., et al., Specificity of presenilin-1- and presenilin-2-dependent γ-secretases towards substrate processing. Journal of Cellular and Molecular Medicine, 2018. 22(2): p. 823-833.

135. Hartmann, T., Cholesterol, Aβ and Alzheimer's disease. Trends in Neurosciences, 2001. 24: p. 45-48.

136. Sawmiller, D., et al., A Novel Apolipoprotein E Antagonist Functionally Blocks Apolipoprotein E Interaction With N-terminal Amyloid Precursor Protein, Reduces β-Amyloid-Associated Pathology, and Improves Cognition. Biological Psychiatry, 2019. 86(3): p. 208-220.

137. Breger, L.S. and M.T. Fuzzati Armentero, Genetically engineered animal models of Parkinson's disease: From worm to rodent. European Journal of Neuroscience, 2019. 49(4): p. 533-560.

138. Dolgacheva, L.P., et al., Role of DJ-1 in the mechanism of pathogenesis of Parkinson's disease. Journal of Bioenergetics and Biomembranes, 2019. 51(3): p. 175-188.

139. Humbert, J., et al., Parkin and synphilin-1 isoform expression changes in Lewy body diseases. Neurobiology of Disease, 2007. 26(3): p. 681-687.

140. Cooper, J.F., et al., α-synuclein expression from a single copy transgene increases sensitivity to stress and accelerates neuronal loss in genetic models of Parkinson's disease. Experimental Neurology, 2018. 310: p. 58-69.

141. Carta, A.R., et al., Advances in modelling alpha-synuclein-induced Parkinson's diseases in rodents: Virus-based models versus inoculation of exogenous preformed toxic species. J Neurosci Methods, 2020. 338: p. 108685.

142. Praticò, D. and S. Sung, Lipid Peroxidation and Oxidative imbalance: Early functional events in Alzheimer's disease. Journal of Alzheimer's Disease, 2004. 6: p. 171-175.

143. Castellani, R.J., et al., Sublethal RNA Oxidation as a Mechanism for Neurodegenerative Disease. International Journal of Molecular Sciences, 2008. 9(5): p. 789-806.

144. Nunomura, A., et al., RNA oxidation in Alzheimer disease and related neurodegenerative disorders. Acta Neuropathologica, 2009. 118(1): p. 151-166.

145. Sultana, R. and D.A. Butterfield, Oxidatively modified, mitochondria-relevant brain proteins in subjects with Alzheimer disease and mild cognitive impairment. Journal of Bioenergetics and Biomembranes, 2009. 41(5): p. 441-446.

146. Puyal, J., et al., [The two faces of autophagy in the nervous system]. Med Sci (Paris), 2009. 25(4): p. 383-90.

147. Bond, C.E. and S.A. Greenfield, Multiple cascade effects of oxidative stress on astroglia. Glia, 2007. 55(13): p. 1348-1361.

148. Ballatori, N., et al., Glutathione dysregulation and the etiology and progression of human diseases. 2009. 390(3): p. 191-214.

149. Martínez, A., et al., Protein Targets of Oxidative Damage in Human Neurodegenerative Diseases with Abnormal Protein Aggregates. Brain Pathology, 2010. 20(2): p. 281-297.

150. Halliwell, B., Oxidative stress and neurodegeneration: where are we now? Journal of

Neurochemistry, 2006. 97(6): p. 1634-1658.

151. Sonnen, J.A., et al., Free radical-mediated damage to brain in Alzheimer's disease and its transgenic mouse models. Free Radical Biology and Medicine, 2008. 45(3): p. 219-230.

152. Zheng, L., et al., Oxidative stress induces macroautophagy of amyloid β-protein and ensuing apoptosis. Free Radical Biology and Medicine, 2009. 46(3): p. 422-429.

153. Reed, T.T., et al., Proteomic identification of nitrated brain proteins in early Alzheimer's disease inferior parietal lobule. Journal of Cellular and Molecular Medicine, 2009. 13(8b): p. 2019-2029.

154. Martin, H.L. and P. Teismann, Glutathione—a review on its role and significance in Parkinson's disease. The FASEB Journal, 2009. 23(10): p. 3263-3272.

155. Tribl, F., et al., Identification of L-ferritin in Neuromelanin Granules of the Human Substantia Nigra: A TARGETED PROTEOMICS APPROACH *. Molecular & Cellular Proteomics, 2009. 8(8): p. 1832-1838.

156. Sarkate, A.P., V.S. Jambhorkar, and B.K. Sakhale, Natural Food Antioxidants, in Plant Antioxidants and Health, H.M. Ekiert, K.G. Ramawat, and J. Arora, Editors. 2020, Springer International Publishing: Cham. p. 1-16.

157. Mehta, J., S. Rayalam, and X. Wang, Cytoprotective Effects of Natural Compounds against Oxidative Stress. Antioxidants, 2018. 7(10): p. 147.

158. Zhao, B., Natural Antioxidants Protect Neurons in Alzheimer's Disease and Parkinson's Disease. Neurochemical Research, 2009. 34(4): p. 630-638.

159. Liu, Z., et al., Oxidative Stress in Neurodegenerative Diseases: From Molecular Mechanisms to Clinical Applications. Oxidative Medicine and Cellular Longevity, 2017. 2017: p. 2525967.

160. Yin, K.J., et al., Amyloid-beta induces Smac release via AP-1/Bim activation in cerebral endothelial cells. The Journal of neuroscience : the official journal of the Society for Neuroscience, 2002. 22(22): p. 9764-9770.

161. Yan, S.D. and D.M. Stern, Mitochondrial dysfunction and Alzheimer's disease: role of amyloid-β peptide alcohol dehydrogenase (ABAD). International Journal of Experimental Pathology, 2005. 86(3): p. 161-171.

162. Maia, L.F., et al., Changes in amyloid-beta and Tau in the cerebrospinal fluid of transgenic mice overexpressing amyloid precursor protein. Sci Transl Med, 2013. 5(194): p. 194re2.

163. Wang, Z.-F., et al., Overexpression of Tau Proteins Antagonizes Amyloid-β-Potentiated Apoptosis Through Mitochondria-Caspase-3 Pathway in N2a Cells. Journal of Alzheimer's Disease, 2010. 20: p. 145-157.

164. Jellinger, K.A., Basic mechanisms of neurodegeneration: a critical update. J Cell Mol Med, 2010. 14(3): p. 457-87.

165. Higgins, G.C., P.M. Beart, and P. Nagley, Oxidative stress triggers neuronal caspase-independent

death: Endonuclease G involvement in programmed cell death-type III. Cellular and Molecular Life Sciences, 2009. 66(16): p. 2773-2787.

166. Todde, V., M. Veenhuis, and I.J. van der Klei, Autophagy: Principles and significance in health and disease. Biochimica et Biophysica Acta (BBA) - Molecular Basis of Disease, 2009. 1792(1): p. 3-13.

167. Martínez-Pinilla, E., et al., Regional and Gender Study of Neuronal Density in Brain during Aging and in Alzheimer's Disease. Front Aging Neurosci, 2016. 8: p. 213.

168. Chang, H.Y., T.K. Sang, and A.S. Chiang, Untangling the Tauopathy for Alzheimer's disease and parkinsonism. J Biomed Sci, 2018. 25(1): p. 54.

169. Bussière, T., et al., Progressive degeneration of nonphosphorylated neurofilament protein-enriched pyramidal neurons predicts cognitive impairment in Alzheimer's disease: stereologic analysis of prefrontal cortex area 9. J Comp Neurol, 2003. 463(3): p. 281-302.

170. Lassmann, H., et al., Cell death in Alzheimer's disease evaluated by DNA fragmentation in situ. Acta Neuropathologica, 1995. 89(1): p. 35-41.

171. Frade, J.M. and M.C. Ovejero-Benito, Neuronal cell cycle: the neuron itself and its circumstances. Cell Cycle, 2015. 14(5): p. 712-20.

172. Ungureanu, A.A., et al., Amyloid beta oligomers induce neuronal elasticity changes in age-dependent manner: a force spectroscopy study on living hippocampal neurons. Sci Rep, 2016. 6: p. 25841.

173. Iannielli, A., et al., Pharmacological Inhibition of Necroptosis Protects from Dopaminergic Neuronal Cell Death in Parkinson’s Disease Models. Cell Reports, 2018. 22(8): p. 2066-2079.

174. Yasuda, T., Y. Nakata, and H. Mochizuki, α-Synuclein and Neuronal Cell Death. Molecular Neurobiology, 2013. 47(2): p. 466-483.

175. Decressac, M., et al., Progressive neurodegenerative and behavioural changes induced by AAV-mediated overexpression of α-synuclein in midbrain dopamine neurons. Neurobiology of Disease, 2012. 45(3): p. 939-953.

176. Tanaka, Y., et al., Inducible expression of mutant α-synuclein decreases proteasome activity and increases sensitivity to mitochondria-dependent apoptosis. Human Molecular Genetics, 2001. 10(9): p. 919-926.

177. Freeman, D., et al., Alpha-Synuclein Induces Lysosomal Rupture and Cathepsin Dependent Reactive Oxygen Species Following Endocytosis. PLOS ONE, 2013. 8(4): p. e62143.

178. Chi, H., H.-Y. Chang, and T.-K. Sang, Neuronal Cell Death Mechanisms in Major Neurodegenerative Diseases. International Journal of Molecular Sciences, 2018. 19(10): p. 3082.

179. Sánchez-Pernaute, R., et al., Insights into Parkinson's disease models and neurotoxicity using non-

invasive imaging. Toxicology and Applied Pharmacology, 2005. 207(2, Supplement): p. 251-256.

180. Hoogeveen, A.T., et al., Characterization and localization of the Huntington disease gene product. Human Molecular Genetics, 1993. 2(12): p. 2069-2073.

181. Rubinsztein, D.C., et al., Analysis of the huntingtin gene reveals a trinucleotide-length polymorphism in the region of the gene that contains two CCG-rich stretches and a correlation between decreased age of onset of Huntington's disease and CAG repeat number. Hum Mol Genet, 1993. 2(10): p. 1713-5.

182. Lee , J.-T., et al., Amyloid-β peptide induces oligodendrocyte death by activating the neutral sphingomyelinase–ceramide pathway. Journal of Cell Biology, 2004. 164(1): p. 123-131.

183. Klunk, W.E., et al., Binding of the Positron Emission Tomography Tracer Pittsburgh Compound-B Reflects the Amount of Amyloid-β in Alzheimer's Disease Brain But Not in Transgenic Mouse Brain. The Journal of Neuroscience, 2005. 25(46): p. 10598.

184. Valla, J., et al., Effects of Image Resolution on Autoradiographic Measurements of Posterior Cingulate Activity in PDAPP Mice: Implications for Functional Brain Imaging Studies of Transgenic Mouse Models of Alzheimer's Disease. NeuroImage, 2002. 16(1): p. 1-6.

185. Toyama, H., et al., PET imaging of brain with the β-amyloid probe, [11C]6-OH-BTA-1, in a transgenic mouse model of Alzheimer's disease. European Journal of Nuclear Medicine and Molecular Imaging, 2005. 32(5): p. 593-600.

186. Strome, E.M. and D.J. Doudet, Animal Models of Neurodegenerative Disease: Insights from In vivo Imaging Studies. Molecular Imaging and Biology, 2007. 9(4): p. 186-195.

187. Frega, M., In Vitro Neuronal Networks, in Neuronal Network Dynamics in 2D and 3D in vitro Neuroengineered Systems. 2016, Springer International Publishing: Cham. p. 31-41.

188. Elfarrash, S., et al., Organotypic slice culture model demonstrates inter-neuronal spreading of alpha-synuclein aggregates. Acta Neuropathologica Communications, 2019. 7(1): p. 213.

189. Froula, J.M., et al., α-Synuclein fibril-induced paradoxical structural and functional defects in hippocampal neurons. Acta Neuropathologica Communications, 2018. 6(1): p. 35.

190. D'Agostino, D.P., R.W. Putnam, and J.B. Dean, Superoxide (·O2−) Production in CA1 Neurons of Rat Hippocampal Slices Exposed to Graded Levels of Oxygen. Journal of Neurophysiology, 2007. 98(2): p. 1030-1041.

191. Raiss, C.C., et al., Functionally different α-synuclein inclusions yield insight into Parkinson's disease pathology. Scientific Reports, 2016. 6(1): p. 23116.

192. Hassink, G.C., et al., Exogenous α-synuclein hinders synaptic communication in cultured cortical primary rat neurons. PLOS ONE, 2018. 13(3): p. e0193763.

193. Courte, J., et al., The expression level of alpha-synuclein in different neuronal populations is the primary determinant of its prion-like seeding. Scientific Reports, 2020. 10(1): p. 4895.

194. Taguchi, K., et al., Differential Expression of Alpha-Synuclein in Hippocampal Neurons. PLOS ONE, 2014. 9(2): p. e89327.

195. Peelaerts, W., et al., α-Synuclein strains cause distinct synucleinopathies after local and systemic administration. Nature, 2015. 522(7556): p. 340-344.

196. Nemani, V.M., et al., Increased Expression of α-Synuclein Reduces Neurotransmitter Release by Inhibiting Synaptic Vesicle Reclustering after Endocytosis. Neuron, 2010. 65(1): p. 66-79.

197. Mobini, S., et al., Advances in ex vivo models and lab-on-a-chip devices for neural tissue engineering. Biomaterials, 2019. 198: p. 146-166.

198. Raimondi, I., et al., Organ-On-A-Chip in vitro Models of the Brain and the Blood-Brain Barrier and Their Value to Study the Microbiota-Gut-Brain Axis in Neurodegeneration. Front Bioeng Biotechnol, 2019. 7: p. 435.

199. Marx, V., Neuroscience models: choose your dimension. Nat Methods, 2018. 15(11): p. 863-866.

200. Zhuang, P., et al., 3D neural tissue models: From spheroids to bioprinting. Biomaterials, 2018. 154: p. 113-133.

201. Lovett, M.L., et al., Innovations in 3-Dimensional Tissue Models of Human Brain Physiology and Diseases. Adv Funct Mater, 2020. 30(44).

202. Hofer, M. and M.P. Lutolf, Engineering organoids. Nat Rev Mater, 2021: p. 1-19.

203. Ahadian, S., et al., Organ-On-A-Chip Platforms: A Convergence of Advanced Materials, Cells, and Microscale Technologies. Adv Healthc Mater, 2018. 7(2).

204. Sung, J.H., et al., Recent Advances in Body-on-a-Chip Systems. Analytical Chemistry, 2019. 91(1): p. 330-351.

205. Feinerman, O., A. Rotem, and E. Moses, Reliable neuronal logic devices from patterned hippocampal cultures. Nature Physics, 2008. 4(12): p. 967-973.

206. Hardelauf, H., et al., Micropatterning neuronal networks. Analyst, 2014. 139(13): p. 3256-3264.

207. Jang, M.J. and Y. Nam, Geometric effect of cell adhesive polygonal micropatterns on neuritogenesis and axon guidance. J Neural Eng, 2012. 9(4): p. 046019.

208. Taylor, A.M., et al., Microfluidic Multicompartment Device for Neuroscience Research. Langmuir, 2003. 19(5): p. 1551-1556.

209. Taylor, A.M., et al., A microfluidic culture platform for CNS axonal injury, regeneration and transport. Nature Methods, 2005. 2(8): p. 599-605.

210. Gladkov, A., et al., Design of Cultured Neuron Networks in vitro with Predefined Connectivity Using Asymmetric Microfluidic Channels. Scientific Reports, 2017. 7(1): p. 15625.

211. Moutaux, E., et al., An integrated microfluidic/microelectrode array for the study of activity-dependent intracellular dynamics in neuronal networks. Lab on a Chip, 2018. 18(22): p. 3425-3435.

212. Soscia, D., et al., Controlled placement of multiple CNS cell populations to create complex neuronal cultures. PLOS ONE, 2017. 12(11): p. e0188146.

213. Kajtez, J., et al., 3D-Printed Soft Lithography for Complex Compartmentalized Microfluidic Neural Devices. Advanced Science, 2020. 7(16): p. 2001150.

214. Ndyabawe, K., et al., Brain-on-a-Chip Device for Modeling Multiregional Networks. ACS Biomaterials Science & Engineering, 2021. 7(1): p. 350-359.

215. Park, J., et al., Three-dimensional brain-on-a-chip with an interstitial level of flow and its application as an in vitro model of Alzheimer's disease. Lab on a Chip, 2015. 15(1): p. 141-150.

216. Jeong, G.S., et al., Networked neural spheroid by neuro-bundle mimicking nervous system created by topology effect. Molecular Brain, 2015. 8(1): p. 17.

217. Kato-Negishi, M., et al., Millimeter-Sized Neural Building Blocks for 3D Heterogeneous Neural Network Assembly. Advanced Healthcare Materials, 2013. 2(12): p. 1564-1570.

218. Harberts, J., et al., Toward Brain-on-a-Chip: Human Induced Pluripotent Stem Cell-Derived Guided Neuronal Networks in Tailor-Made 3D Nanoprinted Microscaffolds. ACS Nano, 2020. 14(10): p. 13091-13102.

219. Booth, R. and H. Kim, Characterization of a microfluidic in vitro model of the blood-brain barrier (μBBB). Lab on a Chip, 2012. 12(10): p. 1784-1792.

220. Kilic, O., et al., Brain-on-a-chip model enables analysis of human neuronal differentiation and chemotaxis. Lab on a Chip, 2016. 16(21): p. 4152-4162.

221. Bang, S., et al., A Low Permeability Microfluidic Blood-Brain Barrier Platform with Direct Contact between Perfusable Vascular Network and Astrocytes. Scientific Reports, 2017. 7(1): p. 8083.

222. Huber, D., et al., Hydrodynamics in Cell Studies. Chemical Reviews, 2018. 118(4): p. 2042-2079.

223. Alrifaiy, A., O.A. Lindahl, and K. Ramser, Polymer-Based Microfluidic Devices for Pharmacy, Biology and Tissue Engineering. Polymers, 2012. 4(3): p. 1349-1398.

224. Ren, K., Y. Chen, and H. Wu, New materials for microfluidics in biology. Current Opinion in Biotechnology, 2014. 25: p. 78-85.

225. Nie, J., J. Fu, and Y. He, Hydrogels: the next generation body materials for microfluidic chips? Small, 2020. 16(46): p. 2003797.

226. Chung, B.G., et al., Microfluidic fabrication of microengineered hydrogels and their application in tissue engineering. Lab on a Chip, 2012. 12(1): p. 45-59.

227. Hwang, J., et al., Microchannel fabrication on glass materials for microfluidic devices. International Journal of Precision Engineering and Manufacturing, 2019. 20(3): p. 479-495.

228. Beebe, D.J., G.A. Mensing, and G.M. Walker, Physics and applications of microfluidics in biology. Annual review of biomedical engineering, 2002. 4(1): p. 261-286.

229. Nguyen, N.-T., S.T. Wereley, and S.A.M. Shaegh, Fundamentals and applications of microfluidics. 2019: Artech house.

230. Taylor, A.M., et al., Microfluidic Local Perfusion Chambers for the Visualization and Manipulation of Synapses. Neuron, 2010. 66(1): p. 57-68.

231. Peyrin, J.-M., et al., Axon diodes for the reconstruction of oriented neuronal networks in microfluidic chambers. Lab on a Chip, 2011. 11(21): p. 3663-3673.

232. Deleglise, B., et al., Synapto-Protective Drugs Evaluation in Reconstructed Neuronal Network. PLOS ONE, 2013. 8(8): p. e71103.

233. Deleglise, B., et al., Dysregulated Neurotransmission induces Trans-synaptic degeneration in reconstructed Neuronal Networks. Scientific Reports, 2018. 8(1): p. 11596.

234. Tan, V.X., et al., Neurotoxicity of the Cyanotoxin BMAA Through Axonal Degeneration and Intercellular Spreading. Neurotoxicity Research, 2018. 33(1): p. 62-75.

235. Lassus, B., et al., Glutamatergic and dopaminergic modulation of cortico-striatal circuits probed by dynamic calcium imaging of networks reconstructed in microfluidic chips. Scientific Reports, 2018. 8(1): p. 17461.

236. Deleglise, B., et al., β-amyloid induces a dying-back process and remote trans-synaptic alterations in a microfluidic-based reconstructed neuronal network. Acta Neuropathologica Communications, 2014. 2(1): p. 145.

237. Kamudzandu, M., et al., A micro-fabricated in vitro complex neuronal circuit platform. Biomedical Physics & Engineering Express, 2019. 5(4): p. 045016.

238. Renault, R., et al., Asymmetric axonal edge guidance: a new paradigm for building oriented neuronal networks. Lab Chip, 2016. 16(12): p. 2188-91.

239. Courte, J., et al., Reconstruction of directed neuronal networks in a microfluidic device with asymmetric microchannels, in Methods in Cell Biology, D.A. Fletcher, J. Doh, and M. Piel, Editors. 2018, Academic Press. p. 71-95.

240. Courte, J., et al., Quantitative study of alpha-synuclein prion-like spreading in fully oriented reconstructed neural networks reveals non-synaptic dissemination of seeding aggregates. bioRxiv, 2021: p. 2021.10.06.463379.

241. Courte, J., et al., Reconstruction of directed neuronal networks in a microfluidic device with asymmetric microchannels. Methods Cell Biol, 2018. 148: p. 71-95.

242. Holloway, P.M., et al., Asymmetric confinement for defining outgrowth directionality. Lab on a Chip, 2019. 19(8): p. 1484-1489.

243. Forró, C., et al., Modular microstructure design to build neuronal networks of defined functional connectivity. Biosensors and Bioelectronics, 2018. 122: p. 75-87.

244. Usenovic, M., et al., Internalized Tau Oligomers Cause Neurodegeneration by Inducing

Accumulation of Pathogenic Tau in Human Neurons Derived from Induced Pluripotent Stem Cells. The Journal of Neuroscience, 2015. 35(42): p. 14234-14250.

245. Wu, J.W., et al., Small misfolded Tau species are internalized via bulk endocytosis and anterogradely and retrogradely transported in neurons. J Biol Chem, 2013. 288(3): p. 1856-70.

246. Takeda, S., et al., Neuronal uptake and propagation of a rare phosphorylated high-molecular-weight tau derived from Alzheimer's disease brain. Nature Communications, 2015. 6(1): p. 8490.

247. Nobuhara, C.K., et al., Tau Antibody Targeting Pathological Species Blocks Neuronal Uptake and Interneuron Propagation of Tau in Vitro. The American Journal of Pathology, 2017. 187(6): p. 1399-1412.

248. Wu, J.W., et al., Neuronal activity enhances tau propagation and tau pathology in vivo. Nature Neuroscience, 2016. 19(8): p. 1085-1092.

249. Calafate, S., et al., Synaptic Contacts Enhance Cell-to-Cell Tau Pathology Propagation. Cell Reports, 2015. 11(8): p. 1176-1183.

250. Wang, Y., et al., The release and trans-synaptic transmission of Tau via exosomes. Molecular Neurodegeneration, 2017. 12(1): p. 5.

251. Song, H.-L., et al., β-Amyloid is transmitted via neuronal connections along axonal membranes. Annals of Neurology, 2014. 75(1): p. 88-97.

252. Choi, Y.J., et al., Neurotoxic amyloid beta oligomeric assemblies recreated in microfluidic platform with interstitial level of slow flow. Scientific Reports, 2013. 3(1): p. 1921.

253. Cho, H., et al., Microfluidic Chemotaxis Platform for Differentiating the Roles of Soluble and Bound Amyloid-β on Microglial Accumulation. Scientific Reports, 2013. 3(1): p. 1823.

254. Bianco, F., et al., Overflow Microfluidic Networks: Application to the Biochemical Analysis of Brain Cell Interactions in Complex Neuroinflammatory Scenarios. Analytical Chemistry, 2012. 84(22): p. 9833-9840.

255. Brahic, M., et al., Axonal transport and secretion of fibrillar forms of α-synuclein, Aβ42 peptide and HTTExon 1. Acta Neuropathologica, 2016. 131(4): p. 539-548.

256. Freundt, E.C., et al., Neuron-to-neuron transmission of α-synuclein fibrils through axonal transport. Ann Neurol, 2012. 72(4): p. 517-24.

257. Gribaudo, S., et al., Propagation of α-Synuclein Strains within Human Reconstructed Neuronal Network. Stem Cell Reports, 2019. 12(2): p. 230-244.

258. Prots, I., et al., alpha-Synuclein oligomers induce early axonal dysfunction in human iPSC-based models of synucleinopathies. Proc Natl Acad Sci U S A, 2018. 115(30): p. 7813-7818.

259. Osaki, T., et al., In Vitro Microfluidic Models for Neurodegenerative Disorders. Adv Healthc Mater, 2018. 7(2).

260. Virlogeux, A., et al., Reconstituting Corticostriatal Network on-a-Chip Reveals the Contribution of the Presynaptic Compartment to Huntington's Disease. Cell Reports, 2018. 22(1): p. 110-122.

261. Lei, Y., et al., An on-chip model for investigating the interaction between neurons and cancer cells. Integrative Biology, 2016. 8(3): p. 359-367.

262. Théry, M., Micropatterning as a tool to decipher cell morphogenesis and functions. Journal of Cell Science, 2010. 123(24): p. 4201-4213.

263. Tomba, C. and C. Villard, Brain cells and neuronal networks: Encounters with controlled microenvironments. Microelectronic Engineering, 2015. 132: p. 176-191.

264. Aebersold, M.J., et al., "Brains on a chip": Towards engineered neural networks. TrAC Trends in Analytical Chemistry, 2016. 78: p. 60-69.

265. Fricke, R., et al., Axon guidance of rat cortical neurons by microcontact printed gradients. Biomaterials, 2011. 32(8): p. 2070-6.

266. Hardelauf, H., et al., Micropatterning neuronal networks. Analyst, 2014. 139(13): p. 3256-64.

267. Szelechowski, M., et al., A viral peptide that targets mitochondria protects against neuronal degeneration in models of Parkinson's disease. Nature Communications, 2014. 5.

268. Renault, R., et al., Combining microfluidics, optogenetics and calcium imaging to study neuronal communication in vitro. PLoS One, 2015. 10(4): p. e0120680.

269. Yamada, A., et al., In-mold patterning and actionable axo-somatic compartmentalization for on-chip neuron culture. Lab Chip, 2016. 16(11): p. 2059-68.

270. Patel, T.P., et al., Automated quantification of neuronal networks and single-cell calcium dynamics using calcium imaging. J Neurosci Methods, 2015. 243: p. 26-38.

271. Schindelin, J., et al., Fiji: an open-source platform for biological-image analysis. Nature Methods, 2012. 9(7): p. 676-682.

272. Breskin, I., et al., Percolation in Living Neural Networks. Physical Review Letters, 2006. 97(18): p. 188102.

273. Deleglise, B., et al., Synapto-protective drugs evaluation in reconstructed neuronal network. PLoS One, 2013. 8(8): p. e71103.

274. Ross, C.A. and M.A. Poirier, Protein aggregation and neurodegenerative disease. Nature Medicine, 2004. 10(7): p. S10-S17.

275. Braak, H., et al., Idiopathic Parkinson's disease: possible routes by which vulnerable neuronal types may be subject to neuroinvasion by an unknown pathogen. Journal of Neural Transmission, 2003. 110(5): p. 517-536.

276. Braak, H., et al., Staging of brain pathology related to sporadic Parkinson's disease. Neurobiology of Aging, 2003. 24(2): p. 197-211.

277. Borghammer, P., How does parkinson's disease begin? Perspectives on neuroanatomical pathways, prions, and histology. Mov Disord, 2018. 33(1): p. 48-57.

278. Brundin, P. and R. Melki, Prying into the Prion Hypothesis for Parkinson's Disease. J Neurosci, 2017. 37(41): p. 9808-9818.

279. Weil, R.S., et al., Current concepts and controversies in the pathogenesis of Parkinson's disease dementia and Dementia with Lewy Bodies. F1000Res, 2017. 6: p. 1604.

280. Aguzzi, A. and L. Rajendran, The Transcellular Spread of Cytosolic Amyloids, Prions, and Prionoids. Neuron, 2009. 64(6): p. 783-790.

281. Kara, E., J.D. Marks, and A. Aguzzi, Toxic Protein Spread in Neurodegeneration: Reality versus Fantasy. Trends in Molecular Medicine, 2018. 24(12): p. 1007-1020.

282. Bourdenx, M., et al., Protein aggregation and neurodegeneration in prototypical neurodegenerative diseases: Examples of amyloidopathies, tauopathies and synucleinopathies. Progress in Neurobiology, 2017. 155: p. 171-193.

283. Blättler, T., et al., PrP-expressing tissue required for transfer of scrapie infectivity from spleen to brain. Nature, 1997. 389(6646): p. 69-73.

284. Brandner, S., et al., Normal host prion protein (PrPC) is required for scrapie spread within the central nervous system. Proc Natl Acad Sci U S A, 1996. 93(23): p. 13148-51.

285. Peng, C., J.Q. Trojanowski, and V.M.Y. Lee, Protein transmission in neurodegenerative disease. Nature Reviews Neurology, 2020. 16(4): p. 199-212.

286. Uemura, N., et al., Cell-to-Cell Transmission of Tau and α-Synuclein. Trends in Molecular Medicine, 2020. 26(10): p. 936-952.

287. Emmanouilidou, E., et al., Cell-Produced α-Synuclein Is Secreted in a Calcium-Dependent Manner by Exosomes and Impacts Neuronal Survival. The Journal of Neuroscience, 2010. 30(20): p. 6838-6851.

288. Saman, S., et al., Exosome-associated tau is secreted in tauopathy models and is selectively phosphorylated in cerebrospinal fluid in early Alzheimer disease. J Biol Chem, 2012. 287(6): p. 3842-9.

289. Flavin, W.P., et al., Endocytic vesicle rupture is a conserved mechanism of cellular invasion by amyloid proteins. Acta Neuropathologica, 2017. 134(4): p. 629-653.

290. Jan, A., et al., The Prion-Like Spreading of Alpha-Synuclein in Parkinson's Disease: Update on Models and Hypotheses. International Journal of Molecular Sciences, 2021. 22(15): p. 8338.

291. Lee, H.-J., et al., Assembly-dependent endocytosis and clearance of extracellular a-synuclein. The International Journal of Biochemistry & Cell Biology, 2008. 40(9): p. 1835-1849.

292. Luk Kelvin, C., et al., Exogenous α-synuclein fibrils seed the formation of Lewy body-like intracellular inclusions in cultured cells. Proceedings of the National Academy of Sciences, 2009.

106(47): p. 20051-20056.

293. Minakaki, G., et al., Autophagy inhibition promotes SNCA/alpha-synuclein release and transfer via extracellular vesicles with a hybrid autophagosome-exosome-like phenotype. Autophagy, 2018. 14(1): p. 98-119.

294. Hansen, C., et al., α-Synuclein propagates from mouse brain to grafted dopaminergic neurons and seeds aggregation in cultured human cells. The Journal of Clinical Investigation, 2011. 121(2): p. 715-725.

295. Desplats, P., et al., Inclusion formation and neuronal cell death through neuron-to-neuron transmission of α-synuclein. Proceedings of the National Academy of Sciences, 2009. 106(31): p. 13010-13015.

296. Zhang, S., et al., Mechanistic basis for receptor-mediated pathological alpha-synuclein fibril cell-to-cell transmission in Parkinson's disease. Proc Natl Acad Sci U S A, 2021. 118(26): p. e2011196118.

297. Rustom, A., et al., Nanotubular Highways for Intercellular Organelle Transport. Science, 2004. 303(5660): p. 1007-1010.

298. Wang, Y., et al., Tunneling-nanotube development in astrocytes depends on p53 activation. Cell Death & Differentiation, 2011. 18(4): p. 732-742.

299. Costanzo, M., et al., Transfer of polyglutamine aggregates in neuronal cells occurs in tunneling nanotubes. Journal of Cell Science, 2013. 126(16): p. 3678-3685.

300. Abounit, S., et al., Tunneling nanotubes spread fibrillar α-synuclein by intercellular trafficking of lysosomes. The EMBO Journal, 2016. 35(19): p. 2120-2138.

301. Victoria, G.S. and C. Zurzolo, The spread of prion-like proteins by lysosomes and tunneling nanotubes: Implications for neurodegenerative diseases. Journal of Cell Biology, 2017. 216(9): p. 2633-2644.

302. De Strooper, B. and E. Karran, The Cellular Phase of Alzheimer's Disease. Cell, 2016. 164(4): p. 603-615.

303. Courte, J., et al., The expression level of alpha-synuclein in different neuronal populations is the primary determinant of its prion-like seeding. Scientific Reports, 2020. 10(1).

304. Lee, S.J., et al., Cell-to-cell transmission of non-prion protein aggregates. Nat Rev Neurol, 2010. 6(12): p. 702-6.

305. Patel, S., et al., Control of cell adhesion on poly(methyl methacrylate). Biomaterials, 2006. 27(14): p. 2890-7.

306. Park, J.Y., et al., Increased poly(dimethylsiloxane) stiffness improves viability and morphology of mouse fibroblast cells. BioChip Journal, 2010. 4(3): p. 230-236.

307. Bartalena, G., et al., Biomaterial surface modifications can dominate cell–substrate mechanics: the

impact of PDMS plasma treatment on a quantitative assay of cell stiffness. Soft Matter, 2012. 8(3): p. 673-681.

308. Chung, S.H. and J. Min, Morphological investigations of cells that adhered to the irregular patterned polydimethylsiloxane (PDMS) surface without reagents. Ultramicroscopy, 2009. 109(8): p. 861-867.

309. Chen, W.-H., et al., Probing Relevant Molecules in Modulating the Neurite Outgrowth of Hippocampal Neurons on Substrates of Different Stiffness. PLOS ONE, 2014. 8(12): p. e83394.

310. Cheng, C.-M., P.R. LeDuc, and Y.-W. Lin, Localized bimodal response of neurite extensions and structural proteins in dorsal-root ganglion neurons with controlled polydimethylsiloxane substrate stiffness. Journal of Biomechanics, 2011. 44(5): p. 856-862.

311. Lantoine, J., et al., Matrix stiffness modulates formation and activity of neuronal networks of controlled architectures. Biomaterials, 2016. 89: p. 14-24.

312. Gokaltun, A., et al., Recent advances in nonbiofouling PDMS surface modification strategies applicable to microfluidic technology. Technology (Singap World Sci), 2017. 5(1): p. 1-12.

313. Liu, W., et al., Enhancement and control of neuron adhesion on polydimethylsiloxane for cell microengineering using a functionalized triblock polymer. Lab Chip, 2019. 19(19): p. 3162-3167.

314. Liu, W., et al., Straightforward neuron micropatterning and neuronal network construction on cell-repellent polydimethylsiloxane using microfluidics-guided functionalized Pluronic modification. Analyst, 2021. 146(2): p. 454-462.

315. Ryu, J.R., et al., Synaptic compartmentalization by micropatterned masking of a surface adhesive cue in cultured neurons. Biomaterials, 2016. 92: p. 46-56.

316. Esch, T., V. Lemmon, and G. Banker, Local Presentation of Substrate Molecules Directs Axon Specification by Cultured Hippocampal Neurons. The Journal of Neuroscience, 1999. 19(15): p. 6417.

317. Kim, W.R., et al., Surface-printed microdot array chips for the quantification of axonal collateral branching of a single neuron in vitro. Lab on a Chip, 2014. 14(4): p. 799-805.

318. Garcia, M., et al., Two-tiered coupling between flowing actin and immobilized N-cadherin/catenin complexes in neuronal growth cones. Proc Natl Acad Sci U S A, 2015. 112(22): p. 6997-7002.

319. Czöndör, K., et al., Micropatterned substrates coated with neuronal adhesion molecules for high-content study of synapse formation. Nature Communications, 2013. 4(1): p. 2252.

320. Lussi, J.W., et al., Pattern stability under cell culture conditions—a comparative study of patterning methods based on PLL-g-PEG background passivation. Biomaterials, 2006. 27(12): p. 2534-41.

321. Groll, J., et al., A novel star PEG-derived surface coating for specific cell adhesion. J Biomed Mater Res A, 2005. 74(4): p. 607-17.

322. Wischerhoff, E., et al., Controlled cell adhesion on PEG-based switchable surfaces. Angew Chem

Int Ed Engl, 2008. 47(30): p. 5666-8.

323. Desai, R.A., N.M. Rodriguez, and C.S. Chen, "Stamp-off" to micropattern sparse, multicomponent features. Methods Cell Biol, 2014. 119: p. 3-16.

324. Thery, M. and M. Piel, Adhesive micropatterns for cells: a microcontact printing protocol. Cold Spring Harb Protoc, 2009. 2009(7): p. pdb prot5255.

325. Slavík, J., et al., Multi-Electrode Array with a Planar Surface for Cell Patterning by Microprinting. Sensors, 2019. 19(24): p. 5379.

326. Albelda, S.M. and C.A. Buck, Integrins and other cell adhesion molecules. The FASEB Journal, 1990. 4(11): p. 2868-2880.

327. Huang, S. and D.E. Ingber, The structural and mechanical complexity of cell-growth control. Nature Cell Biology, 1999. 1(5): p. E131-E138.

328. Chaudhuri, O., et al., Hydrogels with tunable stress relaxation regulate stem cell fate and activity. Nature Materials, 2016. 15(3): p. 326-334.

329. Shellard, A. and R. Mayor, Collective durotaxis along a self-generated stiffness gradient in vivo. Nature, 2021. 600(7890): p. 690-694.

330. Kim, H.N. and N. Choi, Consideration of the Mechanical Properties of Hydrogels for Brain Tissue Engineering and Brain-on-a-chip. BioChip Journal, 2019. 13(1): p. 8-19.

331. Koser, D.E., et al., Mechanosensing is critical for axon growth in the developing brain. Nat Neurosci, 2016. 19(12): p. 1592-1598.

332. Shellard, A. and R. Mayor, Durotaxis: The Hard Path from In Vitro to In Vivo. Dev Cell, 2021. 56(2): p. 227-239.

333. Spadaro, F., et al., Corticotropin-releasing factor acts via a third ventricle site to reduce exploratory behavior in rats. Pharmacol Biochem Behav, 1990. 36(2): p. 305-9.

334. Bizanti, A., P. Chandrashekar, and R. Steward, Jr., Culturing astrocytes on substrates that mimic brain tumors promotes enhanced mechanical forces. Exp Cell Res, 2021. 406(2): p. 112751.

335. Wilson, C.L., S.L. Hayward, and S. Kidambi, Astrogliosis in a dish: substrate stiffness induces astrogliosis in primary rat astrocytes. RSC Adv, 2016. 6(41): p. 34447-34457.

336. Javier-Torrent, M., G. Zimmer-Bensch, and L. Nguyen, Mechanical Forces Orchestrate Brain Development. Trends Neurosci, 2021. 44(2): p. 110-121.

337. Afflerbach, A.-K., et al., Mesenchymal Stem Cells as a Promising Cell Source for Integration in Novel In Vitro Models. Biomolecules, 2020. 10(9): p. 1306.

338. Nikolakopoulou, P., et al., Recent progress in translational engineered in vitro models of the central nervous system. Brain, 2020. 143(11): p. 3181-3213.

339. Bekkers, J.M., Autaptic Cultures: Methods and Applications. Front Synaptic Neurosci, 2020. 12: p.

18.

340. Bekkers, J.M. and C.F. Stevens, Excitatory and inhibitory autaptic currents in isolated hippocampal neurons maintained in cell culture. Proc Natl Acad Sci U S A, 1991. 88(17): p. 7834-8.

341. Šmít, D., et al., Axon tension regulates fasciculation/defasciculation through the control of axon shaft zippering. Elife, 2017. 6.

342. Deleglise, B., et al., Dysregulated Neurotransmission induces Trans-synaptic degeneration in reconstructed Neuronal Networks. Sci Rep, 2018. 8(1): p. 11596.

343. Cohen, M.S., et al., Neurotrophin-mediated dendrite-to-nucleus signaling revealed by microfluidic compartmentalization of dendrites. Proceedings of the National Academy of Sciences, 2011. 108(27): p. 11246-11251.